CORA Cork Open Research Archive
Cartlann Taighde Oscailte Chorcaí

Title	Development of an electrochemical immunosensor for environmental monitoring of polychlorinated biphenyls (PCBs) in soil environment
Authors	Alsefri, Samia
Publication date	2023
Original Citation	Alsefri, S. A. 2023. Development of an electrochemical immunosensor for environmental monitoring of polychlorinated biphenyls (PCBs) in soil environment. PhD Thesis, University College Cork.
Type of publication	Doctoral thesis
Rights	© 2023, Samia Abdullah Alsefri. - https://creativecommons.org/licenses/by-nc/4.0/
Download date	2026-11-05 09:43:22
Item downloaded from	https://hdl.handle.net/10468/15959



UCC
University College Cork, Ireland
Coláiste na hOllscoile Corcaigh

Ollscoil na hÉireann, Corcaigh

National University of Ireland, Cork



Development of An Electrochemical Immunosensor for Environmental Monitoring of Polychlorinated Biphenyls (PCBs) in Soil Environment

Thesis presented by

Samia Abdullah Alsefri, B.Sc. M.Sc.

112220405

Orcid 0000-0003-1959-4155

for the degree of

Doctor of Philosophy

University College Cork

School of Chemistry

Head of School/Department: Prof. Anita Maguire

Supervisor(s): Dr. Eric Moore

[2023]

Dedicated to my beloved parents, Mrs. Norah and Mr. Abdullah, my loving son Master Ahmed, and my sweetheart daughter Miss Tulin. It is also dedicated to my siblings and friends who have always supported and loved me. I would not have been able to achieve all my success without them.

“If we knew what we were doing, it would not be called research, would it?”

- Albert Einstein

Table of Contents

TABLE OF CONTENTS I

LIST OF TABLE AND FIGURES IX

ACKNOWLEDGEMENT XVII

DECLARATION XX

ABBREVIATIONS XXI

ABSTRACT XXIV

RESEARCH PROBLEM XXV

KEY RESEARCH QUESTIONS XXVII

AIMS AND OBJECTIVES. XXVII

THESIS OUTLINE XXIX

CHAPTER 1 1

GENERAL INTRODUCTION 1

1. GENERAL INTRODUCTION 2

1.1 MOTIVATION 2

1.2 POLYCHLORINATED BIPHENYLS (PCBS) 3

1.2.1 ORIGIN, OCCURRENCE AND EXPOSURE OF PCBS 5

1.2.1.1 Environment Pollution of (PCBs) 7

1.2.1.2 Health Effect of PCBs *8*

..... *10*

1.2.2 CURRENT DETECTION METHODS FOR PCBS DETERMINATION 10

1.2.2.1 Chromatographic Techniques 10

1.2.2.2 Immunochemical Methods 11

1.2.2.3 Immunoassays and Immunosensors 12

1.3 IMMUNOASSAYS (ELISA) 13

1.3.1 Immunoassay Format 14

1.3.1.1 Capture ELISA 15

1.3.1.2 Sandwich ELISA 16

1.3.1.3 Competitive ELISA 17

1.3.1.4 Displacement ELISA 19

1.4 BIOSENSORS 21

1.4.1 Classification of Biosensors 25

1.4.1.1 Based on Bioreceptors 25

1.4.1.1.1 Enzymes 26

1.4.1.1.2 Antibodies 30

1.4.1.2 Based on Transducers 33

1.4.1.2.1 Optical Biosensors 34

1.4.1.2.2 Electrochemical Biosensors 34

1.5 FUNDAMENTAL CONCEPTS IN ELECTROCHEMISTRY 35

1.5.1 The Electrochemical Cell 35

1.5.2 The Electrode /Solution Interface (Double Layer Model) 37

1.5.3 Mass Transport 38

1.5.3.1 Diffusion 39

1.5.3.2 Migration 40

1.5.3.3 Convection 40

1.5.4 Electrochemical Techniques 40

1.5.4.1 Voltammetric Transducers 40

1.5.4.1.1 Cyclic Voltammetry 41

1.5.4.1.2 Linear Sweep Voltammetry (LSV) 43

1.5.4.1.3 Differential Pulse Voltammetry (DPV) 44

1.5.4.2 Impedimetric Transducers 46

1.5.4.2.1 Electrochemical Impedance Spectroscopy (ELS) 46

1.5.4.3 Conductometric Transducers 49

1.5.4.4 Potentiometric Transducers 49

1.5.4.5 Amperometric Transducers 50

1.6 CLASSIFICATION OF ELECTROCHEMICAL IMMUNOSENSORS..... 50

1.6.1 Based on the Type of Method Immobilization. 51

1.6.1.1 Physical Adsorption 53

1.6.1.2 Physical Entrapment 53

1.6.1.3 Cross Linking 54

1.6.1.4 Covalent Bonding 54

1.6.2 Based on the Type of Electrode Surface Modification. 54

1.6.2.1 Self-assembled Monolayers (SAMs) 55

1.6.3 Based on the Labeling Strategy. 56

1.7 THEORETICAL CONSIDERATION OF ENZYME KINETICS 60

1.8 SCREEN PRINTED ELECTRODES 62

1.9 STATISTICAL ANALYSIS 62

1.9.1 Validation 63

1.9.1.1 Linear Range 63

1.9.1.2 Limit of Detection 63

1.9.1.3 Selectivity 64

1.9.1.3 Sensitivity 65

1.9.1.4 Accuracy and Precision 66

1.9.1.5 Repeatability and Reproducibility 67

1.9.1.6 Percentage Recovery 67

1.9.1.7 Correlation 68

1.10 REFERENCE 69

CHAPTER 2 97

DEVELOPMENT OF OPTICAL IMMUNOSENSORS BASED ELISA 97

2. DEVELOPMENT OF OPTICAL IMMUNOSENSORS BASED ON INDIRECT COMPETITIVE ENZYME-LINKED IMMUNOSORBENT ASSAY METHODS FOR DETECTION OF AROCLOR1254 IN ENVIRONMENTAL SAMPLES. 98

2.1 ABSTRACT 98

2.2 INTRODUCTION 99

2.3 EXPERIMENTAL 102

2.3.1 Materials 102

2.3.2 Instrumentations 103

2.3.3 Preparations of Buffer Solutions 103

2.3.4 Protein–Hapten Conjugates 105

2.3.5 Primary antibody optimization of Polyclonal Chicken Antibody (IgY) Specific to PCB 105

2.3.6 Time Optimization for Antibody Immobilisation 106

2.3.7 Influence of Blocking Solution 107

2.3.8 Secondary antibody optimization of AP Labeling 107

2.3.9 Chessboard Assay 108

2.3.10 Indirect Competitive Assay 109

2.3.11 Soil Sample Preparation 112

2.4 RESULTS AND DISCUSSION 112

2.4.1 Coating conjugate optimization of Aroclor 1254-BSA. 112

2.4.2 Primary antibody optimization of Polyclonal Chicken Antibody (IgY) Specific to PCB 113

2.4.3 Time Optimization for Antibody Immobilisation 115

2.4.4 Influence of Blocking Solution 116

2.4.5 Secondary antibody optimization of AP Labeling 119

2.4.6 Optimisation Checkerboard ELISA Assay 120

2.4.7 Control Assays 121

2.4.8 Indirect Competitive Assay 123

2.4.9 Analysis of samples 125

2.5 CONCLUSIONS 126

2.6 REFERENCES 128

CHAPTER 3 134

DEVELOPMENT AND CHARACTRISATION OF 134

ELECTROCHEMICAL IMMUNOSENSORS 134

3. ELECTROCHEMICAL DEVELOPMENT OF AN IMMUNOSENSOR FOR DETECTION POLYCHLORINATED BIPHENYLS (PCBS) FOR ENVIRONMENTAL ANALYSIS 135

3.1 ABSTRACT 135

3.2 INTRODUCTION 136

3.3 MATERIALS AND METHODS 141

3.3.1 Reagents and Chemicals 141

3.3.2 Equipment and Instrumentation 142

3.4 ELECTROCHEMICAL CHARACTERIZATION OF THE GOLD ELECTRODE 143

3.4.1 Studies on Electrode Cleaning Protocol 143

3.4.2 Studies on the Influence of Scan Rate 143

3.4.3 Stability Study of the Coated Electrodes 144

3.4.4 Cyclic Voltammetry (CV) 144

3.4.5 Impedance Measurement 145

3.4.6 Amperometric Detection 145

3.5 OPTIMIZATION OF POLYCLONAL CHICKEN ANTIBODY (IGY) SPECIFIC TO PCB. 146

3.6 OPTIMIZATION OF SECONDARY ANTIBODY AP LABELLED. 146

3.7 STUDYING THE INFLUENCE OF BLOCKING. 147

3.8 SPECIFICITY (CROSS-REACTIVITY) 148

3.9 SELF-ASSEMBLED MONOLAYERS 148

3.9.1 Modification of Gold SPE with SAM (LSV) 148

3.10 TOPOGRAPHY CHARACTERIZATION 150

3.10.1 Contact Angle Measurement 150

3.10.2 Scanning Electron Microscopy (SEM) 150

3.10.3 Atomic Force Microscopy (AFM) 150

3.11 INDIRECT COMPETITIVE ASSAY 151

3.12 REAL SAMPLE 152

3.13 RESULTS AND DISCUSSION 153

3.13.1 INFLUENCE OF ELECTRODE CLEANING PROCEDURE 153

3.13.2 INFLUENCE OF SCAN RATE 155

3.13.3 KINETIC STUDIES OF MICHAELIS-MENTEN PLOT 157

3.13.4 ELECTROCHEMICAL CHARACTERIZATION 159

3.13.4 .1 STABILITY STUDY OF THE COATED ELECTRODES 159

3.13.4.2 CYCLIC VOLTAMMETRY 161

3.13.4.3 IMPEDANCE MEASUREMENT 162

3.13.4.4 AMPEROMETRIC DETECTION 165

3.13.5 SPECIFICITY (CROSS-REACTIVITY) 167

3.13.6 OPTIMIZING THE CONCENTRATION OF PCB AB AND SECONDARY ANTIBODY: 168

3.13.7 THE IMPORTANCE OF BLOCKING SOLUTION 171

3.13.8 TOPOGRAPHY CHARACTERIZATION 172

3.13.8.1 CONTACT ANGLE MEASUREMENT 174

3.13.8.2 SCANNING ELECTRON MICROSCOPY (SEM) 175

3.13.8.3 ATOMIC FORCE MICROSCOPY (AFM) 175

3.13.9 INDIRECT COMPETITIVE ASSAY 177

3.13.10 REAL SAMPLE ANALYSIS 180

3.14 CONCLUSIONS 182

3.15 REFERENCE 184

APPENDIX 194

CHAPTER 4 196

DEVELOPMENT LABEL FREE ELECTROCHEMICAL IMMUNOSENSORS 196

4. A NOVEL LABEL-FREE ELECTROCHEMICAL IMMUNOSENSOR BASED ON A SELF-ASSEMBLED MONOLAYER-MODIFIED ELECTRODE FOR POLYCHLORINATED BIPHENYL (PCB) IN ENVIRONMENTAL ANALYSIS 197

4.1 ABSTRACT 197

4.2 INTRODUCTION 198

4.3 MATERIALS AND METHODS 202

4.3.1 Chemicals and Materials 202

4.3.2 Equipment and Instruments 202

4.4 CYCLIC VOLTAMMETRY FOR PRETREATMENT OF ELECTRODES 203

4.5 MODIFICATION OF SPG ELECTRODES 204

4.6 OPTIMIZATION OF LABEL-FREE IMMUNOASSAY 204

4.7 REAL SAMPLE ANALYSIS 205

4.8 RESULTS AND DISCUSSION 206

4.8.1 Optimization of the assay conditions 206

4.8.2 Sensitivity of the immunosensor for PCB Aroclor 1254 determination 209

4.8.3 Reproducibility and stability of the designed immunosensor 214

4.8.4 Real sample analysis 215

4.9 CONCLUSIONS 217

4.10 REFERENCES 218

CHAPTER 5 223

DEVELOPMENT OF THE QUECHERS EXTRACTION METHOD AND COMPARISON WITH (GC-MS) 223

5. DEVELOPMENT OF THE QUECHERS EXTRACTION METHOD FOR THE DETERMINATION OF POLYCHLORINATED BIPHENYLS (AROCLOR 1254) IN SOIL SAMPLES BY USING GC-MS 224

5.1 ABSTRACT 224

5.2 INTRODUCTION 226

5.3 EXPERIMENT 228

5.3.1 Instrumentation and Conditions for GC-MS 228

5.3.2 Chemicals and Instruments 229

5.3.3 Standard and Sample Solution Preparation 230
5.3.4 Extraction and Clean-Up Procedure 232
5.3.5. Method validation 233
5.4. RESULTS AND DISCUSSION 234
5.4.1. Optimization of Extraction Solvent Conditions 234
5.4.2 Optimization of Physical Extraction Condition 238
5.4.3 Method validation 242
5.4.4. ANALYSIS OF AROCLOR 1254 IN SPIKED SOIL SAMPLES (RECOVERY AND PRECISION) 244
5.5 COMPARATIVE SUMMARY OF THE DIFFERENT ASSAY PROCEDURES USED ON SPGES WITH OPTICAL AND GC-MS 248
5.6 CONCLUSION 250
5.7 REFERENCES 252
APPENDIX 259
CHAPTER 6 260
GENERAL CONCLUSIONS AND SUGGESTIONS FOR FUTURE WORK 260
6.1. CONCLUSION 261
6.2. FUTURE WORK 266
6.3 REFERENCES 270
APPENDIX A 272
A.1 Awards 272
A.2 Publications 272
A.3 Oral Presentation 273
A.4 Poster Presentation 274
A.5 Dissemination Activities 275
A.6 Modules 275
A.7 Workshops 276

List of Table and Figures

Figure 1.1 Displays the formula and structure of PCBs, with chlorine atoms replacing hydrogens in various positions on the aromatic rings [33]. 4

Figure 1.2 Sources and routes of human exposure to PCBs [38]. 5

Figure1.3 An overview of the main targets of PCBs with related disorders in humans.[38]. 10

Figure 1.4 ELISA 96 well plate is made from clear polystyrene that is suitable for optical detection. 14

Figure 1.5 The Capture assay the Primary antibody is immobilised on a surface, add blocking buffers, then add the labelled antibody, add the substrate to measure the absorbance signal. 15

Figure 1.6 Typical calibration curve of capture assay represents the direct relationship of the signal and concentration**.** 16

Figure 1.7 Sandwich assay, the capture antibody is immobilised on a surface, add blocking buffers, then add the sample containing the target antigen, add the detection antibody label conjugate, add the substrate to measure the absorbance signal. 17

Figure 1.8 Competitive assay, coating conjugate is immobilized on the surface, add blocking buffers, after addition of both the antigen and the primary antibody adding the enzyme-conjugated labelled antibody, competition occurs between the two for binding to the antibody. The addition of the enzyme's substrate leads to color development and measure the absorbance signal. 18

Figure 1.9 Typical calibration curve for competitive assay represents the inverse relationship of the signal and concentration. 19

Figure 1.10 Displacement assay, coating conjugate is immobilized on the surface, add blocking buffers, after addition of the antigen next the primary antibody adding the enzyme-conjugated labelled antibody, competition occurs between the two for binding to the antibody. The addition of the enzyme's substrate leads to color development and measure the absorbance signal. 20

Figure 1.11 Schematic of different types of biosensors. The biocomponent is immobilized on a biocompatible layer, resulting in a change of physical or chemical properties of the elements that can be detected by a measuring tool. 23
Table 1.1 key steps for biosensor design and operation..... 24
Figure 1.12 Molecular model of alkaline phosphatase (Raymond J. L.). 27
Figure 1.13 Interaction of pNPP substrate with alkaline phosphatase resulting in colour changes that can be measured at 405nm..... 28
Figure 1.14 Interaction of pAPP and alkaline phosphatase was measured by amperometric detection, which 2 electrons were generated. 29
Figure 1.15 A schematic represents a basic structural unit of an IgY, with a single Y shape [130]..... 31
Figure 1.16 Examples of antibodies-antigens arrangement for high avidity and low avidity. 32
Table 1.2 A comparison of monoclonal antibodies and polyclonal antibodies. 33
Figure 1.17 This diagram shows the three electrodes of an electrochemical cell linked to the ampere (A) and volte (V). The working electrode, reference electrode, and counter electrode are symbolised as WE RE and CE, respectively (142). 36
Figure 1.18 The Electrical Double Layer (141). 37
Figure1.19 Basic shape of the current response for a cyclic voltammetry [147]. 41
Figure 1.20 A typical curve of LSV. The slope represents the scan rate of the experiment (volts per unit time). 44
Figure 1.21 DPV waveform, showing; pulse time, tp; waiting time, tw; pulse amplitude, Ep; base potential, Es and the two points of current measurements, τ and τ'..... 45
Figure 1.22 Resulting DPV curve of change in current (i2 - i1, from points τ and τ respectively) versus the base potential..... 45
Figure 1.23 Impedance circuit (Randles model for SAM characterization of gold electrode. 47
Figure 1.24 Nyquist plot for oxidation/reduction reaction of 5 mM [Fe (CN)6]3-/4- in 0.1 M KCl (imaginary impedance versus real impedance) frequency measured from 0.1 Hz to 1 MHz, with amplitude of 0.1 V, Potential applied at +0.21V. 48
Table 1.3 Methods of biocomponent immobilisation to solid support or carrier. 52

Figure 1.25 Surface modification involving the immobillsation of SAM solution on a gold electrode, followed by activation of carbodiimide and succinimide and incubation of antibodies and antigen. 56
Table 1.4 Some selected studies on electrochemical immunosensors in environmental monitoring. Successfully developed electrochemical immunosensor for various analytical detections. 58
Figure1.26 Michaelis-Menten Plot. Km represents the analytically useful region for substrate..... 61
Table 1.5 Table of validation characteristics. 66
Figure 2.2 Schematic of chessboard titration was performed with different concentration of the BSA-Aroclor 1254 coating conjugate and the Polyclonal chicken antibody (IgY) as capture antibody. Each column 1-11 coating conjugate dilution factor. Each row A-G contains capture antibody dilution factor. column 12 and row H contains positive and negative control. 109
Figure 2.5 Capture assay was performed to optimise the concentration of BSA-Aroclor 1254 coating conjugate. 113
Figure 2.6 Calibration curve of capture assay for the optimization of PCB Polyclonal chicken antibody..... 115
Figure 2.7 Absorbance signals measured at different incubation times between the antibody and the surface of the solid. The points correspond to the average absorbance ±S.D. signal calculated for n=3 repetitions. 116
Figure 2.8 Investigates the most suitable blocking buffer to be used for indirect competitive assay. It was using this different blocking solution. Bovine serum albumin (BSA), 1% (w/v) in Tris buffer, pH 7, non-fat dried milk powder 1%(w/v) in PBS, pH 7 and Fish gelatin (1% (w/v) in PBS, pH 7 the most commonly used protein blockers are BSA and was given good result. 118
Figure 2.9 Optimization of blocking buffer use different blocking buffer percentages of BSA blocking at 1% of BSA, 2% OF BSA and 3% OF BSA and the obtain result it was no big difference between the three of them. 118
Figure 2.10 Optimization of antibody dilution for detection. In the case of the antibody, the immobilization time was 60 minutes. The dilution points correspond to the average absorbance ± S.D. signal calculated for n=3 repetitions. 119

Figure 2.11 3D chessboard capture ELISA was carried out with different concentrations of BSA- Aroclor 1254 coating conjugate and PCB polyclonal antibody. 121

Figure 2.13 Competitive assay for Aroclor 1254 measured after the exposure to the pNPP. 124

Figure 3.1 Structure of Arcolor 1254. 138

..... 140

Figure 3.2 The graphic depicts the synthesis of SAM from 11-MUA on a gold electrode in combination with antibody immobilization. 140

Figure 3.3 The steps involved in the formation of self-assembled monolayers on the gold electrode. 149

Figure 3.4 Studies on different chip-cleaning procedures. CV was scanned in mM [Fe (CN)6]$^{3-/4-}$ redox coupled with a 50 mV/s scan rate. 150

Table 3.1 The values of peak-to-peak separation using different cleaning protocols**.** 155

Figure 3.5 Influence of the scan rates on the CV signals measured in 5 mM {Fe (CN)6}$^{3-/-4}$ in 1 M KCl. The potential applied was from - 0.2 to 0.6 V. 156

Table 3.2 Influence of the scan rate on the half-peak potential and the peak current for the oxidation component of the process. The scan rates studied were 5 mv/s, 10 mv/s, 20 mv/s, 50 Mv/s, 70 mv/s, 100 mv/s, 150 mv/s, and 200 mv/s. 157

Figure 3.6 Michaelis-Menten plot for different concentration of the substrate pAPP. 158

Figure 3.7 Electrochemical characterization of modified electrode. **(A)** A stability study of the coated BSA-Aroclor 1254 on a gold electrode surface was performed using linear sweep voltammetry. Prior to the measurements, the coated electrode was stored at 4 ◦C. Three electrodes were measured every day for 10 days. 160

Figure 3.7 (B) The voltammogram of CV for the bare gold electrode and the gold electrode after SAM modification with 11-MUA. 161

Figure 3.7 (C) Impedance spectra of the bare gold electrode,after 20 h SAM, activation with EDC/NHS and immobilization with 5 µg/mL−1 BSA-Aroclor 1254. The redox couple was 5 Mm [Fe (CN)6]3−/4− in 0.1 KCl. Frequency measured from 0.1 Hz to 1 MHz, with amplitude of 0.1 V, potential applied at 0.21 V. The inserted circuit is

Randle's equivalent, where Rs represents the dynamic solution resistance, Rct represents the charge transfer resistance of the immobilize recognition layer, CdI indicates the capacitance measured between the gold electrode and the electrolyte solution on a double layer basis, and Zw is the Warburg element describing the time frequency..... 164

Figure 3.7 (D) Amperometric detection of a chip modified AP containing bilayer (competitive assay) was measured in DEA buffer pH 9.5 at potential of 0.45 V vs. Ag/AgCl. The substrate pAPP was injected at 40 s..... 166

Table 3.3 Parameter evaluation for the Randle's model on a gold electrode. 163

Table 3.4 The cross-reactivities of the antibody against Aroclor 1254 and other Aroclor using competitive assay..... 168

Figure 3.8 (A) Optimized concentration of Polyclonal Chicken antibody (IgY) specific to PCB (primary antibody) using capture assay. Detection was LSV (n=3). The optimized concentration of PCB was 0.123 µg/ml..... 170

Figure 3.8 (B) show that a dilution of 1/5000 Goat anti-chicken IgY gave a large current signal without a significant amount of nonspecific and hence this dilution was used for all further assays..... 170

Figure 3.9 The influence of blocking step. The capture assay was carried out using AP labelled**.**..... 171

Figure 3.10 Typical topography of the bare electrode surfaces of gold SPE and modified with SAM. Contact angle graphs of bare electrode (A) and SAM-modified electrode (B); SEM micrographs of bare electrode (C) and 11MUA-SAM-modified electrode (D); top cross-section (×100 magnification); AFM micrographs (E) bare Au, (F) 11-MUA SAM (20 h), (G) EDC/NHS (1 h), (H) BSA-Aroclor 1254 coating conjugate. 174

Table 3.5 The water contact angle of gold electrodes is treated with thiol SAM. ... 175

Table 3.6 Surface roughness and particle diameters of bare and modified gold electrodes..... 176

Figure 3.11 A competitive assay was conducted in which the performance of the gold electrode modified with 11-MUA was compared with the assay performance using (a) a bare gold electrode and (b) SAM modification gold electrode. 178

Table 3.7 Comparison with previously reported electrochemical PCB immunosensors with present work. 179
Table 3.8 MUA-SAM/EDC/NHS/SPGE and ELISA (immunoassay) for the determination of Aroclor 1254 in environmental samples. 181
Figure A.1 Nyquist plot: influence of SAM immobilization time on gold electrode using 5 mM 11-MUA. 194
Figure 4.1 Functionalization steps of PCB immunoassay on SPGE, reprinted from reference [31]. 201
Figure 4.2 Metrohm DropSens, gold screen-printed electrode. 203
Figure 4.3 (A) Optimized concentration of PCB-BSA conjugate using capture assay. Detection was DPV (n=3). The optimized concentration of the PCB-BSA conjugate was 5 µg/ml. 207
Figure 4.3 (B) Optimized concentration of PCB using capture assay. Detection was DPV (n=3). The optimized concentration of PCB was 0.246 µg/ml, which is less than the optical, that was 0.465 µg/ml. 208
Figure 4.3 (C) Competition time for immunosensor response. Detection was DPV (n=3). 209
Figure 4.4 (A) Differential pulse voltammetry (DPV) responses the designed immunosensor to Aroclor 1254 concentrations(a) 0.011 ng/mL, (b) 0.033 ng/mL, (c) 0.101 ng/mL, (d) 0.304 ng/mL, (e) 0.91 ng/mL, (f) 2.7 ng/mL, (g) 8.2 ng/mL, (h) 25 ng/mL, (i) 74 ng/mL, and (j) 220 ng/mL.). **(B)** Plot of DPV current with respect to logarithms of different Aroclor 1254 concentrations. **(C)** EIS spectra for $[Fe(CN)6]^{3-/4-}$ after the binding of Aroclor 1254 at the immunosensor probe with different concentrations (a-j). **(D)** Plot of EIS the corresponding calibration obtained from EIS responses with respect to logarithms of different Aroclor 1254 concentrations. **(E)** The Bode impedance plots log of frequency vs. Magnitude Z(ohm). 213
Table 4.1 Performances of diverse electrochemical detection. 214
Figure 4.5 The stability of Aroclor 1254 detection by the immunosensor in 30 days. 215
Table 4.2 SPGE electrochemical and ELISA (immunoassay) approaches for the determination of Aroclor 1254 in soil samples (n=3). 216
Figure 5.1 Graphical Abstract. 226

Figure 5.2 Agilent 6890/5973 gas chromatography-mass Spectrometry (GC-MS) instrument. 229
Figure 5.3 Schematic illustration of the modified QuEChERS extraction method. .. 233
Figure 5.4 (a) The effect of water addition on extraction efficiency for the target Aroclor 1254 at 10 ng/ml. 236
..... 237
Figure 5.4 (b) The effect of acetonitrile and hexane as extraction solvents for the target Aroclor 1254 at 5 ng/mL and 10 ng/mL (n = 3). 237
Figure 5.4 (c) The effects of different solvent volumes for the target Aroclor 1254 at 10 ng/mL (n = 3). 237
Figure 5.5 (A) Effect of shaking: 4 min, 15 mL of acetonitrile/water (75%: 25%, v/v), 5 g of soil, 4 g MgSO4, 1 NaCl. 240
Figure 5.5(B) Effect of speed: 10 min, 15 mL of acetonitrile/water (75%: 25%, v/v), 5 grams of soil, 4 grams MgSO4, 1 NaCl. 240
Figure 5.5 (C) Effect of centrifuge time: 4500 rpm, 15 mL of acetonitrile/water (75%: 25%, v/v), 5 g of soil, 4 g MgSO4, 1 NaCl. 241
Figure 5.5 (D) Comparison of recovery rates for different sorbents in the QuEChERS extraction method (n = 3) The conditions for the experiment were: 5 grams of soil, 15 mL of acetonitrile/water (75%: 25%, v/v), 4 grams of MgSO4, 1 gram of NaCl, 4500 rpm. 241
Figure 5.6 (a) GC analysis for the blank sample. (b) GC-MS calibration curve for standard Aroclor 1254. 243
Figure 5.7 (a) GC/MS Total ion chromatogram of Aroclor 1254 (red line) and the blank (black line) for 10 µg /kg soil sample after QuEChERS extraction. (b) GC/MS Total ion chromatogram of Aroclor 1254 (red line) and the blank (black line) for 5 µg /kg soil sample after QuEChERS extraction. 246
Table 5.1 Comparison of the present study with other studies. For the present work recovery and RSD was included at different Aroclor 1254 concentrations in soil samples (n=3). 247
Table 5.2 Comparison of optical and electrochemical immunosensors performance with GC-MS. 249

Figure 6.1 Schematic view of analytical methods over various electrochemical methods for SMX detection towards nanomaterial interfacial aspects [4]. 266
Figure 6.2 Summary of microfluidics, such as substrates materials, fabrication technologies, detection method and types of microfluidics [7]. 267
Figure 6.3 Applications of smartphone-based wireless electrochemical sensors. .. 268

Acknowledgement

All thanks to ALLAH, for all the blessings. He has bestowed on me. Without his blessings, this achievement would not have been possible.

First, I would like to thank the Ministry of Higher Education of Saudi Arabia for the financial support. Without their sponsorship and support, I would not have had this opportunity. I would like to thank my supervisor, Dr. Eric Moore, for his tremendous guidance, support, and encouragement. Thanks to his kind and humble nature, this significantly impacted my research journey. During challenging times, his encouragement motivated me to persevere and overcome obstacles. His positive attitude and belief in my abilities have instilled confidence in me. I would like to take this opportunity to thank you for making such a positive impact on my life. I appreciate your concern and useful advice. I will be forever grateful to you. I consider myself fortunate to have worked under his supervision.

On the other hand, during my journey from 2019 to 2023 the COVID-19 pandemic has had a significant impact on every aspect of our lives, and the research for this thesis was not immune to its effects. The pandemic caused many delays, interruptions, and challenges in the data collection and analysis process. However, these pandemic taught men how to adapt to unexpected circumstances. I got support from my family, friends, and colleagues during this time.

Secondly, the last five years at Tyndall and University College Cork, UCC have been fulfilling for me, and I have had the opportunity to increase my network of professional individuals. Today, I am grateful to all the people I met who made my life and work interesting and enjoyable through sharing their knowledge and perspectives. I would also like to thank the many friends I have made here. I would

like to thank all the people who in one way or another have been with me, supported me, and worked with me during the five years during which this thesis was completed. I would like to thank Eileen Hurley, leader of the Life Science Interface Laboratory for the wonderful help - thank you for being there for me when I really needed you. A special thanks to Dr Anna Hogan from the School of Chemistry in UCC for the help with GC-MS and different techniques measurements. Thanks also to my colleagues in the Sensing and Separation group for being reliable and supportive people. Ibtihaj Albalawi, Hanan Alatawi, Justina Ugwah, Edel Whelton, Niamh O'Mahoney, Emma O'Sullivan and Yineng wang, you are my second family here, please accept my thanks for everything that you've done to help me. Words cannot express how grateful I am for your kindness. You are wonderful friends, and I appreciate your love, support, and generosity.

Thirdly, a special thanks to my friends Dr. Shifa Felemban, Dr. Thanih Balbaied and Dr. Areej Alyami who supported me whenever I needed it. Provided me with advice and guided me to become a better researcher. Supporting me during my challenging times and pushing me when I need motivation. You cannot imagine how much strength your support gave me during those difficulties. You all shared with me unforgettable moments during the PhD. My life would not be the same without you and I am grateful to have you as friends. Love you all.

Finally, my deepest gratitude goes to my entire family, to whom this thesis is dedicated. I owe everything to my parents who encouraged and helped me at every stage of my personal and academic life, especially my mum, who continuously supported me over the past four years by raising and nurturing my children. Mum, a day would not go by without you checking on me, encouraging me, and pushing me

forward to complete this journey. Without your support this achievement would not have been possible. I owe a debt of gratitude to my son Ahmed and my daughter Tulin. Thank you for being patient, mature and believing in me as I know 4 years is not a fleeting time being away from you. Thanks for all your prayers and for your unconditional love that you sent to me across the sea. My apologies for missing most of your childhood, but now that this academic journey has ended, we can look forward to making beautiful memories together in the future. You are my angels and all my life; I will be grateful to you. I consider myself the luckiest person in the world to have such a lovely and caring family standing beside me with their love and unconditional support.

Last but not least, thanks to God.

It is time to go back home; my kids are waiting for me.

“It always seems impossible until it’s done.”

– Nelson Mandela

Declaration

This is to certify that the work I am submitting is my own and has not been submitted for another degree, either at University College Cork or elsewhere. All external references and sources are clearly acknowledged and identified within the contents. I have read and understood the regulations of University College Cork concerning plagiarism and intellectual property.

Samia Alsefri

Abbreviations

ΔEp	peak-to-peak separation
11-MUA	11-mercaptoundecanoic acid
ACN	acetonitrile
AFM	atomic force microscopy
Ag/AgCl	silver/silver chloride
AP	alkaline phosphatase
Au	gold
BSA	bovine serum albumin
CV	cyclic voltammetry
DEA	diethanolamine
DMOS	dimethyl dulfoxide
DPV	Differential Pulse Voltammetry
EDC	1-Ethyl-3-(3-(dimethylamino)-propyl) carbodiimide
EIS	electrochemical impedance spectroscopy
ELISA	enzyme-linked immunosorbent assay
GC-MS	Gas Chromatography-Mass Spectrometry
HPLC	high performance liquid chromatography

Hz	hertz
IC50	half maximal inhibitory concentration
K3Fe (CN)6	potassium ferricyanide
K4Fe (CN)6	potassium ferrocyanide
KCl	potassium chloride
LOD	limit of detection
LR	linear Range
LSV	linear sweep voltammetry
MeOH	methanol
NaCl	sodium chloride
NaCNBH4	sodium cyanoborohydride
NaOH	sodium hydroxide
NHS	N-hydroxy succinimide
OD	Optical Density
PAb	polyclonal antibodies
pAPP	p-aminophenyl phosphate
PBS	Phosphate-buffered saline
PCB	polychlorinated biphenyls
pNPP	p-nitrophenyl phosphate

R_{ct}	charge transfer resistance
R_s	solution resistance
SAM	self-assembled monolayer
SEM	scanning electron microscopy.
SPGE	screen-printed gold electrodes
TRIS	tris(hydroxyl methyl)aminomethane

Abstract

Polychlorinated biphenyls, PCBs are a type of chemical contaminant known as persistent organic pollutants (POPs). They consist of biphenyl molecules covalently bonded with one to ten chlorine atoms. PCBs pose a threat to ecosystems and food safety due to their high toxicity, long-term stability, poor degradation, and bioaccumulation. The current methods, although sensitive, have their limitations, for example, time-consuming, laborious, and costly. Further, the instrumentation cannot be used for on-site analysis.

The aim of this research is to develop a novel electrochemical method that will be capable of providing a direct, portable, cost-effective, and easy method for analysing and monitoring PCBs in the environment. For the first time, a self-assembled monolayer was used to modify an electrode as a method for fabricating a transducer for detection of PCBs by using a gold electrode, it was modified with 11-mercaptoundecanoic acid (11-MUA), and the activation of the carboxylic acid terminal was performed by cross-linking 1-ethyl-3-(3-dimethylaminopropyl) carbodiimide (EDC) and N-hyrodsuccinmide (NHS). The electrochemical behaviour of the electrode was investigated by CV (Cyclic Voltammetry), LSV (Linear Sweep Voltammetry) and EIS (Electrochemical Impedance Spectroscopy) using a ferrocyanide/ferricyanide redox pair. It was found that the indirect competitive assay showed the best performance for Aroclor1254 detection, with a commercial Polyclonal chicken antibody (IgY) specific to PCB was used as primary antibody. The limit of detection was found at 0.20 ng/ml using bare gold electrode. However, the sensitivity of the sensor was increased after the electrode surface modification was found at 0.09 ng/ml. A novel electrochemical immunosensor method showed a good performance with a 3-fold decrease in sensitivity achieved after the surface modification. The electrode coated with coating conjugate was found stable for more than 25 days at 4 ˚C.

In conclusion, this Ph.D. thesis demonstrates that the integration of electrochemical techniques with immunoassay methods can achieve detection limits as low as required for in-situ and real-time analysis of soil samples. It was found that the electrochemical immunosensor method showed better results compared to ELISA and that was verified with GC-MS. The usage of this a novel electrochemical immunosensor as a complement to the electrochemical studies not only enhanced the quality of the research but also contributed to the construction and improvement of immunosensors. As a result, they represent an accurate and a new robust method that can be applied to microsensors and microfluidic systems for the effective control and prevention of PCBs in the environment.

Research Problem

The presence of PCBs is still a significant problem for the environment, since they are easily detectable at high levels [1]. Consequently, in addition to reducing and/or removing the number of their toxic discharges into the environment, it is still necessary to develop techniques and methods for detecting and monitoring these hazardous pollutants in a cost-effective, sensitive, and selective manner to enable effective remediation to take place. As a result of their widespread usage in the past, PCBs have a significant environmental threat and pose a health risk [2,3]. Additionally, Babacar Ngom, emphasized that there is a high demand for rapid, sensitive, and accurate methods of detection of biological and chemical contaminants [4] . Traditional methods for detecting biological contaminants are time-consuming and expensive despite their sensitivity, while methods for detecting chemical contaminants rely on expensive and complex instrumentation with the same level of accuracy and specificity, hindering processors from taking immediate corrective measures when contaminants are detected [5].

As a result, the development of portable, rapid, sensitive, and selective immunosensor technologies that can overcome the discussed analytical constraints is of crucial importance [6,7] .They are less expensive and can also be widely available for screening PCBs and other pollutants of concern. Immunosensor technology is known for its high performance and high sample throughput, with a significant reduction in analysis time [8]. Specifically, these techniques are suitable for continuous, rapid, and in-situ screening of environmental pollutants. Numerous techniques based on immunochemistry have been created to determine the

interactions between antibodies and antigens (Ab-Ag) and are currently being studied by researchers. Among these methods are electrochemical detection techniques, including amperometry and voltammetry [9] as well as potentiometry [10]. Additionally, other methods such as optical and piezoelectric methodologies, have been described [11].

Several analytical techniques and methods have been developed to analyze PCBs, including non-portable laboratory bench-based analysis such as gas chromatography (GC) with electron capture detector (ECD), mass selective detector (MSD) and mass spectrometry (MS). Although these methods are accurate, sensitive, and reliable, they can be tedious, expensive, and require large volumes of toxic solvents, making them unsuitable for large-scale continuous PCB screening [12,13]. Therefore, it is important to develop cost-effective, easy-to-use, and equally sensitive, selective, and accurate detection techniques. This research focuses on the development of a label-free, reagent-less electrochemical immunosensor based on self-assembled monolayer-modified electrodes, which enhance the sensor's sensitivity and selectivity. It is expected that this immunosensor will eliminate the need for labeling procedures and reduce the experimental timeframes and high level of expertise required for conventional methods. Considering the analytical constraints, the following research questions were formulated.

Key Research Questions

The fabrication of an immunosensor requires the use of a transducer and biological material which is immobilized on the transducer. The following are the key research questions from this thesis:

- Can a robust method be developed that can easily be adopted for on-site analysis?
- Can the limit of detection be improved on of sensitivity for detections of PCBs in soil?
- Is it possible to develop a portable electrochemical immunosensor for on-site detection of PCBs in the environment?

The purpose of this study is to determine the optimum conditions for the efficient use of the developed PCBs method. In addition, the method will be evaluated for reliability, reproducibility, and validity. With these questions in mind, the following objectives were set.

Aims and Objectives.

The major objective for this research is to develop a novel device that can be easily used besides its portability for the determination of polychlorinated biphenyls (PCBs) in the environment, mainly focusing on soil samples. Voltametric detection with screen-printed electrode allows simple instrumentation and could be used as a small portable device for field measurements. In this research, for the first time, we developed a novel electrochemical immunosensor based on a self-assembled monolayer-modified electrode that can be used for monitoring and detecting of Polychlorinated Biphenyl (PCB) in environmental analysis as an alternative method to

the costly, time-consuming, and high expertise-requiring methods. This can be achieved through the following objectives:

1. To optimize various conditions and regents that is viable for PCBs detection and quantification by applying ELISA method. This technique allows for the screening of multiple samples, and analysis can be completed reasonably quickly.

2. To develop electrochemical immunosensors by integrating immunoassay into SPGE, optimizing for rapid and precise detection through modification of the electrode with self-assembled monolayer, optimizing conditions for antibody immobilization, and evaluating antibody compatibility with the transducer.

3. To integrate the label electrochemical immunosensors method to label free electrochemical immunosensors with the purpose of increasing the sensitivity and reducing the assay time.

4. To validate the performance of the optimised immunosensors compared to other alternative detection devices.

Develop an electrochemical immunosensor, using Voltametric detection with the screen-printed electrode allows simple instrumentation and could be used as a small portable device for field measurements.

Thesis Outline

The thesis is divided into six chapters. Following the introduction, the further chapters in this thesis are divided as follows:

Chapter 1

Provides a general introduction about the analyte of interest, the PCBs, all the fundamental concepts and principles of immunoassay including formats of ELISA, method immobilisation and the enzymes substrate reaction. Further discusses the electrochemistry development including the electrochemical cell, the electrochemical techniques, and the classification of electrochemical immunosensors that are used in this research. A review of previously published work on electrochemical sensors for environmental analysis is summarized.

Chapter 2

In the first paper, an optical immunosensor using a 96-well microtiter plate as a solid surface has been developed. A polyclonal chicken antibody (IgY) specific to PCB antibody was obtained, under the optimal combination of coating antigen and antibody. A sensitive indirect competitive enzyme-linked immunosorbent assay (icELISA) has been developed to measure Aroclor1254 in environmental samples. Several experimental parameters have been optimized, including coating conjugates, the concentration of antibodies, incubation time, types of blocking solution and different reagents have been optimized. The results obtained based on the ELISA were used to integrate the immunoassay methods to develop electrochemical immunosensors in the next chapter.

The paper that makes up this chapter is titled "**The development of optical immunosensors based on indirect competitive enzyme-linked immunosorbent assay methods for detection of Aroclor1254 in environmental samples**" The paper is currently being **Under review** for publication in journal of the Royal Society of Chemistry.

Chapter 3

In the second paper, the article discusses the development of an electrochemical immunosensor for detecting Aroclor 1254. The immunosensor was developed by immobilizing polyclonal primary anti-PCB antibodies onto a gold screen-printed electrode that was modified with 11-mercaptoundecanoic acid (11-MUA). The carboxylic acid terminal of the electrode was activated using cross-linking 1-ethyl-3-(3-dimethylaminopropyl) carbodiimide (EDC) and N-hydroxysuccinimide (NHS). Characterization of the self-assembled monolayers (SAM) development on the gold electrode was carried out using various techniques such as cyclic voltammetry (CV), electrochemical impedance spectroscopy (EIS), atomic force microscopy (AFM), scanning electron microscopy (SEM), and contact angle measurement. Potentially offer rapid sample screening in a portable, disposable format, which was used for integrating the novel electrochemical immunosensors and could contribute to the effective control and prevention of PCBs in the environment. This chapter has been published in a peer reviewed journal with title paper that makes up this chapter is titled" **Electrochemical Development of an Immunosensor for Detection Polychlorinated biphenyls (PCBs) for Environmental Analysis.**"

Chemosensors 2021, 9(11),307; https://doi.org/10.3390/chemosensors9110307

Chapter 4

This chapter presents a novel label-free electrochemical immunosensor for the detection of PCBs. The immunosensor is based on a self-assembled monolayer-modified electrode and uses a PCB-BSA conjugate to compete with free PCBs for binding to the anti-PCB polyclonal primary antibody (IgY). A secondary antibody is then used to enhance the sensor's sensitivity for the detection of PCBs in a sample. The immunosensor is immobilized on an 11-mercaptoundecanoic acid (11-MUA)-modified gold electrode via a carbodiimide-coupling reaction using cross-linking 1-ethyl-3-(3-dimethylaminopropyl) carbodiimide (EDC) and N-hydroxysuccinimide (NHS) on the electrode surface. The developed immunosensor shows good linearity in ng/mL and limit of detection (LOD) of 0.11 ng/ml for PCBs detection, making it a cost-effective and sensitive solution for sample screening. This label-free electrochemical immunosensor has potential for real-time monitoring of PCBs in soil samples or other samples, as it is portable and disposable. The chapter has been published in a peer reviewed journal with the title" **A Novel Label-Free Electrochemical Immunosensor Based on a Self-Assembled Monolayer-Modified Electrode for Polychlorinated Biphenyl (PCB) in Environmental Analysis**".

Electrochem 2022, 3(3), 451-462; https://doi.org/10.3390/electrochem3030031

Chapter 5

In the fourth paper, The QuEChERS extraction method and gas chromatography with mass spectrometry were used for the development of an analytical method to detect polychlorinated biphenyls (PCBs) in soil samples. The study optimized various parameters such as shaking, centrifuging time, type of solvent, and clean-up adsorbents. The best results were obtained with acetonitrile/water as the extraction solvent and diatomaceous earth as the dispersive solid-phase extraction sorbent. The method was shown to be simple, sensitive, efficient, and environmentally friendly. The approach based on QuEChERS for the determination of Aroclor 1254 in soil has not been published before, and it is believed that this approach will eliminate the significant challenge of sample extraction in GC-MS processing, which was a procedural challenge in previous analyses. GC-MS results were compared to results obtained from immunoassays (ELISAs) and electrochemical immunosensors. This chapter has been published in a peer reviewed journal with title titled" **Development of the QuEChERS Extraction Method for the Determination of Polychlorinated Biphenyls (Aroclor 1254) in Soil Samples by Using GC-MS**".

Separations 2023, 10(4), 250; https://doi.org/10.3390/separations10040250

Chapter 6

The novel research and development which was detailed in chapters 2 to 5 were summarised. Suggestions and some ideas were given for better improvement for future research. Finally, the publications and oral and poster presentation given while doing the thesis was arranged in the appendix.

CHAPTER 1

General Introduction

1. General Introduction

1.1 Motivation

PCBs are persistent organic pollutants manufactured domestically 80 years ago. But, since 1945, they have been used in a wide range of industries and commerce, including electrical, heat transfer, hydraulic, and plasticizers in paint, plastics, and rubber. PCBs exposure was associated with increased blood PCB concentrations in individuals working in PCB-contaminated workplaces due to repetitive risks and significant correlations with PCB exposure. Though banned since the 1970's in many countries, they can still be found in the workplace and the environment. One of the main characteristics attributed to the usefulness of PCBs and their harmfulness is their high thermal and chemical resistance. Their stability makes them able to stay in the environment for a long time after they are emitted, which makes them easily bio accumulable. This is because they do not readily break down when heated or treated with chemicals. Over the past few decades, PCBs have received increasing attention and awareness because they can cause skin conditions, liver damage, reproductive disorders, immune system dysfunction, and cancer. PCBs can be found in soils and water, which makes it necessary to track their spread as they move. For this reason, we need developed sensing devices that provide a direct, portable, cost-effective, and easy method for detecting and monitoring PCBs.

1.2 Polychlorinated Biphenyls (PCBs)

Polychlorinated biphenyls (PCBs) are a type of organic compounds that consist of biphenyl with one to ten chlorine atoms attached covalently [14–17]. The structure of these compounds includes two aromatic rings with 1 to 10 chlorine atoms, as shown in Figure 1.1. The Stockholm Convention on Persistent Organic Pollutants has enlisted numerous POPs, which include chlorinated (and brominated) aromatics like polychlorinated biphenyls (PCBs) [18–20]. PCBs appear as oily liquids or solids, ranging from colorless to light yellow, and have no smell or taste. They are one of the 12 categories of persistent organic pollutants (POPs) and comprise 209 PCB congeners [21–23]. These congeners exhibit significant structural variability, resulting in differences in their chemical and physical characteristics, including persistence and bioaccumulation. Based on the number of chlorine atoms, congeners with four or fewer chlorine substituents are classified as low-chlorine PCBs, while those with more than four chlorine atoms are classified as high-chlorine PCBs [24,25]. These chemicals have a harmful impact on the environment and all living organisms, and pose a significant risk to human health [26,27].

PCBs mostly exist as mixtures of congeners, with the commonest commercial mixtures being called Aroclors. The number attached after Aroclor compounds is reflect the percentage of chlorine in the mixture, e.g., Aroclor 1254 is 54 % chlorine by weight, with more highly chlorinated mixtures typically being more persistent and toxic [28]. PCB mixtures are resistant to extreme temperatures and pressures, making them useful in a variety of industrial and commercial applications, including as dielectric fluids, heat exchange liquids, inks, plasticizers, and transformers [29].

Despite the ban of PCB manufacture and use in most countries in the late 70's and early 80's due to their toxicity and potential harm to human health, they continue to be slowly and continuously released into the environment from old equipment and waste dumps. As a result, they can still be found in environmental matrices such as air, soil, sediment, and wastewater [30,31]. Furthermore, these PCBs are easily absorption by microplastics, which act as vectors for these organic contaminants, facilitating their dispersion in a variety of environmental compartments. Due to their physical and chemical stability, the degradation behavior of PCBs has received significant attention in recent years [32]. Therefore, it is crucial to develop highly selective, robust, and reusable assays to detect trace amounts of PCB residues, particularly the most toxic PCB species in environmental samples with a complex matrix. On the other hand, the widespread use of PCBs can cause issues in soil, aquatic environments, air, and even in the human body. The monitoring of PCBs in environmental samples is therefore essential for the identification and control of contaminated areas.

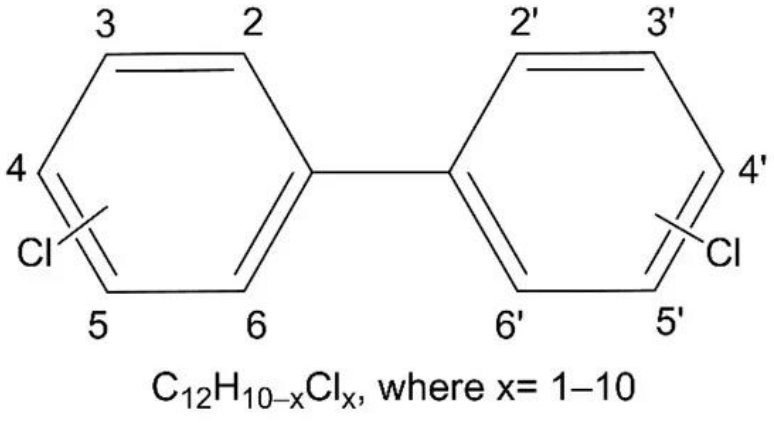


Figure 1.1 Displays the formula and structure of PCBs, with chlorine atoms replacing hydrogens in various positions on the aromatic rings [33].

1.2.1 Origin, Occurrence and Exposure of PCBs

Since PCBs are widely present in the environment, it is likely that everyone has been exposed to them. PCB contamination may pose a higher risk to those who live near hazardous waste sites. These chemicals can enter the body through contaminated food, inhalation, or skin contact. The body absorbs PCBs readily, and they tend to accumulate in fatty tissue. Due to their poor elimination, PCBs can build up in the body over time [33–37]. Figure 1.2 shows the main routes for PCB release into the environment and the relative human exposure routes.

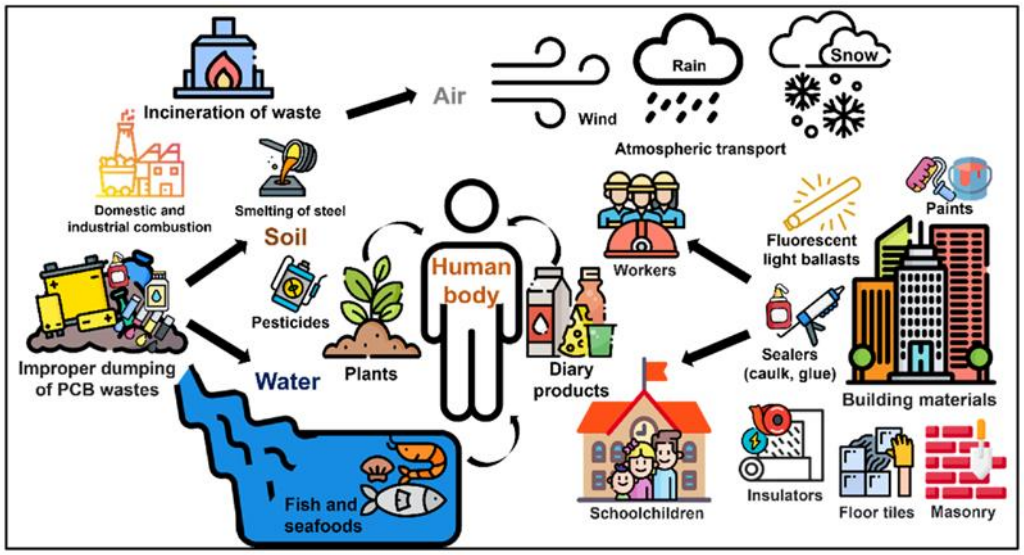


Figure 1.2 Sources and routes of human exposure to PCBs [38].

Over the past few decades, PCBs have been widely used in a variety of industries. They are released during industrial processes such as smelting and cooking, as well as during the combustion of coal, wood, crude oil, gasoline, and diesel fuel [39,40]. The presence of PCBs in the atmosphere has been detected at high levels in industrial areas, which are primarily produced unintentionally [41].

Old appliances like refrigerators and toaster ovens over 30 years old may leak PCBs, which can be inhaled or absorbed through the skin. Exposure can also occur through contaminated food, hazardous waste sites, workplace accidents, and disposal of PCBs [42,43]. Contaminated soil and dust can lead to ingestion or inhalation of PCBs, and tilling dry soil can result in ingestion of small amounts. PCBs stored in a mother's body can cross the placenta and affect unborn babies, and they are excreted in breast milk, posing a risk for babies [3,44,45].

PCBs are commonly found in contaminated fish, meat, and dairy products, with bottom-feeding freshwater fish like catfish, buffalo, and carp having the highest levels. PCBs are usually not found in high amounts in grazing animals and dairy products as plants take up only small amounts of PCBs from the soil. Small amounts of PCBs may also be found on the outer surfaces of fruits and vegetables due to contaminated dust [46,47].

Since PCBs are not easily dissolved in water, exposure through water is usually not a concern. Nevertheless, some private wells using old submersible pumps containing PCB oil may become contaminated if the pump seal fails. People do not come into contact with PCBs in surface waters unless they come into contact with contaminated sediments [48,49].

A PCB transformer or ballast may be found in old fluorescent lights in schools, offices, and homes. It is possible for PCBs to leak from these ballasts and contaminate exposed surfaces and the air if they fail. PCB levels can be measured in the air after light ballast failure [50,51].

PCBs can also be a potential source of exposure in the workplace, with industrial accidents being the primary cause of PCB poisoning in humans. Occupations such as firefighting and hazardous waste cleanup in response to electrical system fires and accidents are vulnerable to PCB exposure [3,52].

Therefore , it is important to create sample preparation techniques that are simple and effective for selectively enriching ultra-trace levels of PCBs prior to accurate detection [53].

1.2.1.1 Environment Pollution of (PCBs)

Due to point source releases, PCBs do not occur naturally in the environment, they are man-made chemicals which they are produced through a chemical synthesis process in which chlorine atoms are substituted for some of the hydrogen atoms on biphenyl molecules. The release of PCBs into the environment is caused by spills, leaks from electrical and other equipment, as well as improper disposal and storage of PCBs. More than half of the PCBs produced have been released into the environment [54–58]. PCBs can be transported long distances and bind strongly to soil and sediment, so they tend to remain in the environment for a prolonged period and for most of its congeners, the half-life ranges from months to years [14]. A significant amount of PCBs leach from soil slowly, particularly the more highly chlorinated congeners, and translocate to plants via soil in an insignificant amount. The presence of these agents has been detected in the air, water, soil, and sediments all over the world [59].

There are different levels of PCBs acceptable in soil, depending on the country and the intended use. As part of the EU's Waste Framework Directive (2008/98/EC) and the Persistent Organic Pollutants Regulation (Regulation (EC) No 850/2004), maximum limits for PCBs in soil are based on the land's intended use. In the EU maximum limit for PCBs in agricultural or residential soils and industrial soils is 20 mg/kg (milligrams per kilogram) is 50 mg/kg respectively.

PCBs are long-lasting in the environment before breaking down and they may enter the food chain. It is possible to find low levels of PCBs in fish, shellfish, meat, poultry, milk, dairy products, and other foods [60]. Because PCBs are widely distributed in the environment, the public may be exposed to them through soil/dust, air, water, or food residues.

1.2.1.2 Health Effect of PCBs

PCBs pose serious health risks to humans via three main exposure routes: oral ingestion, inhalation, and dermal absorption. For adults, dietary consumption is the primary source of exposure. However, inhalation poses a higher carcinogenic risk, particularly in children [61]. Furthermore, the persistent nature of PCBs in the environment can lead to adverse health effects in humans and animals. As a result, improving PCB detection methods is crucial for the global environment [32,62,63]. As a result of their oncogenic effects, PCBs were classified by the International Agency for Research on Cancer in 2015 as a Group 1 carcinogen as a major toxicological concern worldwide [64,65]. Different types of cancer have been linked to PCB exposure, including thyroid, testicular, prostate, breast, non-hodgkin's lymphoma, and colorectal cancer [66,67]. PCB exposure increases the risk of cancer by 20 % in

men. Women with breast cancer are more likely to develop aggressive cancers and metastatic disease after exposure to PCBs [68–71].

The presence of PCBs is associated with both carcinogenic risk and metabolic disease [72,73]. Exposure to PCBs may lead to insulin resistance, which increases the risk of metabolic disorders. Studies have shown that plasma PCB levels are related to cardiovascular disease risk factors such as hypertension, type 2 diabetes, obesity, and dyslipidemia [74,75]. Furthermore, PCBs are endocrine-disrupting substances, causing cancer in mammals as well as damage to the reproductive system, immune system, stomach, skin, liver, and other organs [33].

People who have been exposed to PCBs for an extended period are more likely to suffer from skin conditions, such as acne and rashes. There has been evidence that workers exposed to elevated levels of PCB suffer from liver damage. According to some studies, workers exposed to PCBs may experience nose and lung irritation, gastrointestinal discomfort, depression, and fatigue. PCBs may cause cancer in humans, according to the US Environmental Protection Agency and the WHO International Agency for Research on Cancer [76,77].

The behaviors of children such as crawling on bare dirt surfaces, eating soil, and frequent hand-to-mouth activities make them particularly susceptible to PCB exposure. Breast milk can also contain PCBs, which may be passed on to infants. Several studies have demonstrated that children exposed to PCBs may exhibit abnormal immune responses as well as problems with motor skills and short-term memory [15,20,78]. Certain cancers have been observed in groups of workers who have been exposed to elevated levels of PCBs (as well as other chemicals).

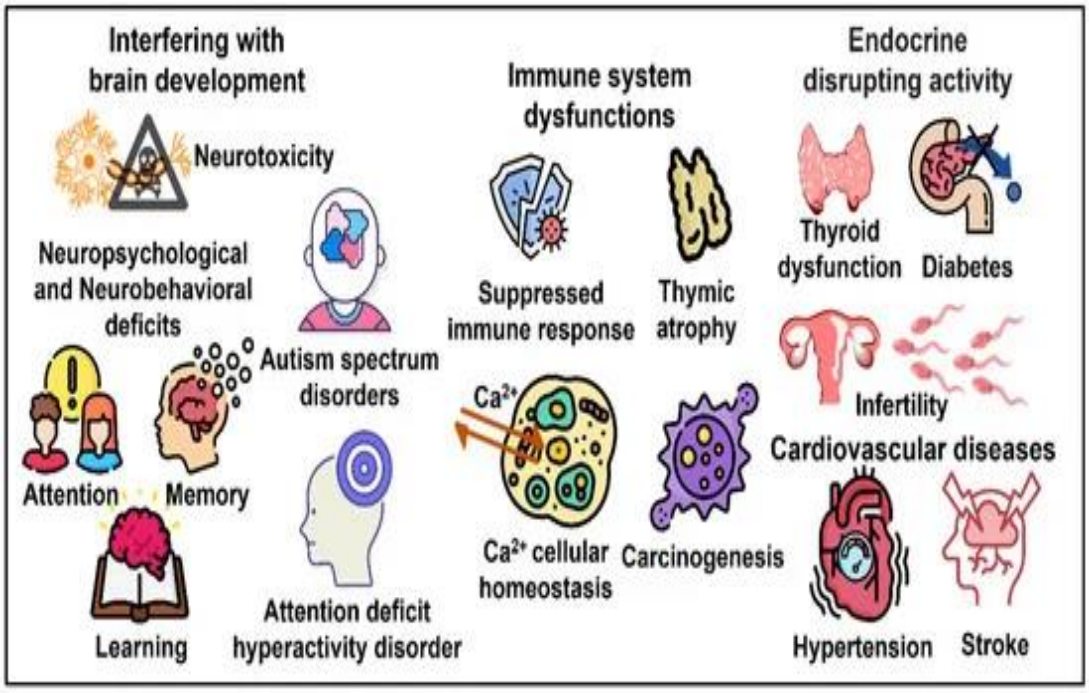


Figure1.3 An overview of the main targets of PCBs with related disorders in humans [38].

1.2.2 Current Detection Methods for PCBs Determination

There are a number of studies being conducted to develop new techniques and methods for determination of PCBs in air, water, soil, and sediment. Presently, the most common techniques used for PCB detection are Chromatography, ELISA and Biosensors. Each of these techniques has its benefits and drawbacks. In the following section, we will discuss it in detail.

1.2.2.1 Chromatographic Techniques

In order to determine the presence of PCBs in different matrices such as air, soil, water, food, and oil, a variety of traditional methods are commonly used. GC is the oldest complex laboratory-based and widely used instrumentation technique, coupled with an electron capture detector (ECD), a high-resolution mass

spectrometry system (HRMS), or a low-resolution mass spectrometry system (LRMS). As well as liquid-liquid extraction (LLE), solid phase extraction (SPEX) and supercritical fluid extraction (SFE), high performance liquid chromatography (HPLC) can also be used. In addition, different methods of detection can also be used, such as flame ionization, ultraviolet (UV) or fluorescence detection [79–81].

There are several advantages to these techniques, including their high sensitivity, selectivity, and accuracy. The major disadvantage of these chromatographic techniques is that their development is expensive, especially for large-scale analyses, and they are also costly to run, difficult to use, time-consuming, and require large quantities of expensive and toxic solvents [82–84]. In most cases, sample preparation is required prior to chromatographic separation [85,86]. A further disadvantage of conventional analysis procedures is that they require instrumentation that is not suitable for on-site analysis [87]. For the reasons outlined above, immunochemical methods present as a better method for detection.

1.2.2.2 Immunochemical Methods

Immunoreaction-based methods including enzyme linked immune-sorbent assay (ELISA) which is the most popular immunoassays, A chemical-colorimetric test kit is used to determine whether a sample contains 50 ppm or more PCBs. As a result, ELISA test kits became increasingly popular in the 1970's and 1980's [88,89] . These were based on the concept of using an enzyme as a reporter label. They are generally performed in microtiter plates, this method, although sensitive, detection of multiple samples at one time, microtiter plates require time and skilled personnel to operate, and they are inefficient for: carrying out multiple analyses at once, detecting and

transducing continuously. Moreover, these technique are expensive and a lab-based application [90]. Regarding this, immunosensors are a promising alternative to optical immunoassays for monitoring important analytes in the environment due to their high sensitivity and selectivity [91–93]. Furthermore, they provide real-time monitoring of immunoreactions at detector surfaces.

As mentioned earlier, traditional methods have some advantages. In order to ensure reliability, they require multiple external controls for quantitative analysis. Furthermore, large sample volumes, expensive instruments, and expensive reagents are usually required. Furthermore, environmental pollutants require more sensitive, simpler, and real-time monitoring methods.

According to reports, biosensors, especially immunosensors, are highly effective techniques for rapid, easy, continuous, and on-site analysis of environmental pollutants. They have the ability to overcome the limitations of traditional methods.

1.2.2.3 Immunoassays and Immunosensors

Immunoassays and immunosensors are analytical techniques that use antibodies or other immunoreceptors to detect and quantify specific molecules in a sample. There is a critical difference between immunosensors and immunoassays; an immunoassay system is based on the interaction between the antibody and the antigen in which the recognition process of the antigen occurs elsewhere [17,94]. Despite this, in immunosensors, the immunocomplex formation and diagnosis take place on the

same platform. Both techniques were used to complete this thesis. In the following section, we will discuss it in detail.

1.3 Immunoassays (ELISA)

Immunoassays are based on the ability of antibodies to bind specifically to different substances. Immunoassay uses the principle where the quantification of the assay can be observed by the development of colour towards the enzyme that attached to the reactants after the addition of suitable substrate [95,96]. These are frequently utilized for assessing the levels of different hormones, allergens, viruses, and bacteria. Perhaps one of the best-known immunoassays for environmental monitoring is enzyme linked immunosorbent assay (ELISA). ELISA is a technique used in immunology to detect the presence of antibody or an antigen in the sample .As an analytical tool immunoassay have been adapted to detect a wide range of analytes, achieving very low detection limits in most cases [89]. The first immunoassay was described in 1959 and since then it has developed into a fundamental and well-established analytical tool in biochemistry. In ELISA, immobilization and incubation steps are applied to bind the reagents to a solid phase-bound substance [97]. The common microplate that has been used in this assay is 96 well plate Figure 1.4. The washing step is introduced to separate the bound and unbound regent. This washing step is the key element to the success exploitation of ELISA. An enzymatic interaction with the substrate will quantify the reaction, through the use of an enzyme-labelled reaction. The signal that occurred as the changes of colour is associated with the presence of antigens and antibodies. There are a variety of types of immunoassays and the selection of ELISA format relies on the specific needs of the assay and the

availability of reagents. For instance, when detecting small molecules, the competitive assay is the most suitable option, and the following section discusses some of the most common formats used.



Figure 1.4 ELISA 96 well plate is made from clear polystyrene that is suitable for optical detection.

1.3.1 Immunoassay Format

The two well-known formats in ELISA are direct and indirect assay. The direct ELISA uses the method of directly labelling the antibody itself, while the indirect ELISA could be used when no labelled primary antibody is available. The advantage of indirect ELISA is that the commercial conjugates could be used. However, a variety of ELISA methods are available depending on the specific requirements of the assay. These include capture assay, sandwich assay, competitive assay, and displacement assay.

1.3.1.1 Capture ELISA

The diagram for antigen capture assay is shown in Figure 1.5. In an ELISA test, the target antigen is present on a coated plate and labelled antibodies are used to detect it. The detection can be measured using colorimetric, chemiluminescent, or fluorescent methods. The indirect ELISA, on the other hand, involves an unlabelled primary antibody in combination with a labelled secondary antibody, which is designed to bind to all antibodies of a specific species, making it suitable for use with a variety of primary antibodies. For example, it can be used with all mouse monoclonal antibodies by utilizing a labelled secondary antibody directed against anti-mouse antibodies. Figure 1.6 shows the typical curve for direct capture assay. The signal observed is proportional towards the biocomponent concentration.

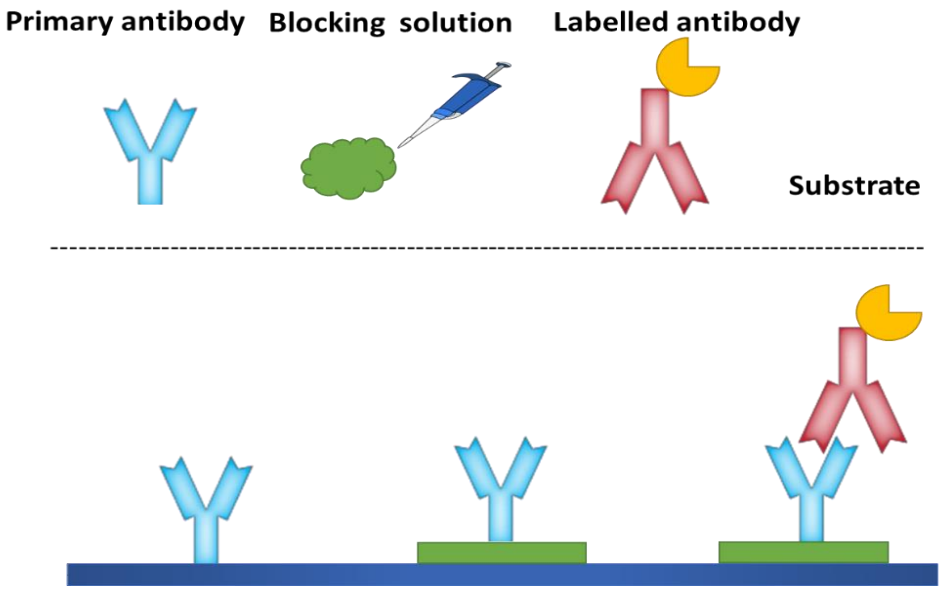


Figure 1.5 The capture assay the primary antibody is immobilised on a surface, add blocking buffers, then add the labelled antibody, add the substrate to measure the absorbance signal.

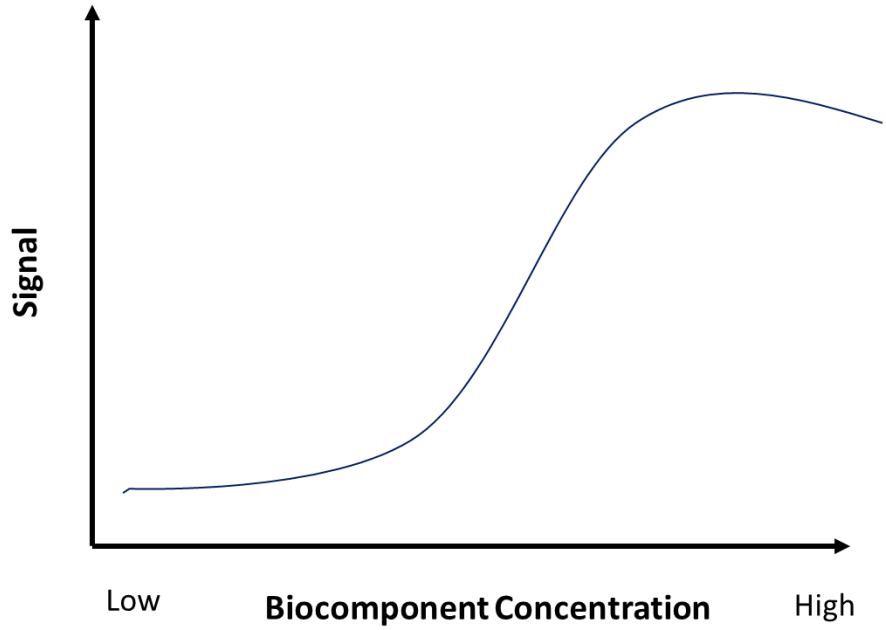


Figure 1.6 Typical calibration curve of capture assay represents the direct relationship of the signal and concentration**.**

1.3.1.2 Sandwich ELISA

The sandwich ELISA is a method that quantifies the amount of antigen between two layers of antibodies, which includes the capture and detection antibodies. In order for this method to be effective, the antigen being measured must have a minimum of two antigenic sites that can bind to antibodies, as two antibodies are required for the sandwich. As shown in Figure 1.7, the process begins with the coating of the plate with a capture antibody. A sample containing the target analyte is then added, and any antigen present binds to the capture antibody. Detecting antibodies are then added, which bind to the antigen. The secondary antibody is enzyme-labelled and

binds to the detecting antibody. As a final step, a substrate is added, which is transformed into a detectable signal by the enzyme.

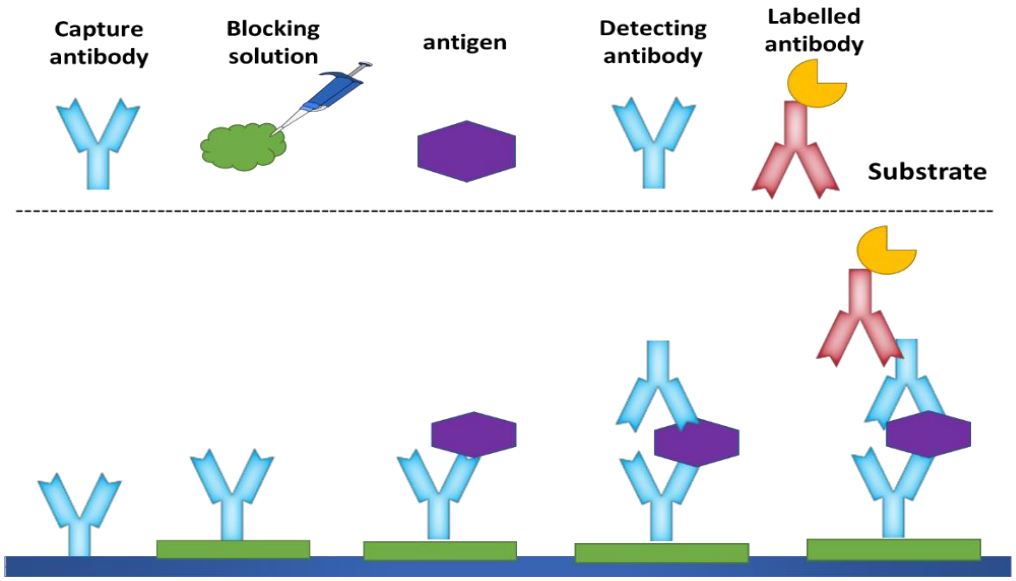


Figure 1.7 Sandwich assay, the capture antibody is immobilised on a surface, add blocking buffers, then add the sample containing the target antigen, add the detection antibody label conjugate, add the substrate to measure the absorbance signal.

1.3.1.3 Competitive ELISA

Competitive ELISAs are commonly used when the antigen is small and contains only one epitope, or antibody binding site. In this method, the purified antigen is labelled instead of the antibody. The unlabelled antigen from samples competes with the labelled antigen for binding to the capture antibody. If the antigen is present in the samples, there will be a decrease in signal from purified antigen compared to assay wells with labelled antigen alone. Figure 1.8 provides a schematic for the competitive ELISA method.

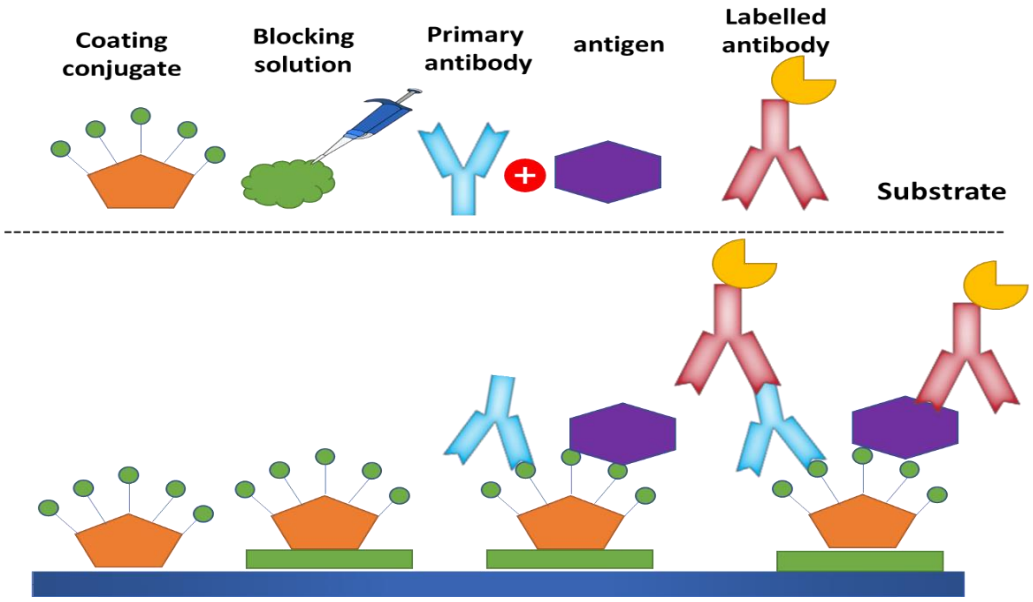


Figure 1.8 Competitive assay, coating conjugate is immobilized on the surface, add blocking buffers, after addition of both the antigen and the primary antibody adding the enzyme-conjugated labelled antibody, competition occurs between the two for binding to the antibody. The addition of the enzyme's substrate leads to color development and measure the absorbance signal.

The process of competitive ELISA involves incubating an unlabelled antibody with its corresponding antigen. The resulting complexes of antibody and antigen are then introduced to a well coated with the antigen. Any unbound antibody has the potential to bind to the antigen on the microwell plate. Following this step, the plate is washed to eliminate any unbound antibody and antigen. A secondary antibody that is specific to the primary antibody is then added, which is linked to an enzyme. Substrate is added to produce the detectable signal at higher concentration, the antigen presence results in less free antibody to bind. Therefore. reverse trend in signal is obtained for example the high concentrations give the weakest signal and low concentration of the analyte give the higher signal. Figure 1.9 shows the typical calibration curve for a

competitive assay. The signal observed is inversely proportional towards the biocomponent concentration.

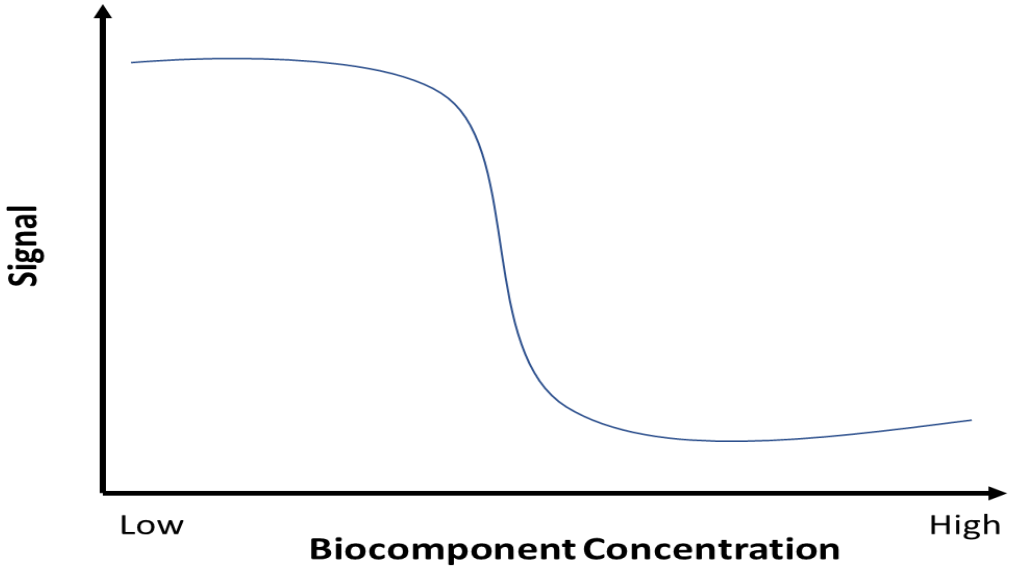


Figure 1.9 Typical calibration curve for competitive assay represents the inverse relationship of the signal and concentration.

1.3.1.4 Displacement ELISA

For displacement ELISA, the protocol used are similar to the competitive assay as mentioned in Section 1.3.1.3, except for this protocol requires one additional step, thus requiring 1 hour more incubation time. Figure 1.10 illustrates the steps involved in competitive assay. Unlike the competitive assay which involves the step of mixing and immobilizing the primary antibodies with the antigen in one step, a displacement assay requires different separation steps of primary antibody and antigen. Prior to the introduction of the antigen, the primary antibody that binds to the coating conjugate will be replaced with this substance. After the addition of labelled antibody

and the substrates, the signal was measured where the signal achieved is inversely proportional to the concentration of the antigen added. The typical calibration curve for a Displacement assay is similar to those achieved for the competitive assay, refer to Figure1.9.

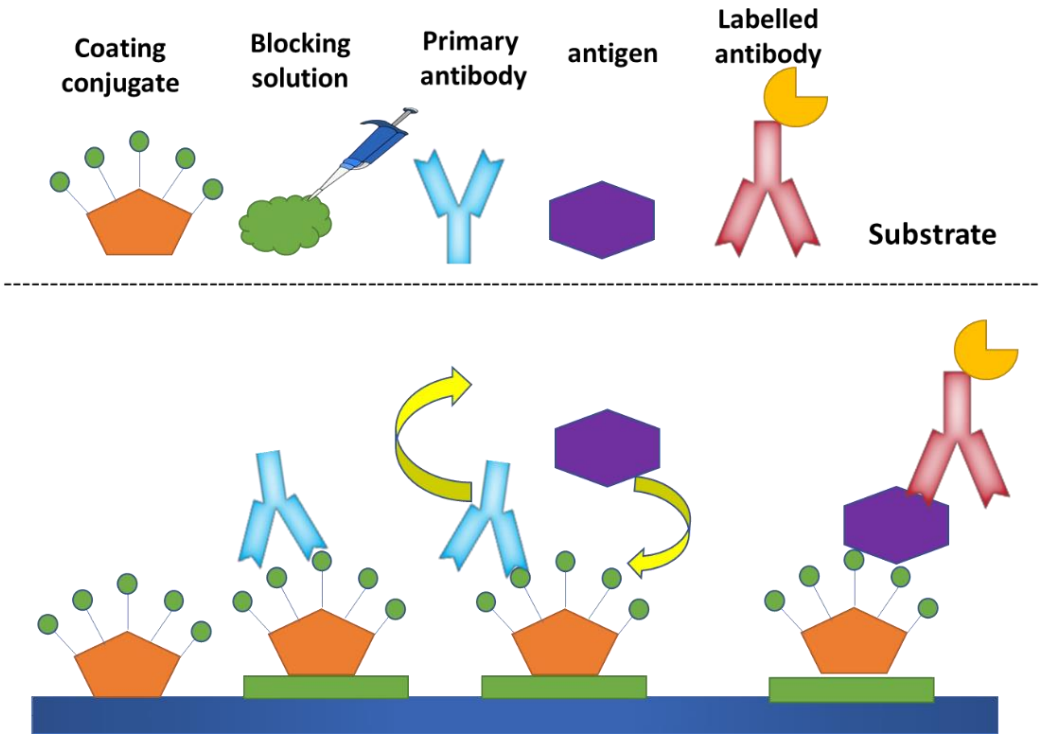


Figure 1.10 Displacement assay, coating conjugate is immobilized on the surface, add blocking buffers, after addition of the antigen next the primary antibody adding the enzyme-conjugated labelled antibody, competition occurs between the two for binding to the antibody. The addition of the enzyme's substrate leads to color development and measure the absorbance signal.

1.4 Biosensors

The concept of sensors is well known, since every human is endowed with five different types of sensors: touch, smell, hearing, sight, and taste. In order to improve the quality of our lives, scientists have developed instruments that are similar to the five senses, but with significant improvements in performance. As a result of this development, thermometers and telescopes have become common tools in everyday life. There are several types of sensors that can be classified based on their performance and function, including physical sensors, chemical sensors, and biosensors [98]. Both indoor and outdoor environments can be measured using physical sensors. A physical sensor is used to measure various physical characteristics such as temperature, distance, pressure, mass, and magnetism. In contrast, chemical sensors are devices that are used to detect chemical reactions. An example of a chemical sensor is the pH meter, which measures voltage changes caused by changes in alkalinity, and litmus paper, which measures dye colour changes corresponding to alkalinity changes.

In 1962, Leland C. Clark developed the first biosensor for the detection of enzymes [99]. Since then, biosensors have been extensively studied and applied to a variety of applications, ranging from public health and environmental monitoring to homeland security and food safety [100–103]. Significant progress has been made in the development of biosensors over the years. The current generation of biosensors can detect even the smallest amounts of potentially harmful and deadly biological pathogens in a fast, efficient, and cost-effective manner. Although some biosensors

require expensive equipment to operate, others are portable, making them suitable for use in underdeveloped regions of the world [104].

A biosensor is an analytical device that consists of two main components: a bioreceptor and a physical transducer. A bioreceptor is a biological component that determines the target analyte, bioreceptor such as (tissue, microorganisms, organelles, cell receptors, enzymes, antibodies, nucleic acids, etc) [105]. In close contact with a physicochemical transducer that converts biological responses into electrical signals that are then processed in a data processing system. Transducers may be thermometric, magnetic, electrochemical, piezoelectric, optical, or micromechanical [106]. Classification of biosensors can be based either on their method of signal transduction or on their principle of biorecognition. IUPAC's 1999 recommendations define a biosensor as a device with an independently integrated receptor that is capable of providing selective quantitative or semi-quantitative analytical information using a biological recognition component [107]. It is possible to classify biosensors based on the type of biological signalling mechanism utilized or the type of signal transduction employed [108] . The size and shape of biosensors vary, and they are able to detect and measure even very low concentrations. Biosensors typically consist of (a) an analyte, (b) a bioreceptor, (c) a transducer, (d) electronics, and (e) a display. Figure 1.11. Below depicts the principal parts of a biosensor.

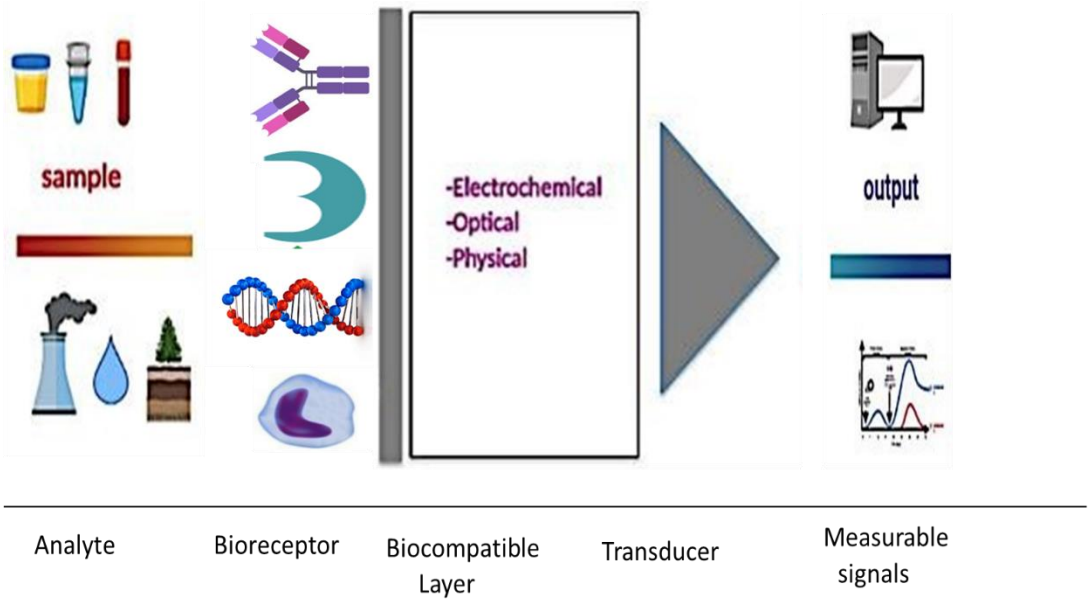


Figure 1.11 Schematic of different types of biosensors. The biocomponent is immobilized on a biocompatible layer, resulting in a change of physical or chemical properties of the elements that can be detected by a measuring tool.

Biosensor-based techniques have been rapidly developed for environmental monitoring over the past few decades. Significant advances and improvements for environment biosensors have been shown in the aspects of sensitivity, selectivity, and simplicity. Detection of specific compounds, such as organic compounds, toxic metals, hazardous industrial chemicals, and pathogenic bacteria, requires improved transducers, enhanced biocomponents, and an integrated approach between the two entities in order to create functional and robust analytical instruments [109].

Biosensors have been employed in applications ranging from industrial process control to environmental monitoring. The development of biosensors as diagnostic tools is ongoing.

There are several detections from which improvements can be expected over the next few years, for both the sensing layer and the transducer. Higher selectivity, improved stability and better sensitivity are perhaps the present requirement for future development.

The general design of a biosensors in its simplest form can be divided into four key steps, table below which are fundamental to its function and characterization.

Table 1.1 key steps for biosensor design and operation.

Biocomponents are immobilized on the surface of the transducer.
Analyte introduction and subsequent capture by the biocomponent.
Biocomponents produce responses and is converted into a detectable signal.
This signal is amplified, digitalized, and analysed using some form of processing device.

Biosensors offer analysis at a reduced cost, they are cheap to produce and if used in conjunction with other traditional analytical techniques such as GC and HPLC they can be a valued and important asset, especially in the screening of large quantities of samples. The continual improvement of the microelectronic industry also has a key role for biosensor development as detection techniques can now be made into handheld devices, which when coupled to a biosensor offer the possibility of field analysis and lab in a brief-case approach.

1.4.1 Classification of Biosensors

Biosensors consist of two main components: bioreceptors and transducers. A biosensor can be classified based on its bioreceptor (enzymatic biosensors are the most common type of biosensor), immunosensors (have high specificity and sensitivity and are especially useful in diagnosing), aptamers or nucleic acid-based biosensors (possess high specificity for bacteria and nucleic acids) and whole-cell or microbial biosensors [110]. The second category of biosensors is based on the transducer: electrochemical (which can be further divided into potentiometric, amperometric, impedance, and conductometric), electronic, thermal, optical , and mass-based or gravimetric [111,112].

1.4.1.1 Based on Bioreceptors

According to the biorecognition principle, biosensors can be classified as catalytic or affinity sensors [113] . A catalytic biosensor produces a new biochemical product as a result of the interaction between the analyte and the bioreceptor. This biosensor can detect enzymes, microorganisms, tissues, and whole cells. When using an affinity (non-catalytic) biosensor, the analyte is bound irreversibly to the receptor, so that no new biochemical reactions are produced during the interaction. Detection targets for this type of sensor include antibodies, cell receptors, and nucleic acids [114]. A biological recognition system converts information from the biochemical domain, usually analyte concentration, into a chemical or physical output signal with a defined sensitivity. The specificity of biosensors depends on the biorecognition elements used as this molecule recognizes specific target analyte before the signal is converted by transducers [115]. In general, biological recognition elements are macromolecules

that catalyze biochemical reactions immobilized on physical transducers. Due to their high selectivity and ease of use, enzymes are the most commonly used biological elements in the development of biosensors.

1.4.1.1.1 Enzymes

An enzyme is a protein that catalyses the chemical reaction in living systems. In an enzymatic reaction, the enzyme converts the substrates into the molecules at significant rates [116]. The reactions involving enzymes are usually specific because of their characteristics (i.e. complementary shape, charge and hydrophilicity/ hydrophobicity) which is only reacted to the certain substrates. Enzyme labels have been widely used in affinity biosensors, particularly in immunosensors. The ideal enzyme label must have a very high catalytic activity toward a particular substrate. Different enzymes labels are employed in immunosensors including peroxidase [117]. glucose oxidase [118], catalase an enzyme immunosensor for the electrochemical determination of the tumour antigen α-fetoprotein [119] and many more. In this research, alkaline phosphatase was used as a labeled enzyme. Figure 1.12 shows the molecular model of alkaline phosphatase [120].



Figure 1.12 Molecular model of alkaline phosphatase [206].

The two most commonly used enzymes in ELISA are alkaline phosphatase and horseradish peroxidase. AP is dimeric glycoprotein with a molecular weight of ca. 140,000 g mol^{-1} [121]. AP is often used in molecular technologies laboratories and one of the commonly used is in immunoassay as an enzyme label. The optimal pH for AP is between the ranges of pH 8 to pH 10, as APs are most effective in an alkaline environment.

In order to determine the enzyme activities, the ELISA technique can be used. It depends on how well the enzyme and substrate react to each other, thus it is important to choose the right substrates for the targeted enzymes. The most used AP substrate for spectrophotometric detection is p-nitrophenyl phosphate (pNPP) [122,123].

The buffer used with the substrate PNPP is usually diethanolamine (DEA) in alkaline condition (i.e. pH 9.5). Figure 1.13 shows the enzymatic conversion of the substrate caused the colour change that indicates the presence of the enzymes. The absorbance signal obtained at 405 nm was produced when the p-NPP was converted to p-nitrophenol (p-NP) and phosphate from the enzymatic reaction, with the yellow colour was observed after the reaction [124]. The higher intensity of yellow colour can be seen, the higher the absorbance signal will be observed, and the intensity of the yellow colour is representative of the concentration of the analyte present.

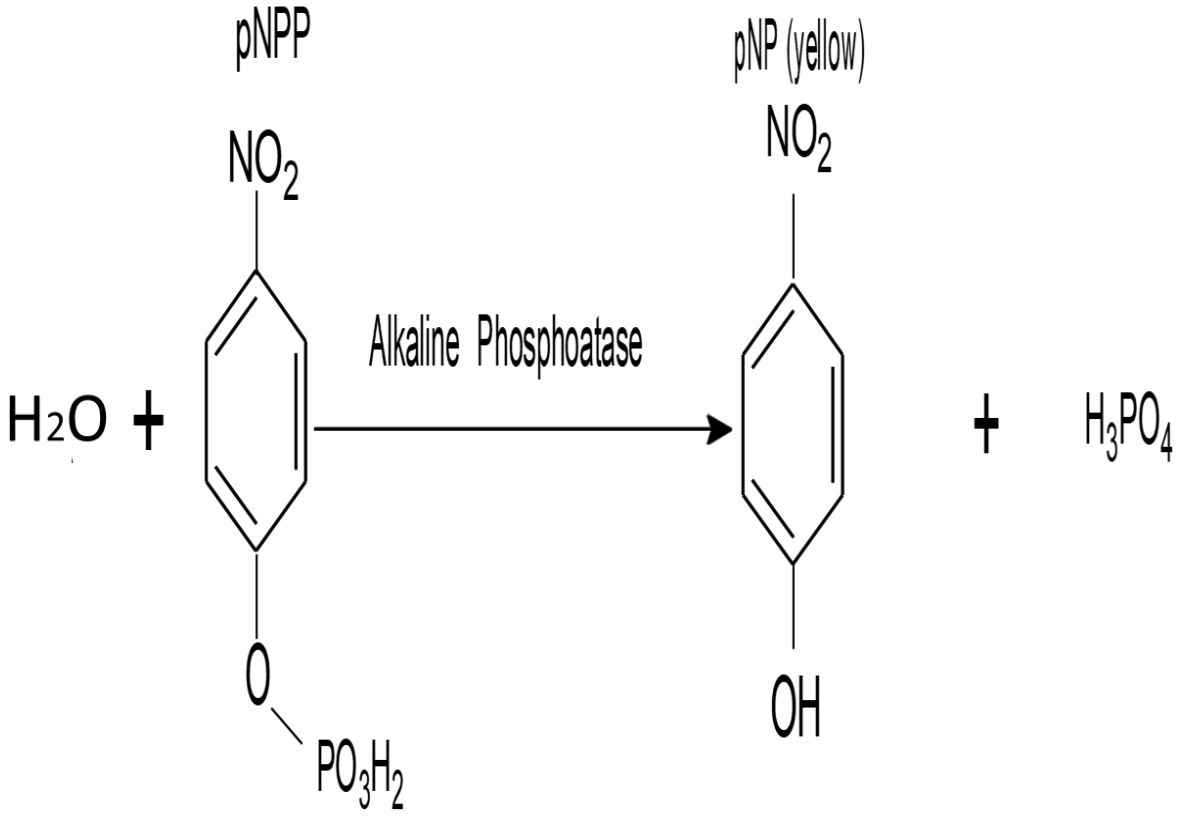


Figure 1.13 Interaction of pNPP substrate with alkaline phosphatase resulting in colour changes that can be measured at 405nm.

For electrochemical detection, the most used AP substrate is p-aminophenyl phosphate (pAPP) [125]. AP catalyses the dephosphorylation of pAPP to p-aminophenol (pAP) and phosphate, followed by the oxidation of pAP to form p-quinone imine at low potential of + 300 mV vs. Ag/AgCl [126]. Two electrons were generated in this reaction which occurred at the surface area of the working electrode. Figure 1.14 shows the enzymatic reaction between the pAPP and alkaline phosphatase.

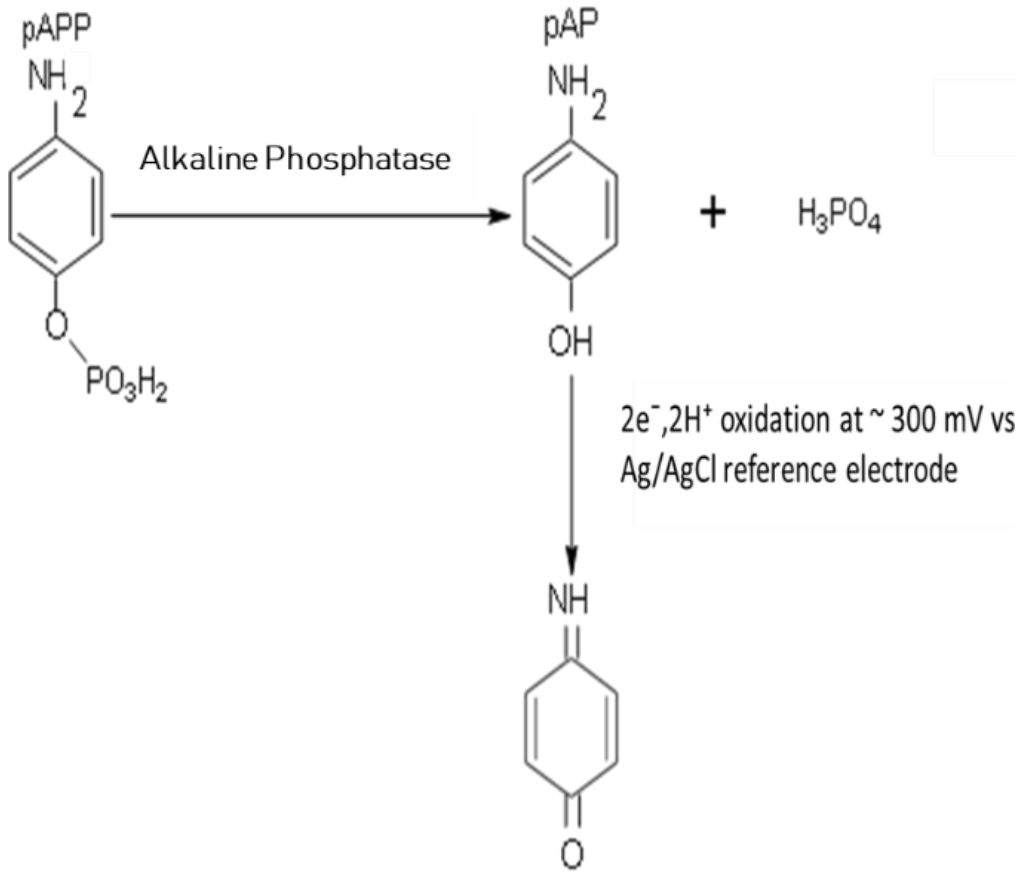


Figure 1.14 Interaction of pAPP and alkaline phosphatase was measured by amperometric detection, which 2 electrons were generated.

1.4.1.1.2 Antibodies

Since antibodies are affinity biorecognition elements, they have been utilized for over two decades due to their wide application range and strong antigen-antibody interactions. The antibody, also known as immunoglobulin (Ig) in a Y-shape, consists of two heavy and two light polypeptide chains connected by disulfide bonds, is an immune response to an antigen [127]. Since they can bind to specific targets, they are widely used in research, diagnosis, and therapy. There are five different types of antibodies: IgG, IgA, IgM, IgD and IgE. These types of immunoglobulins differ from each other in the number and positions of the disulfide bridges [128]. In this research have been use IgY, is the type of antibody produced in birds and IgY is the avian counterpart to mammalian IgG.

IgY (immunoglobulin Y) consists of two heavy chains and two light chains linked by disulfide bonds, similar to other antibodies. In the heavy and light chains, the variable regions are highly diverse and determine the specificity of the antibody for a particular antigen.

The structure of IgY is similar to that of IgG, with two heavy chains (H) of approximately 67 to 70 kDa and two light chains (L) of approximately 25 kDa. Similar to IgG, the light chains have a constant region (CL) and a variable region (VL). There is a significant difference between IgY and IgG when it comes to heavy chains. The heavy chains of IgG have three constant regions (CH1-CH3), while the heavy chains of IgY have four constant regions (CH1-CH4) (Figure 1.15). IgY has a higher molecular weight (180 kDa) than IgG (150 kDa) due to a further constant domain and the corresponding carbohydrate chains [129]. In an antibody, there are two main regions:

the fragment antigen-binding (Fab) region, which binds to antigens, and the fragment crystallizing (Fc) region, which interacts with receptors on the surface of cells.

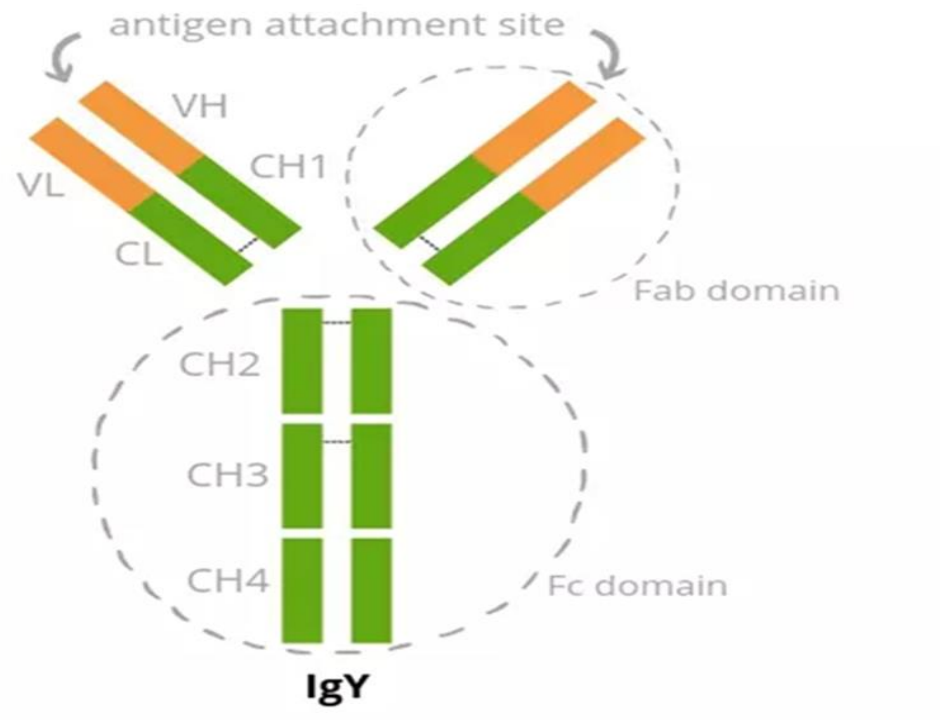


Figure 1.15 A schematic represents a basic structural unit of an IgY, with a single Y shape [130].

Antibody avidity can be defined as the overall stability of the antibody-antigen interactions, in the aspects of their affinity, geometric arrangement and valency between the antibody and antigen. Stronger interactions between antigen and antibody could be achieved by using higher affinity antibody.

Basically, to achieve optimal interactionist is preferable to entail high affinity and high avidity of the antigen-antibody binding. For example, to bind the second and the third antibodies together, they must be forming the same species as the primary antibodies. Otherwise, the Fc portion of the primary antibody could not be detected

by them. (Figure 1.16) represents antibody -antigen arrangements for high avidity and low avidity interactions [130].

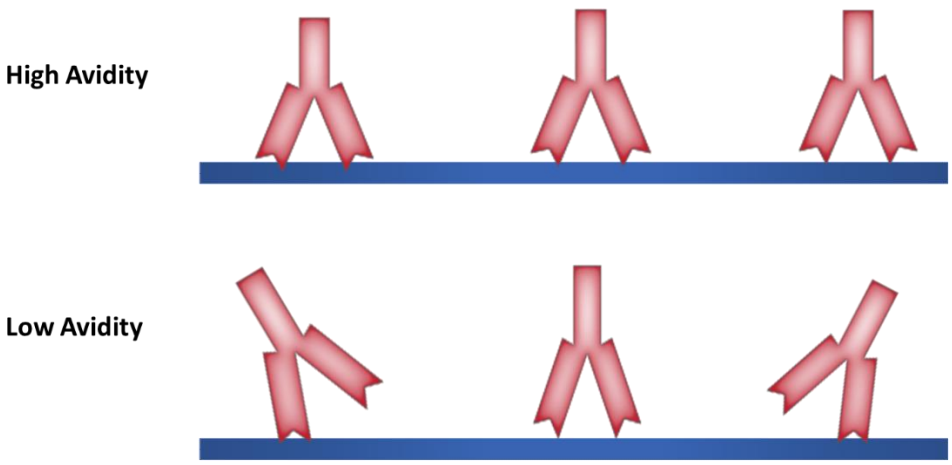


Figure 1.16 Examples of antibodies-antigens arrangement for high avidity and low avidity.

Several aspects such as size, charge, amino acid composition and carbohydrate content make them different to each other. Cloning of antibodies will produce monoclonal and polyclonal antibodies. Preparations of antibodies could be either monoclonal or polyclonal. Monoclonal antibodies are produced by a single clone of antibody-producing cells [131]. Polyclonal antibodies are produced by the immunized cells containing many different antibodies against the various mixtures of antigens injected [132]. Table 1.2 shows the difference between monoclonal antibodies and polyclonal antibodies.

Table 1.2 A comparison of monoclonal antibodies and polyclonal antibodies.

Monoclonal antibodies.	Polyclonal antibodies.
Preparation is expensive. Similar affinities Antibody that is monospecific Only one epitope can be detected. Suitable for binding antigens within a mixture of molecules	Preparation costs are lower. Affinity differences. Reproduction was not possible. Multiple epitopes are recognized. Commonly used in research assays.

1.4.1.2 Based on Transducers

Transducers are perhaps the most important part of the biosensor; it is a device that transforms biochemical interactions into measurable electronic signals. It can have a dramatic effect on both the specificity and sensitivity of the system. Thus, it is important to find the best transducer capable of giving the optimum detection for a particular system. In biosensors, transducers of different types are used, including optical, electrochemical, and piezoelectric transducers. In general, electrochemical biosensors are most commonly employed (approximately 70 %), followed by optical biosensors (approximately 25 %) due to their ease of operation and rapid response immunosensors [133].

1.4.1.2.1 Optical Biosensors

The most common class of biosensors reported is the optical biosensor. It is an analytical device consisting of an optical transducer and a biorecognition element. Different biological materials can be used as biorecognition elements, including enzymes, antibodies, antigens, receptors, nucleic acids, whole cells, and tissues. The transduction process in optical biosensors results in a change in the absorption, transmission, reflection, refraction phase, amplitude, frequency, and/or polarization of light. Biorecognition elements cause physical or chemical changes as a result. Measurement of absorbance is the simplest method of optical detection in biosensors, in which changes in analytes concentration are measured as a result of their adsorption of a certain wavelength of light. In general, optical biosensing can be divided into two general categories: label-free and label-based. Briefly, label-free sensing generates a signal directly from the interaction of the analyte with the transducer. In contrast, in label-based sensing, the optical signal is generated by calorimetry, fluorescence, or luminescence methods [134,135].

1.4.1.2.2 Electrochemical Biosensors

The electrochemical biosensor is a specialized type of biosensor that detects biological entities by converting the information into an electrical signal such as voltage, current, or impedance [99,136]. The various kinds of electrochemical biosensors are categorized according to the mode of measurements including amperometric, voltammetric, impedimetric, and potentiometric transducers [137].The amperometric transducer measures changes in current, the potentiometric transducer measures changes in potential, the voltammetric transducer measures

changes in current, and the impedimetric transducer measures variations in the medium's impedance between electrodes [138,139]. The main advantage of electrochemical transducers is that they can be miniaturized and made portable, making them especially useful for in-field, medical, environmental, or food analysis.

1.5 Fundamental Concepts in Electrochemistry

1.5.1 The Electrochemical Cell

Electrochemical detection occurs when a redox reaction takes place. There are two parts to a redox reaction: oxidation and reduction. In a chemical reaction, oxidation involves the loss of electrons, whereas reduction involves the addition of electrons. The reactions of oxidation and reduction occur simultaneously because, when an electron is lost, it is gained somewhere else - this causes current to be generated.

Electrochemical reactions can occur spontaneously if there is a natural transfer of electrons in accordance with the standard reduction potential, which is also referred to as Galvanic. The strength of the electron pulls increases with higher potential values. Alternatively, the reaction can be electrolytic, in which an electrochemical cell is used to apply electrical energy, facilitating chemical reactions that would otherwise not occur. Molecules that lose electrons are called oxidized or reductant, while molecules that gain electrons are called reduced or oxidant. Electron loss and gain takes place on surfaces known as electrodes, which are dipped in a solution. An electrolyte is a solution that is crucial to the flow of ions during oxidation and reduction processes. On cathodic and anodic electrodes, electrons flow from anode to cathode during oxidation and reduction reactions.

The flow of electric current in an electrochemical cell can be classified into two types: Faradaic and non-Faradaic. Faradaic current refers to the current generated by redox reactions, whereas non-Faradaic current is produced by the electrode double layer. To minimize non-Faradaic current, increasing the signal to noise ratios can be an effective approach [140] .

Electrochemical experimentation commonly involves the use of a 3-electrode system for current measurement. Figure 1.17 displays the components of an electrochemical setup. The potential is established between the working electrode (WE) and the reference electrode (RE), while the current flows between the WE and counter electrode (CE). Voltammetry techniques, such as cyclic voltammetry, linear sweep voltammetry, and amperometry, can be utilized for the measurement of both potential and current [141] .

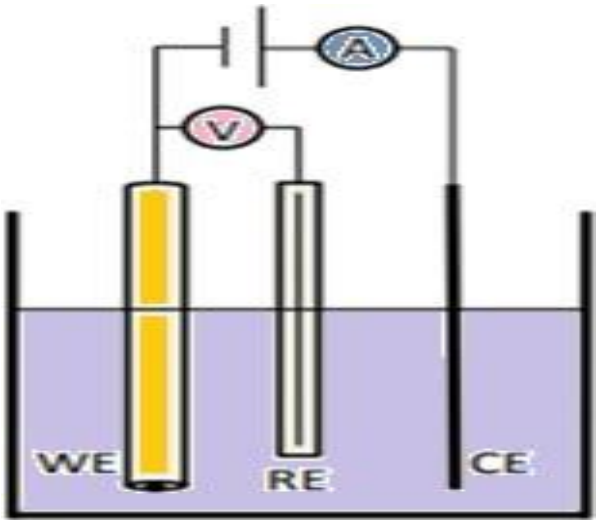


Figure 1.17 This diagram shows the three electrodes of an electrochemical cell linked to the ampere (A) and volte (V). The working electrode, reference electrode, and counter electrode are symbolised as WE RE and CE, respectively (142).

The working electrode plays a crucial role in determining the effectiveness of electrochemical assays, as it facilitates the transfer of electrons to or from the analyte [142]. To accomplish this, conductive materials such as metals, semiconductors, or graphite are typically used to construct the working electrode, and the choice of materials depends on the intended reaction. The reference electrode, such as Ag/AgCl, is the second main electrode, serving the vital function of maintaining the potential within the electrochemical cell. Lastly, the counter electrode is also critical, as its surface area must be significantly larger than that of the working electrode to prevent kinetic limitations from occurring. Since the reaction takes place in a solution, the ionic strength of the electrolyte must be maintained to reduce the solution's resistance.

1.5.2 The Electrode /Solution Interface (Double Layer Model)

An electrical double layer is formed between the electrode and the solution when potential is applied to the cell. This occurs when the electrode surface becomes charged, attracting ions dissolved in the solution. As the attracted ions have opposite charges, they form inner and outer layers, as shown in Figure 1.18.

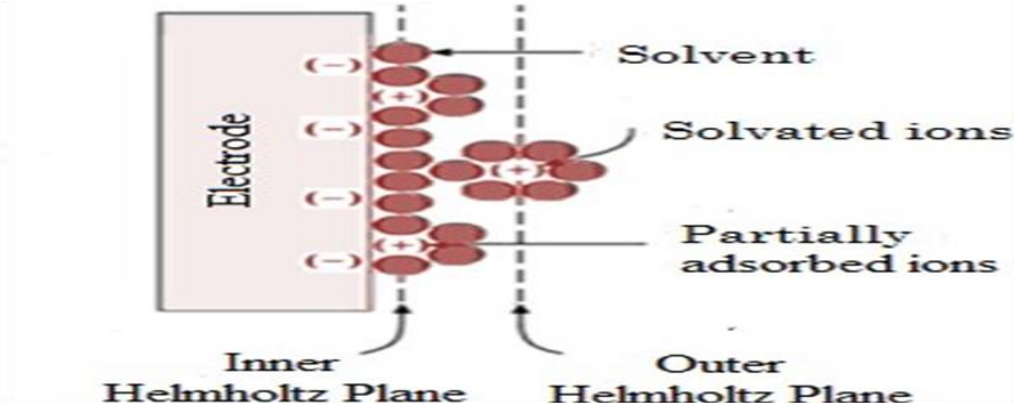


Figure 1.18 The Electrical Double Layer (141).

The inner layer of the electrical double layer is situated closer to the electrode surface and is referred to as the inner Helmholtz plane. It is composed of solvent molecules and ions that are specifically adsorbed. The outer layer, on the other hand, is positioned a bit further from the surface and is known as the outer Helmholtz plane. It is made up of ions that are solvated [142].

1.5.3 Mass Transport

Mass transport refers to the rate at which molecules or particles are transported and can have a significant impact on the overall reaction rate. The Nernst-Planck equation is a common equation used to measure the rate of one-dimensional mass transport at a fixed point, as shown in Equation 1.1.

$$J(x,t) = -D\frac{\partial C(x,t)}{\partial x} - \frac{zFDC}{RT}\frac{\partial \emptyset(x,t)}{\partial x} + C(x,t)V(x,t) \quad \text{(Eq.1.1)}$$

The Nernst-Planck equation (Equation 1.1) describes one-dimensional mass transport at a fixed point, where J(x,t) is the flux, D is the diffusion coefficient (cm^{-2} s^{-1}), ∂C(x,t)/∂x is the concentration gradient (at distance x and time t), ∂∅(x,t)/∂x is the potential gradient, z and C are the charge and concentration of the electroactive species, and V(x,t) is the hydrodynamic velocity (in the x direction). There are three modes of mass transport that can influence electrochemical reactions, namely diffusion, migration, and convection [140].

1.5.3.1 Diffusion

A diffusion is the spontaneous movement of particles or molecules in response to a concentration gradient [143]. The phenomenon occurs in all solutions in which there are uneven concentrations of reagents, typically moving from areas of high concentration to areas of low concentration [140]. According to Fick's First Law (Equation 1.2), diffusion rate is directly proportional to concentration gradient.

$$J(x,t) = -D\frac{\partial C(x,t)}{\partial x} \qquad \text{(Eq.1.2)}$$

According to Fick's Second Law in Equation 1.3, there is a proportional relationship between the current and the concentration gradient of electroactive species, indicating that the diffusional flux is time dependent.

$$\frac{\partial C(x,t)}{\partial t} = D\frac{\partial^2 C(x,t)}{\partial x^2} \qquad \text{(Eq.1.3)}$$

As a result of the concentration gradients established between the interfacial region and the bulk solution, diffusion is a common phenomenon in all voltammetry experiments. Nevertheless, the current response in diffusion-only experiments is dependent on the flux at the electrode surface, which depends on the electrode's size and geometry.

1.5.3.2 Migration

Migration refers to the movement of charged species in response to the electrical field, where they are either attracted or repelled from the interface by electrostatic forces. Migration can be effectively eliminated by adding a fully dissociated electrolyte, which serves as the ionic charge carrier.

1.5.3.3 Convection

Convection is a molecular motion that occurs due to the presence of force or bulk motion in the solution [140]. This motion can result from various factors such as vibrations, stirring or rotation. Natural convection is generated by small thermal or density differences in the solution, and it functions to mix the solution in a random and unpredictable manner.

1.5.4 Electrochemical Techniques

In general, electrochemical techniques are employed to obtain information on the processes or reactions that occur when an electric potential is applied to the study system. The following sections will outline the electrochemical techniques employed in this thesis.

1.5.4.1 Voltammetric Transducers

Voltammetric transducers are capable of measuring and recording the current as a function of the applied potential. Peak currents obtained are directly proportional to the species concentration and are equivalent to specific chemicals. There are several advantages of this method, including low noise, higher sensitivity, and the ability to

detect a variety of compounds with different peak potentials at the same time. In order to obtain information about chemical reactions, the current produced by the analyte is plotted at the potential applied to the working electrode [144].

1.5.4.1.1 Cyclic Voltammetry

Cyclic voltammetry (CV) is generally utilized to study the electrochemical properties of solutions containing analytes. This method is well established electrochemical method to study the surface chemistry on gold surface [145]. The principle of CV is that the current is related to the reduction of ions and the concentration of the ions in solution is related to the sweep rate, area and diffusion of molecules in solution. The potential is applied between the reference electrode and the working electrode, and the current is measured between the counter electrode and the working electrode. A basic Shape of the current response for a cyclic voltammetry is illustrated in Figure 1.19.

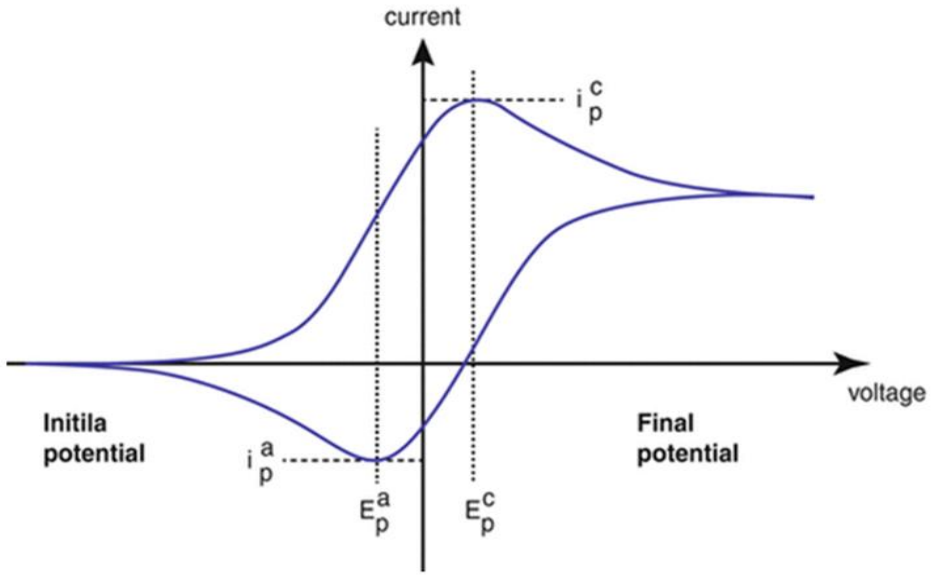


Figure1.19 Basic shape of the current response for a cyclic voltammetry [147].

For example, the redox reaction of Fe^{2+} is explained as follows. During the scan from - 0.2 to 0.6 V (starting from point A), the applied potential is sufficiently positive at 0.1 V to allow oxidation of Fe^{2+} to occur at the electrode surface. This oxidation is accompanied by anodic current, which increases rapidly until the surface concentration of Fe^{2+} approaches zero, as signalled by the peaking of the current at point B. The current then decays as the solution surrounding the electrode is depleted of Fe^{2+} due to its oxidation to Fe^{3+}.After the direction of the potential scan is switched at 0.6 V (point C) to a negative scan, the oxidation continues until the applied potential becomes sufficiently negative to cause reduction of Fe^{3+} (point D).

The half reactions of oxidation and reduction of Fe^{2+} are explained in the Equation 1.4 and Equation 1.5

$$Fe^{2+} \xrightarrow{\text{oxidation}} Fe^{3+} + e^- \qquad \text{(Eq 1.4)}$$

$$Fe^{3+} + e^- \xrightarrow{\text{reduction}} Fe^{2+} \qquad \text{(Eq 1.5)}$$

A cyclic voltammogram may be used to obtain quantitative data regarding analyte concentration using the Randles Sevcik equation (Equation 1.6).

$$i_p = (2.69 \times 10^5)\, n^{3/2} A D^{1/2} C v^{1/2} \qquad \text{(Eq 1.6)}$$

Where i_p is the peak current of ferricyanide/ferrocyanide, n is the number of electrons transferred, A is the electrode surface area (cm^2), D is the diffusion coeffision ($cm^{-2}\ s^{-1}$), C is the concentration ($mol\ cm^{-3}$), v is the scan rate ($V\ s^{-1}$).

Half peak-potential (the current is half of the peak current) between oxidation and reduction peak was calculated according to the Equation 1.7.

$$E\,{}^{1}/_{2} = \frac{Epa+Epc}{2} \qquad \text{(Eq 1.7)}$$

The point as current is half for the separation of anodic and cathodic peaks is about 59/n mV at 25 °C, where n is the number of electrons involved in the reaction.

1.5.4.1.2 Linear Sweep Voltammetry (LSV)

Linear sweep voltammetry, is a technique used to measure current by applying a potential that is swept linearly over time [146]. It detects the oxidation or reduction peak of a species by measuring the current when the species begins to be oxidized or reduced. The potential is scanned from a lower to an upper limit in LSV, and a typical LSV curve is shown in Figure 1.20. The scan rate of the voltage can be calculated using the slope of the curve.

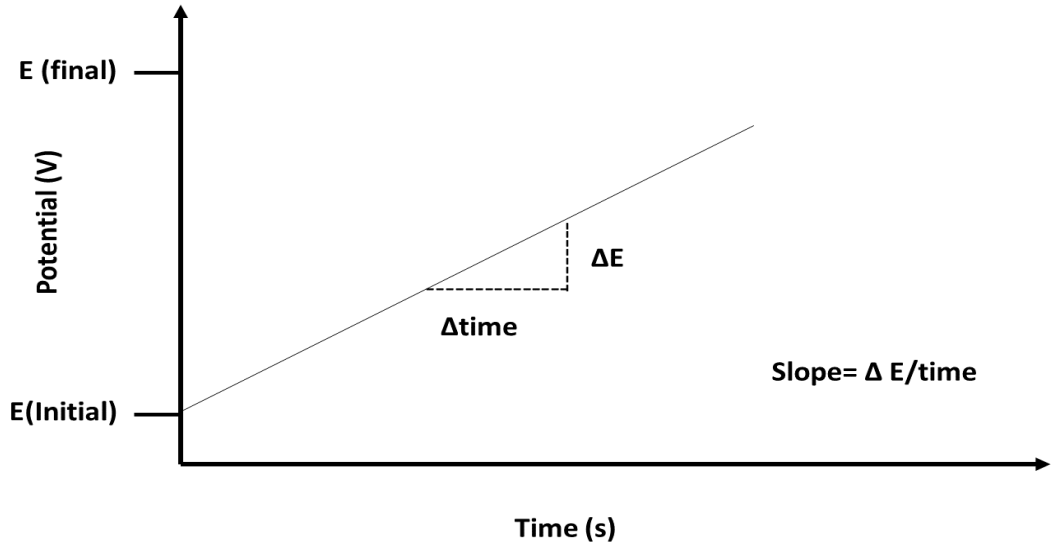


Figure 1.20 A typical curve of LSV. The slope represents the scan rate of the experiment (volts per unit time).

1.5.4.1.3 Differential Pulse Voltammetry (DPV)

Pulse voltammetric methods are based on the difference in rate of decay of the charging current and faradaic currents after when the potential between the WE and RE as a pulse of increasing amplitude [147]. In DPV the current measured before and after the application of each pulse, with the difference in current been plotted against the base potential and been at a maximum around the redox potential of the reacting species or analyte. DPV is considered to be a highly sensitive method having a high signal to noise ratio, as shown in Figures 1.21 and 1.22.

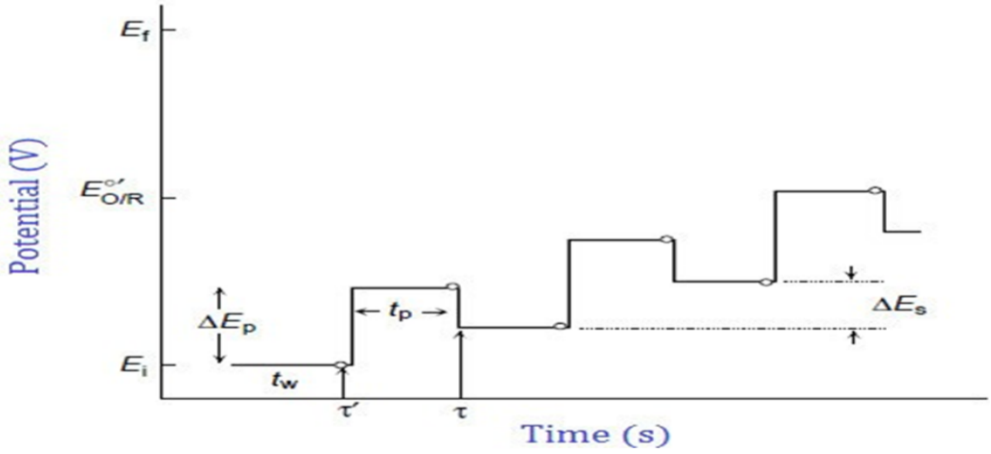


Figure 1.21 DPV waveform, showing; pulse time, tp; waiting time, tw; pulse amplitude, Ep; base potential, Es and the two points of current measurements, τ and τ'.

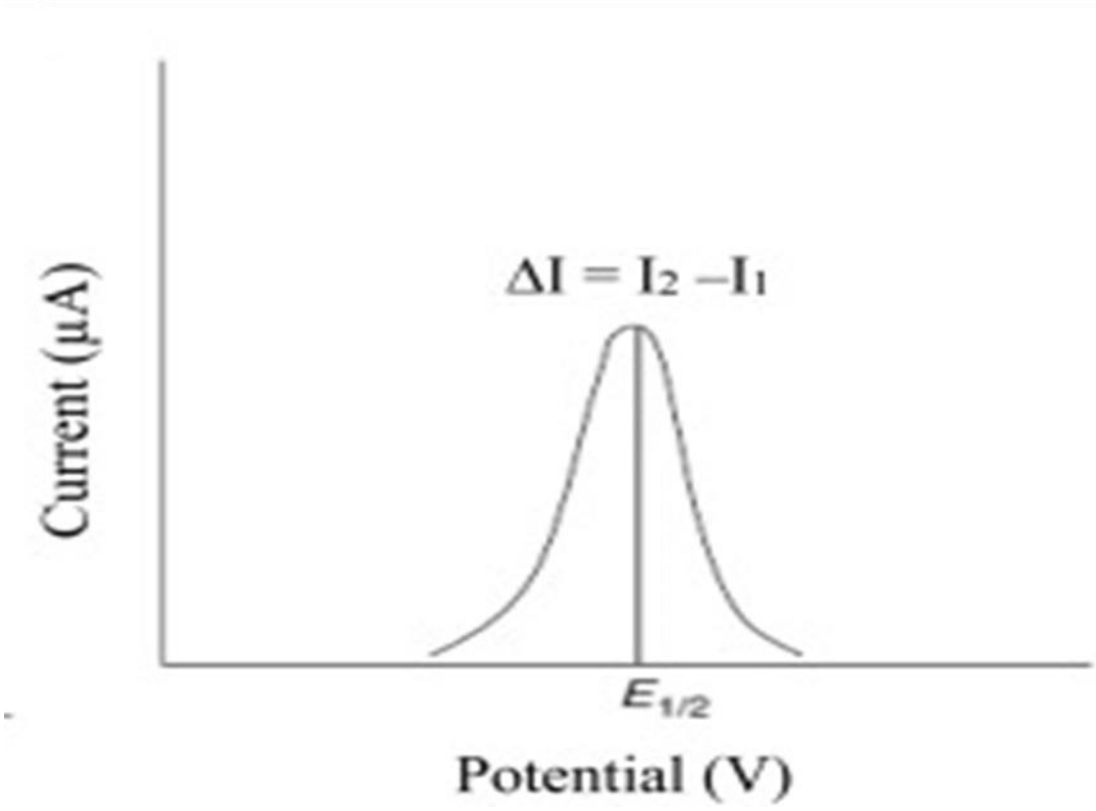


Figure 1.22 Resulting DPV curve of change in current (i2 - i1, from points τ and τ respectively) versus the base potential.

The current is monitored before and after a pulse of potential is applied. The data output is obtained as the difference of the currents at the two sampled points. The area under the curve is proportional to the concentration of the species.

1.5.4.2 Impedimetric Transducers

This type of transducer can detect alterations in impedance produced by the immobilization of biomaterials onto the electrodes, leading to modifications in capacitance and electron transfer between them. The use of electrochemical impedance spectroscopy (EIS) is commonly linked with this type of transducer, and it is used to evaluate the characteristics and functionality of electrodes that have been functionalized with biomaterials [148].

1.5.4.2.1 Electrochemical Impedance Spectroscopy (ELS)

EIS is a sensitive technique used for monitoring the electrical response of a system after periodic small amplitudes of alternate current AC signals are applied. As a result of the analysis of the system, we are able to obtain information regarding the interface and the reactions that occur at that interface.

The use of EIS appears to be promising since it provides a sensitive method for studying electron transfer across thin monolayers [149]. A number of research papers have been published. This detection method has been widely used for the investigation of the electrochemical behaviour of self-assembled monolayers using EIS in the past two decades with modified gold electrodes for the detection of haemoglobin [150], myoglobin [151], penicillin G in milk [152], and glucose [153].

EIS data is commonly analysed by fitting it to an equivalent electrical circuit model. Electrical elements such as resistors, capacitors, and inducers are commonly used in circuit models. A Randles circuit is an equivalent electrical circuit consisting of an active electrolyte resistance R_s in series with a double-layer capacitance C_{dl} and a faradaic impedance. The Randles Model for EIS characterisation on modified gold electrodes is illustrated in Figure 1.23.

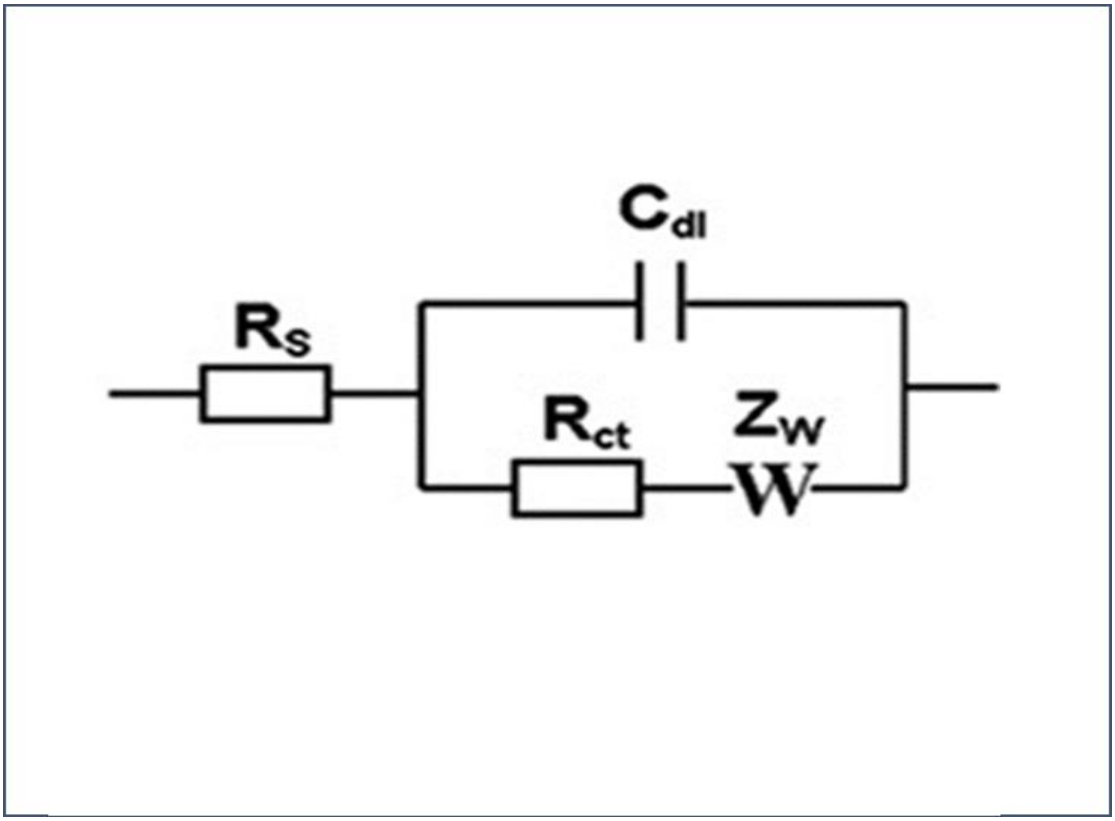


Figure 1.23 Impedance circuit (Randles model for SAM characterization of gold electrode.

An Randles model circuit consists of R_s representing dynamic solution resistance, C_{dl} representing the double layer capacitance between electrodes and electrolyte solution, R_{ct} representing charge transfer resistance in the immobilized recognition layer, and Z_w representing the Warburg element describing mass transport in relation to time (frequency).

A Nyquist plot could also be used to represent the impedance data, as was done in this thesis, where the imaginary (Z") and versus real (Z') components of the impedance are plotted. A Nyquist plot of the Randles impedance is shown in Figure 1.24 with the semi-circle at higher frequencies and the straight line at an angle of 45˚ to the real axis at lower frequencies.

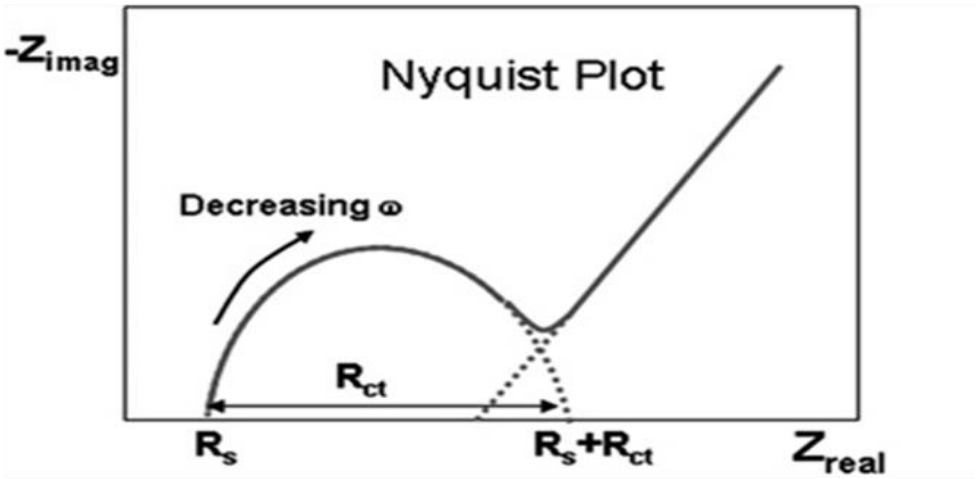


Figure 1.24 Nyquist plot for oxidation/reduction reaction of 5 mM $[Fe(CN)6]^{3-/4-}$ in 0.1 M KCl (imaginary impedance versus real impedance) frequency measured from 0.1 Hz to 1 MHz, with amplitude of 0.1 V, Potential applied at +0.21V.

In the model circuit shown in Figure 1.23, the C_{dl} value could only be calculated after frequency information was provided. Equation 1.8 shows the Warburg impedance calculation.

$$\omega_Z \, Im_{max} = \frac{1}{C_{dl} R_{ct}} \qquad \text{(Eq 1.8)}$$

1.5.4.3 Conductometric Transducers

Conductometric transducers work on the principle that a change in the number, charge, or molarity of ions causes a change in conductivity, which is used to measure the overall conductance of a sample [154]. Ionic species may be consumed or produced depending on the reaction involved. The method is not very specific, but it can become selective if an enzyme is introduced to the detector. A conductometric device has several advantages, including the fact that it does not require a reference electrode, is inexpensive, is capable of being miniaturized, and provides a direct electrical response [112]. In contrast to other electrochemical methods, this method is less sensitive and highly dependent on buffer capacity.

1.5.4.4 Potentiometric Transducers

The potentiometric sensor is designed to measure the potential of an electrode without any current flowing. The difference in potential between the working and reference electrodes is measured and used as a signal, with the reference electrode providing a fixed reference potential. The potentiostat can control the sensor with minimal interference from IR (ohmic) drop [155] . This sensor has the advantage of being easy to operate, and by using a field effect transistor (FET), it can be made smaller and used automatically. However, the technique still lacks specificity, as it can bind to other ions present in the sample, resulting in non-specific binding [156] .

1.5.4.5 Amperometric Transducers

Amperometric transducers measure currents resulting from electrochemical oxidation or reduction of an electroactive species containing a biorecognition element in the presence of a constant potential (voltage) applied to the working electrode. The applied potential drives the electron transfer reaction of the electroactive species, causing it to gain or lose electrons [157]. As a result of this reaction, the current obtained is a direct measure of the rate of electron transfer, which is representative of the recognition process, and proportional to the concentration of the analyte.

1.6 Classification of Electrochemical Immunosensors

Electrochemical immunosensor is a combination of a specific antigen-antibody interaction with the sensitive bio-electrode detection [158]. When the analyte of interest binds to the recognition element, it triggers a measurable change in the electrical properties of the electrode, which is then detected and quantified. In electrochemical immunosensors, the change of the electrical properties of an electrode, such as potential, current, conductance or impedance is measured due to the Ab-Ag interaction that caused by the immunoreactions [159].

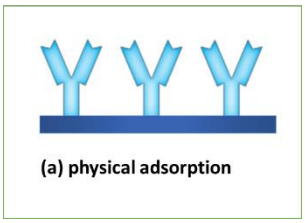
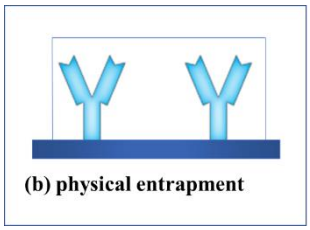
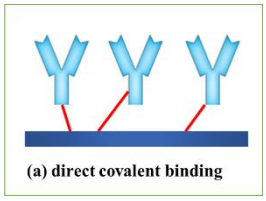
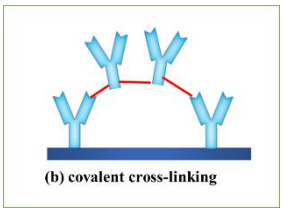
This technique introduces a miniaturised device that allows for simple, low-cost instrumentation, needs only small sample volume, and does not require sample preparation which is very time consuming [160]. This method can be used to achieve very low detection limits.

Electrochemical immunosensors can be classified based on various factors, such as the type of electrode surface modification, the type of method immobilization and the type of labelling strategy. Understanding these different classifications is important in designing and optimizing the performance of electrochemical immunosensors for various applications in healthcare, food safety and environmental monitoring. A comparison of the sensitivity and specificity of labelled and label-free detections has been addressed in this thesis.

1.6.1 Based on the Type of Method Immobilization.

Various techniques can be used to immobilize the biological component onto the transducer. Among these techniques, physical immobilization (which is reversible) and chemical immobilization (which is irreversible) are commonly employed. The appropriate technique to be used depends on several factors, such as the chosen biorecognition element, the transducer, the physical-chemical environment, and the characteristics of the analyte [161,162] . The key concept for the manufacture and development of a biosensor is the immobilisation of the biocomponents in order to stabilise them so that they can be used repeatedly.

Table 1.3 Methods of biocomponent immobilisation to solid support or carrier.

Method	Description
Physical (Reversible) Immobilization  	The method involves affixing enzymes onto the transducer surface without the need for chemical bonding. Enzyme immobilization techniques include (a) physical adsorption and (b) physical entrapment.
Chemical (Irreversible) Immobilization  	This technique involves creating robust chemical bonds, such as covalent binding or linking, between functional groups of biorecognition elements and the transducer surface. Chemical immobilization methods are classified into two categories based on chemical bonding: (a) direct covalent binding and (b) covalent cross-linking.

1.6.1.1 Physical Adsorption

This is one of the most straightforward methods for immobilizing biomolecules onto a transducer surface. Although the principle is practical, it is primarily used for immobilizing antibodies or proteins. The process involves exposing the biomolecules to an activated solid support for a specific duration and under specific conditions, allowing the biological agents to adsorb onto the carrier's surface. Physisorption of the biomolecule occurs through electrostatic interaction, hydrogen bonding, hydrophobic interactions, or a combination of these mechanisms [163].

1.6.1.2 Physical Entrapment

The primary benefit of immobilizing biocomponents through physical entrapment is that it involves trapping biomolecules within a gel or polymer, allowing them to remain close enough to the transducer surface for signal detection while preserving the immobilized species' chemical properties. The technique entails trapping the biomolecules within a lattice that permits the diffusion of smaller molecules such as the substrate to interact with them. This method is ideal for larger biomolecules such as antibodies, providing a greater degree of freedom for electrochemical interaction between the substrate and label. However, for larger antigens, this immobilization technique may be less effective as the antigen may encounter difficulty diffusing through the lattice. One of the oldest biosensor designs involved sandwiching the biomaterial between two membranes, allowing both antigen and small substrate to move freely while limiting the biomaterial's mobility. Examples of commonly used gels or polymers include nylon, starch, and polyacrylamide [164].

1.6.1.3 Cross Linking

Cross-linking is a well-known method for immobilizing enzymes, and glutaraldehyde and hexamethylene are common bi-functional agents used for this purpose. The linker binds to the enzyme's amino groups and the solid support, resulting in a stable polymer. These bi-functional reagents can link several enzymes together, producing a thin film on the solid support. One drawback of this method is that enzyme activity decreases, but the advantage is increased enzyme loading due to the spatial arrangement of products. Swelling of the bulky layer formed can also be problematic as large analytes may not diffuse through it [164].

1.6.1.4 Covalent Bonding

This immobilization method involves the direct covalent attachment of the biocomponent to the transducer's surface. It is similar to the cross-linking method mentioned earlier, but it creates a monolayer of protein on the surface instead of a randomly oriented layer. The most commonly used chemical for covalently attaching antibodies to transducer surfaces is 1-ethyl-3-(3-dimethylaminopropyl) carbodiimide (EDC). This method's advantage is that the thin layer formed offers excellent diffusivity [164,165].

1.6.2 Based on the Type of Electrode Surface Modification.

The surface of electrodes is modified to improve their performance in a variety of electrochemical applications. Surface properties can be modified in order to enhance an electrode's sensitivity, selectivity, stability, and durability [166]. As a result, electrochemical sensing, become more efficient. There are several types of electrode

surface modifications that are commonly used to enhance the performance and functionality of electrodes in various electrochemical applications such as chemical treatments, physical modifications, and deposition of thin films or coatings. In this thesis we used Self-Assembled Monolayer (SAM) is a type of chemical modification of an electrode surface. It involves the adsorption of a monolayer of organic molecules onto the surface of the electrode through a self-assembly process. The following section provides a detailed description of the modification of the electrode surface.

1.6.2.1 Self-assembled Monolayers (SAMs)

The important feature in immunoassay is the ability to immobilise the desire protein on specific targeted area with no non-specific binding. Self-assembled monolayers (SAMS) are used in order to reduce random orientation of the antibodies binding to the surface. Tremendous studies on SAM for biomaterial coating or modification are increased as they offered good properties in terms of cleanliness, uniformity and stable [167]. Modifications of alkanethiols on gold are the most extensively studied SAM substrate system, where the thiols react readily with gold surface to create uniform monolayers [168]. Since gold strongly adsorbed the protein molecules because of thiol-gold (hydrophobic) interaction, they provide adequate surface for immobilisation of biomaterials [169]. SAM formed on the adsorption of long chain alkanethiols on the gold electrode surface could permit control over the properties of the interface at the molecular scale as they provide well-ordered organic surfaces [170]. SAM formation is observed to be stable up to several months in air or in contact

with water or ethanol. They desorb at temperatures greater than 70 °C or when irradiated with UV light in the presence of oxygen. Figure 1.25 shows the schematic for SAM modification on gold electrode involving different immobilisation steps of chemicals, protein, and antigen.

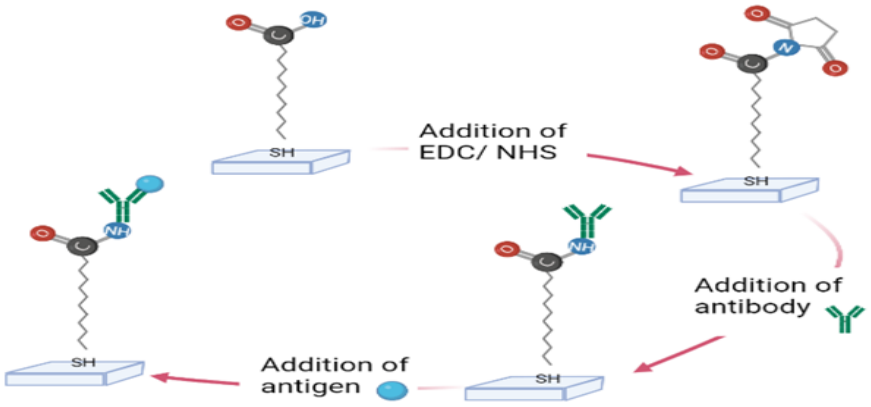


Figure 1.25 Surface modification involving the immobillsation of SAM solution on a gold electrode, followed by activation of carbodiimide and succinimide and incubation of antibodies and antigen.

1.6.3 Based on the Labeling Strategy.

The detection approaches of electrochemical immunosensors can be divided into label-free assays and labelled assays. In label-free assays, analytes are measured directly through biochemical reactions on transducers, whereas in labelled assays, the analyte is sandwiched between a capture agent and a labelled agent with a special label, such as an enzyme, quantum dot, fluorophore, or radioisotope, in order to obtain signal.

label free immunosensors, in other words direct immunosensors, are capable of detecting the physical or chemical changes arising directly from the immune antigen-antibody complex formation without needing to label. In this type of immunosensor, there is no need to use the label and it can be applied for fast, real-time analysis [171–174].While labelled immunosensors and called indirect immunosensors are based on the signal generating from one or several labels allowing highly sensitive and versatile detection. In indirect measurements such as enzymes, e.g., horseradish peroxidase [175], catalase and glucose oxidase [176] , alkaline phosphatase [177], and electroactive compounds as a mediator such as ferrocene, Prussian blue is usually used in the electrochemical immunosensor, especially when antigens and antibodies are not intrinsically electroactive. Moreover, several nanomaterials such as gold nanoparticles (Au NPs) or different quantum dots (QDs) can be used to amplify the signal. Hence, the application of label free immunosensor in environmental monitoring has become increasingly favoritized in the last decades. However, each detection approach (label free/label) electrochemical immunosensors have some advantages and some drawbacks. The advantages of label electrochemical immunosensors include high sensitivity, specificity, and multiplexing capability. However, they can be more complex and expensive than label-free immunosensors, and the labelling step can introduce variability and reduce the stability of the sensor. In contrast to label, label free immunosensors have some advantages such as do not require a labelling step, simplicity, lower cost, reduces time, higher stability also can offer the potential for real-time monitoring of target analytes [172,173,178,179] However, label-free immunosensors can be more challenging to develop and optimize than labelled immunosensors, as they rely on the direct detection of the

antigen-antibody interaction rather than a labelled signal. The future of label-free electrochemical immunosensors based on SAMs is promising, and further research could lead to the development of more robust, sensitive, and portable sensors for various applications, including food safety and environmental monitoring [180–182].Herein, we report the research progress of electrochemical immunosensors applied in environmental monitoring that were published in the last years Table 1.4.

Table 1.4 Some selected studies on electrochemical immunosensors in environmental monitoring. Successfully developed electrochemical immunosensor for various analytical detections.

Immunosensor	Electrochemical Technique	Analyte	Matrix	Linear Range	LOD	Reference
Label-free impedimetric	gold electrode + SAM (impedimetric immunoassay)	total PCB	insulating oil	0.01–10 µg/L	0.001 µg/L	[183]
Label-free electrochemical	DZN/thiolated aptamer/Au NP/SPGEs CV EIS	Diazinon (DZN)	plasma of Male wistar rat	0.1–1000 nM	0.0169 nM	[184]
Label-free electrochemical	NiHCF NPs/rGO/ gold electrode (DPV) (EIS)	PCB 77	water	1–100 ng/L	0.22 ng/L	[185]

Immunosensor	Electrochemical Technique	Analyte	Matrix	Linear Range	LOD	Reference
Label-free electrochemical	GCE/MNF/EDC-NHS/Ab/BSA (EIS)	atrazin	water	------	0.22 × 10−21 g /mL	[186]
label free immunosensor	384 micro well plate EIS	17β-Estradiol (E2)	water	1–200 pg ml^{-1}	1 pg ml^{-1}	[187]
label-free electrochemical immunosensor	sulfo-LC-SPDP/ gold surface DPV QCM EIS	Aeromonas salmonicida	seawater	1 CFU mL^{-1}	1 and 107 CFU mL^{-1}	[188]
Label-free electrochemical immunosensor	N-HRGO/TH modified GCE EIS/CV	COVID-19	saliva	0.3 pg mL^{-1}	1 pg mL−1−10 ng mL−1,	[189]
Labelled-electrochemical	MoS2-rGO/Thi/AuNP/GCE	PCB77	water /soil	0.3 fg mL−1–0.1 ng mL−1	80 ag /mL	[190]
Labelled-electrochemical	SnS2/β-CD modified screen-printed electrode. (DPV) (CV)	Aroclor 1016	--------	0.625 to 80 µM	5 µM	[191]
Labelled-electrochemical	Ab2-OMCSi-Zn probes (Ab1-CS/GN/GCE) DPV	procalcitonin (PCT)	serum	0.05 pg/mL to 80 ng/mL	0.013 pg/mL	[192]
Labelled-electrochemical	11-MUA-SAM/EDC/NHS/SPGE	benzo[a]pyrene (BaP)	water	40-60 mg/L	0.01 mg/L	[193]
Labelled-electrochemical	Carbon-rich monolayer on ITO EIS	Pyrene	Water	1.75–7.00 ppt	1.75 ppt	[194]

1.7 Theoretical Consideration of Enzyme Kinetics

In enzyme kinetics, several aspects need to be taken into consideration. These include the concentration of enzyme, concentration of ligand (substrate, products, inhibitors, and activators), pH, ionic strength and temperature during the reaction [195][196] . Enzyme electrodes have been widely used in electro chemical devices for monitoring a variety of substrates in the environment, clinical applications, and food samples. It consists of a layer of an enzyme immobilised on the appropriate electrode [197][198] Equation 1.9 illustrates the operation of an enzyme electrode, where a reaction is catalysed by immobilising the enzyme layers on the electrode, generating a detectable species.

$$S+C \xrightarrow{\text{Enzyme}} P+C \qquad \text{(Eq. 1.9)}$$

S and C are the substrate and core actant (cofactor) and P and C' are corresponding products. There are many variables aspects that may vary the response characteristics of enzymes electrode.

According to Michaelis-Menten mechanism, an enzyme-substrate complex is formed in the first step and either the substrate is released unchanged or after modification to form products [199]. Equation 1.10 represents the enzymatic reactions of a single substrate.

$$E + \mathrm{S} \underset{K-1}{\overset{K\,1}{\rightleftharpoons}} ES \xrightarrow{k2} E + P \qquad \text{(Eq.1.10)}$$

This reaction involves the combination of a substrate (S) and an enzyme (E) to form an intermediate complex (ES). This intermediate is subsequently breaks down onto product (P) and liberates the enzyme [198,200]. The rate v of the enzyme-catalysed reaction, at a fixed enzyme concentration could be explained by the Michaelis-Menten equation, as shown in Equation 1.11.

$$V = \frac{V_m\,(S)}{(K_m + (S))} \qquad \text{(Eq.1.11)}$$

K_m is the Michaelis-Menten constant and V_m the maximum rate of the reaction. Figure 1.26 shows the variation of the rate of an enzyme-catalysed reaction with substrate concentration. K_m corresponds to the substrate concentration, in which the concentration is determined by the half of V_m. It was determined at the half rate of V_{max}, For the development of enzyme electrodes, it is ideal to have the highest V_m and the lowest K_m.

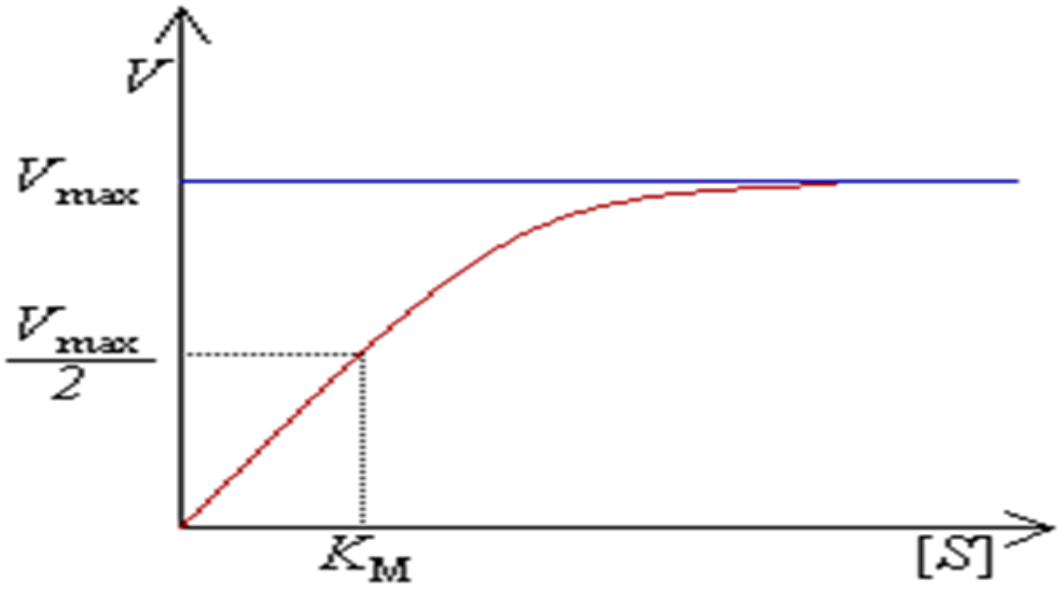


Figure1.26 Michaelis-Menten Plot. K_m represents the analytically useful region for substrate.

1.8 Screen Printed Electrodes

The electrochemical process relies on solid electrodes made from gold, carbon, and platinum as inert materials. The electrodes serve as support surfaces for the immobilization of the recognition element and the transducing device. Most electrodes are modified in order to increase sensitivity and selectivity to a particular analyte by immobilizing a selective layer on the transducer surface. These electrodes have the advantages of being inexpensive, planar, miniature, disposable, and thick film electrodes. In most cases, these electrodes are pocket-sized and are easy to monitor on site. The use of screen-printed electrodes in electroanalysis is now common due to their high conductivity, ease of fabrication, electrochemical activity, and low cost [201]. Commercially available electrodes made from carbon and platinum have been successfully used in sensor applications. For the purposes of this thesis, SPEs refer only to gold-based electrodes. Electrodes of this type have been used to detect electroactive compounds such as dopamine, detect heavy metals, and construct biosensors using enzymes and antibodies.

1.9 Statistical Analysis

To create a biosensor system that is efficient and proficient, it is crucial to meet both static and dynamic requirements. These specifications can be employed to enhance the effectiveness of biosensors for commercial use. In order to set standards for statistical analysis, a meticulous validation process is necessary. The main goal of this validation process is to assess the performance of the analytical technique and to prove that the analytical system is functioning under a state of statistical control. This

"state of statistical control" implies that all sources of error have been identified and characterized statistically, and they remain consistent [202].

1.9.1 Validation

Validation of an analytical method is the process by which it is established, by laboratory studies, that the performance characteristics of the method meet the requirements for the intended analytical applications. In this section we provide validation features which include linear Range, limit of detection, sensitivity, selectivity, as well as accuracy and precision."

When outlining the results these characteristics should be clearly identified in the method description so that the suitability of the method for the specific application can be assessed.

1.9.1.1 Linear Range

The range of calibration for an analytical method refers to the range of concentrations of analytes in a sample that has been shown to be precise, accurate, and linear. This range is usually determined through linearity studies and varies depending on the purpose of the procedure.

1.9.1.2 Limit of Detection

It is the lowest amount of a substance that the sensor signal can distinguish without a control sample. This characteristic is considered highly valuable when estimated accurately. The analyst can expect to detect the smallest concentration of analyte with a certain level of confidence, and the International Union of Pure and Applied Chemistry (IUPAC) recommends relating the limit of detection to the smallest

measure of response that can be detected with reasonable certainty in a given analytical method [203]. According to this definition, the equation 1.12 is used to determine the detection limit in terms of concentration (CL) or amount (qL) based on (xL), the smallest detectable measure of response.

$$CL \text{ (or } qL) = ks_B/b$$

The recommended value for the limit of detection (LOD) can be calculated using Equation 1.12, which takes into account the standard deviation of the blank (sB) and the sensitivity of the method (b), expressed as the slope of the calibration curve. According to IUPAC, a value of k = 3 is recommended for LOD based on the confidence interval.

1.9.1.3 Selectivity

Selectivity pertains to the degree to which a specific constituent within a substance can be identified without being impacted by other constituents in the same substance. A technique that is completely selective for a certain factor is considered to be precise; however, very few analytical methods are entirely precise for a given factor, and therefore cross-react with other substances. This is because both the factor of interest and other substances contribute to the analytical signal and cannot be distinguished from one another. The impact of this interference on the signal can be either positive or negative, depending on the type of interaction between the factor of interest and interfering species.

1.9.1.3 Sensitivity

The sensitivity of a method is defined as the smallest concentration difference in a variable that can be detected with a certain level of probability, and it can be determined by calculating the slope of a calibration curve. To determine the concentration of an unknown variable, most analytical methods require the establishment of a calibration curve, which involves plotting the instrumental response (y) against the variable concentration (x) and using linear regression analysis to determine the relationship between y and x in the linear range. Equation 1.13 expresses the calibration function.

$$y = mx + C$$

Equation 1.13: Equation of a straight line

Assuming that "c" represents the y-intercept and "m" represents the slope, having more data points to construct the calibration curve will improve the accuracy of the slope as long as the calibration curve is within the method's linear response range. It's crucial to ensure that the measurement matrix used to analyse the samples and establish the calibration curve is physically and chemically identical for both the samples and standards.

1.9.1.4 Accuracy and Precision

The concept of "accuracy" refers to the deviation between the real or expected value and the value that is actually obtained. Typically, accuracy is a combination of systematic error or bias and random error. Random errors stem from unpredictable and unregulated changes in the conditions of the analytical system during various analyses. Examples of sources that can lead to random errors include changes in instrumental conditions, discrepancies in the physical and chemical properties of samples or reagents across different occasions, and inconsistencies in reading results/scales that can be attributed to the analyst. Table 1.5 provides a breakdown of the sources that give rise to systematic errors or biases.

Table 1.5 Table of validation characteristics.

Sample instabilities between sample collection and analysis
Deficiencies in determining all relevant forms of the variable
Calibration with bias
Incorrect blank estimation

In general, 'precision' refers to the degree of agreement between repeated analyses. This degree of agreement can be numerically defined by using the parameter standard deviation or relative standard deviation.

1.9.1.5 Repeatability and Reproducibility

A crucial aspect of designing an analytical device is ensuring that it consistently produces results within an acceptable margin of error across multiple tests. Repeating experiments multiple times (n > 3) and obtaining the same results eliminates any uncertainty regarding the accuracy of the obtained results. This is an indicator of the device's effectiveness, as it allows other operators in different laboratories to achieve identical results when performing the same tests. This process also validates the device's performance.

1.9.1.6 Percentage Recovery

The term "percentage recovery" is frequently used in organic and inorganic chemistry when determining the yield of a reaction or purification process. This metric is indicative of the quality of the experiment and the accuracy of the procedures employed. The percentage recovery is typically calculated using equation 1.14.

$$\%\ \text{Recovery} = \frac{\text{Amount recovered}}{\text{Initial amount}} \text{x} \frac{100}{1}$$

Equation 1.14: % Recovery:

1.9.1.7 Correlation

The correlation coefficient is a metric used to quantify how well a curve or line fits a particular plot. The closer the value of the correlation coefficient is to one, the more precise the fit is considered to be, while the opposite is also true. Typically, the correlation coefficient is represented by R2.

1.10 Reference

1. Stuart-Smith, S.J.; Jepson, P.D. Persistent threats need persistent counteraction: Responding to PCB pollution in marine mammals. *Mar. Policy* **2017**, *84*, 69–75, doi:10.1016/j.marpol.2017.06.033.

2. Ayris, S.; Harrad, S. The fate and persistence of polychlorinated biphenyls in soil. *J. Environ. Monit.* **1999**, *1*, 395–401, doi:10.1039/a903017d.

3. Ross, G. The public health implications of polychlorinated biphenyls (PCBs) in the environment. *Ecotoxicol. Environ. Saf.* **2004**, *59*, 275–291.

4. Ngom, B.; Guo, Y.; Wang, X.; Bi, D. Development and application of lateral flow test strip technology for detection of infectious agents and chemical contaminants: a review. *Anal. Bioanal. Chem.* **2010**, *397*, 1113–1135.

5. Teles, F.S.R.R. Biosensors and rapid diagnostic tests on the frontier between analytical and clinical chemistry for biomolecular diagnosis of dengue disease: A review. *Anal. Chim. Acta* **2011**, *687*, 28–42.

6. Ricci, F.; Volpe, G.; Micheli, L.; Palleschi, G. A review on novel developments and applications of immunosensors in food analysis. *Anal. Chim. Acta* **2007**, *605*, 111–129.

7. Bojorge Ramírez, N.; Salgado, A.M.; Valdman, B. The evolution and developments of immunosensors for health and environmental monitoring: problems and perspectives. *Brazilian J. Chem. Eng.* **2009**, *26*, 227–249.

8. Bender, S.; Sadik, O.A. Direct electrochemical immunosensor for polychlorinated biphenyls. *Environ. Sci. Technol.* **1998**, *32*, 788–797.

9. Harfield, J.C.; Batchelor-McAuley, C.; Compton, R.G. Electrochemical determination of glutathione: a review. *Analyst* **2012**, *137*, 2285–2296.

10. Aydin, E.B.; Aydin, M.; Sezgintürk, M.K. Advances in electrochemical immunosensors. *Adv. Clin. Chem.* **2019**, *92*, 1–57.

11. Kłos-Witkowska, A. The phenomenon of fluorescence in immunosensors. *Acta Biochim. Pol.* **2016**, *63*, 215–221.

12. Ahmed, F.E. Analysis of polychlorinated biphenyls in food products. *TrAC trends Anal. Chem.* **2003**, *22*, 170–185.

13. Baroudi, F.; Al-Alam, J.; Chimjarn, S.; Delhomme, O.; Fajloun, Z.; Millet, M. Conifers as environmental biomonitors: A multi-residue method for the concomitant quantification of pesticides, polycyclic aromatic hydrocarbons and polychlorinated biphenyls by LC-MS/MS and GC–MS/MS. *Microchem. J.* **2020**, *154*, 104593, doi:10.1016/J.MICROC.2019.104593.

14. Jones, K.C.; De Voogt, P. Persistent organic pollutants (POPs): state of the science. *Environ. Pollut.* **1999**, *100*, 209–221.

15. Alharbi, O.M.L.; Khattab, R.A.; Ali, I. Health and environmental effects of persistent organic pollutants. *J. Mol. Liq.* **2018**, *263*, 442–453.

16. Vasseghian, Y.; Hosseinzadeh, S.; Khataee, A.; Dragoi, E.-N. The concentration of persistent organic pollutants in water resources: A global systematic review, meta-analysis and probabilistic risk assessment. *Sci. Total Environ.* **2021**, *796*,

149000.

17. Alsefri, S.; Balbaied, T.; Moore, E. Electrochemical Development of an Immunosensor for Detection Polychlorinated biphenyls (PCBs) for Environmental Analysis. **2021**, doi:10.3390/chemosensors9110307.

18. Rodrigues, J.P.; Duarte, A.C.; Santos-Echeandía, J.; Rocha-Santos, T. Significance of interactions between microplastics and POPs in the marine environment: a critical overview. *TrAC Trends Anal. Chem.* **2019**, *111*, 252–260.

19. Ricciardi, M.; Pironti, C.; Motta, O.; Miele, Y.; Proto, A.; Montano, L. Microplastics in the aquatic environment: Occurrence, persistence, analysis, and human exposure. *Water* **2021**, *13*, 973.

20. Pironti, C.; Ricciardi, M.; Motta, O.; Miele, Y.; Proto, A.; Montano, L. Microplastics in the environment: Intake through the food web, human exposure and toxicological effects. *Toxics* **2021**, *9*, 224.

21. Xu, W.; Wang, X.; Cai, Z. Analytical chemistry of the persistent organic pollutants identified in the Stockholm Convention: A review. *Anal. Chim. Acta* **2013**, *790*, 1–13.

22. Zhu, X.; Zhou, D.; Cang, L.; Wang, Y. TiO2 photocatalytic degradation of 4-chlorobiphenyl as affected by solvents and surfactants. *J. Soils Sediments* **2012**, *12*, 376–385, doi:10.1007/s11368-011-0464-y.

23. Mills Iii, S.A.; Thal, D.I.; Barney, J. A summary of the 209 PCB congener nomenclature. *Chemosphere* **2007**, *68*, 1603–1612.

24. Erickson, M.D. Analytical chemistry of PCBs. **1997**.

25. Grimm, F.A.; Hu, D.; Kania-Korwel, I.; Lehmler, H.-J.; Ludewig, G.; Hornbuckle, K.C.; Duffel, M.W.; Bergman, Å.; Robertson, L.W. Metabolism and metabolites of polychlorinated biphenyls. *Crit. Rev. Toxicol.* **2015**, *45*, 245–272.

26. James, R.C.; Busch, H.; Tamburro, C.H.; Roberts, S.M.; Schell, J.D.; Harbison, R.D. Polychlorinated biphenyl exposure and human disease. *J. Occup. Med.* **1993**, 136–148.

27. Spaeth, K. Polychlorinated Biphenyls (PCBs). **2011**.

28. Bernhard, T.; Petron, S. Analysis of PCB Congeners vs . Arcolors in Ecological Risk Assessment. *Issue Pap.* **2001**, 7.

29. Alvares, A.P.; Kappas, A. The inducing properties of polychlorinated biphenyls on hepatic monooxygenases. *Clin. Pharmacol. Ther.* **1977**, *22*, 809–816.

30. Zhu, M.; Yuan, Y.; Yin, H.; Guo, Z.; Wei, X.; Qi, X.; Liu, H.; Dang, Z. Environmental contamination and human exposure of polychlorinated biphenyls (PCBs) in China: A review. *Sci. Total Environ.* **2022**, *805*, 150270.

31. Jones, P.A.; Sloan, R.J.; Brown, M.P. PCB congeners to monitor with caged juvenile fish in the upper Hudson River. *Environ. Toxicol. Chem. An Int. J.* **1989**, *8*, 793–803.

32. Wang, H.; Zhang, C.; Zhang, X.; Wang, S.; Xia, Z.; Zeng, G.; Ding, J.; Ren, N. Construction of Fe3O4@ β-CD/g-C3N4 nanocomposite catalyst for degradation of PCBs in wastewater through photodegradation and heterogeneous Fenton oxidation. *Chem. Eng. J.* **2022**, *429*, 132445.

33. Othman, N.; Ismail, Z.; Selamat, M.I.; Sheikh Abdul Kadir, S.H.; Shibraumalisi, N.A. A Review of Polychlorinated Biphenyls (PCBs) Pollution in the Air: Where and How Much Are We Exposed to? *Int. J. Environ. Res. Public Health* **2022**, *19*, 13923.

34. Carpenter, D.O. Polychlorinated biphenyls (PCBs): routes of exposure and effects on human health. *Rev. Environ. Health* **2006**, *21*, 1–24.

35. Egendorf, S.P.; Gailey, A.D.; Schachter, A.E.; Mielke, H.W. Soil toxicants that potentially affect children's health. *Curr. Probl. Pediatr. Adolesc. Health Care* **2020**, *50*, 100741.

36. Li, W.; Achal, V. Environmental and health impacts due to e-waste disposal in China–A review. *Sci. Total Environ.* **2020**, *737*, 139745.

37. Fisher, B.E. Most unwanted. *Environ. Health Perspect.* **1999**, *107*, A18–A23.

38. Gauger, K.J.; Kato, Y.; Haraguchi, K.; Lehmler, H.-J.; Robertson, L.W.; Bansal, R.; Zoeller, R.T. Polychlorinated biphenyls (PCBs) exert thyroid hormone-like effects in the fetal rat brain but do not bind to thyroid hormone receptors. *Environ. Health Perspect.* **2004**, *112*, 516–523.

39. Montano, L.; Pironti, C.; Pinto, G.; Ricciardi, M.; Buono, A.; Brogna, C.; Venier, M.; Piscopo, M.; Amoresano, A.; Motta, O. Polychlorinated biphenyls (PCBs) in the environment: occupational and exposure events, effects on human health and fertility. *Toxics* **2022**, *10*, 365.

40. Dumanoglu, Y.; Gaga, E.O.; Gungormus, E.; Sofuoglu, S.C.; Odabasi, M. Spatial and seasonal variations, sources, air-soil exchange, and carcinogenic risk assessment for PAHs and PCBs in air and soil of Kutahya, Turkey, the province of thermal power plants. *Sci. Total Environ.* **2017**, *580*, 920–935.

41. Hao, Y.; Li, Y.; Han, X.; Wang, T.; Yang, R.; Wang, P.; Xiao, K.; Li, W.; Lu, H.; Fu, J. Air monitoring of polychlorinated biphenyls, polybrominated diphenyl ethers and organochlorine pesticides in West Antarctica during 2011–2017: Concentrations, temporal trends and potential sources. *Environ. Pollut.* **2019**, *249*, 381–389.

42. Hu, J.; Zheng, M.; Liu, W.; Nie, Z.; Li, C.; Liu, G.; Xiao, K. Characterization of polychlorinated dibenzo-p-dioxins and dibenzofurans, dioxin-like polychlorinated biphenyls, and polychlorinated naphthalenes in the environment surrounding secondary copper and aluminum metallurgical facilities in China. *Environ. Pollut.* **2014**, *193*, 6–12.

43. Robinson, B.H. E-waste: an assessment of global production and environmental impacts. *Sci. Total Environ.* **2009**, *408*, 183–191.

44. Kumar, S.; Singh, V. E-Waste: Generation, environmental and health impacts, recycling and status of e-waste legislation. *J. Emerg. Technol. Innov. Res.* **2019**, *6*, 592–600.

45. Gantsho, N. Health effects of polychlorinated biphenyls (PCBs): allergies in the workplace. *Curr. Allergy Clin. Immunol.* **2011**, *24*, 162–164.

46. Awasthi, A.K.; Zeng, X.; Li, J. Relationship between e-waste recycling and human health risk in India: a critical review. *Environ. Sci. Pollut. Res.* **2016**, *23*, 11509–11532.

47. Ahmed, F.E. Chemical Health Risk Assessment–Critique of Existing Practices and Suggestions for Improvement. In *Seafood Safety*; National Academies Press (US), 1991.

48. Diaz, J.H.; Hu, C. Health risks and benefits of seafood consumption. *Trop. Med. Health* **2009**, *37*, 79–95.

49. Pawełczyk, A. Assessment of health risk associated with persistent organic pollutants in water. *Environ. Monit. Assess.* **2013**, *185*, 497–508.

50. Ritter Paul Sibley, Ken Hall, Patricia Keen, Gevan Mattu, Beth Linton, Len, K.S. Sources, pathways, and relative risks of contaminants in surface water and groundwater: a perspective prepared for the Walkerton inquiry. *J. Toxicol. Environ. Heal. Part A* **2002**, *65*, 1–142.

51. Weschler, C.J. Changes in indoor pollutants since the 1950s. *Atmos. Environ.* **2009**, *43*, 153–169, doi:10.1016/j.atmosenv.2008.09.044.

52. Mathematics, A. POLYCHLORINATED BIPHENYLS (PCBs): A NEW HAZARD FOR HISTORIC BUILDINGS Emily J. Sinitski Submitted. **2016**, 1–23.

53. Borja, J.; Taleon, D.M.; Auresenia, J.; Gallardo, S. Polychlorinated biphenyls and their biodegradation. *Process Biochem.* **2005**, *40*, 1999–2013, doi:10.1016/j.procbio.2004.08.006.

54. Zeng, J.; Wang, Q.; Gao, J.; Wang, W.; Shen, H.; Cao, Y.; Hu, M.; Bi, W.; Gan, N.

Magnetic stir bars with hyperbranched aptamer as coating for selective, effective headspace extraction of trace polychlorinated biphenyls in soils. *J. Chromatogr. A* **2020**, *1614*, 460715.

55. Vane, C.H.; Kim, A.W.; Beriro, D.J.; Cave, M.R.; Knights, K.; Moss-Hayes, V.; Nathanail, P.C. Polycyclic aromatic hydrocarbons (PAH) and polychlorinated biphenyls (PCB) in urban soils of Greater London, UK. *Appl. Geochemistry* **2014**, *51*, 303–314.

56. Kim, A.W.; Vane, C.H.; Moss-Hayes, V.L.; Beriro, D.J.; Nathanail, C.P.; Fordyce, F.M.; Everett, P.A. Polycyclic aromatic hydrocarbons (PAHs) and polychlorinated biphenyls (PCBs) in urban soils of Glasgow, UK. *Earth Environ. Sci. Trans. R. Soc. Edinburgh* **2017**, *108*, 231–247.

57. Ododo, M.M.; Wabalo, B.K. Polychlorinated Biphenyls (PCBs) and Their Impacts on Human Health : A Review. *J. Environ. Pollut. Hum. Heal.* **2019**, *7*, 73–77, doi:10.12691/jephh-7-2-3.

58. Di Lenola, M.; Barra Caracciolo, A.; Grenni, P.; Ancona, V.; Rauseo, J.; Laudicina, V.A.; Uricchio, V.F.; Massacci, A. Effects of Apirolio Addition and Alfalfa and Compost Treatments on the Natural Microbial Community of a Historically PCB-Contaminated Soil. *Water. Air. Soil Pollut.* **2018**, *229*, doi:10.1007/s11270-018-3803-4.

59. Biziuk, M. Environmental fate and global distribution of polychlorinated biphenyls Related papers Environmental Fate and Global Distribution of Polychlorinated Biphenyls ARTICLE in REVIEWS OF ENVIRONMENTAL CONTAMINATION AND TOXICOLOGY · FEBRUARY 2009., doi:10.1007/978-1-

4419-0032-6_5.

60. Martin, I.; Cowie, C. *Using Science to Create a Better Place: Compilation of Data for Priority Organic Pollutants for Derivation of Soil Guideline Values*; Environment Agency, 2008; ISBN 184432964X.

61. De Mul, A.; Bakker, M.I.; Zeilmaker, M.J.; Traag, W.A.; van Leeuwen, S.P.J.; Hoogenboom, R.L.A.P.; Boon, P.E.; van Klaveren, J.D. Dietary exposure to dioxins and dioxin-like PCBs in The Netherlands anno 2004. *Regul. Toxicol. Pharmacol.* **2008**, *51*, 278–287.

62. Aslam, I.; Baqar, M.; Qadir, A.; Mumtaz, M.; Li, J.; Zhang, G. Polychlorinated biphenyls in indoor dust from urban dwellings of Lahore, Pakistan: Congener profile, toxicity equivalency, and human health implications. *Indoor Air* **2021**, *31*, 1417–1426.

63. Liu, X.; Sakthivel, R.; Cheng, C.-Y.; Luo, J.; Song, L.; Wu, J.; He, W.; Younis, U.; Chung, R.-J. 3A-Amino-3A-Deoxy-(2AS, 3AS)-β-Cyclodextrin Hydrate/Tin Disulfide Modified Screen-Printed Carbon Electrode for the Electrochemical Detection of Polychlorinated Biphenyls., doi:10.1186/s11671-019-3236-z.

64. Verma, M.L.; Rani, V. Biosensors for toxic metals, polychlorinated biphenyls, biological oxygen demand, endocrine disruptors, hormones, dioxin, phenolic and organophosphorus compounds: a review. *Environ. Chem. Lett.* **2021**, *19*, 1657–1666.

65. Combustions, I.; Cancer, I.A. for R. on IARC monographs on the evaluation of carcinogenic risks to humans, vol. 100 (E). *Lyon IARC* **1997**.

66. Lim, J.; Nam, C.; Yang, J.; Rha, K.H.; Lim, K.-M.; Jee, S.H. Serum persistent organic pollutants (POPs) and prostate cancer risk: A case-cohort study. *Int. J. Hyg. Environ. Health* **2017**, *220*, 849–856.

67. Lerro, C.C.; Jones, R.R.; Langseth, H.; Grimsrud, T.K.; Engel, L.S.; Sjödin, A.; Choo-Wosoba, H.; Albert, P.; Ward, M.H. A nested case-control study of polychlorinated biphenyls, organochlorine pesticides, and thyroid cancer in the Janus Serum Bank cohort. *Environ. Res.* **2018**, *165*, 125–132.

68. Cheng, Z.; Zhang, X.; Bassig, B.; Hauser, R.; Holford, T.R.; Zheng, E.; Shi, D.; Zhu, Y.; Schwartz, S.M.; Chen, C. Serum polychlorinated biphenyl (PCB) levels and risk of testicular germ cell tumors: a population-based case-control study in Connecticut and Massachusetts. *Environ. Pollut.* **2021**, *273*, 116458.

69. Parada Jr, H.; Sun, X.; Tse, C.-K.; Engel, L.S.; Hoh, E.; Olshan, A.F.; Troester, M.A. Plasma levels of polychlorinated biphenyls (PCBs) and breast cancer mortality: The Carolina Breast Cancer Study. *Int. J. Hyg. Environ. Health* **2020**, *227*, 113522.

70. Koual, M.; Cano-Sancho, G.; Bats, A.-S.; Tomkiewicz, C.; Kaddouch-Amar, Y.; Douay-Hauser, N.; Ngo, C.; Bonsang, H.; Deloménie, M.; Lecuru, F. Associations between persistent organic pollutants and risk of breast cancer metastasis. *Environ. Int.* **2019**, *132*, 105028.

71. Faroon, O.; Ruiz, P. Polychlorinated biphenyls: New evidence from the last decade. *Toxicol. Ind. Health* **2016**, *32*, 1825–1847.

72. Arrebola, J.P.; Fernández, M.F.; Martín-Olmedo, P.; Molina-Molina, J.M.; Sánchez-Pérez, M.J.; Sánchez-Cantalejo, E.; Molina-Portillo, E.; Expósito, J.; Bonde, J.P.; Olea, N. Adipose tissue concentrations of persistent organic pollutants and total cancer risk in an adult cohort from Southern Spain: preliminary data from year 9 of the follow-up. *Sci. Total Environ.* **2014**, *500*, 243–249.

73. Charles, D.; Berg, V.; Nøst, T.H.; Bergdahl, I.A.; Huber, S.; Ayotte, P.; Wilsgaard, T.; Averina, M.; Sandanger, T.; Rylander, C. Longitudinal changes in concentrations of persistent organic pollutants (1986–2016) and their associations with type 2 diabetes mellitus. *Environ. Res.* **2022**, *204*, 112129.

74. Mansouri, E.H.; Reggabi, M. Association between type 2 diabetes and exposure to chlorinated persistent organic pollutants in Algeria: A case-control study. *Chemosphere* **2021**, *264*, 128596.

75. Aminov, Z.; Carpenter, D.O. Serum concentrations of persistent organic pollutants and the metabolic syndrome in Akwesasne Mohawks, a Native American community. *Environ. Pollut.* **2020**, *260*, 114004.

76. Pruvost-Couvreur, M.; Béchaux, C.; Rivière, G.; Le Bizec, B. Impact of sociodemographic profile, generation and bioaccumulation on lifetime dietary and internal exposures to PCBs. *Sci. Total Environ.* **2021**, *800*, 149511.

77. Matovu, H.; Li, Z.-M.; Henkelmann, B.; Bernhöft, S.; De Angelis, M.; Schramm, K.-W.; Sillanpää, M.; Kato, C.D.; Ssebugere, P. Multiple persistent organic

pollutants in mothers' breastmilk: Implications for infant dietary exposure and maternal thyroid hormone homeostasis in Uganda, East Africa. *Sci. Total Environ.* **2021**, *770*, 145262.

78. Guo, F.; Yin, S.; Wang, H.; Zhang, J.; Liu, Y.; Aamir, M.; Liu, W. Polychlorinated biphenyls (PCBs) in the colostrum samples from the Yangtze River Region: Exposure profile and risk assessment. *Environ. Pollut.* **2021**, *285*, 117253.

79. Cancer, I.A. for R. on *IARC monographs on the evaluation of the carcinogenic risk of chemicals to humans. Vol. 21. Sex hormones (II).*; Distributed for IARC by WHO, Geneva, Switzerland, 1979; ISBN 9283212215.

80. Sawatsubashi, T.; Tsukahara, C.; Baba, K.; Ohi, E.; Shinoda, A.; Miura, N. Development of new-type rapid analysis technology of polychlorinated biphenyls by using liquid chromatographic clean-up material (polyvinyl alcohol gel). *J. Chromatogr. A* **2008**, *1177*, 138–149.

81. Schantz, M.M.; Bøwadt, S.; Benner Jr, B.A.; Wise, S.A.; Hawthorne, S.B. Comparison of supercritical fluid extraction and Soxhlet extraction for the determination of polychlorinated biphenyls in environmental matrix standard reference materials. *J. Chromatogr. A* **1998**, *816*, 213–220.

82. Żwir-Ferenc, A.; Biziuk, M. Solid Phase Extraction Technique--Trends, Opportunities and Applications. *Polish J. Environ. Stud.* **2006**, *15*.

83. Hawthorne, S.B.; Miller, D.J. Directly coupled supercritical fluid extraction—gas chromatographic analysis of polycyclic aromatic hydro-carbons and polychlorinated biphenyls from environmental solids. *J. Chromatogr. A* **1987**,

403, 63–76.

84. Hackett, M.; Wang, H.; Miller, G.C.; Bornhop, D.J. Ultraviolet-visible detection for capillary gas chromatography and combined ultraviolet-mass spectrometry using a remote flow cell. *J. Chromatogr. A* **1995**, *695*, 243–257.

85. *Direct Electrochemical Immunosensor for Polychlorinated Biphenyls*; **1998**.

86. Rezaee, M.; Yamini, Y.; Faraji, M. Evolution of dispersive liquid–liquid microextraction method. *J. Chromatogr. A* **2010**, *1217*, 2342–2357.

87. Ferrario, J.; Byrne, C.; Dupuy Jr, A.E. Background contamination by coplanar polychlorinated biphenyls (PCBs) in trace level high resolution gas chromatography/high resolution mass spectrometry (HRGC/HRMS) analytical procedures. *Chemosphere* **1997**, *34*, 2451–2465.

88. Laschi, S.; Fránek, M.; Mascini, M. Screen-printed electrochemical immunosensors for PCB detection. *Electroanalysis* **2000**, *12*, 1293–1298, doi:10.1002/1521-4109(200011)12:16<1293::AID-ELAN1293>3.0.CO;2-5.

89. Engvall, E. [28] Enzyme immunoassay ELISA and EMIT. In *Methods in enzymology*; Elsevier, 1980; Vol. 70, pp. 419–439 ISBN 0076-6879.

90. Lequin, R.M. Enzyme immunoassay (EIA)/enzyme-linked immunosorbent assay (ELISA). *Clin. Chem.* **2005**, *51*, 2415–2418.

91. Shah, K.; Maghsoudlou, P. Enzyme-linked immunosorbent assay (ELISA): the basics. *Br. J. Hosp. Med.* **2016**, *77*, C98–C101.

92. Ahmad, A.; Moore, E. Electrochemical immunosensor modified with self-

assembled monolayer of 11-mercaptoundecanoic acid on gold electrodes for detection of benzo[a]pyrene in water. *Analyst* **2012**, *137*, 5839–5844, doi:10.1039/c2an35236b.

93. Haji-Hashemi, H.; Norouzi, P.; Safarnejad, M.R.; Ganjali, M.R. Label-free electrochemical immunosensor for direct detection of Citrus tristeza virus using modified gold electrode. *Sensors Actuators B Chem.* **2017**, *244*, 211–216, doi:10.1016/J.SNB.2016.12.135.

94. Khesuoe, M.P.; Okumu, F.O.; Matoetoe, M.C. Development of a silver functionalised polyaniline electrochemical immunosensor for polychlorinated biphenyls †. **2016**, doi:10.1039/c6ay01733a.

95. Cristea, C.; Florea, A.; Tertiș, M.; Săndulescu, R. Immunosensors. In *Biosensors-micro and nanoscale applications*; IntechOpen, 2015 ISBN 9535121731.

96. Hage, D.S. Immunoassays. *Anal. Chem.* **1999**, *71*, 294–304.

97. Vashist, S.K.; Luong, J.H.T. Immunoassays: an overview. *Handb. Immunoass. Technol.* **2018**, 1–18.

98. McBain, A.M. Enzyme immunoassay as an analytical tool in clinical chemistry **1988.**

99. Banica, F.-G. *Chemical sensors and biosensors: fundamentals and applications*; John Wiley & Sons, **2012**; ISBN 1118354230.

100. Clark Jr, L.C.; Lyons, C. Electrode systems for continuous monitoring in cardiovascular surgery. *Ann. N. Y. Acad. Sci.* **1962**, *102*, 29–45.

101. Mao, K.; Zhang, H.; Pan, Y.; Yang, Z. Biosensors for wastewater-based epidemiology for monitoring public health. *Water Res.* **2021**, *191*, 116787.

102. Dennison, M.J.; Turner, A.P.F. Biosensors for environmental monitoring. *Biotechnol. Adv.* **1995**, *13*, 1–12.

103. Oh, Y.; Lee, Y.; Heath, J.; Kim, M. Applications of animal biosensors: a review. *IEEE Sens. J.* **2014**, *15*, 637–645.

104. Mishra, G.K.; Barfidokht, A.; Tehrani, F.; Mishra, R.K. Food safety analysis using electrochemical biosensors. *Foods* **2018**, *7*, 141.

105. Alhadrami, H.A. Biosensors: Classifications, medical applications, and future prospective. *Biotechnol. Appl. Biochem.* **2018**, *65*, 497–508.

106. Byfield, M.P.; Abuknesha, R.A. Biochemical aspects of biosensors. *Biosens. Bioelectron.* **1994**, *9*, 373–399.

107. Turner, A.; Karube, I.; Wilson, G.S. *Biosensors: fundamentals and applications*; Oxford university press, **1987**.

108. Thevenot, D.R.; Toth, K.; Durst, R.A.; Wilson, G.S. Electrochemical biosensors: recommended definitions and classification. *Pure Appl. Chem.* **1999**, *71*, 2333–2348.

109. Perumal, V.; Hashim, U. Advances in biosensors: Principle, architecture and applications. *J. Appl. Biomed.* **2014**, *12*, 1–15, doi:https://doi.org/10.1016/j.jab.2013.02.001.

110. Srivastava, S.K.; Van Rijn, C.J.M.; Jongsma, M.A. Biosensor-based detection of

tuberculosis. *RSC Adv.* **2016**, *6*, 17759–17771.

111. Farré, M.; Kantiani, L.; Pérez, S.; Barceló, D. Sensors and biosensors in support of EU Directives. *TrAC Trends Anal. Chem.* **2009**, *28*, 170–185.

112. Ronkainen, N.J.; Halsall, H.B.; Heineman, W.R. Electrochemical biosensors. *Chem. Soc. Rev.* **2010**, *39*, 1747–1763.

113. Grieshaber, D.; MacKenzie, R.; Vörös, J.; Reimhult, E. Electrochemical biosensors-sensor principles and architectures. *Sensors* **2008**, *8*, 1400–1458.

114. Palchetti, I.; Mascini, M. Biosensor technology: a brief history. In *Sensors and Microsystems: AISEM 2009 Proceedings*; Springer, **2009**; pp. 15–23.

115. Naresh, V.; Lee, N. A review on biosensors and recent development of nanostructured materials-enabled biosensors. *Sensors* **2021**, *21*, 1109.

116. Chambers, J.P.; Arulanandam, B.P.; Matta, L.L.; Weis, A.; Valdes, J.J. Biosensor recognition elements. *Curr. Issues Mol. Biol.* **2008**, *10*, 1–12.

117. Bennett, T.P.; Frieden, E. Modern topics in biochemistry; structure and function of biological molecules. **1966**.

118. Dai, Z.; Yan, F.; Chen, J.; Ju, H. Reagentless amperometric immunosensors based on direct electrocehmistry of HRP for determination of carcinoma antigen. *Anal. Chem.* **2003**, *75*, 125.

119. Kuhlmann, W.D.; Peschke, P. Glucose oxidase as label in histological immunoassays with enzyme-amplification in a two-step technique: coimmobilized horseradish peroxidase as secondary system enzyme for

chromogen oxidation. *Histochemistry* **1986**, *85*, 13–17.

120. Aizawa, M.; Morioka, A.; Suzuki, S. An enzyme immunosensor for the electrochemical determination of the tumor antigen α-fetoprotein. *Anal. Chim. Acta* **1980**, *115*, 61–67.

121. Kim, E.E.; Wyckoff, H.W. Reaction mechanism of alkaline phosphatase based on crystal structures: Two-metal ion catalysis. *J. Mol. Biol.* **1991**, *218*, 449–464, doi:https://doi.org/10.1016/0022-2836(91)90724-K.

122. Wang, J.H.; Wang, K.; Bartling, B.; Liu, C.-C. The detection of alkaline phosphatase using an electrochemical biosensor in a single-step approach. *Sensors* **2009**, *9*, 8709–8721.

123. Bianchi, A.; Giachetti, E.; Vanni, P. A continuous spectrophotometric assay for alkaline phosphatase with glycerophosphate as substrate. *J. Biochem. Biophys. Methods* **1994**, *28*, 35–41.

124. Morgenstern, S.; Kessler, G.; Auerbach, J.; Flor, R. V; Klein, B. An automated p-nitrophenylphosphate serum alkaline phosphatase procedure for the AutoAnalyzer. *Clin. Chem.* **1965**, *11*, 876–888.

125. Gong, H.; Little, G.; Cradduck, M.; Draney, D.R.; Padhye, N.; Olive, D.M. Alkaline phosphatase assay using a near-infrared fluorescent substrate merocyanine 700 phosphate. *Talanta* **2011**, *84*, 941–946.

126. Wijayawardhana, C.A.; Halsall, H.B.; Heineman, W.R. Micro volume rotating disk electrode (RDE) amperometric detection for a bead-based immunoassay. *Anal. Chim. Acta* **1999**, *399*, 3–11.

127. Ronkainen-Matsuno, N.J.; Thomas, J.H.; Halsall, H.B.; Heineman, W.R. Electrochemical immunoassay moving into the fast lane. *TrAC Trends Anal. Chem.* **2002**, *21*, 213–225.

128. Ma, H.; O'Kennedy, R. The structure of natural and recombinant antibodies. *Pept. Antibodies Methods Protoc.* **2015**, 7–11.

129. Schroeder Jr, H.W.; Cavacini, L. Structure and function of immunoglobulins. *J. Allergy Clin. Immunol.* **2010**, *125*, S41–S52.

130. Pereira, E.P. V; van Tilburg, M.F.; Florean, E.O.P.T.; Guedes, M.I.F. Egg yolk antibodies (IgY) and their applications in human and veterinary health: A review. *Int. Immunopharmacol.* **2019**, *73*, 293–303, doi:10.1016/j.intimp.2019.05.015.

131. Ereño-Orbea, J.; Sicard, T.; Cui, H.; Carson, J.; Hermans, P.; Julien, J.-P. Structural basis of enhanced crystallizability induced by a molecular chaperone for antibody antigen-binding fragments. *J. Mol. Biol.* **2018**, *430*, 322–336.

132. Crowther, J.R. *The ELISA guidebook*; Springer, **2009**; Vol. 566;.

133. Leenaars, M.; Hendriksen, C.F.M. Critical steps in the production of polyclonal and monoclonal antibodies: evaluation and recommendations. *ILAR J.* **2005**, *46*, 269–279.

134. Halilovic, A.; Merdan, E.; Kovacevic, Z.; Pokvic, L.G. Review of Biosensors for Environmental Field Monitoring. *2019 8th Mediterr. Conf. Embed. Comput. MECO 2019 - Proc.* **2019**, 10–14, doi:10.1109/MECO.2019.8760166.

135. Damborský, P.; Švitel, J.; Katrlík, J. Optical biosensors. *Essays Biochem.* **2016**, *60*, 91–100, doi:10.1042/EBC20150010.

136. Das, P.; Fatehbasharzad, P.; Colombo, M.; Fiandra, L.; Prosperi, D. Multifunctional Magnetic Gold Nanomaterials for Cancer. *Trends Biotechnol.* **2019**, *37*, 995–1010, doi:10.1016/j.tibtech.2019.02.005.

137. Ahmad, R.; Khan, M.; Mishra, P.; Jahan, N.; Ahsan, M.A.; Ahmad, I.; Khan, M.R.; Watanabe, Y.; Syed, M.A.; Furukawa, H. Engineered hierarchical CuO nanoleaves based electrochemical nonenzymatic biosensor for glucose detection. *J. Electrochem. Soc.* **2021**, *168*, 17501.

138. Dhal, A.; Kalyani, T.; Ghorai, S.; Kumar, N.; Kumar, S. Recent development of electrochemical immunosensor for the diagnosis of dengue virus NSI protein : A review. *Sensors Int.* **2020**, *1*, 100030, doi:10.1016/j.sintl.2020.100030.

139. Aspland, J.R.; Hennion, M.-C. Chapter 6 - Immunochemical Methods and Biosensors. In *Trace Determination of Pesticides and their Degradation Products in Water*; Barceló, D., Hennion, M.-C., Eds.; Techniques and Instrumentation in Analytical Chemistry; Elsevier, **1997**; Vol. 19, pp. 429–517.

140. Hasan-abad, A.M.; Esmaili, M.A.; Ghotaslou, A.; Atapour, A.; Khoshroo, A.; Naghian, E.; Diseases, A.; Hospital, S.B.; Sciences, M.; Health, N. A Review: Electrochemical Biosensors for Testosterone Detection. **2022**, *14*, 1060–1077.

141. Forster, R.J.; Keyes, T.E.; Zoski, C.G. Handbook of Electrochemistry **2007**.

142. Eliaz, N.; Gileadi, E. *Physical electrochemistry: fundamentals, techniques, and applications*; John Wiley & Sons, **2019**; ISBN 3527341390.

143. Murphy, B.; Horner, G.; Tarcy, D.; Bylikin, S. *Oxford IB Diploma Programme: Chemistry Course Companion*; Oxford University Press-Children, **2014**; ISBN 0198307691.

144. Agar, J.N. Diffusion and convection at electrodes. *Discuss. Faraday Soc.* **1947**, *1*, 26–37.

145. Bard, A.J.; Faulkner, L.R. Fundamentals and applications: electrochemical methods. *Electrochem. Methods* **2001**, *2*, 580–632.

146. Kaifer, A.E.; Gómez-Kaifer, M. *Supramolecular electrochemistry*; John Wiley & Sons, **2008**; ISBN 3527613617.

147. Takeda, M.; Shiku, H.; Ino, K.; Matsue, T. Electrochemical chip integrating scalable ring–ring electrode array to detect secreted alkaline phosphatase. *Analyst* **2011**, *136*, 4991–4996.

148. Dossi, N.; Susmel, S.; Toniolo, R.; Pizzariello, A.; Bontempelli, G. Application of microchip electrophoresis with electrochemical detection to environmental aldehyde monitoring. *Electrophoresis* **2009**, *30*, 3465–3471.

149. Kumar, S.; Kalkal, A. Electrochemical detection: Cyclic voltammetry/differential pulse voltammetry/impedance spectroscopy. In *Nanotechnology in Cancer Management*; Elsevier, **2021**; pp. 43–71.

150. Yu, C.J.; Wan, Y.; Yowanto, H.; Li, J.; Tao, C.; James, M.D.; Tan, C.L.; Blackburn, G.F.; Meade, T.J. Electronic detection of single-base mismatches in DNA with ferrocene-modified probes. *J. Am. Chem. Soc.* **2001**, *123*, 11155–11161.

151. Xing, Y.F.; O'Shea, S.J.; Li, S.F.Y. Electron transfer kinetics across a dodecanethiol monolayer self assembled on gold. *J. Electroanal. Chem.* **2003**, *542*, 7–11, doi:10.1016/S0022-0728(02)01440-7.

152. Hleli, S.; Martelet, C.; Abdelghani, A.; Burais, N.; Jaffrezic-Renault, N. Atrazine analysis using an impedimetric immunosensor based on mixed biotinylated self-assembled monolayer. *Sensors Actuators B Chem.* **2006**, *113*, 711–717.

153. Billah, M.; Hays, H.C.W.; Millner, P.A. Development of a myoglobin impedimetric immunosensor based on mixed self-assembled monolayer onto gold. *Microchim. Acta* **2008**, *160*, 447–454.

154. Kumlanghan, A.; Liu, J.; Thavarungkul, P.; Kanatharana, P.; Mattiasson, B. Microbial fuel cell-based biosensor for fast analysis of biodegradable organic matter. *Biosens. Bioelectron.* **2007**, *22*, 2939–2944.

155. Wang, J.; Carmon, K.S.; Luck, L.A.; Suni, I.I. Electrochemical impedance biosensor for glucose detection utilizing a periplasmic E. coli receptor protein. *Electrochem. Solid-State Lett.* **2005**, *8*, H61.

156. Mikkelsen, S.R.; Rechnitz, G.A. Conductometric tranducers for enzyme-based biosensors. *Anal. Chem.* **1989**, *61*, 1737–1742.

157. Pohanka, M.; Skládal, P. Electrochemical biosensors--principles and applications. *J. Appl. Biomed.* **2008**, *6*.

158. Morgan, C.L.; Newman, D.J.; Price, C.P. Immunosensors: technology and opportunities in laboratory medicine. *Clin. Chem.* **1996**, *42*, 193–209.

159. Skládal, P. Advances in electrochemical immunosensors. *Electroanalysis* **1997**, *9*, 737–745.

160. Bartlett, P.N.; Whitaker, R.G.; Green, M.J.; Frew, J. Covalent binding of electron relays to glucose oxidase. *J. Chem. Soc. Chem. Commun.* **1987**, 1603–1604.

161. Mostafa, G.A.E. Electrochemical biosensors for the detection of pesticides. *Open Electrochem. J.* **2010**.

162. Wen, W.; Yan, X.; Zhu, C.; Du, D.; Lin, Y. Recent advances in electrochemical immunosensors. *Anal. Chem.* **2017**, *89*, 138–156.

163. Martinkova, P.; Kostelnik, A.; Válek, T.; Pohanka, M. Main streams in the construction of biosensors and their applications. *Int. J. Electrochem. Sci. Vol. 12, issue 8* **2017**.

164. Arya, A.; Gangwar, A.; Kumar, A. Biosensors in animal biotechnology. In *Nanotechnology in Modern Animal Biotechnology*; Elsevier, **2019**; pp. 75–95.

165. Sneha, H.P.; Beulah, K.C.; Murthy, P.S. Enzyme immobilization methods and applications in the food industry. In *Enzymes in food biotechnology*; Elsevier, **2019**; pp. 645–658.

166. Sassolas, A.; Blum, L.J.; Leca-Bouvier, B.D. Immobilization strategies to develop enzymatic biosensors. *Biotechnol. Adv.* **2012**, *30*, 489–511, doi:https://doi.org/10.1016/j.biotechadv.2011.09.003.

167. Nguyen, H.H.; Kim, M. An overview of techniques in enzyme immobilization. *Appl. Sci. Converg. Technol.* **2017**, *26*, 157–163.

168. Sharma, S.; Singh, N.; Tomar, V.; Chandra, R. A review on electrochemical detection of serotonin based on surface modified electrodes. *Biosens. Bioelectron.* **2018**, *107*, 76–93.

169. Tosatti, S.; Michel, R.; Textor, M.; Spencer, N.D. Self-Assembled Monolayers of Dodecyl and Hydroxy-dodecyl Phosphates on Both Smooth and Rough Titanium and Titanium Oxide Surfaces. **2002**, doi:10.1021/la011459p.

170. Hofer, R.; Textor, M.; Spencer, N.D. Alkyl phosphate monolayers, self-assembled from aqueous solution onto metal oxide surfaces. *Langmuir* **2001**, *17*, 4014–4020.

171. Díaz-González, M.; González-García, M.B.; Costa-García, A. Recent advances in electrochemical enzyme immunoassays. *Electroanal. An Int. J. Devoted to Fundam. Pract. Asp. Electroanal.* **2005**, *17*, 1901–1918.

172. Mrksich, M.; Whitesides, G.M. Using self-assembled monolayers to understand the interactions of man-made surfaces with proteins and cells. *Annu. Rev. Biophys. Biomol. Struct.* **1996**, *25*, 55–78.

173. Rapp, B.E.; Gruhl, F.J.; Länge, K. Biosensors with label-free detection designed for diagnostic applications. *Anal. Bioanal. Chem.* **2010**, *398*, 2403–2412.

174. Jiang, X.; Li, D.; Xu, X.; Ying, Y.; Li, Y.; Ye, Z.; Wang, J. Immunosensors for detection of pesticide residues. *Biosens. Bioelectron.* **2008**, *23*, 1577–1587.

175. Luppa, P.B.; Sokoll, L.J.; Chan, D.W. Immunosensors—principles and applications to clinical chemistry. *Clin. Chim. acta* **2001**, *314*, 1–26.

176. Aizawa, M.; Morioka, A.; Matsuoka, H.; Suzuki, S.; Nagamura, Y.; Shinohara, R.; Ishiguro, I. An enzyme immunosensor for IgG. *J. Solid-Phase Biochem.* **1976**, *1*, 319–328.

177. Wang, H.; Li, X.; Mao, K.; Li, Y.; Du, B.; Zhang, Y.; Wei, Q. Electrochemical immunosensor for α-fetoprotein detection using ferroferric oxide and horseradish peroxidase as signal amplification labels. *Anal. Biochem.* **2014**, *465*, 121–126.

178. Tang, J.; Tang, D.; Li, Q.; Su, B.; Qiu, B.; Chen, G. Sensitive electrochemical immunoassay of carcinoembryonic antigen with signal dual-amplification using glucose oxidase and an artificial catalase. *Anal. Chim. Acta* **2011**, *697*, 16–22.

179. Yin, Z.; Liu, Y.; Jiang, L.-P.; Zhu, J.-J. Electrochemical immunosensor of tumor necrosis factor α based on alkaline phosphatase functionalized nanospheres. *Biosens. Bioelectron.* **2011**, *26*, 1890–1894.

180. Sadik, O.A.; Van Emon, J.M. Applications of electrochemical immunosensors to environmental monitoring. *Biosens. Bioelectron.* **1996**, *11*, i–x.

181. Fowler, J.M.; Wong, D.K.Y.; Halsall, H.B.; Heineman, W.R. Recent developments in electrochemical immunoassays and immunosensors. *Electrochem. sensors, Biosens. their Biomed. Appl.* **2008**, 115–143.

182. Haji-Hashemi, H.; Safarnejad, M.R.; Norouzi, P.; Ebrahimi, M.; Shahmirzaie, M.; Ganjali, M.R. Simple and effective label free electrochemical immunosensor for Fig mosaic virus detection. *Anal. Biochem.* **2019**, *566*, 102–106,

doi:10.1016/J.AB.2018.11.017.

183. Gogola, J.L.; Martins, G.; Caetano, F.R.; Ricciardi-Jorge, T.; dos Santos, C.N.D.; Marcolino-Junior, L.H.; Bergamini, M.F. Label-free electrochemical immunosensor for quick detection of anti-hantavirus antibody. *J. Electroanal. Chem.* **2019**, *842*, 140–145.

184. Ge, C.-Y.; Rahman, M.M.; Zhang, W.; Lopa, N.S.; Jin, L.; Yoon, S.; Jang, H.; Xu, G.-R.; Kim, W. An electrochemical immunosensor based on a self-assembled monolayer modified electrode for label-free detection of α-synuclein. *Sensors* **2020**, *20*, 617.

185. Date, Y.; Aota, A.; Sasaki, K.; Namiki, Y.; Matsumoto, N.; Watanabe, Y.; Ohmura, N.; Matsue, T. Label-Free Impedimetric Immunoassay for Trace Levels of Polychlorinated Biphenyls in Insulating Oil. **2014**, doi:10.1021/ac4035289.

186. Hassani, S.; Akmal, M.R.; Salek-Maghsoudi, A.; Rahmani, S.; Ganjali, M.R.; Norouzi, P.; Abdollahi, M. Novel label-free electrochemical aptasensor for determination of Diazinon using gold nanoparticles-modified screen-printed gold electrode. *Biosens. Bioelectron.* **2018**, *120*, 122–128, doi:https://doi.org/10.1016/j.bios.2018.08.041.

187. Fan, L.; Wang, G.; Liang, W.; Yan, W.; Guo, Y.; Shuang, S.; Dong, C.; Bi, Y. Label-free and highly selective electrochemical aptasensor for detection of PCBs based on nickel hexacyanoferrate nanoparticles/reduced graphene oxides hybrids. *Biosens. Bioelectron.* **2019**, *145*, 111728, doi:10.1016/J.BIOS.2019.111728.

188. Supraja, P.; Tripathy, S.; Krishna Vanjari, S.R.; Singh, V.; Singh, S.G. Label free, electrochemical detection of atrazine using electrospun Mn2O3 nanofibers: Towards ultrasensitive small molecule detection. *Sensors Actuators B Chem.* **2019**, *285*, 317–325, doi:https://doi.org/10.1016/j.snb.2019.01.060.

189. Singh, A.C.; Bacher, G.; Bhand, S. A label free immunosensor for ultrasensitive detection of 17β-Estradiol in water. *Electrochim. Acta* **2017**, *232*, 30–37, doi:https://doi.org/10.1016/j.electacta.2017.02.120.

190. Messaoud, N. Ben; dos Santos, M.B.; Vieira, A.; Garrido-Maestu, A.; Espiña, B.; Queirós, R.B. A novel portable label-free electrochemical immunosensor for ultrasensitive detection of Aeromonas salmonicida in aquaculture seawater. *Anal. Bioanal. Chem.* **2022**, *414*, 6591–6600, doi:10.1007/s00216-022-04219-9.

191. Zhai, Q.; Wang, X.; Hu, C.; Zhu, L.; Zhang, C.; Dai, L. Label-free electrochemical immunosensor for highly sensitive COVID-19 spike protein detection. *Sensors and Actuators Reports* **2022**, *4*, 100124, doi:https://doi.org/10.1016/j.snr.2022.100124.

192. Mohammadi, A.; Heydari-Bafrooei, E.; Foroughi, M.M.; Mohammadi, M. Electrochemical aptasensor for ultrasensitive detection of PCB77 using thionine-functionalized MoS 2-rGO nanohybrid. **2020**, doi:10.1016/j.microc.2020.104747.

193. Liu, X.; Sakthivel, R.; Cheng, C.-Y.; Luo, J.; Song, L.; Wu, J.; He, W.; Younis, U.; Chung, R.-J. 3A-Amino-3A-Deoxy-(2AS, 3AS)-β-Cyclodextrin Hydrate/Tin Disulfide Modified Screen-Printed Carbon Electrode for the Electrochemical

Detection of Polychlorinated Biphenyls. *Nanoscale Res. Lett.* **2020**, *15*, 1–13.

194. Fang, Y.; Hu, Q.; Yu, X.; Wang, L. Ultrasensitive electrochemical immunosensor for procalcitonin with signal enhancement based on zinc nanoparticles functionalized ordered mesoporous carbon-silica nanocomposites. *Sensors Actuators B Chem.* **2018**, *258*, 238–245, doi:https://doi.org/10.1016/j.snb.2017.11.062.

195. Sheryna Jusoh, N.; Fauzan Tuan Omar, T.; Ahmad, A. MALAYSIAN JOURNAL OF ANALYTICAL SCIENCES THIOL MODIFIED AMPEROMETRIC IMMUNOSENSOR FOR BENZO[a]PYRENE DETECTION IN SURFACE RIVER WATER SAMPLES (Immunosensor Amperometrik Diubahsuai Tiol untuk Pengesanan Benzo[a]pirina dalam Sampel Air Sungai Permukaan). *Malaysian J. Anal. Sci.* **2019**, *23*, 849–860, doi:10.17576/mjas-2019-2305-10.

196. Muñoz, J.; Crivillers, N.; Mas-Torrent, M. Carbon-Rich Monolayers on ITO as Highly Sensitive Platforms for Detecting Polycyclic Aromatic Hydrocarbons in Water: The Case of Pyrene. *Chem. Eur. J.* **2017**, *23*, 15289–15293.

197. Saio, F.; Omura, H.; Hayano, K. Adenosine deaminase activity in soils. *Soil Sci. Plant Nutr.* **1986**, *32*, 107–112.

198. Segel, H.I. The Hanes-Woolf plot. *Enzym. Kinet. A Wiley Intersci. Publ. New York* **1975**.

199. Willner, I.; Riklin, A.; Shoham, B.; Rivenzon, D.; Katz, E. Development of novel biosensor enzyme electrodes: Glucose oxidase multilayer arrays immobilized onto self-assembled monolayers on electrodes. *Adv. Mater.* **1993**, *5*, 912–915.

200. Cornish-Bowden, A. *Fundamentals of enzyme kinetics*; John Wiley & Sons, 2013; ISBN 3527665498.

201. Atkins, P.; De Paula, J.; Friedman, J. Chemical equilibrium. *Atkins' Phys. Chem.* **2002**, *7*, 222–251.

202. Atkins, P.W.; De Paula, J. Molecular reaction dynamics. *Atkins' Phys. Chem.* **2002**, 956–961.

203. Turner, A.P.F. Biosensors: sense and sensibility. *Chem. Soc. Rev.* **2013**, *42*, 3184–3196.

204. Eisenhart, C. Realistic evaluation of the precision and accuracy of instrument calibration systems. *Precis. Meas. calibration Stat. concepts Proced.* **1969**, 2147.

205. Long, G.L.; Winefordner, J.D. Limit of detection. A closer look at the IUPAC definition. *Anal. Chem.* 1983, *55*, 712A-724A.

206. Kim, E.E.; Wyckoff, H.W. Reaction mechanism of alkaline phosphatase based on crystal structures: Two-metal ion catalysis. J. Mol. Biol. **1991**, 218, 449–464, doi: https://doi.org/10.1016/0022-2836(91)90724-K.

University College Cork, Ireland
Coláiste na hOllscoile Corcaigh

CORA
Cork Open Research Archive
Cartlann Taighde Oscailte Chorcaí

Alsefri, S. A. 2023. Development of an electrochemical immunosensor for environmental monitoring of polychlorinated biphenyls (PCBs) in soil environment. PhD Thesis, University College Cork.

Please note that Chapter 2 (pp. 97-133) is unavailable due to a request by the author.

CORA Cork Open Research Archive http://cora.ucc.ie

CHAPTER 3

Development and Characterization of Electrochemical Immunosensors

3. Electrochemical Development of an Immunosensor for Detection Polychlorinated biphenyls (PCBs) for Environmental Analysis

Note: This work has been published in the journal of **Chemosensors** Acta, **2021**, *9*(11),307

3.1 Abstract

Polychlorinated biphenyls (PCBs) are a highly toxic family of synthetic chemical compounds. PCBs are widely spread in the environment and their toxicity can cause serious ailments to living organisms such as cancer; therefore, developing a device for the detection of PCBs in the environment is significant. In this paper, polyclonal primary anti-PCB antibodies were immobilized onto a gold screen-printed electrode with the purpose of creating an electrochemical immunosensor for the detection of Aroclor 1254. It was modified with 11-mercaptoundecanoic acid (11-MUA), and the activation of the carboxylic acid terminal was performed by cross-linking 1-ethyl-3-(3-dimethylaminopropyl) carbodiimide (EDC) and N-hyrodsuccinmide (NHS) on the electrode surface. Cyclic voltammetry, electrochemical impedance spectroscopy (EIS), linear sweep voltammetry, atomic force microscopy (AFM), scanning electron microscopy (SEM), and contact angle measurement were employed to characterize of self-assembled monolayers (SAM) development on the gold electrode. Using a competitive assay, a 0.09 ng/ml limit of detection and a linear range of 0.101–220 ng/ml were determined. The self-assembled monolayers (SAM) were successful in

encapsulating the PCBs on the immunosensor. The electrochemical detection showed better resolution when compared to traditional methods such as the ELISA optical technique. The novel electrochemical immunosensor approach that is discussed in this paper has the potential to offer rapid sample screening in a portable, disposable format and could contribute to the effective control and prevention of PCBs in the environment.

Key words: polychlorinated biphenyls; disposable screen-printed gold electrode; linear sweep voltammetry; immunosensors; immunoassays; self-assembled monolayers.

3.2 Introduction

Polychlorinated biphenyls (PCBs) are a family of artificial organic compounds with two to ten chlorine atoms attached to the biphenyl [1,2]. Since 1929, PCBs have been commercially manufactured under the trade name Aroclor. Aroclor consists of a combination of chlorinated biphenyls, including over 100 different unique PCBs. Congeners are defined and numbered according to the total amount of chlorine in the mixture [3]. Aroclor 1254 ($C_{12}H_5Cl_5$) is one of the commercial products, and it is a viscous, light-yellow liquid with an average molecular weight of 328, containing approximately 21 % $C_{12}H_6Cl_4$, 48 % $C_{12}H_5Cl_5$, 23 % $C_{12}H_4Cl_6$, and 6 % $C_{12}H_3Cl_7$ with an average chlorine content of 54 % [4]. Figure 3.1 shows the structure of Arcolor 1254.

These compounds have been used as plasticizers, surface coatings, inks, additives for insulating liquids, pesticides, and lubricants [5,6], all of which have contaminated the environment. Further contamination may result from the disposal of obsolete electrical equipment containing PCBs, as well as leaks from industrial sites. Furthermore, PCBs have significant teratogenic, carcinogenic, and mutagenic impacts on the human body. PCBs are persistent in the environment and until today a large proportion of PCBs are still present in old transformers and power capacitors, which have the potential to be released into the environment. PCB congeners also enhance the degree of structural uniformity and chlorination increases. Lastly, the PCBs high stability and lipophilicity nature resulted in them being widely distributed in the world ecosystem. PCBs occur in all environments matrixes and can be found in a variety of environmental media (water, atmosphere, soil, sediment, and creatures) [7–10]. These chemicals have become a significant danger to the environment and the health and safety of humans. All of these facts make the development of an effective and economical testing method for PCBs very important [11,12].

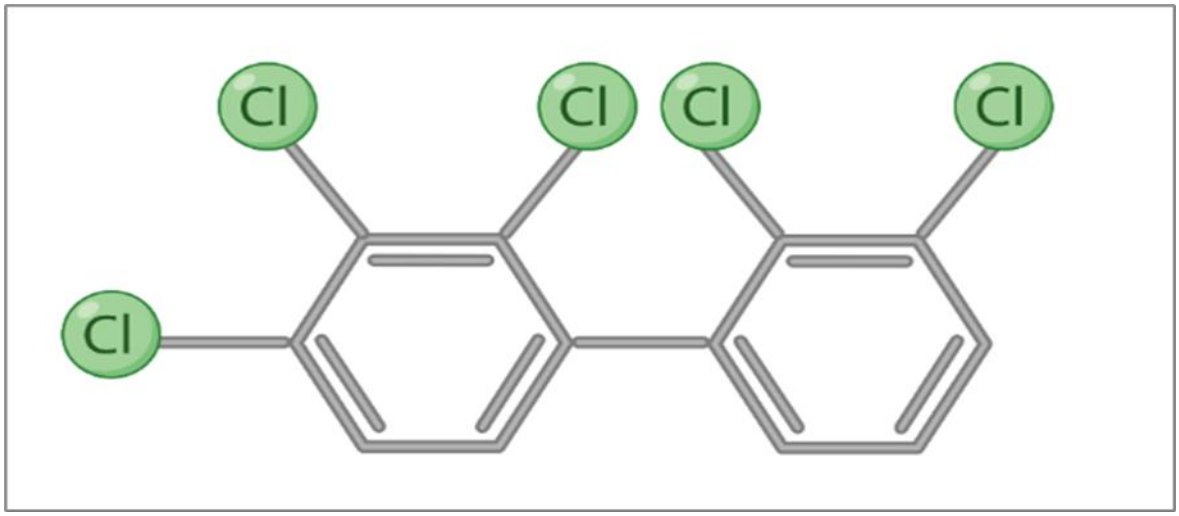


Figure 3.1 Structure of Arcolor 1254.

The methods used to determine PCBs so far are: tandem mass spectrometry [13,14], bioanalytical techniques [15], and spectral analysis [16]. These methods, although sensitive, are generally time-consuming and expensive and typically require sample preparation before the chromatographic separation [17,18]. On the other hand, electrochemical techniques have been utilized in a variety of prospective applications and environmental research due to their relative advantages, such as low costs, easy operation, and fast response.

Only a few papers have been published to date that are based on electrochemical immunosensors for PCBs [19,20]. All of these have used modified materials to enhance the immobilization of antibodies, such as nanoparticles [19,21–23], self-assembled monolayers (SAM), including [24,25] cysteamine [26] and 11-mercaptoundecanoic acid (11-MUA) [24]. SAM is typically formed by activating the carboxylic acid groups with [1-ethyl-3-(3-dimethylaminopropyl) carbodiimide] (EDC) in conjunction with N-hydroxy succinimide (NHS) before protein immobilization through the use of an

alkylthiol reaction [27]. This reaction decreases the random orientation of the antibodies that bind the surface proteins to the carboxylic acid end-groups enhancing the immunosensor sensitivity and selectivity [24,28]. Research has shown that SAM forms better on a gold surface [29–31] as the gold strongly absorbs the protein molecules and creates a hydrophobic interaction through the strong S–Au bonds [32,33]. This facilitates the immobilization of the desired protein on the specific target area and limits non-specific binding [34]. Electrode surfaces provide no sites for covalent bonding, making it necessary to coat a thin film of functional groups to covalently bond with the amino groups of the used antibodies [35]. In this research paper, the anti-PCB were compounded onto the chip (made of the gold sensor) by covalent coupling technique and with the aid of [1-ethyl-3-(3-dimethylamino propyl) carbodiimide] (EDC) in collaboration with N-hydroxy succinimide (NHS) [36,37]. Figure 3.2 illustrates the fabrication of an immunosensor in a gold electrode with 11-MUA SAM, as well as its activation by EDC/NHS. The desired protein and antigen are then presented.

The indirect competitive assay using (alkaline phosphate) AP as an enzymatic label was used. A bovine albumin (BSA) conjugate, BSA-PCB was the basis for the PCB immobilization procedure. After the experiment, the amount of anti-PCB that reacted with immobilized PCB was determined using a secondary antibody with alkaline phosphate, labelled *p*-aminophenyl phosphate (*p*APP), which detected the presence of alkaline phosphate. A Liner sweep volumetry was used as the electrochemical detection technique. A number of characterization methods were reported including

contact angle measurement, cyclic voltammetry, impedance measurement, SEM, and AFM. To the best of our knowledge, this is the first study to investigate the SAM modified on gold electrodes with PCBs compounds. The measurement of the electrochemical detection for the biochip was achieved via detection of the quantity of antibodies that react with the target Aroclor 1254 compound. The assay was then compared with the traditional optical method (ELISA).

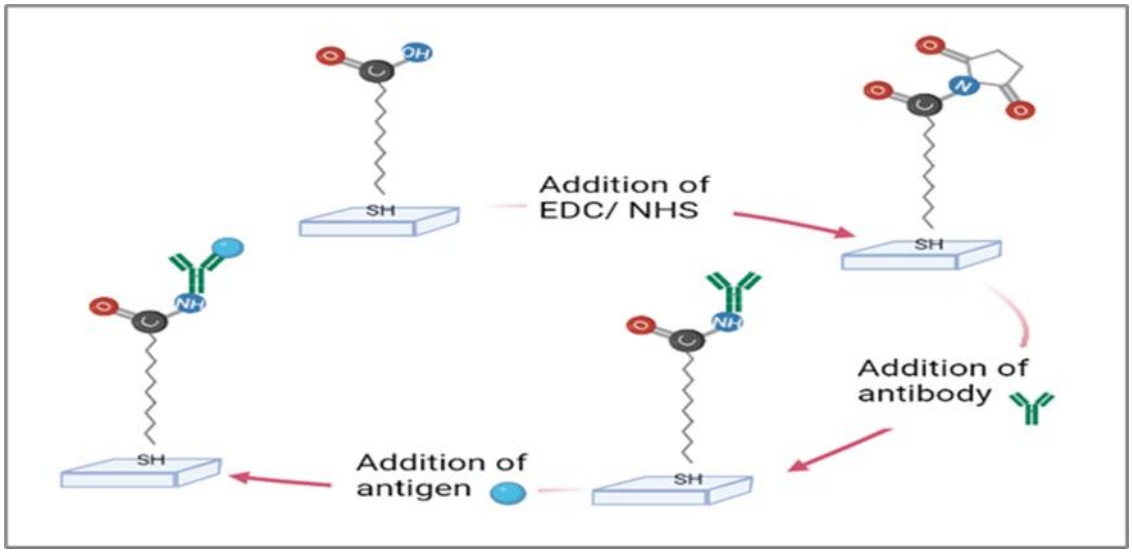


Figure 3.2 The graphic depicts the synthesis of SAM from 11-MUA on a gold electrode in combination with antibody immobilization.

3.3 Materials and Methods

3.3.1 Reagents and Chemicals

Polyclonal chicken antibody (IgY) specific to PCB, alkaline phosphatase (AP) labelled goat anti-chicken (IgY) antibodies were bought from GmbH (Heidelberg, Germany). Aroclor 1254 and PCB were bought from (Cole-Parmer Instrument Company Ltd., Eaton Socon, Saint Neots, UK). A total of 2 mg of PCB-BSA conjugate (Aroclor 1254) was bought from (BioTeZ Berlin-Buch GmbH (Heidelberg, Germany)). *p*-nitrophenyl phosphate (*p*NPP) substrate, diethanolamine reagent (DEA) phosphate-buffered saline (PBS), sodium hydrogen carbonate, sodium chloride, Tween-20, tris (hydroxymethyl) aminomethane, potassium chloride (KCl) and bovine serum albumin (BSA) were bought from Sigma (Dublin, Ireland). To adjust pH, hydrochloric acid (HCl) 37 %, sodium hydroxide, ammonium hydroxide solution and sodium cyanoborohydride ($NaCNBH_4$) were bought from Sigma (Dublin, Ireland). 11-mercaptoundecanoic acid (11-MUA), 1-ethyl-3-(3-dimethylaminopropyl) carbodiimide (EDC), NHS, potassium ferricyanide ($K_3[Fe\ (CN)_6]$), potassium ferrocyanide ($K_3[Fe\ (CN)_6]$), acetone, 1-isopropyl alcohol, ethanol, and alkaline phosphatase (AP) were also bought from Sigma (Dublin, Ireland). For the electrochemical tests, the substrate was *p*-aminophenyl phosphate (*p*APP) salt, which was bought from Sigma (Dublin, Ireland). Disposable electrochemical screen-printed gold electrodes (AuE), model C220 BT, were purchased from (Drop Sens, Asturias, Spain). To ensure optimal detection, a standard 96 well ELISA microplate was bought from Greiner bio-one (Frickenhausen, Germany). All other reagents were

analytical grade or higher, with daily buffer solutions made using nanopore water (18.2 MΩ-cm).

3.3.2 Equipment and Instrumentation

Optical detection was carried out using the EL Read 2000 microplate reader provided by biochrom.co.UK. Incubation was made possible using a Biometra OV3 Incubator (Gottingen, Germany), which was set at 37 °C. Cyclic voltammetry was recorded using a PalmSens handheld potentiostat (Palm Instrument BV Houten, Houten, The Netherlands). Impedance measurements were performed in a faraday cage with minimal noise using a CHI potentiostat 1100/620B (CH Instruments Inc., Austin, TX, USA). The removal of the surface organic molecules was achieved using a plasma cleaner (Harrick Plasma Ithaca, New York, NY, USA). A nitrogen spray gun facilitated the drying of SPEs between measurements using the Contact Angle Instrument (OCA) by Data Physics Instruments GmbH (Filderstadt, Germany). SEM measurements were carried out on an FEI Quanta 650 Scanning electron microscope (FEI Company, Hillsboro, OR, USA). AFM measurements were carried out using "SCANASYST-AIR" by Bruker AFM Probes (Bruker AFM Probes, Camarillo, CA, USA). Specificity (Cross-Reactivity) obtained using a PalmSens handheld potentiostat (Palm Instrument BV Houten, Houten, The Netherlands) and Data obtained from Origin Pro 8.5.1 software. Measurements were taken at room temperature between −0.2 and 0.6 V in $[Fe(CN)_6]^{3-/4-}$ and 0.1 M of KCl solution with a scan rate of 50 mVs^{-1}.

3.4 Electrochemical Characterization of the Gold Electrode

3.4.1 Studies on Electrode Cleaning Protocol

For electrochemical measurements, it is necessary to ensure that the electrode surfaces are clean. As a result, showing in Figure 3.4, the optimization of various SPGE cleaning protocols was carried out. At a scan rate of 50 mV s^{-1}, the chips were cycled in 5 mM [Fe (CN)6] $^{3-/4-}$ in 0.1 M KCl. The potential was chosen between −0.2 and 0.6 versus Ag/AgCl. The following are the different chip-cleaning protocols: (a) SPGE was given a plasma cleaner treatment for 20–30 min; (b) SPGE was ultrasonically cleaned for 5 min in acetone, then for another 5 min in 1-isopropyl alcohol before being rinsed with deionized water for 5 min; (c) on a hot plate, a 1:1:5 mixture of 29 % ammonia solution, 30 % H_2O_2, and ultrapure water was heated to 80 °C, and the SPGEs were immersed in the solution for 5 min; (d) the SPGE was cycled from 0 to +1.6 V in 0.5 M for 3 scans in 0.5 M sulfuric acid, H_2SO_4. The SPEs need to be cleaned before use. The electrodes were cleaned with isopropanol, nano pure water and dried with a nitrogen gun to remove the photoresist.

3.4.2 Studies on the Influence of Scan Rate

In order to study the influence of the scan rate, the electrode was scanned between −0.2 and 0.6 V in 5 mM [Fe (CN)6] $^{3-/4-}$ in 0.1 M KCl to investigate the effect of the scan rate. Different scan rates of 5–200 mV s^{-1} versus Ag/AgCl were used in the experiments.

3.4.3 Stability Study of the Coated Electrodes

A stability study was performed on the coated BSA-Aroclor 1254 coating conjugate on the gold electrodes by immobilizing the electrodes with a few layers of the assay components, which is similar to the steps mentioned in Section 3.11. Using an Indirect competitive Assay, the gold electrode was coated with 5 μg/ml of BSA-Aroclor 1254 coating conjugate overnight and kept at a temperature of 4 °C. The next morning the electrodes were washed, dried, and placed in a blocking solution (BSA-tris buffer) for one hour. The electrodes were then rinsed with a washing buffer and nonpure water. The biochips were stored dry at 4 °C for further use. A complete capture assay test was performed on three electrodes daily for 10 days using LSV.

3.4.4 Cyclic Voltammetry (CV)

CV was performed in 0.1 M KCl with a 5 mM ferri/ferrocyanide redox pair with an applied voltage ranging from -0.2 to +0.6 V. The scan rate was set at 0.05 V s^{-1}. In this experiment, screen-printed electrodes (SPEs) were utilized. The gold electrode had a working area of 4 mm. The Ag/AgCl reference electrode was used to refer to all potentials reported in this study.

3.4.5 Impedance Measurement

A frequency response analysis (FRA) was utilized to apply a modest amplitude AC signal to the biochip for impedance measurements. The impedance behaviour of the electrode was evaluated by analysing the AC voltage and current response at frequencies ranging from 0.1 Hz to 1 MHz. The measurements were performed in the presence of a 5 mM redox probe $[Fe(CN)_6]^{3-/4-}$ in 0.1 M KCl at an applied potential of +0.2 V and an amplitude of 0.1 V.

3.4.6 Amperometric Detection

PalmSens (Palm Instrument BV Houten, Houten, The Netherlands). was used to carry out amperometric detection using a portable potentiostat. Before each measurement, a coating was applied to the chips with layers of a biocomponent assay, which was stored in 14,000 µL DEA buffer with pH 9.5 and at a temperature of 4 ˚C. The aim of this was to prevent loss of activity of the antibodies. The detection was carried out on the coated electrode using the AP as the labelled enzyme and the *p*APP as the substrate. The measurement was set to 60 s, and the potential was applied at 450 mV versus Ag/AgCl. The measurement of the current was taken to acquire stability in the baseline. At 45 s, 100 µL of *p*APP was injected into the working electrode. The final concentration of the *p*APP in the buffer was 5 µg/ml. The increase in the current was taken as the data signal for evaluation. As *p*APP is sensitive to light and moisture, the solution was made daily.

3.5 Optimization of Polyclonal Chicken Antibody (IgY) Specific to PCB.

The objective of this assay was to optimise the concentration of PCB primary antibody on the biochip working electrode using the capture assay for PCB detection. This assay was carried out by immobilising a BSA- Aroclor 1254 coating conjugate at 5 µg /ml to completely cover the working electrode and allowed to bind for overnight at 4 ◦C. Then, the biochips were washed with washing buffer three times and were dried with nitrogen.30 µl of blocking solution was pipetted onto the surface, making sure that the working area was completely covered and were allowed to bind for 30 minutes at 37 ˚C. Then, the biochips were washed again using washing buffer and were dried with nitrogen. A serial dilution of Polyclonal chicken antibody (IgY) primary antibody in 12 different concentrations was prepared 10 µl of each concentration was added to the working area and the biochips were incubated for 1 hour at 37 ˚C. 10 µl of goat anti-chicken (IgY) (AP) labeled was added and allowed to bind for another 30 minutes. The electrodes were washed and dried and ready to be measured using Linear sweep voltammetry detection.

3.6 Optimization of Secondary Antibody AP Labelled.

Capture assays were performed using a fixed concentration of BSA-Aroclor 1254 coating conjugate at 5 µg /ml to completely cover the working electrode and allowed to bind for overnight at 4 ◦C. Then, the biochips were washed with washing buffer three times and were dried with nitrogen.30 µl of blocking solution was pipetted onto the surface, making sure that the working area was completely covered and were allowed

to bind for 30 minutes at 37 ˚C. Then, the biochips were washed again using a washing buffer and were dried with nitrogen. 10 µl of 0.123 µg/ml of Polyclonal Chicken antibody (IgY) specific to PCB was added to the working area and the biochips were incubated for 1 hour at 37 ˚C. 10 µl of different concentration of secondary antibody dilution was added and allowed to bind for another 30 minutes at 37 ˚C. The electrodes were washed and dried and ready to be measured using Linear sweep voltammetry detection.

3.7 Studying the Influence of Blocking.

The importance of the blocking procedure was studied using capture assay. The biochips were prepared in three sets, with three biochips for each set (n=3). Set A consisted of a blank, in which the bare electrode was pAPP. For set B, 5 µl of BSA-Aroclor 1254 coating conjugate (5 µg/ml) was spread to the area of working electrode and allowed to bind for overnight at 4 ˚C. Then, the biochips were washed with washing buffer three times and were dried with nitrogen. The blocking step was skipped. 10 µl of 0.123 µg/ml of Polyclonal Chicken antibody (IgY) specific to PCB was added to the working area and the biochips were incubated for 30 minutes at 37 °C. 10 µl of goat anti-chicken (IgY) (AP) labeled was added and allowed to bind for another 30 minutes at 37°C. The same procedures as mentioned above were applied to set C, where for blocking step, 30 µl of blocking solution was pipetted onto the surface, making sure that the working area was completely covered and were allowed

to bind for 30 minutes at 37 °C. The electrodes were washed and dried and ready to be measured using Linear sweep voltammetry detection.

3.8 Specificity (Cross-Reactivity)

The specificity was determined by testing the cross-reactivity (CR) of the antibody with a variety of Aroclors. The reaction was carried out using liner sweep voltammetry (LSV) by adding these compounds (instead of Aroclor 1254 in the respective assays) at 11 serial dilutions, using the same concentration range (0.01 to 660 ng /ml) that was used to detect the target (Aroclor 1254). The CR values can be calculated using the following formula:

$$\text{cross} - \text{reactivity}\ (\%) = \frac{\text{IC50 of Aroclor 1254}}{\text{IC50 of other compounds}} \times 100$$

3.9 Self-Assembled Monolayers

3.9.1 Modification of Gold SPE with SAM (LSV)

In order to prepare self-assembled monolayers (SAM) on the gold working electrodes, solutions of 5 mM 11-mercaptoundecanoic acid (11-MUA) were separately prepared in absolute ethanol (N_2 bubbled for 30 min to eliminate the presence of oxygen) [38–40]. The gold electrodes were immersed in the SAM solution for 20 h at room temperature. Upon removing the biochips from the solution, the electrodes were rinsed thoroughly with absolute ethanol to remove any unbound molecules. They were then dried with N_2. To activate the carboxylic terminal end after SAM formation, the

electrodes were immersed in a solution of 50 mM EDC and NHS for 1 h and were rinsed with deionized water and dried with N_2. CVs were carried out in 5 mM $[Fe(CN)_6]^{3-/4-}$ and 0.1 M of KCl solution, and the potential that was applied was in the range (0.2 to 0.6 V) [34,35]. The scan rate applied was 50 mV s^{-1}. Figure 3.3 shows the steps involved in the formation of self-assembled monolayers on the gold electrodes. Immobilization of protein on the gold surface after the activation of EDC/NHS was performed by incubating 5 µg/ml of BSA-Aroclor 1254 coating conjugate at 37 ◦C for 1 h.

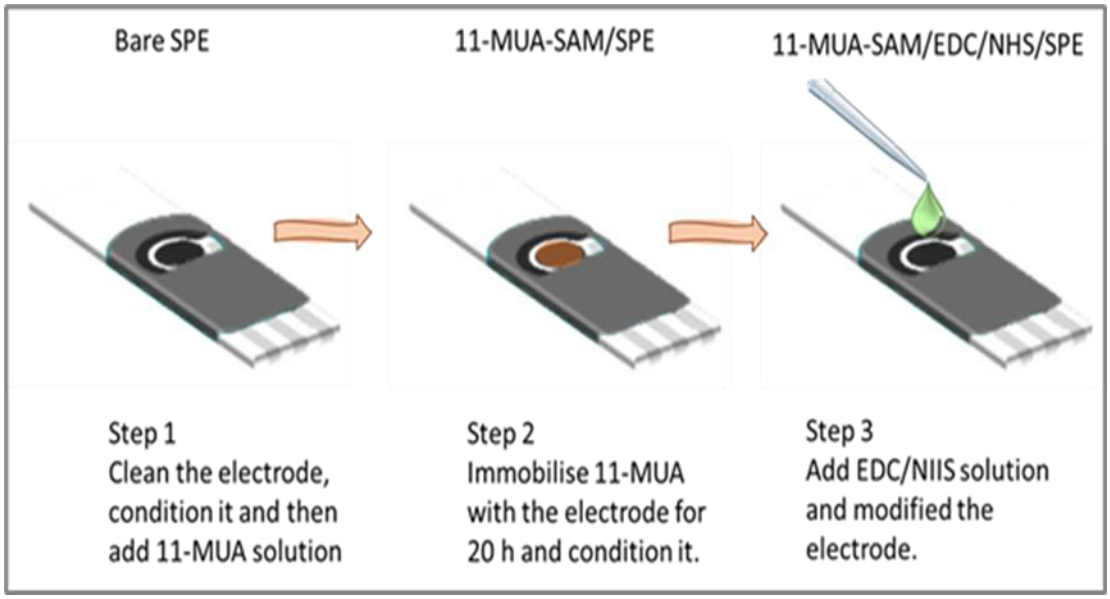


Figure 3.3 The steps involved in the formation of self-assembled monolayers on the gold electrode.

3.10 Topography Characterization

3.10.1 Contact Angle Measurement

The sessile drop contact angle method was utilized to evaluate the surface hydrophobicity of the SAM substrates. A 1 µL drop of deionized water was supplied to the surface of the gold electrodes at a medium rate of 1 µL per second. Measurements were repeated on each electrode for three drops.

3.10.2 Scanning Electron Microscopy (SEM)

SEM measurements at the surface of the bare gold electrode were observed using a FEI Quanta 650 Scanning electron microscope (SEM). The SEM was coated and imaged at ×100 magnifications for clean bare AuE and SAM-modified AuE. These were observed and compared before and after the modification.

3.10.3 Atomic Force Microscopy (AFM)

The experiments were performed using an atomic force microscope (Bruker AFM Probes, Camarillo, CA, USA), which used “scanasyst-Air” as its measurement mode. The force constant of the scanasyst-Air was 2 N/m. The frequency used for the tapping mode was 95 ± 45 kHz with a scan size of 0.5 µm. For the purposes of comparison, three scans were taken per sample. Data acquisition was performed using NanoScope Analysis 1.9 software.

3.11 Indirect Competitive Assay

Indirect competitive assay was applied by ELISA or by linear sweep voltammetry. Immobilization of antibodies was carried out directly on microwell plates or on the clean electrode surface to enhance the maximum signal. The immobilization of biocomponents was performed on the working electrode and wells. A total of 100 µL or 10 µL of the coating antigen BSA-Aroclor1254 (5 µg/ml) (pH 7.4) was added to microwell plates or electrode surfaces and incubated overnight at 4 ◦C. The microwell plates or electrodes surfaces were then washed three times with 0.05 M Tris, pH 7.4 (0.05% Tween 20) and blocked with 1% BSA-Tris Solution (0.05 M Tris-HCl) for 1 h or 30 min at 37 ◦C. After incubation, the microwell plates or electrode surface was washed three times to remove any unbound coating conjugate. For the competition step, the serial dilution of Aroclor 1254 PCB was mixed with polyclonal chicken antibody (IgY) specific to PCB with concentrations of 0.465 µg/ml or 0.123 µg/ml used for ELISA or linear sweep voltammetry. The mixture was left to incubate for 15 min. A volume of 100 or 10 µL was introduced to the microwell plates or electrode surface. The microwell plates and electrode surfaces were allowed to bind for 1 h or 30 min at 37 ◦C. To standardize the assay, a 1/5000 dilution of commercially available (AP) labeled goat anti-chicken (IgY) antibodies was prepared, and 100 or 10 µL of the solution was added to the microwell plates or electrode surfaces and allowed to react for 1 h or 30 min at 37 ◦C. After washing, 100 or 10 µL of the substrate solution *p*NPP or *p*APP diluted in DEA buffer (pH 9.5, 1 mg/ ml) was added to surfaces. The electrochemical substrates were incubated, and measurements were taken using the PalmSens potentiostat.

3.12 Real Sample

The analysis was carried out in a river water sample were collected from River Lee (Cork, Ireland) in April 2020, and the tap water was taken from Kane Building (chemistry department)—UCC (University College Cork). To protect the water samples from contaminants, glass vessels with Teflon caps were used for storage. Immediately after collecting the samples, they were diluted with equal amounts of methanol to prevent losses to the polystyrene tubes or the glass containments. To remove all the suspended materials in the sample, 0.45 μm filter aid materials were used before testing. The water samples used in this experiment contained 50% methanol. The final assay result was multiplied by a factor of 2 [41]. For the highly contaminated samples, those outside the assay's calibration range were further diluted and analysed. For the soil sample analysis, ten grams of soil were placed in a glass flask and spiked with a known amount of Aroclor 1254 before being extracted for recovery studies. A measure of 5 g of the spiked sample was added to 10 ml of methanol. The flask was sealed, shaken frequently for 2 min, and then left at room temperature for 30 min. The sample was centrifuged at 2500 rpm for 10 min. After waiting 5 min for the solid particles to settle, the soil was filtered through a 0.45 μm nitrocellulose filter. The extract was then evaporated to a volume of 1 ml before processing, as described in Section 3.11.

3.13 Results and Discussion

3.13.1 Influence of Electrode Cleaning Procedure

Cleaning and substrate preparation are important steps in studying the surface phenomenon, because they can improve the surface state for better electrochemical activity to take place. There are different common pre-treatment methods for producing a clean gold surface, and most are performed just before the modification of the surface. Different pre-treatment procedures, either individual or combined, are employed. Common pre-treatment methods include thermal treatment, mechanical polishing with a slurry of alumina, oxygen plasma cleaning, chemical oxidation with piranha solution or ethanol, and electrochemical polishing using potential cycling [42][43]. In this study, we used four different protocols to clean the electrode, as follows: plasma cleaning, ultrasonicating, NH_3 + $H2O_2$, and $H2SO_4$. Electrode cleanliness can be measured by examining the potential difference of the peak-to-peak separation (ΔEp) of anodic and cathodic peaks. According to Fischer et al., a smaller ΔEp indicates a cleaner surface, where any increase in the ΔEp value indicates that some sort of contamination has occurred on the electrode surface [44]. Considering that the theoretical value of ΔEp is 59 mV for the single-electron transfer of [Fe (CN)6] $^{3-/4-}$, the closest experimental value of ΔEp (58 mV) was achieved when the CV was performed using the plasma-cleaner-treated electrode. Compared with the other cleaning protocols, the plasma cleaning method shows well-defined peaks (see Figure 3.4). For this reason, we used this method as our cleaning procedure for further

electrochemical investigations. The data generated from the curves are summarized in Table 3.1.

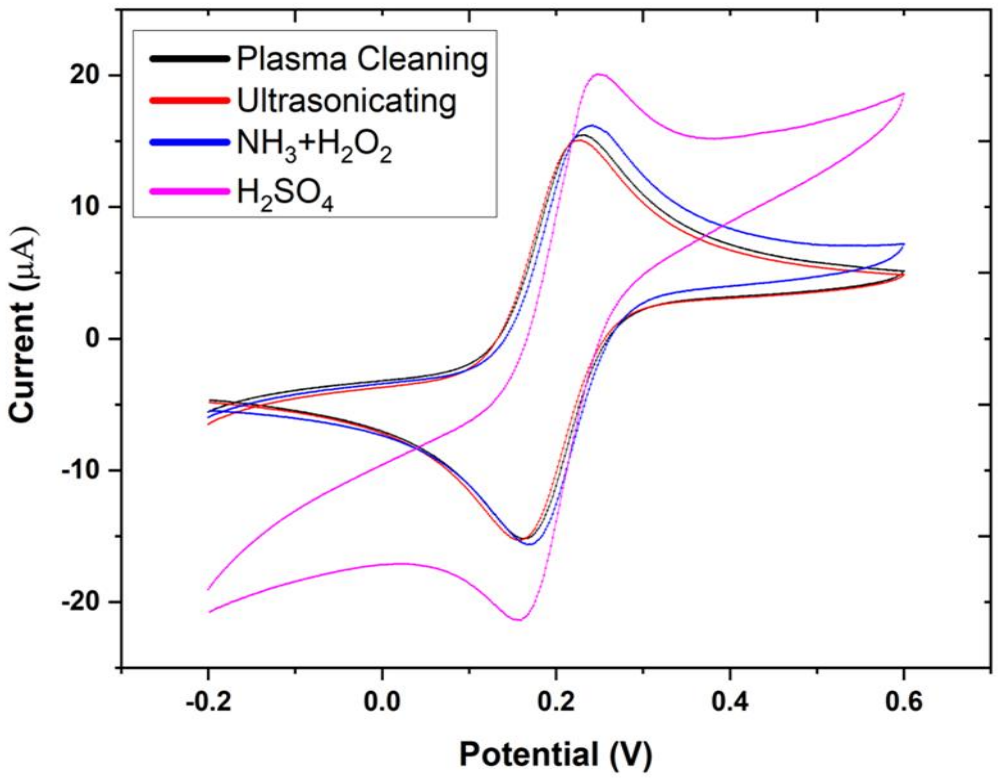


Figure 3.4 Studies on different chip-cleaning procedures. CV was scanned in mM [Fe (CN)6]$^{3-/4-}$ redox coupled with a 50 mV/s scan rate.

Table 3.1 The values of peak-to-peak separation using different cleaning protocols**.**

Cleaning protocols	**E_{pa}(V)**	**E_{PC}(V)**	**ΔE_P (mV)**
Plasma cleaning	0.226	0.168	58
Ultrasonicating	0.226	0.160	66
$NH_3H_2O_2$	0.242	0.172	70
H_2SO_4	0.246	0.160	86

*$\Delta E_P = E_{Pa} - E_{pc}$

3.13.2 Influence of Scan Rate

The influence of the scan rates was investigated by performing the CVs over the range 5–200 mV s^{-1}. As shown in Figure 3.5, a large peak separation was observed when the scan rates were increased. The redox couple used was 5 mM ferricyanide/ferrocyanide in 0.1 MKCL. The peak-to-peak separation achieved for the scan rate of 50 mV s^{-1} was 64 mV s^{-1}, which is a better performance compared to those reported by M. Lu with 75 mV s^{-1} [45] . A good linear correlation was obtained between the anodic peak height and the square root of the applied scan rates, as shown in Figure 3.5 The values of the correlation coefficients (R2) of the anodic peak (0.999) and the cathodic peak (0.998) confirm that the electrochemical system was under the diffusion control process. Table 3.2 shows the calculated CV data for the oxidation of 5 mM [Fe (CN)6] $^{3-/4-}$ in 1 M kCL with different scan rates. The measurements were performed at room temperature, 25 ˚C. Table 3.2 shows that the data of Ipa increased as the scan rate increased. It also shows the ΔEpa for each scan rate within the practical range (70–40 mV). In addition,

the theoretical value of 58 mV was recorded twice at that range, at scan rates of 100 and 200 mV/s. Furthermore, it shows all the redox reactions across the different scan rates applied at ≈200 mV.

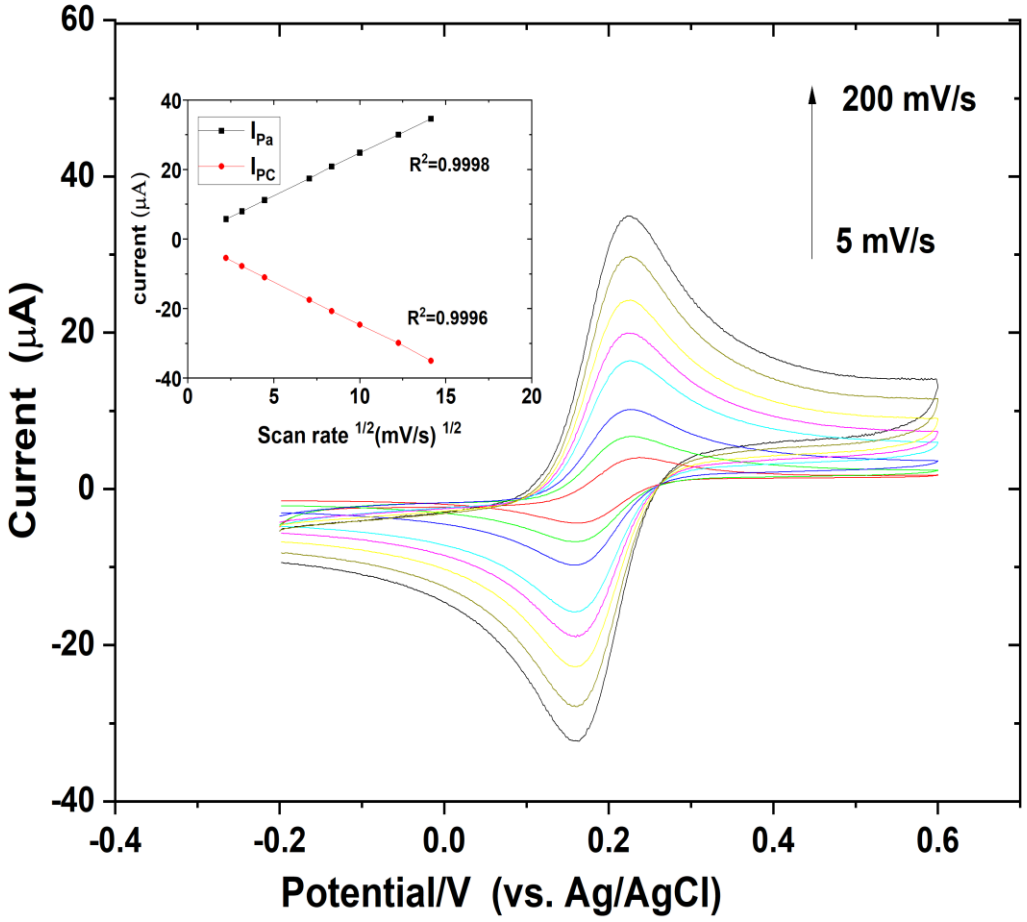


Figure 3.5 Influence of the scan rates on the CV signals measured in 5 mM $\{Fe(CN)6\}^{3-/-4}$ in 1 M KCl. The potential applied was from - 0.2 to 0.6 V.

Table 3.2 Influence of the scan rate on the half-peak potential and the peak current for the oxidation component of the process. The scan rates studied were 5 mv/s, 10 mv/s, 20 mv/s, 50 mv/s, 70 mv/s, 100 mv/s, 150 mv/s, and 200 mv/s.

Scan rate (mV/s)	Ipa (µA)	ΔEp (mV)	Emid vs. Ag/Ag CL (mv)
200	34.59	58	193
150	30.01	64	194
100	24.80	58	193
70	20.83	62	191
50	17.38	64	192
20	11.18	68	192
10	7.98	68	194
5	5.71	70	198

[a] Measured from the value ½ (Epc +Epa) versus Ag/AgCl reference electrode; [b] ΔEp = (Epc-Epa); [c] Ep anodic data as a function of scan rate.

3.13.3 Kinetic Studies of Michaelis-Menten Plot

Capture assay for optimizing electrochemical substrate of pAPP. Kinetic Studies plots were tested to ascertain the concentration of pAPP substrate that would yield a signal of 95 % of I_{max}. Figure 3.6 represents the Michaelis-Menten plot for various

concentrations of pAPP in reaction with AP labelled. The K_m for the pAPP substrates was 0.65mM and the corresponding concentration of substrate at 95 % of Imax Was 96.42 µA. the Figure 3.6 hence indicates Michaelis-Menten plot for different concentrations of the substrate pAPP. For amperometric measurement, the total concentration of pAPP substrate prepared in DEA buffer pH 9.5 and in the presence of 0.1 M KCI done as per the 95% of I_{max} value obtained from Michaelis - Menten plot.

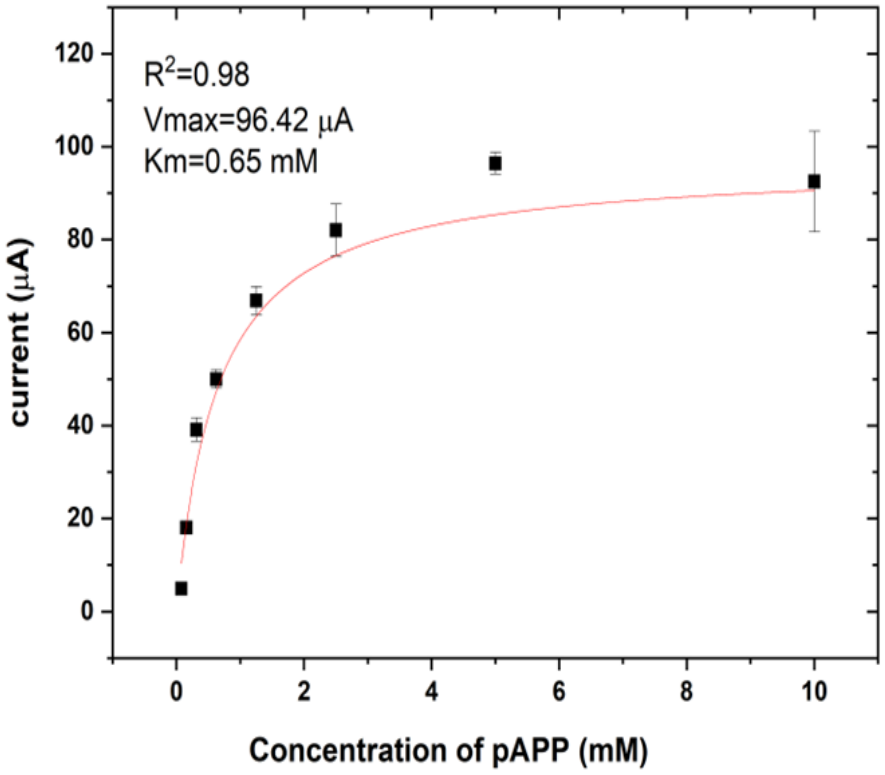


Figure 3.6 Michaelis-Menten plot for different concentration of the substrate pAPP.

3.13.4 Electrochemical Characterization

LSV and CV, as shown in Figure 3.7 A,B were utilized to investigate the SAM redox process in relation to the gold electrode [46,48]; however, their limitations made this difficult. For example, it was difficult to avoid double layer charging and to measure current on low overpotential [47,49]. For these reasons, EIS was applied, as shown in Figure 3.7 C [50]. EIS is a sensitive method for investigating electron transport over a thin monolayer [48,50]. Amperometry was utilized in the presence of *p*AP, which is transformed to *p*-aminophenol, to prove the enzymatic process before adding the target analyte (*p*AP). At +300 mV (vs. Ag/AgCl), detection of *p*AP was possible. Electrodes may be amperometrically measured because of the low substrate specificity of AP (Figure 3.7 D).

3.13.4 .1 Stability Study of the Coated Electrodes

Before the linear sweep voltammetry deduction was used, the electrodes underwent a complete capture assay. A total of 0.123 µg/ml of the primary antibody was immobilized on the electrode surface, followed by the addition of the labelled secondary antibody in 1/5000 dilution. In total, 10 µL of the substrate solution *p*APP was diluted in DEA buffer (pH 9.5, 1 mg /ml) and added to the electrode surfaces. The electrochemical substrates were incubated, and measurements were taken using the PalmSens potentiostat. The electrodes were washed and dried before using LSV. Measurements were performed daily for 10 days using the three electrodes (n = 3).

Figure 3.7 A shows the 10-day performance of the coated BSA-Aroclor 1254 coating conjugate on the gold electrode using LSV detection. From the graphs, it was observed that the coated electrode remained stable for the first 5 days with a decrease in signal being observed from day 6.

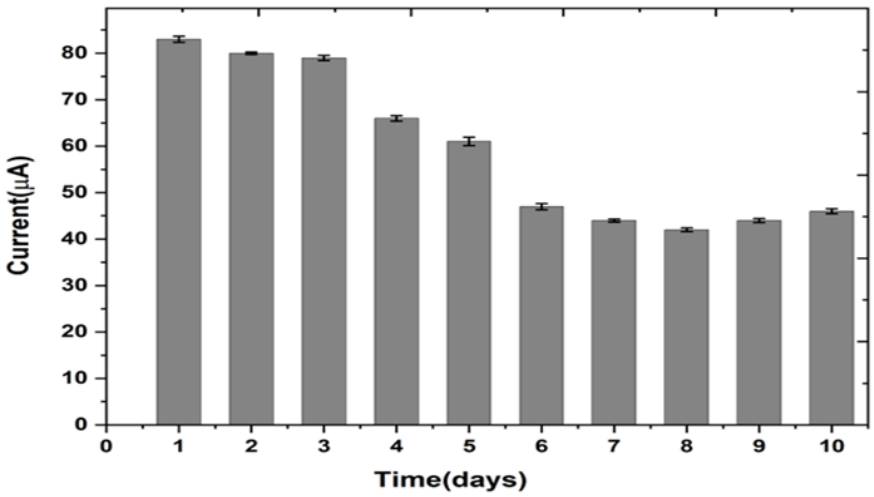


Figure 3.7 Electrochemical characterization of modified electrode. **(A)** A stability study of the coated BSA-Aroclor 1254 on a gold electrode surface was performed using linear sweep voltammetry. Prior to the measurements, the coated electrode was stored at 4 °C. Three electrodes were measured every day for 10 days.

3.13.4.2 Cyclic Voltammetry

To identify the electrochemical properties of the electrode modification, an 11-MUA self-assembly on the gold electrode CV was used. The peaks of the ferricyanide/ferrocyanide couple were utilized to investigate the SAM electron-transfer efficiency on the gold surfaces. It was found that when the SAM molecules bonded to the gold electrode surface, this gradually inhibited electron transport. Figure 3.7 B displays the electrode CVs before and after SAM modification with 11-MUA. Findings indicated a decrease in $[Fe(CN)_6]^{3-/4-}$ cathodic and anodic peak current following the gold surface's immobilization of 11-MUA SAM. This is consistent with the findings of Lu et al. [51]. Water-soluble NHS and EDC to carboxylic acid immobilization ended as SAMs increased protein coverage [52]. The coating conjugate and primary monoclonal antibody were immobilized using the competitive ELISA method.

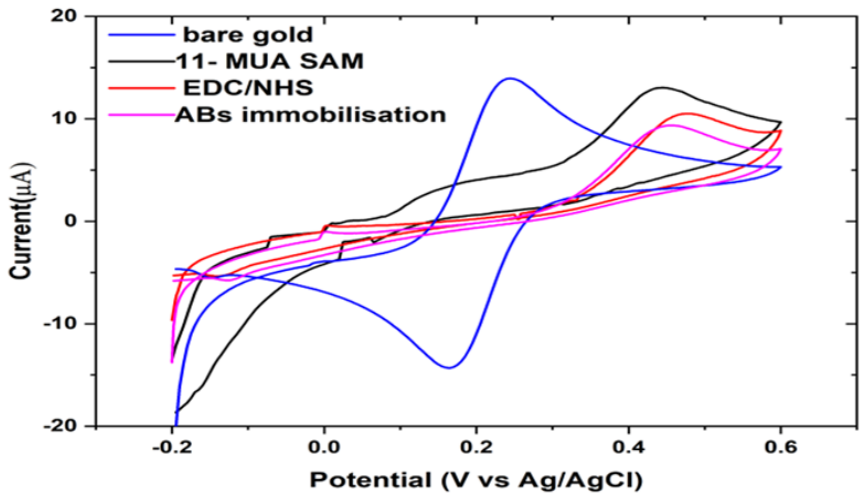


Figure 3.7 (B) The voltammogram of CV for the bare gold electrode and the gold electrode after SAM modification with 11-MUA.

3.13.4.3 Impedance Measurement

To gather further kinetic data, impedance was next applied in this study over a broader time constant limit. The impedance measurements applied ranged from 0.1 Hz to 1 MHz. An amplitude of 0.1 V and a potential of 0.21 V were used. It was observed that at higher frequencies, a semi-circle followed by a straight line appeared at the lower frequencies for the bare gold electrode, demonstrating the presence of Warburg resistance, as shown in Figure 3.7 C. The diffusion processes occurred at the surface of the electrode when it was connected to the equivalent circuit that corresponded to the charge-transfer resistance (Re) [53]. With regard to the bare gold (Au) electrodes, there was an increase in impedance value, and the 11-MUA gold electrode was immobilized for electron transfer [54]. A highly insulated surface on the gold electrode was formed after SAM formation. Upon the addition of the protein layer (BSA-Aroclor 1254) coating conjugate, the impedance value significantly increased at both high and low frequencies. This increase relates to the higher molecular weight of protein-BSA (M = 66.5 kDa), compared to 11-MUA (M = 218.36 g/mol). This result is supported by the fact that almost all the faradaic current was blocked, which increased the surface resistance [27]. The Randle's equivalent shown in Figure 3.7 C depended on mass transport and is comparable to data obtained for electron transfer in an earlier study [54]. The parameter assessment for the Randle's equivalent circuit on the gold electrode for 11-MUA SAM is shown in Table 3.3. Findings indicated that the value C_{dl} for the monolayer electrode was lower than the one recorded for the bare gold electrode (1.18×10^{-6} F/cm^{-2}). This low C_{dl} value is a sign that the electrodes are coated

by well-formed SAM of carboxylic-acid-ended long chain thiols [55]. Upon the activation of EDC/NHS and the addition of the protein layer, the C_{dl} values fell to 8.10 × 10^{-7} and 5.74 × 10^{-7} F/cm^{-2}, in that order. This was due to the presence of the immobilized protein (BSA-Aroclor 1254 coating conjugate) on the gold surface, which resulted in the reduced access of the solution ions to the gold surface.

Table 3.3 Parameter evaluation for the Randle's model on a gold electrode.

Surface	**RS (Ω)**	**Rct (KΩ)**	**Cdl (F/cm^2) × 10^{-6}**
Bare gold	7.52	0.385	8.20
SAM (20 h)	7.79	12.56	1.18
EDC/NHS (1 h)	7.74	27.13	0.81
BSA-Arcoler 1254	7.79	34.92	0.57

Data obtained from CHI 1100/620B software.

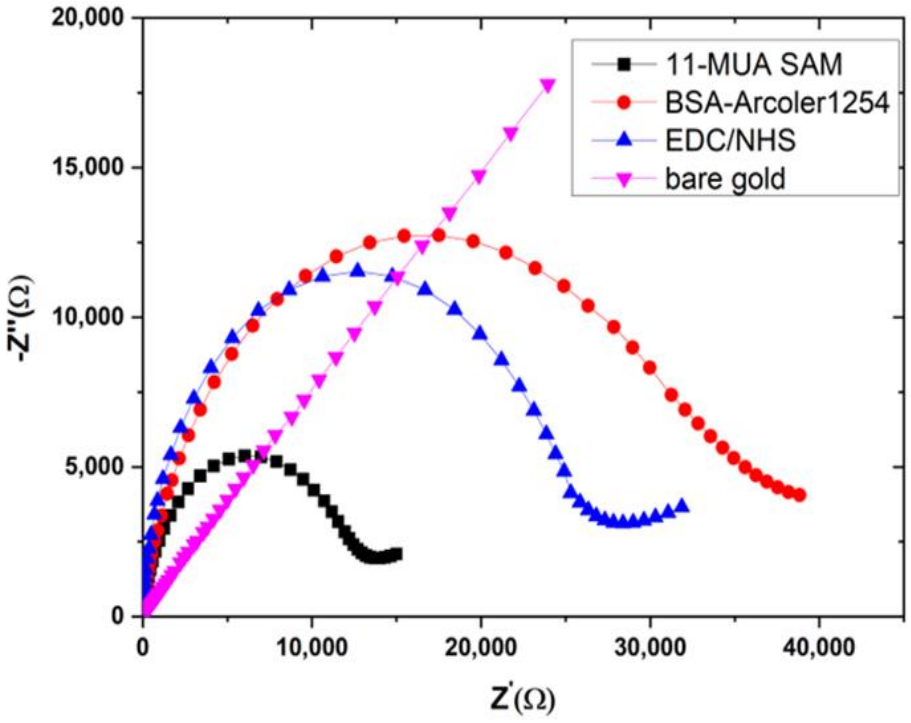


Figure 3.7 (C) Impedance spectra of the bare gold electrode, after 20 h SAM, activation with EDC/NHS and immobilization with 5 µg/ml BSA-Aroclor 1254. The redox couple was 5 Mm [Fe (CN)6]$^{3-/4-}$ in 0.1 KCl. Frequency measured from 0.1 Hz to 1 MHz, with amplitude of 0.1 V, potential applied at 0.21 V. The inserted circuit is Randle's equivalent, where Rs represents the dynamic solution resistance, R_{ct} represents the charge transfer resistance of the immobilize recognition layer, C_{dl} indicates the capacitance measured between the gold electrode and the electrolyte solution on a double layer basis, and Zw is the Warburg element describing the time frequency.

3.13.4.4 Amperometric Detection

Amperometry can detect the current flow resulting from the enzymatic redox reaction in real-time. Before the amperometric measurements were taken, the electrodes were washed and stored in DEA buffer. *p*APP was the substrate that was used for the amperometric sensor. Figure 3.7 D shows the amperometric response of the immunoassay system. Findings revealed that when the *p*APP was introduced at 50 s, the amperometric signal increased and reached a steady-state value in less than 80 s. A steady background amperometric signal was also obtained when there was no addition of *p*-aminophenyl phosphate (*p*APP), which demonstrated electrode stabilization. The enzyme that was utilized for electrochemical detection was AP, which was also used for the ELISA work. Enzyme AP converts *p*NPP into the molecule *p*-nitrophenol, which is spectrophotometrically detectable in conventional ELISAs. Considerable differences in redox potentials between phosphorylated and free forms were observed due to a lack of electrode fouling by electro polymerization and a low redox potential when converted to (*p*AP) at (+300 mV (vs. Ag/AgCl) *p*AP is detectable [46,47]. Measurement of the electrodes both amperometrically and spectrophotometrically was possible due to the low substrate specificity of AP.

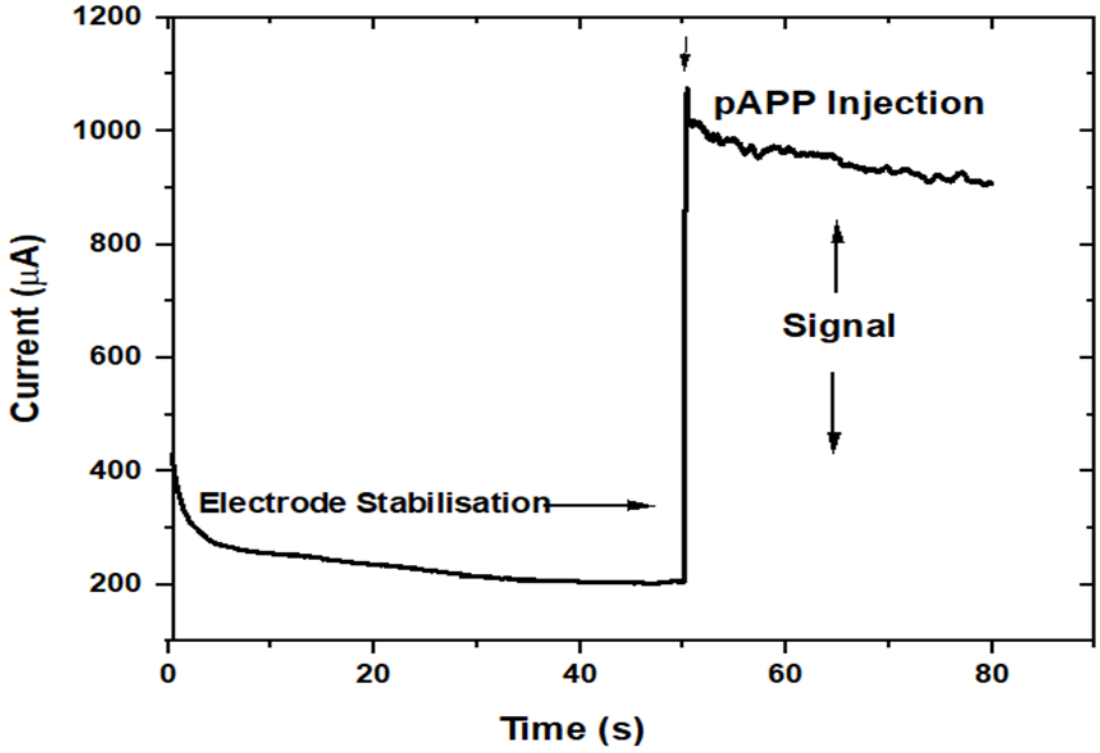


Figure 3.7 (D) Amperometric detection of a chip modified AP containing bilayer (competitive assay) was measured in DEA buffer pH 9.5 at potential of 0.45 V vs. Ag/AgCl. The substrate pAPP was injected at 40 s.

3.13.5 Specificity (Cross-Reactivity)

The specificity of the assay was evaluated by the CR (cross-reactivity) of the polyclonal antibody with five different types of compounds of Aroclors such as (Aroclor 1248, Aroclor 1016, Aroclor 1242, Aroclor 1260, Aroclor 1262). The CR values were calculated according to the following formula: CR (%) = (IC50 of Aroclor 1254)/ (IC50 of other compounds) ×100. The cross-reactivity of five Aroclors compounds against Aroclor 1254 was measured, and the results are displayed in Table3.4. A low IC50 value was recorded for Aroclor 1254, which proved the sensitivity of the assay toward the PCBs detection. Based on the CR values, the assay evidently provided higher responses to formulations with highly chlorinated biphenyls (Aroclors 1254, 1260, and 1262), which had a similar structure arrangement to Aroclor 1254. On the other hand, it recorded the lowest cross-reactivity with a lower chlorination level (Aroclor 1248, 1242, 1016) because of the significant difference in their molecular structures with Aroclor 1254. Therefore, this method showed good specificity for the detection of Aroclor 1254.

Table 3.4 The cross-reactivities of the antibody against Aroclor 1254 and other Aroclor using competitive assay.

Compound	IC50 (ng/ml)	CR (%)
Aroclor 1254	3.94	100
Aroclor 1248	14.4	27.36
Aroclor 1260	5.20	75.765
Aroclor 1242	11.57	34
Aroclor 1262	6.30	62.53
Aroclor 1016	13.27	29.6

3.13.6 Optimizing the Concentration of PCB Ab and Secondary Antibody:

The objective of this assay was to optimise the concentration of PCB primary antibody on the biochip working electrode using the capture assay for PCB detection. This assay was carried out by immobilising a BSA-Aroclor 1254 coating conjugate at 5 µg /ml to completely cover the working electrode. The biochips were blocked with the bocking solution containing 1 % BSA in Tris Buffer pH 7.4. A serial dilution of different concentrations of primary antibody was prepared in 12 different concentrations start from 10 µg/ ml. measured using Linear sweep voltammetry detection. The graph in Figure 3.8 (A) shows the optimized concentration of PCB primary antibody was 0.123

μg/ml. Clearly, optimization of the assay components was required. Hence, capture assays were performed using a fixed concentration of Polyclonal Chicken antibody (IgY) specific to PCB and varying secondary antibody dilution. Blank results had no primary antibody) to ensure that increased secondary antibody concentration did not also lead to an increase in non-specific binding of the secondary antibody to the sensor surface. Figure 3.8 (B) shows that a dilution of 1/5000 goat anti-chicken (IgY) antibodies gave a large current without a significant amount of non-specific binding and hence this dilution was used for all further assays. The capture assay was then repeated using the optimized secondary antibody concentration.

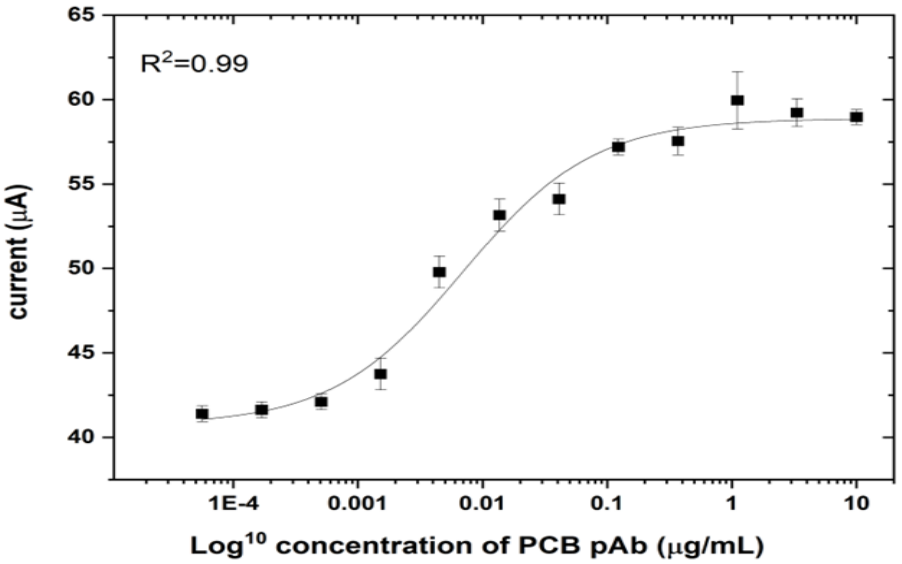


Figure 3.8 (A) Optimized concentration of Polyclonal Chicken antibody (IgY) specific to PCB (primary antibody) using capture assay. Detection was LSV (n=3). The optimized concentration of PCB was 0.123 μg/ml.

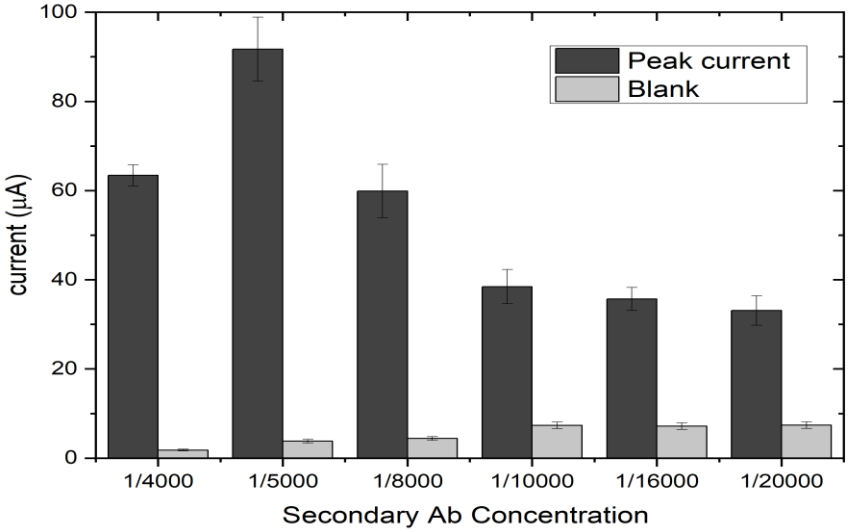


Figure 3.8 (B) show that a dilution of 1/5000 Goat anti-chicken IgY gave a large current signal without a significant amount of nonspecific and hence this dilution was used for all further assays.

3.13.7 The Importance of Blocking Solution

The study was thus key in establishment of the important of the blocking steps. The first control was the substrate of pAPP, second control was the assay without the blocking steps and the last one was the normal assay. From the graph in Figure 3.9 there is a very low signal for blank. This observation was expected as there were no biocomponents immobilized on the electrode surface. For the assay without blocking step, the signal observed had high standard deviation not as that observed for normal assay. With the fact that the blocking step was skipped in the second control, it can be concluded that non-specific binding has occurred. This phenomenon happened probably due to the interference of antibody and antigen interactions, which led to the binding of the unexpected region of antibodies with low avidity, thus resulting in high signal and low precising.

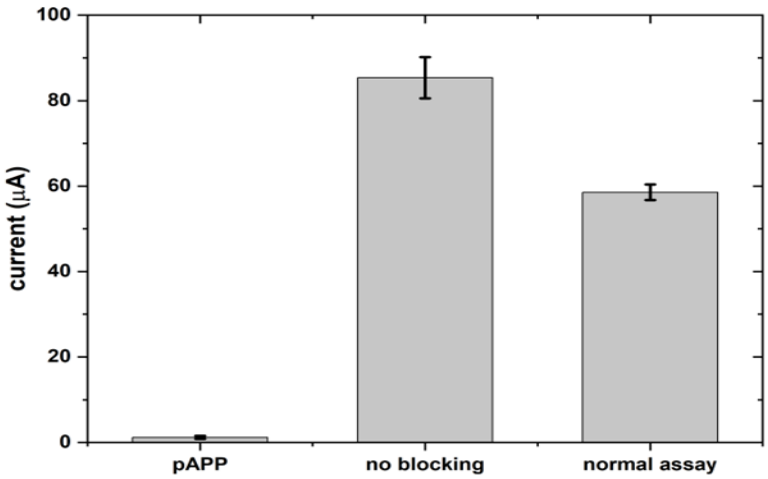
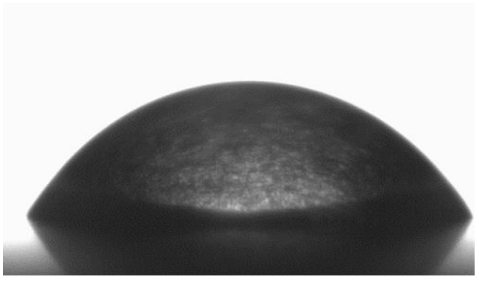


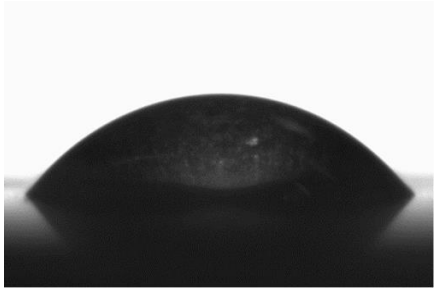
Figure 3.9 The influence of blocking step. The capture assay was carried out using AP labelled**.**

3.13.8 Topography Characterization

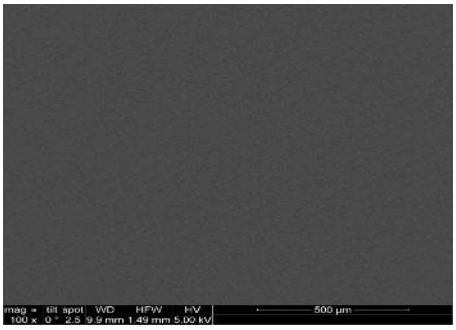
In order to study SAM behavior, a characterization of the monolayer on the gold electrode was carried out using contact angle, SEM and AFM. The contact angle data showed significant variations in hydrophobicity/hydrophilicity when the substrate was modified. The gold immobilized SAM electrode was tested using contact angles for structural information about the modified surface, as shown in Figure 3.10 A, B. SEM and AFM are complementary techniques in assessing SAM formation. SAMs are usually smooth, structurally ordered and chemically defined at the microscopic scale [42]. Therefore, they are ideal for SEM and AFM measurements. Comparisons were made before and after SAM and protein immobilization was performed on the same gold surface. Furthermore, the interaction between SAM and proteins immobilized on the gold electrode was examined. The bare gold and the modified electrode images were taken at ×100 magnification using SEM corresponding to the various stacks, as shown in Figure 3.10 C, D. AFM high-resolution images were taken to measure the roughness of the gold surface electrode during the electrode modification process. This process began with the bare electrode (Figure 3.10 E), then the electrode when 11-MUA was adsorbed (Figure 3.10 F), then the electrode after the activation of EDC/NHS (Figure 3.10 G), and, finally, the electrode after the protein layer of BSA-Aroclor 1254 was formed (Figure 3.10H).



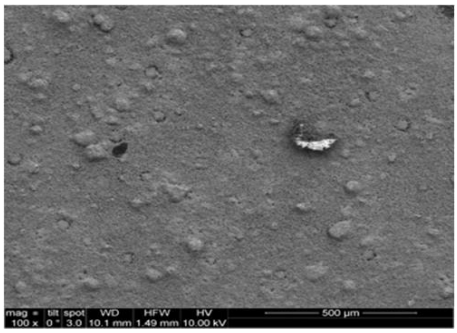
(**A**)



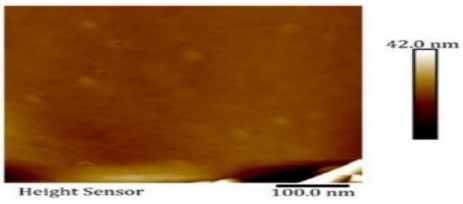
(**B**)


mag = tilt spot WD HFW HV
100 x 0 ° 2.5 9.9 mm 1.49 mm 5.00 kV
500 µm

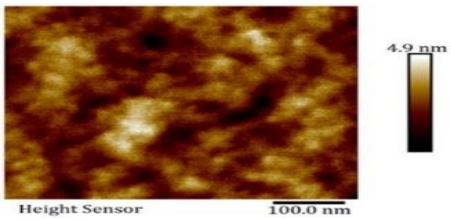
(**C**)


mag = tilt spot WD HFW HV
100 x 0 ° 3.0 10.1 mm 1.49 mm 10.00 kV
500 µm

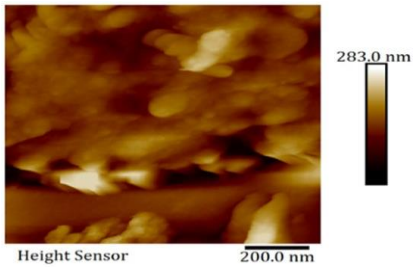
(**D**)


42.0 nm
Height Sensor
100.0 nm

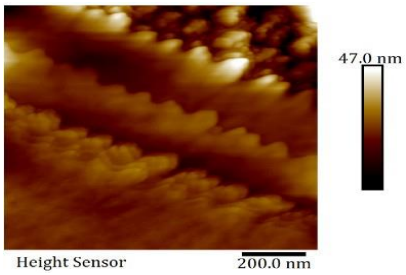
(**E**)


4.9 nm
Height Sensor
100.0 nm

(**F**)


283.0 nm
Height Sensor
200.0 nm

(**G**)


47.0 nm
Height Sensor
200.0 nm

(**H**)

Figure 3.10 Typical topography of the bare electrode surfaces of gold SPE and modified with SAM. Contact angle graphs of bare electrode (A) and SAM-modified electrode (B); SEM micrographs of bare electrode (C) and 11MUA-SAM-modified electrode (D); top cross-section (×100 magnification); AFM micrographs (E) bare Au, (F) 11-MUA SAM (20 h), (G) EDC/NHS (1 h), (H) BSA-Aroclor 1254 coating conjugate.

3.13.8.1 Contact Angle Measurement

The thiol end groups utilized in the fabrication of the modified SAM gold electrodes impacted on the water contact angle. The contact angle for bare gold electrodes is 59.4 degrees [24,43]. However, as shown in Figure 3.10 A, B, after 20 h of SAM synthesis, the contact angle value decreased in comparison with the gold bare electrode value, showing the presence of a hydrophilic surface. Hydroxyl-terminated (OH) and methyl-terminated (CH_3) SAMs will usually possess a smaller hydrophobic surface over amine-terminated (NH_2) or carboxylic acid-terminated (COOH) SAMs [42,44]. Previous research has indicated that the low contact angle value of carboxylic acid-terminated monolayers suggests that the monolayer surface is covered with dense arrays of thiol tail groups. Findings by Wang et al. indicated that SAM carboxyl acid terminus had a minimum contact angle of 10°, depending on the kind of SAM synthesis utilized [42,45]. On the other hand, the contact angle for SAM produced in ethanolic solution has been measured as 35°. This corresponds with the contact angle values obtained twenty hours after SAM modification, as indicated in Table 3.5. SAM adjustment had 2.2 % percent relative standard deviation and decreased the water contact angle for five tests that were recorded per electrode.

Table 3.5 The water contact angle of gold electrodes is treated with thiol SAM.

	Before SAM	After SAM
Contact angle θ (°)	56.9	35.4
Relative standard deviation (%)	3.7 %	2.2 %

Measurement was taken five times for each electrode.

3.13.8.2 Scanning Electron Microscopy (SEM)

The surfaces of the electrodes were photographed using SEM so as to identify at a high resolution the spatial variations in the electrodes before and after modification. The bare gold electrode surface appeared smoother (Figure 3.10 C) than the modified electrode and had a more uneven structure (Figure 3.10 D). As was previously reported [21], the images in Figure 3.10 D show the transition in the surface morphology of the electrodes as the various stacks attached to the gold surface.

3.13.8.3 Atomic Force Microscopy (AFM)

AFM was applied at 0.5 uM^2 to evaluate the interactions between SAM and the proteins that were immobilized on the bare gold electrodes. Figure 3.10 E shows that there was a smooth surface structure for the bare gold electrodes to a resolution of 42 nm. The topography image after the adsorption of 11-MUA revealed a flat surface, with the calculated average of the surface roughness being 2.80 nM (Figure 3.10 F). It was found that the protein layer of the BSA coating conjugate, which formed on the

surface, resulted in greater roughness (Figure 3.10 H) than the surface following the activation of EDC/NHS (Figure 3.10 G). Surface roughness and particle diameter are important because they can aid in the study of the effects of tribological behavior on surfaces. Table 3.6 shows the surface roughness and particle diameter size of the gold electrode before and after the introduction of SAM, EDC/NHS, and the protein layer. It has been reported that surface roughness increases with the addition of protein [46]; however, this research found that the surface roughness decreased after the addition of the protein. The maximum particle diameter was 141.20 nm. As has been argued by Kim [47], it may be possible that the roughness could be due to the different shapes of the protein layer. In addition, it shows inhomogeneous particles size after the addition of the BSA-Arcolor 1254 coating conjugate. This is due to the aggregation of antibodies.

Table 3.6 Surface roughness and particle diameters of bare and modified gold electrodes.

	Bare Gold Electrode	**SAM (20 h)**	**EDC/NHS (1 h)**	**BSA-Alcoler1254 Coating Conjugate**
Surface Roughness	4.74	2.8	2.88	2.94
Min particles diameter (nm)	11.86	-	-	11.86
Max particles diameter (nm)	107.74	-	-	141.2

*Data obtained from NanoScope Analysis 1.9 software.

3.13.9 Indirect Competitive Assay

Linear sweep voltammetry was performed to generate the curves of indirect competitive assay using bare gold electrodes and SAM modified electrodes, as shown in Figure 3.11. Prior to surface modification, the biochips were cleaned using a plasma cleaner. After SAM formation, and to eliminate any unbound molecules from the surface of the gold, the electrodes were cleaned using absolute ethanol. Following SAM formation, a mixture of EDC and NHS was immobilized onto the surface of the gold electrode. The resulting intermediate NHS esters were stable at neutral conditions and did not hydrolyze easily. The unmodified bare gold electrode had a limit of detection (LOD) of 0.202 ng/ml and $R2$ value of 0.96. These findings are lower than other investigators' reported values, but they are still within reasonable parameters [24]. A linear range from 0.304 to 220 ng/ml was attained. When the electrode was changed, it was found that the modification electrode displayed a LOD of 0.09 ng/ml, a sensitivity level that was much lower than that of the unmodified electrode. The sensor recorded a linear detection range of between 220 and 0.101 ng/ml with an $R2$ value of 0.99. This novel modification had good value among other literature reviews, as illustrated in Table 3.7.

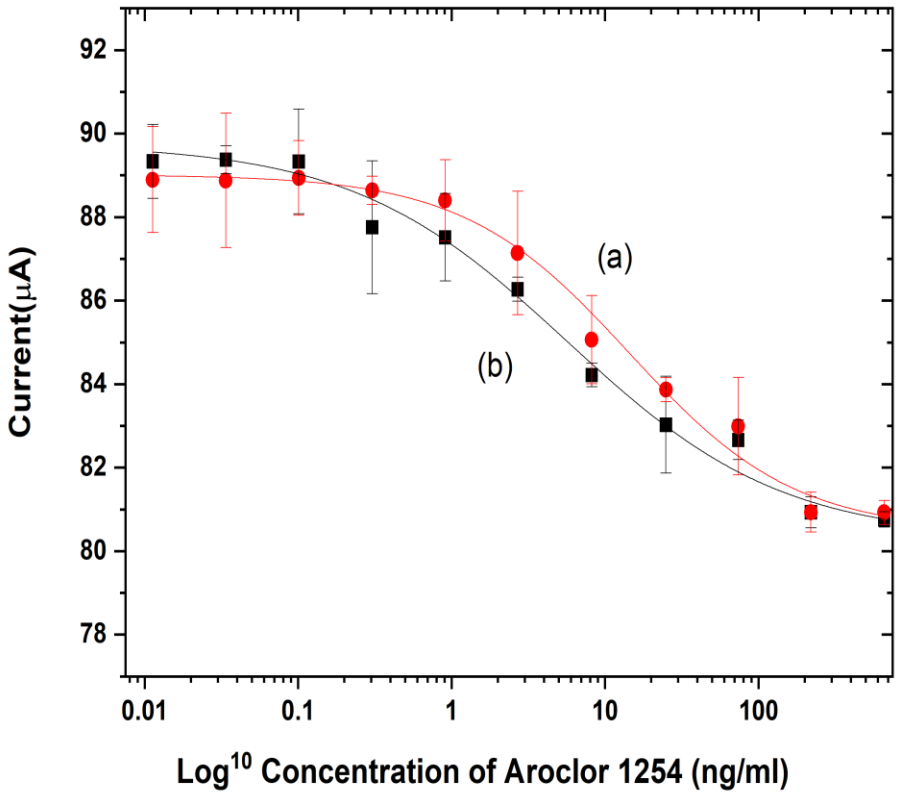


Figure 3.11 A competitive assay was conducted in which the performance of the gold electrode modified with 11-MUA was compared with the assay performance using (a) a bare gold electrode and (b) SAM modification gold electrode.

Table 3.7 Comparison with previously reported electrochemical PCB immunosensors with present work.

Immunosensor	Analyte	LOD	Linear Range	Ref.
MoS2-rGO/Thi/AuNP/GCE	PCB77	80 ag /mL	0.3 fg/mL–0.1 ng /mL	[58,59]
SnS2/β-CD modified screen-printed electrode	Aroclor1016	5 µM	0.625 to 80 µM	[19]
β-CDP/rGO/PPy/PGE	PCB	0.50 pM	1.0 pM–10.0 µM	[5]
Gold bare electrode	Aroclor of 1254	0.20 ng/ml	0.304–220 ng/ml	This work
Au SPE/11MUA-SAM/EDC/NHS	Aroclor of 1254	0.09 ng/ml	0.1 to 220 ng/ml	This work

3.13.10 Real Sample Analysis

11-MUA-SAM/EDC/NHS/SPGE was applied to determine Aroclor 1254 in soil, tap and river water samples collected using the standard addition technique. The river and tap samples were further diluted with tris-BSA buffer solution pH 7.4 and analysed by LSV and ELISA. As highlighted in Table 3.8, the developed sensor's results showed that the recovery values of the spiked samples were in the range of 91–97% for all samples, which indicated highly reliable results, with an RSD value that was below 3% (n = 3). On the other hand, the Aroclor 1254 results obtained by ELISA showed that the recovery values of the spiked samples were in the range of 107.26–120% with an RSD of approximately 7 % (n = 3) Therefore, the 11-MUA-SAM/EDC/NHS/SPGE was an effective technique in determining Aroclor 1254 in environmental samples. Similarly, the analytical results that were obtained from the 11-MUA-SAM/EDC/NHS/SPGE showed that the procedures of the sample analysis were significantly easy as it benefits from a lower determination time and fewer potential errors produced from the elaborate sample preparation. These results were more effective and reliable when compared to the results obtained from ELISA measurements, which is a traditional technique. In terms of detecting Aroclor 1254, it was clear from the results that ELISA could not accurately quantify the variables that were being tested. Therefore, this meant that the developed electrode was more sensitive and precise when compared to the standard instrument, which made the results obtained more satisfactory. The results of the fundamental analysis also showed that the developed sensor had other benefits such as high accuracy, selectivity, and sensitivity in the determination of the PCBs in the environmental samples.

Table 3.8 MUA-SAM/EDC/NHS/SPGE and ELISA (immunoassay) for the determination of Aroclor 1254 in environmental samples.

Techniques	Sample	Added (ng/ml)	Found (ng/ml)	Recovery %	RSD % (n = 3)
11-MUA-SAM/EDC/NHS/SPGE	River water	75	72.75	97	1.34
11-MUA-SAM/EDC/NHS/SPGE	Tap water	75	68.25	91	2.35
11-MUA-SAM/EDC/NHS/SPGE	Soil	75	71.46	95	1.19
ELISA	River water	75	90	120	6.88
ELISA	Tap water	75	80.44	107.26	4.96
ELISA	Soil	75	84.43	112	5.82

3.14 Conclusions

The modification of Au SPE/11MUA-SAM/EDC/NHS in this paper was successfully employed to determine PCBs (Aroclor 1254). In this paper, contact angle, SEM and AFM, the typical topography characterization techniques were used to examine the surface of bare and modified electrodes. In addition, investigation of biochips' electrochemical behaviour was carried out by way of impedance and cyclic voltammetry, through the use of 5 mM potassium ferricyanide/ferrocyanide in the presence of 0.1 M KCI as the redox probe. This redox pair was selected as they are one of the most studied redox complexes in electrochemistry. LSV and amperometry were used to test the stability of the coated electrode as well as the enzymatic redox reaction. The competitive assay was applied to test the developed SPE. The findings demonstrated a significant increase in sensitivity and analytical performance when compared to the SPE. Utilizing the 11-MUA SAM solution, modification of the electrode with the gold surface for detecting Aroclor 1254 determined an LOD of 0.09 ng/ml and a linear range (220–0.101 ng/ml).

In an immunoassay, immobilizing protein to targeted sites without non-specific binding is critical. SAM was employed to reduce the random orientation of antibodies attaching to the surface. Findings indicated that the presence of SAM on the gold electrode increased the binding of the antibody to the surface, and therefore, sensor sensitivity was increased. It was observed that the electrode became more insulated after the immersion of EDC/NHS and BSA-Aroclor 1254 coating conjugate. Overall, the developed chip showed good performance and stability and could be utilized for detection of PCB

compounds using the proposed electrochemical immunosensor. This immunosensor could be used in conjunction with a portable device, allowing for in-field measurements. Moreover, much more work could be carried out to improve the commercialization of the described technique, such as minimizing the number of stages for the assay and the incubation time. In addition, further study could seek to increase the sensitivity and performance of the individual sensor measurements. This would also reduce the steps required for immunoassay testing in the field. Therefore, the integration into a real-time portable lab- on-a-chip solution could represent a future platform for monitoring organic pollution such as PCBs in the environment and avoid costly and non-efficient analysis of the samples in dedicated laboratories.

3.15 Reference

1. Varanasi, P.; Fullana, A.; Sidhu, S. Remediation of PCB contaminated soils using iron nanoparticles. *Chemosphere* **2007**, *66*, 1031–1038.

2. Chana, A.; Concejero, M.A.; De Frutos, M.; Gonzá Lez, M.J.; Herradón, B. Computational Studies on Biphenyl Derivatives. Analysis of the Conformational Mobility, Molecular Electrostatic Potential, and Dipole Moment of Chlorinated Biphenyl: Searching for the Rationalization of the Selective Toxicity of Polychlorinated Biphenyls (PCBs)†. *Chem. Res. Toxicol.* **2002**, *15*, 1514–1526.

3. Cao, S.; Capozzi, S.L.; Kjellerup, B.V.; Davis, A.P. Polychlorinated biphenyls in stormwater sediments: Relationships with land use and particle characteristics. *Water Res.* **2019**, *163*, 114865.

4. The Risk Assessment Information System. Available online: https://rais.ornl.gov/tox/profiles/aroclor_1254_f_V1.html (accessed on 9 October **2021**).

5. Zheng, X.; Li, H.; Xia, F.; Tian, D.; Hua, X.; Qiao, X.; Zhou, C. An Electrochemical Sensor for Ultrasensitive Determination the Polychlorinated Biphenyls. *Electrochim. Acta* **2016**, *194*, 413–421.

6. Yang, G.; Zhuang, H.; Chen, H.; Ping, X.; Bu, D. A gold nanoparticle-based immunosorbent bio-barcode assay combined with real-time immuno-PCR for the detection of polychlorinated biphenyls. *Sens. Actuators B Chem.* **2015**, *214*, 152–158.

7. Gabryszewska, M.; Gworek, B. Impact of municipal and industrial waste incinerators on PCBs content in the environment. *PLoSONE* **2020**, *15*, e0242698.

8. Deng, A.P.; Kolárˇ, V.; Ulrich, R.; Fránek, M. Direct competitive ELISA for the determination of polychlorinated biphenyls in soil samples. *Anal. Bioanal. Chem.* **2002**, *373*, 685–690.

9. Yang, G.; Zhuang, H.; Chen, H.; Ping, X. An indirect competitive enzyme-linked immunosorbent assay for the determination of 3,4-dichlorobiphenyl in sediment using a specific polyclonal antibody†. *Anal. Methods* **2014**, *6*, 893–899.

10. Petrovic, M.; Sremacki, M.; Radonic, J.; Mihajlovic, I.; Obrovski, B.; Vojinovic Miloradov, M. Health risk assessment of PAHs, PCBs and OCPs in atmospheric air of municipal solid waste landfill in Novi Sad, Serbia. *Sci. Total Environ.* **2018**, *644*, 1201–1206.

11. Reddy, A.V.B.; Moniruzzaman, M.; Aminabhavi, T.M. Polychlorinated biphenyls (PCBs) in the environment: Recent updates on sampling, pretreatment, cleanup technologies and their analysis. *Chem. Eng. J.* **2019**, *358*, 1186–1207.

12. Wei, Y.; Kong, L.-T.; Yang, R.; Wang, L.; Liu, J.-H.; Huang, X.-J. Electrochemical impedance determination of polychlorinated biphenyl using a pyrene cyclodextrin-decorated single-walled carbon nanotube hybridw. *Chem. Commun* **2011**, *47*, 5340–5342.

13. Zhang, J.; Pan, M.; Gan, N.; Cao, Y.; Wu, D. Employment of a novel magnetically multifunctional purifying material for determination of toxic highly chlorinated polychlorinated biphenyls at trace levels in soil samples. *J. Chromatogr. A* **2014**, *1364*, 36–44.

14. Ayris, S.; Currado, G.M.; Smith, D.; Harrad, S. GC/MS procedures for the determination of PCBs in environmental matrices.*Chemosphere* **1997**, *35*, 905–917.

15. Van Emon, J.M.; Chuang, J.C. Development and application of immunoaffinity chromatography for coplanar PCBs in soil and sediment. *Chemosphere* **2013**, *90*, 1–6.

16. Cheng, J.; Wang, P.; Su, X.-O. Surface-enhanced Raman spectroscopy for polychlorinated biphenyl detection: Recent developments and future prospects. *TrAC Trends Anal. Chem.* **2020**, *125*, 115836.

17. West, C.; Lesellier, E. A unified classification of stationary phases for packed column supercritical fluid chromatography. *J. Chromatogr. A* **2008**, *1191*, 21–39.

18. Ramón-Azcón, J.; Valera, E.; Rodríguez, Á.; Barranco, A.; Alfaro, B.; Sanchez-Baeza, F.; Marco, M.P. An impedimetric immunosen-sor based on interdigitated microelectrodes (IDμE) for the determination of atrazine residues in food samples. *Biosens. Bioelectron.* **2008**, *23*, 1367–1373.

19. Liu, X.; Sakthivel, R.; Cheng, C.-Y.; Luo, J.; Song, L.; Wu, J.; He, W.; Younis, U.; Chung, R.-J. 3A-Amino-3A-Deoxy-(2AS, 3AS)-β-Cyclodextrin Hydrate/Tin Disulfide Modified Screen-Printed Carbon Electrode for the Electrochemical Detection of Polychlorinated Biphenyls. *Nanoscale Res. Lett.* **2020**, *15*, 4.

20. Yu, Y.; Chen, X.; Wei, Y.; Liu, J.-H.; Huang, X.-J. Strategy for Polychlorinated Biphenyl Detection Based on Specific Inhibition of Charge Transport Using a Nanogapped Gold Particle Film. *Anal. Chem.* **2012**, *84*, 9818–9824.

21. Moldovan, C.; Mihailescu, C.; Stan, D.; Ruta, L.; Iosub, R.; Gavrila, R.; Purica, M.; Vasilica, S. Characterization of self-assembled monolayers (SAMs) on silicon substrate comparative with polymer substrate for *Escherichia coli* O157:H7 detection§. *Appl. Surf. Sci.* **2009**, *255*, 8953–8959.

22. Centi, S.; Laschi, S.; Fránek, M.; Mascini, M. A disposable immunomagnetic electrochemical sensor based on functionalised magnetic beads and carbon-based screen-printed electrodes (SPCEs) for the detection of polychlorinated biphenyls (PCBs). *Anal. Chim. Acta* **2005**, *538*, 205–212.

23. Khesuoe, M.P.; Okumu, F.O.; Matoetoe, M.C. Development of a silver functionalised polyaniline electrochemical immunosensor for polychlorinated biphenyls†. *Anal. Methods* **2016**, *8*, 7087–7095.

24. Ahmad, A.; Moore, E. Electrochemical immunosensor modified with self-assembled monolayer of 11-mercaptoundecanoic acid on gold electrodes for detection of benzo[a]pyrene in water. *Analyst* **2012**, *137*, 5839–5844.

25. Briand, E.; Salmain, M.; Herry, J.M.; Perrot, H.; Compère, C.; Pradier, C.M. Building of an immunosensor: How can the composition and structure of the thiol attachment layer affect the immunosensor efficiency? *Biosens. Bioelectron.* **2006**, *22*, 440–448.

26. Mendes, R.K.; Ferreira, D.C.M.; Carvalhal, R.F.; Peroni, L.A.; Kubota, L.T. Development of an Electrochemical Immunosensor for. *J. Braz. Chem. Soc.* **2009**, *20*, 795–801.

27. Tlili, A.; Abdelghani, A.; Ameur, S.; Jaffrezic-Renault, N. Impedance spectroscopy and affinity measurement of specific antibody– antigen interaction. *Mater. Sci. Eng. C* **2006**, *26*, 546–550.

28. Gutiérrez-Zúñiga, G.G.; Hernández-López, J.L. Sensitivity improvement of a sandwich-type ELISA immunosensor for the detection of different prostate-specific antigen isoforms in human serum using electrochemical impedance spectroscopy and an ordered and hierarchically organized interfacial supramolecular architecture. *Anal. Chim. Acta* **2016**, *902*, 97–106.

29. Chaki, N.K.; Vijayamohanan, K. Self-assembled monolayers as a tunable platform for biosensor applications. *Biosens. Bioelectron.***2002**, *17*, 1–12.

30. Arya, S.K.; Solanki, P.R.; Datta, M.; Malhotra, B.D. Recent advances in self-assembled monolayers based biomolecular electronic devices. *Biosens. Bioelectron.* **2009**, *24*, 2810–2817.

31. Ulman, A. Self-Assembled Monolayers of 4-Mercaptobiphenyls and the Garcia MRSEC for Polymers at Engineered Interfaces.*Acc. Chem. Res.* **2001**, *34*, 855–863.

32. Gooding, J.J.; Ciampi, S. The molecular level modification of surfaces: From self-assembled monolayers to complex molecular assemblies. *Chem. Soc. Rev* **2011**, *40*, 2704–2718.

33. Sayikli Şimşek, Ç.; Nur Sonuç Karaboğ a, M.; Sezgintürk, M.K. A new immobilization procedure for development of an electrochemical immunosensor for parathyroid hormone detection based on gold electrodes modified with 6-mercaptohexanol and silane. *Talanta* **2015**, *144*, 210–218.

34. Bonroy, K.; Frederix, F.; Reekmans, G.; Dewolf, E.; De Palma, R.; Borghs, G.; Declerck, P.; Goddeeris, B. Comparison of random and oriented immobilisation of antibody fragments on mixed self-assembled monolayers. *J. Immunol. Methods* **2006**, *312*, 167–181.

35. Tsugimura, K.; Ohnuki, H.; Wu, H.; Endo, H.; Tsuya, D.; Izumi, M. Oriented antibody immobilization on self-assembled monolayers applied as impedance biosensors. *J. Phys. Conf. Ser.* **2017**, *924*, 012015.

36. Andreescu, S.; Sadik, O.A. Trends and challenges in biochemical sensors for clinical and environmental monitoring. *Pure Appl. Chem.* **2004**, *76*, 861–878.

37. Mollarasouli, F.; Kurbanoglu, S.; Ozkan, S.A. The role of electrochemical immunosensors in clinical analysis. *Biosensors* **2019**,*9*, 86.

38. Bakshi, S.; Mehta, S.; Kumeria, T.; Shiddiky, M.J.A.; Popat, A.; Choudhury, S.; Bose, S.; Nayak, R. Rapid fabrication of homoge- neously distributed hyper-branched gold nanostructured electrode based electrochemical immunosensor for detection of protein biomarkers. *Sens. Actuators B Chem.* **2021**, *326*, 128803.

39. Xiao, X.; Li, H.; Wang, M.; Zhang, K.; Si, P. Examining the effects of self-assembled monolayers on nanoporous gold based amperometric glucose biosensors. *Analyst* **2014**, *139*, 488–494.

40. Haji-Hashemi, H.; Norouzi, P.; Safarnejad, M.R.; Ganjali, M.R. Label-free electrochemical immunosensor for direct detection of Citrus tristeza virus using modified gold electrode. *Sens. Actuators B Chem.* **2017**, *244*, 211–216.

41. Lawruk, T.S.; Lachman, C.E.; Jourdan, S.W.; Fleeker, J.R.; Hayes, M.C.; Herzog, D.P.; Rubio, F.M. Quantitative determination of PCBs in soil and water by a magnetic particle-based immunoassay. *Environ. Sci. Technol.* **1996**, *30*, 695–700.

42. Wang, M.S.; Palmer, L.B.; Schwartz, J.D.; Razatos, A. Evaluating Protein Attraction and Adhesion to Biomaterials with the Atomic Force Microscope. *Langmuir* **2004**, *20*, 7753–7759.

43. Narayan, T.; Kumar, S.; Kumar, S.; Augustine, S.; Yadav, B.K.; Malhotra, B.D. Protein functionalised self-assembled monolayer based biosensor for colon cancer detection. *Talanta* **2019**, *201*, 465–473.

44. Chuang, W.-H.; Lin, J.-C. Surface characterization and platelet adhesion studies for the mixed self-assembled monolayers with amine and carboxylic acid terminated functionalities. *J. Biomed. Mater. Res. Part A* **2007**, *82*, 820–830.

45. Baio, J.E.; Weidner, T.; Brison, J.; Graham, D.J.; Gamble, L.J.; Castner, D.G. Amine terminated SAMs: Investigating why oxygen is present in these films. *J. Electron Spectrosc. Relat. Phenom.* **2009**, *172*, 2–8.

46. Rechendorff, K.; Hovgaard, M.B.; Foss, M.; Zhdanov, V.P.; Besenbacher, F. Enhancement of Protein Adsorption Induced by Surface Roughness. *Appl. Phys. Lett* **2003**, *5*, 10885–10888.

47. Kim, S.Y.; Yu, J.; Son, S.J.; Min, J. Signal enhancement in a protein chip array using a 3-D nanosurface. *Ultramicroscopy* **2010**, *110*, 659–665.

48. Finklea, H.O.; Hanshew, D.D. American Chemical Society Electron-Transfer Kinetics in Organized Thiol Monolayers with Attached Pentaammine(pyridine)ruthenium Redox Centers. *J. Am. Chem. Soc.* **1992**,

114, 3173–3181.

49. Miller, C.; Cuendet, P.; Grätzel, M. Adsorbed ω-hydroxy thiol monolayers on gold electrodes: Evidence for electron tunneling to redox species in solution. *J. Phys. Chem.* **1991**, *95*, 877–886.

50. Xing, Y.F.; O'Shea, S.J.; Li, S.F.Y. Electron transfer kinetics across a dodecanethiol monolayer self-assembled on gold. *J. Electroanal. Chem.* **2003**, *542*, 7–11.

51. Patel, N.; Davies, M.C.; Heaton, R.J.; Roberts, C.J.; Tendler, S.J.B.; Williams, P.M. A scanning probemicroscopy study of the physisorption and chemisorption of protein molecules onto carboxylate terminated self-assembledmonolayers. *Appl. Phys. AMater. Sci. Process.* **1998**, *66*, 569–574.

52. Lu, X.; Li, M.; Yang, C.; Zhang, L.; Li, Y.; Jiang, L.; Li, H.; Jiang, L.; Liu, C.; Hu, W. Electron Transport through a Self- Assembled Monolayer of Thiol-End-Functionalized Tetraphenylporphines and Metal Tetraphenylporphines. *Langmuir* **2006**, *22*, 3035–3039.

53. Radi, A.E.; Muñoz-Berbel, X.; Cortina-Puig, M.; Marty, J.L. An electrochemical immunosensor for ochratoxin A based on immobilization of antibodies on diazonium-functionalized gold electrode. *Electrochim. Acta* **2009**, *54*, 2180–2184.

54. Molinero, V.; Calvo, E.J. Electrostatic interactions at self-assembled molecular films of charged thiols on gold. *J. Electroanal. Chem.* **1998**, *445*, 17–25.

55. Cecchet, F.; Marcaccio, M.; Margotti, M.; Paolucci, F.; Rapino, S.; Rudolf, P. Redox mediation at 11-mercaptoundecanoic acid self-assembled monolayers on gold. *J. Phys. Chem. B* **2006**, *110*, 2241–2248.

56. Fähnrich, K.A.; Pravda, M.; Guilbault, G.G. Disposable amperometric immunosensor for the detection of polycyclic aromatic hydrocarbons (PAHs) using screen-printed electrodes. *Biosens. Bioelectron.* **2003**, *18*, 73–82.

57. Moore, E.J.; Pravda, M.; Kreuzer, M.P.; Guilbault, G.G. Comparative study of 4-aminophenyl phosphate and ascorbic acid 2-phosphate, as substrates for alkaline phosphatase based amperometric immunosensor. *Anal. Lett.* **2003**, *36*, 303–315.

58. Kaya, S.I.; Cetinkaya, A.; Bakirhan, N.K.; Ozkan, S.A. Trends in sensitive electrochemical sensors for endocrine disruptive compounds. *Anal. Chem.* **2020**, *28*, e00106.

59. Mohammadi, A.; Heydari-Bafrooei, E.; Foroughi, M.M.; Mohammadi, M. Electrochemical aptasensor for ultrasensitive detection of PCB77 using thionine-functionalized MoS 2-rGO nanohybrid. *Microchem. J.* **2020**, *155*, 104

Appendix

To obtain the optimal incubation time for SAM formation, we studied the influence of SAM immobilisation time on the gold electrode, using 11-MUA. Measurements were carried out on the same gold electrode, with the incubation taking place at room temperature. As shown in Figure A.1, the impedance values increased in proportion to the incubation time. However, the gold electrode immobilised for 1,2,4,20 hours and from the graph we found that the immobilised for 20 hours gave the better result. Generally, the SAM formation involving 11-MUA on the gold surface was immobilised for between 12 and 20 hours [34][45]. Following this, we proceeded with a 20-hour SAM immobilisation time of 11-MUA for further experiments.

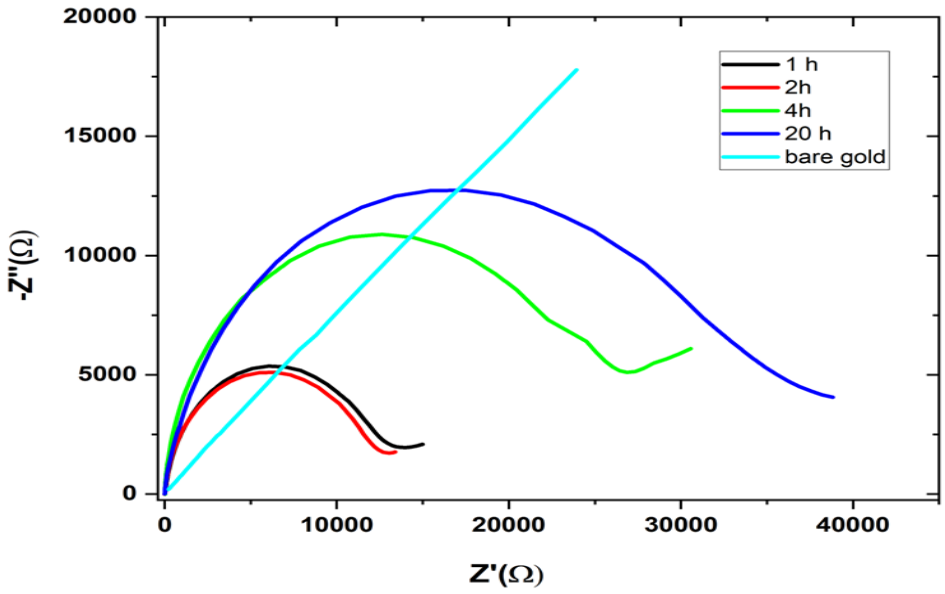
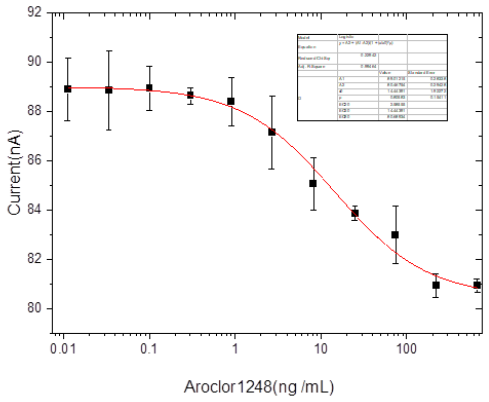
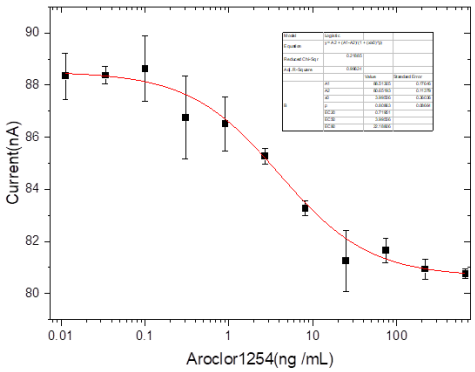
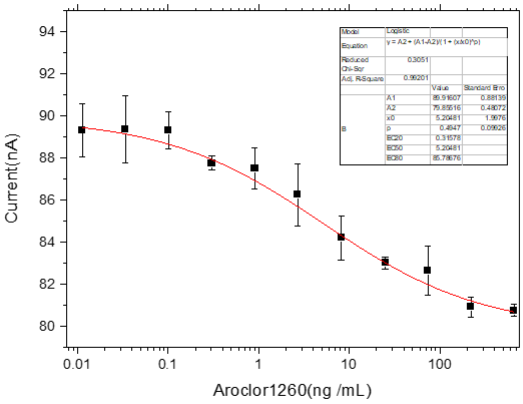


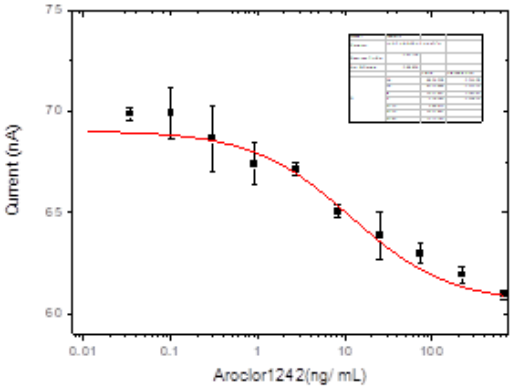
Figure A.1 Nyquist plot: influence of SAM immobilization time on gold electrode using 5 mM 11-MUA.

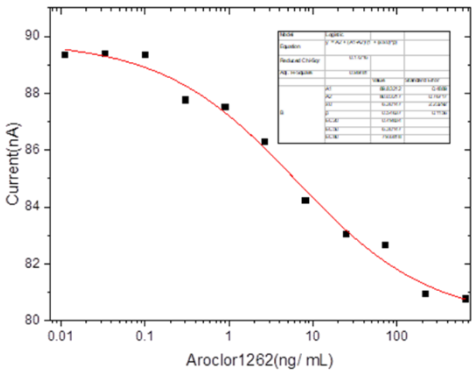
Cross-Reactivity

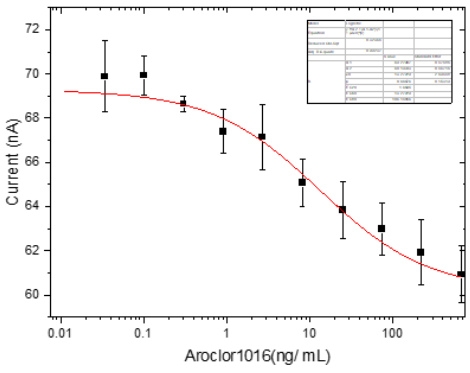












CHAPTER 4

Development Label Free Electrochemical Immunosensors

4. A Novel Label-Free Electrochemical Immunosensor Based on a Self-Assembled Monolayer-Modified Electrode for Polychlorinated Biphenyl (PCB) in Environmental Analysis

Note: This work has been published in the journal of **Electrochem** Acta,**2022**, 3(3), 451-462.

4.1 Abstract

PCBs (polychlorinated biphenyls) are a very large group of organic compounds that have between two and ten chlorine atoms attached to the biphenyl. These compounds have an acute impact as environmental pollutants, causing cancer and other adverse health effects in humans. It is therefore imperative to develop techniques for the cost-effective detection of PCBs at very low concentrations in ecosystems. In this paper, a novel label-free, indirect, competitive electrochemical immunosensor was first developed with a PCB-BSA conjugate. It is shown herein to compete with free PCBs for binding to the anti-PCB polyclonal primary antibody (IgY). Then, we used a secondary antibody to enhance the sensitivity of the sensor for the detection of PCB in a sample. It has been successfully immobilized on an 11-mercaptoundecanoic acid (11-MUA)-modified gold electrode via a carbodiimide-coupling reaction using cross-linking 1-ethyl-3-(3-dimethylaminopropyl) carbodiimide (EDC) and N-hydroxy succinimide (NHS) on the electrode surface. The immunosensor was investigated by cyclic voltammetry (CV), impedance spectroscopy (EIS) and differential pulse voltammetry (DPV) in a standard solution of [Fe (CN)6]$^{3-/4-}$. A linear range of 0.011–220 ng/ml and a limit of detection (LOD) of 0.11 ng/ml for PCBs

detection were achieved by the developed immunosensor, showing advantages over conventional assays. The novel label-free electrochemical immunosensor discussed in this paper is a solution for simple, rapid, cost-effective sample screening in a portable, disposable format. The proposed immunosensor has good sensitivity, and it can prove to be an adequate real-time monitoring solution for PCBs in soil samples or other samples.

Key words: polychlorinated biphenyls; label-free disposable screen-printed gold electrode; differential pulse voltammetry; immunosensors; self-assembled monolayers (SAM).

4.2 Introduction

Polychlorinated biphenyls (PCBs) are organic compounds containing two to ten chlorine atoms attached to the biphenyl [1,2]. Aroclor 1254 ($C_{12}H_5Cl_5$) is a mixture of polychlorinated biphenyls, and is a viscous, light-yellow liquid with a molecular weight of 328, containing 21 % $C_{12}H_6Cl_4$, 48 % $C_{12}H_5Cl_5$, 23 % $C_{12}H_4Cl_6$, and 6 % $C_{12}H_3Cl_7$, with an average chlorine content of 54% [3]. Owing to its severe harm to the environment, the chemical was banned despite its wide use in industry. Nevertheless, it is still present in electrical power generation, plastic manufacturing, chemical production, printing, and other industries; therefore, PCB contamination is still a global issue. It can be found in air, soil, and aquatic environments, and in human bodies [4–6]. PCBs disrupt endogenous

hormones and immune functions, and can lead to tumor formation [7,8]. It is therefore important and urgent to develop reliable, on-site screening systems that use simple analytical methods with high specificity and sensitivity for PCB detection. These methods can be applied to trace levels of PCBs that pose a major threat to the environment and to public health.

For PCB detection, standard methods such as gas chromatography–mass spectrometry (GC-MS) and high-performance liquid chromatography–mass spectrometry (HPLC-MS) have been commonly used [9–11]. Although they are sensitive and accurate, these instrumental analyses have some limitations and are mainly used in laboratory settings. Therefore, immunoassay techniques seem to be a viable solution for portable devices. For example, enzyme-linked immunosorbent assays (ELISA) [12–14] have detection limits of less than 1.0 μg/ml with high specificity [15,16]. Traditional ELISA involves many steps and long incubations, which must be reduced in order to enable rapid, on-site detection of PCBs. Therefore, electrochemical methods will replace optical ones because they enable faster response times and miniaturization. Electrochemical biosensors can be labelled or label-free [17]; label-free-based immunoassays have attracted considerable attention recently due to their fast, simple, and low-cost on-site analysis, and the fact that do not require the modification of biological samples [18–21]. A competitive immunoassay is the common scheme used with label-free immunosensors [3,6,17,22], whereby the formation of antibody–antigen complexes change the thickness and mass of an electrode surface, which in turn blocks the transfer of electrons to the

electrode surface [23,24]. Therefore, the key factor here is the immobilization of the antibody or antigen on the electrode surface with no nonspecific binding.[25,26]

In view of the rarity of studies using label-free electrochemical immunosensors for PCB detection [7,8,13,27–30], in this study, a novel, sensitive, and label-free electrochemical immunosensor was developed based on an indirect competitive assay on modified electrodes for the quantification of total polychlorinated biphenyls (PCBs). Detailed instructions for electrode modification were provided in our previous study [3]. This study applied the Aroclor 1254–bovine serum albumin (BSA) conjugate, which became the solution for the competition assay and enabled our development of the immunosensor modified with 11-mercaptodecylic acid (MUA). PCB-BSA competed with antigens in solution for poly- clonal antibodies (anti-PCB), resulting in two types of anti-PCB: one which binds freely to PCB in solution, while the other binds to PCB-BSA. Secondary antibodies were then applied, which in turn competed with these two types of anti-PCB, changing the electro- chemical signals, and increasing the sensitivity of the immunosensor. Differential pulse voltammetry (DPV) was applied to record the interaction of antibodies with PCB antigens on the modified electrode, using [Fe (CN)6]$^{3-/4-}$ solution as a redox probe. PCBs were therefore competitively bound to this particular antibody, resulting in Aroclor 1254–BSA complex formation, which then dissociated from the electrode, causing significant decreases in DPV. Capture assays were used in optimization, and the analyte concentrations remained constant, allowing the use of direct ELISA. Competitive assays were used in the sensitivity measurements, and the analyte concentration gradually changed, allowing the use of indirect ELISA.

PCBs were determined using the proposed immunosensor in both standard and real samples. The details of the preparation, characterization, and possible application of the immunosensors were investigated as follows. The presented immunosensor's linear dynamic range and limit of detection were compared with a labelled immunosensor, ELISA, and other previously described immunoassays for PCB detection. We believe that the findings of this study, a label-free detection technique, will have a significant impact on the development of an ultrasensitive platform for detecting and quantifying PCBs in the environment. Figure 4.1 illustrates the functionalization process of SPGE and the detection process of the PCB contaminant.

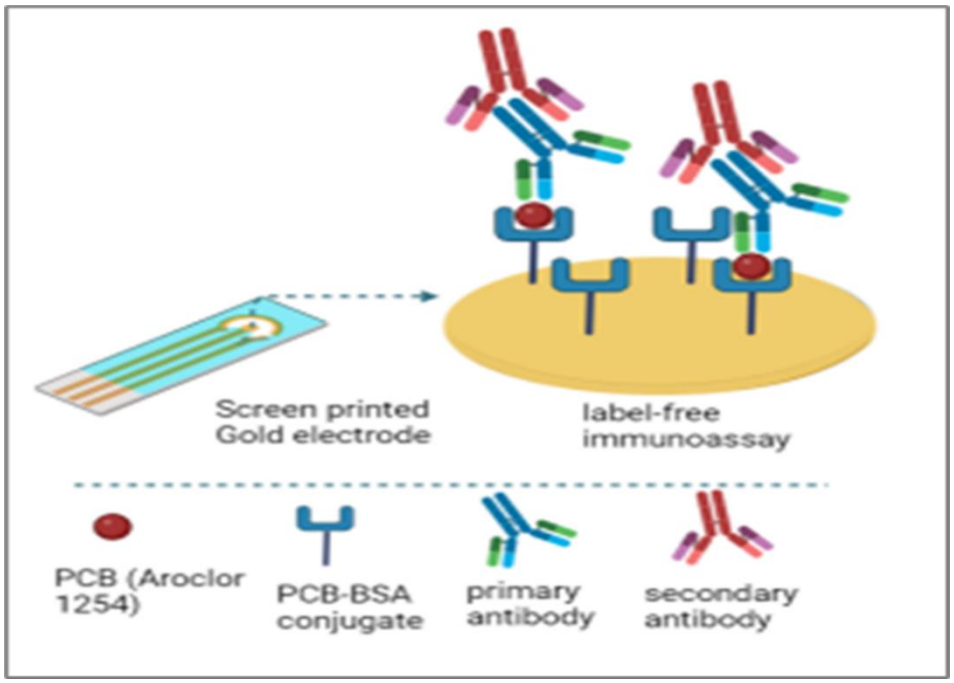


Figure 4.1 Functionalization steps of PCB immunoassay on SPGE, reprinted from reference [31].

4.3 Materials and Methods

4.3.1 Chemicals and Materials

Aroclor 1254 PCB was purchased from Cole-Parmer Instrument Company Ltd., Eaton Socon, Saint Neots, UK. Reagents, such as buffers (Tris base: PBS phosphate-buffered saline, DEA—diethanolamine); solutions ($NaHCO_3$—sodium bicarbonate, NaCl—sodium chloride, KCl potassium chloride, HCl 37 % hydrochloric acid, $NaBH_3CN$—sodium cyanoborohydride,NH_4OH—ammonium hydroxide, NaOH—sodium hydroxide); chemicals (NHS—N-hydroxy succinimide 98%, EDC—1-ethyl-3-(3-dimethylaminopropyl) carbodiimide, 11-MUA—11-mercaptoundecanoic acid 95%, K4[$Fe(CN)_6$] potassium ferro-cyanide, K3[$Fe(CN)_6$] potassium ferricyanide, BSA—bovine serum albumin); Tween-20 detergent; acetone; alcohol (1-isopropyl; ethanol); and clean soil, were bought from Sigma (Dublin, Ireland). Other biochemicals, including polyclonal chicken antibody (IgY), specific to PCB; goat anti-chicken IgY (heavy and light chain) unconjugated antibody; and PCB-BSA conjugate (Aroclor 1254), were purchased from GmbH (Heidelberg, Germany). All the reagents were of analytical grade or higher, and all the buffers and solutions were made from water filtered with nanopores (18.2 MΩ-cm).

4.3.2 Equipment and Instruments

For the optical assays, a microplate reader (EL Read 2000 from biochrom.co, Cambridge, UK) and 96-well ELISA microplates (Greiner bio-one from Frickenhausen, Ger many) were used. For electrochemical assays, a Palm Sens potentiostat (Palm Instrument BV Houten, The Netherlands) and disposable electrochemical screen-printed gold electrodes (AuE)

with a size L 3.4 W 1.0 H 0.05 cm and a diameter of 4 mm (Drop Sens, Asturias, Spain) were used. For incubation and pretreatments, a 37°C Biometra OV3 Incubator (Gottingen, Germany) and a plasma cleaner (Harrick Plasma Ithaca, Ithaca, NY, USA) were used. Between measurements, nitrogen spray guns were used to dry the SPEs.

4.4 Cyclic Voltammetry for Pretreatment of Electrodes

For electrochemical measurements, it is necessary to ensure that the electrode surfaces are clean. The SPEs were treated with plasma cleaner for 30 minutes to remove any organic compounds. After treatment with plasma cleaner, the SPEs were stored in clean and dry containers and ready to be used for electrochemical detections. This experiment was described in chapter 3. The SPE used is screen-printed gold electrode containing gold working electrode (0.11 cm^2), gold counter electrode and Ag/AgCl Silver reference electrode (Figure 4.2).



Figure 4.2 Metrohm DropSens, gold screen-printed electrode.

4.5 Modification of SPG Electrodes

Our method for modifying the electrode was discussed in our previous paper [3]. We briefly describe the method here: 5 mM of 11-MUA used as SAM was applied on the gold working electrodes. 11-MUA was diluted in absolute ethanol and bubbled with N_2 for the purpose of reducing the oxygen [23,32,33]; then, the electrodes were immersed in this mixture for 20 h at 25 °C. Next, the electrodes were rinsed thoroughly with ethanol and dried with N_2. After that, 50 mM EDC and NHS solution was used to immerse electrodes for 1 h, and then the electrodes were rinsed with deionized water and dried again with N_2. The electrodes were then exposed to protein as a final step. A measure of 5 µg /ml of Aroclor 1254–BSA coating conjugate was immobilized for 1 h at 37 °C.

4.6 Optimization of Label-Free Immunoassay

These different experimental parameters were optimized using an Aroclor 1254 solution at 25 ng /ml concentration without a competition test (we used fixed-concentration PCBs at 25 ng /ml Aroclor 1254 concentration). Therefore, instead of performing the competitive assay, we applied a capture assay with DPV techniques to optimize several conditions, including the concentrations of BSA–Aroclor 1254, the concentrations of anti-PCB Ab, and the competition time. Under optimized experimental conditions, the label-free immunoassay was performed using an indirect competitive immunoassay scheme using DPV, which was applied in order to find the calibration plot and compare the other methods. The electrode surfaces were incubated at 37 °C for one hour with 10 µL of BSA–Aroclor 1254 coating antigen (5 µg /ml) (pH 7.4). For washing the electrode

surfaces, 0.05 M Tris, pH 7.4 (0.05% Tween 20) was sprayed on them three times, and then the electrodes were blocked for 30 min at 37 ◦C with 1% BSA–Tris (0.05 M Tris–HCI). To eliminate unbound coating conjugates, the electrode surface was washed three times following the incubation process. Aroclor 1254 PCB, serially diluted with PCB-specific polyclonal chicken antibody (IgY), was mixed and left to incubate for 15 min with 0.246 µg/ml of the polyclonal chicken antibody (IgY). The electrode surface was exposed to 10 µL of each dilution, and binding occurred for 30 min at 37 ◦C. The SPGE surface was coated with a 1/5000 dilution of unlabelled anti-rabbit IgG antibody and allowed to react for 30 min at 37 ◦C in order to standardize the assay. A 30 µL-volume wash buffer was used to wash the electrodes before the electrochemical reading. The DPV analysis utilized a voltage range from -0.2 to +0.6 V at a scan rate of 0.05 V s^{-1} and a response amplitude of 0.05 V. In addition to the step potential, the modulation time and interval time were all fixed during the assay: 0.01 V and 0.1 s, respectively, were used in 0.1 M KCl in 4 mL PBS, containing a 5 mM redox probe $[Fe(CN)6]^{3-/4-}$.

4.7 Real Sample Analysis

For the real sample analysis, ten grams of soil were placed in a glass flask and spiked with a known amount of Aroclor 1254 before being extracted for recovery studies. A measure of 5 g of the spiked sample was added to 10 mL of methanol. The flask was sealed, shaken frequently for 2 min, and then left at room temperature for 30 min. The sample was centrifuged at 2500 rpm for 10 min [34,35]. After waiting 5 min for the solid particles to

settle, the soil was filtered through a 0.45 µm nitrocellulose filter. The extract was then evaporated to a volume of 1 mL before processing, as described in Section 4.6.

4.8 Results and Discussion

4.8.1 Optimization of the assay conditions

Different concentrations of BSA–Aroclor 1254 conjugate and anti-PCB Ab, and different competition times were selected to test the immunosensor. This test was performed using a capture assay and the concentration of BSA–Aroclor 1254 conjugate varied from 20 µg/ml to 0.155 µg/ml in this study. The BSA–Aroclor 1254 conjugate was immobilized on the sensor surface in three independent experiments. As the concentration of BSA–Aroclor 1254 increased, there was an increase in the peak sensor currents. The concentration of the BSA–Aroclor 1254 conjugate (5–20 µg /ml) did not affect the DPV current further; therefore, 5 µg/ml was chosen as the optimal concentration to use during the experiments, as shown in Figure 4.3 (A). Furthermore, 5 µg /ml BSA–Aroclor 1254 coating conjugate were immobilized on the electrodes and used to cover the electrodes completely, followed by blocking the chips with 1% BSA in Tris buffer (pH 7.4). The primary PCB antibody was serially diluted in concentrations ranging between 10 µg /ml and 0.0005 ng /ml, as shown in Figure 4.3 (B), the optimal concentration of anti-PCB Ab was 0.246 µg/ml. The competitive times for PCB–BSA and PCBs standards were also optimized because of the competition with the finite anti-PCBs, which is a factor that affects the DPV response of the biosensor, Figure 4.3 (C) shows the peak current progressed at a dramatic rate until it reached minimal intensity at 25 min (containing 25

ng/mL Aroclor 1254 concentration). A majority of the PCB was bound specifically to anti-PCB as shown in the data from 10 to 35 min. It is therefore optimal to have a 25-minute competition time.

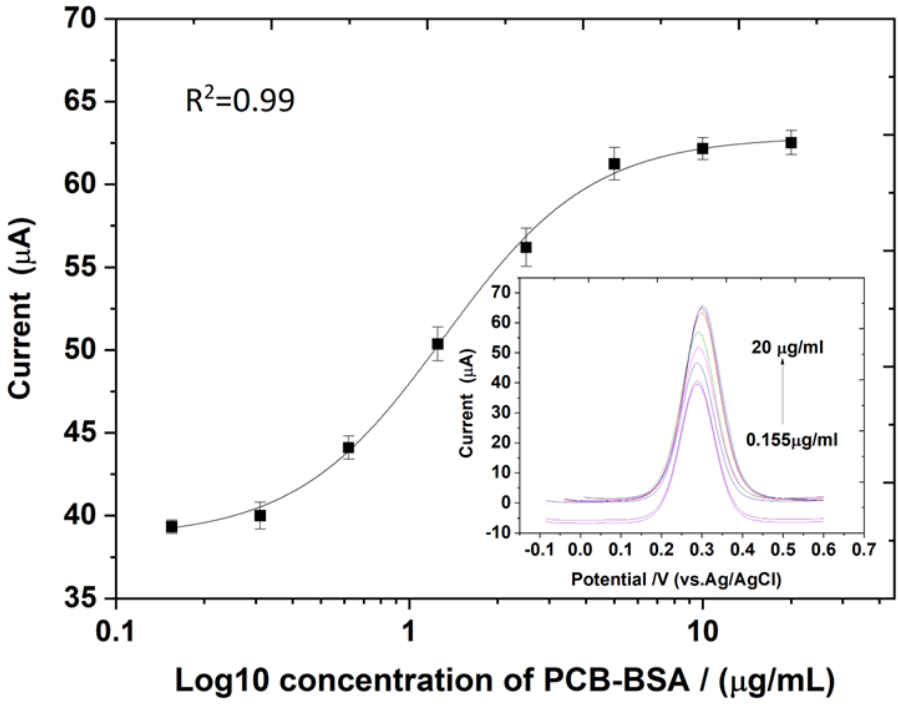


Figure 4.3 (A) Optimized concentration of PCB-BSA conjugate using capture assay. Detection was DPV (n=3). The optimized concentration of the PCB-BSA conjugate was 5 μg/ml.

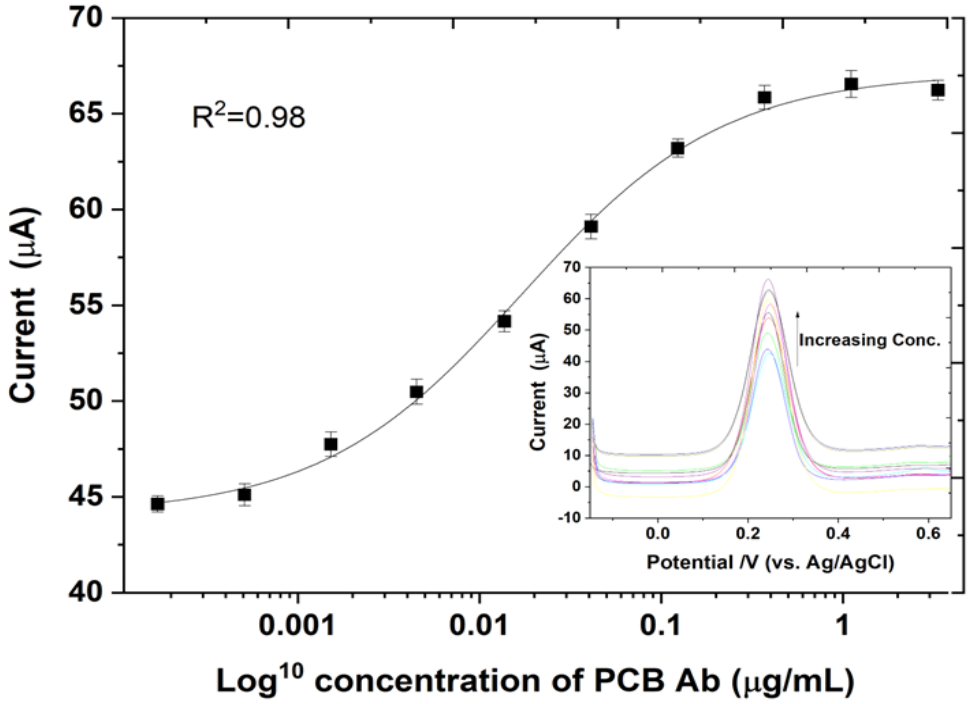


Figure 4.3 (B) Optimized concentration of PCB using capture assay. Detection was DPV (n=3). The optimized concentration of PCB was 0.246 µg/ml, which is less than the optical, that was 0.465 µg/ml.

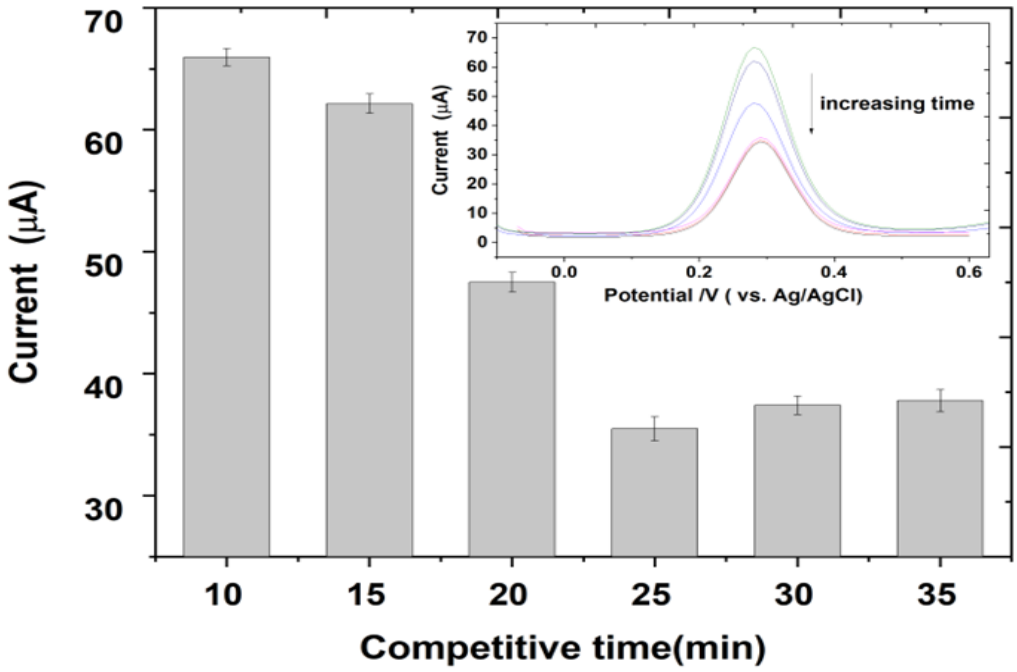
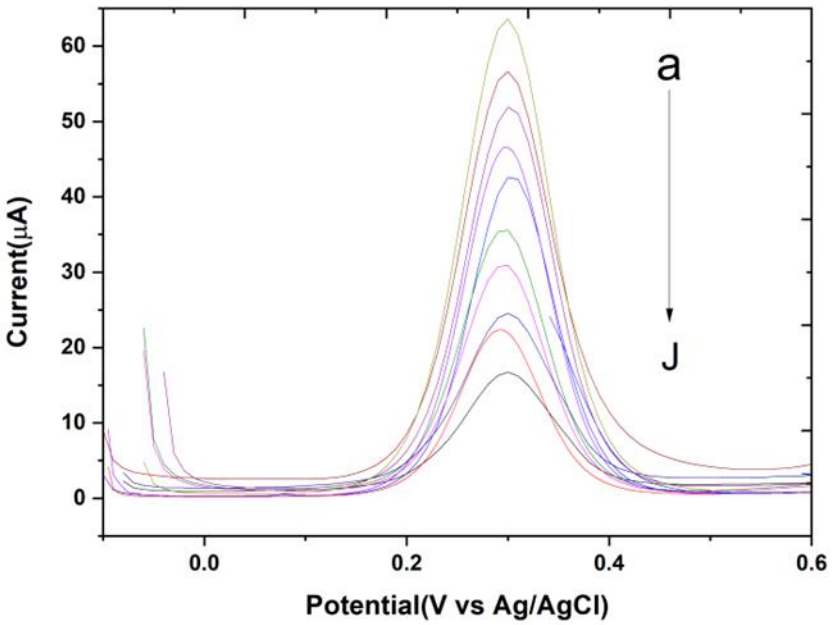


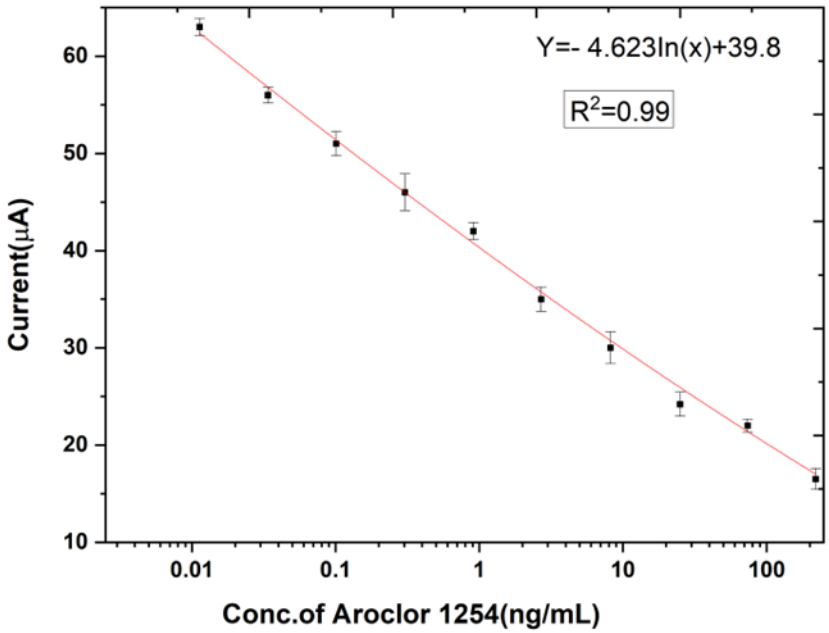
Figure 4.3 (C) Competition time for immunosensor response. Detection was DPV (n=3).

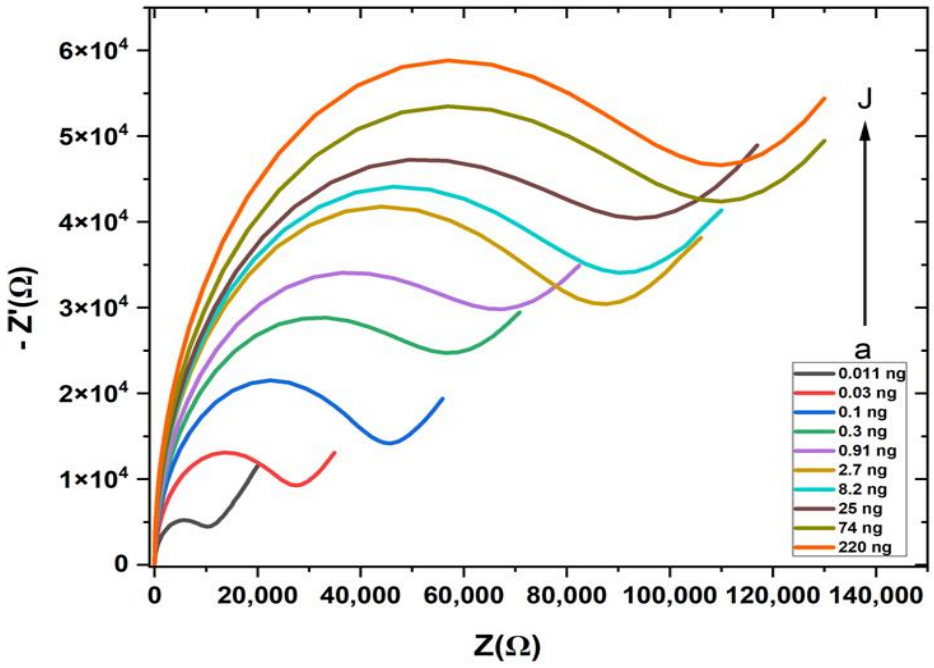
4.8.2 Sensitivity of the immunosensor for PCB Aroclor 1254 determination

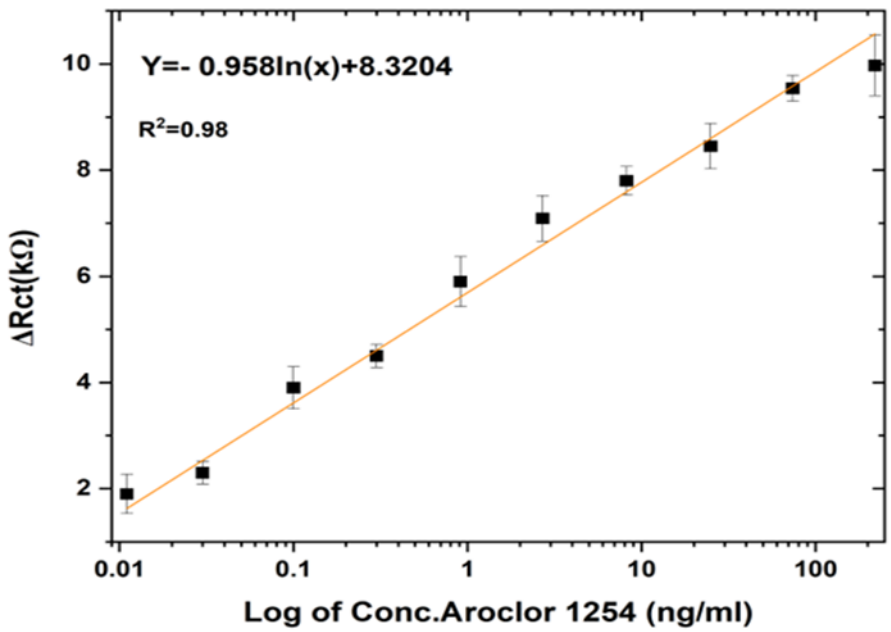
Aroclor 1254 was examined under optimized conditions using DPV in PBS (pH 7.4) to assess its effects on analytical capability. The DPV redox peak currents shown in Figure 4.4 (A) are clearly shown to decrease with increasing concentrations of Aroclor 1254. Results indicate that Aroclor 1254 and PCB-BSA were successfully incorporated. Figure 4.4 (B) shows the current had a linear relationship with Aroclor-1254 concentration on samia-logarithmic scale. The concentration was between 0.011 ng/mL and 220 ng/ml. Additionally, the linear regression equation fit is shown (Y=- 4.623In(x)+39.8) (R2 = 0.99), and the limit of detection was estimated to be 0.11 ng/ml. This was estimated to be three

times that of the SD of the blank sample/slope. Further, we detect the Aroclor-1254 by the EIS method since it exhibits better analytical performance and to prove the concept. Figure 4.4 (C) depicts the Nyquist plots for the binding of Aroclor-1254 antigen at the immunosensor probe with the concentration of ranging from 0.011 to 220 ng/ml. The diameter of the semicircle was increased with increasing the Aroclor 1254 concentration, indicating that the competition between the free Arocior -1254 and the immobilized BSA- Aroclor 1254 for binding to the anti-PCB antibody is, indeed, existent. as shown in Figure 4.4 (D) that the corresponding R_{ct} was positively proportional to the concentration of Aroclor-1254, enhancing the linear relationship between the EIS response and the Aroclor-1254 concentration logarithm from 0.011 to 220 ng/ml ,this corresponds to the linear regression equation of ΔR_{ct} (kΩ) = (Y=- 0.958In(x)+ 8.3204), the correlation coefficient was (R2 = 0.989), which resulted with a limit of detection (LOD) of 0.91 ng/ml (S/N = 3) which is consistent with the DPV responses. Figure 4.4 (E) shown the Bode plot represents the relationship of Z of the system versus the frequency range was applied (only Z values at frequency range of 10^4 Hz down to 10^5 Hz are plotted). The variation of difference in Rct showed a linear behaviour with the logarithmic concentration of Aroclor 1254.Comparing Table 4.1 with other existing PCB-detection methods, the immunosensor demonstrated a wider linear dynamic range and an acceptable detection limit with a sensitivity of 4.62 $\mu A \cdot ng^{-1}$ and $0.958X10^4$ Ω ng^{-1} ml for DPV and EIS respectively.


a
J
Current(μA)
Potential(V vs Ag/AgCl)
0
10
20
30
40
50
60
0.0
0.2
0.4
0.6


Y=- 4.623ln(x)+39.8
R2=0.99
Current(μA)
Conc.of Aroclor 1254(ng/mL)
10
20
30
40
50
60
0.01
0.1
1
10
100


6×10^4
5×10^4
4×10^4
3×10^4
2×10^4
1×10^4
0
- Z'(Ω)
0
20,000
40,000
60,000
80,000
100,000
120,000
140,000
Z(Ω)
J
a
0.011 ng
0.03 ng
0.1 ng
0.3 ng
0.91 ng
2.7 ng
8.2 ng
25 ng
74 ng
220 ng


Y=- 0.958ln(x)+8.3204
R²=0.98
10
8
6
4
2
ΔRct(kΩ)
0.01
0.1
1
10
100
Log of Conc.Aroclor 1254 (ng/ml)

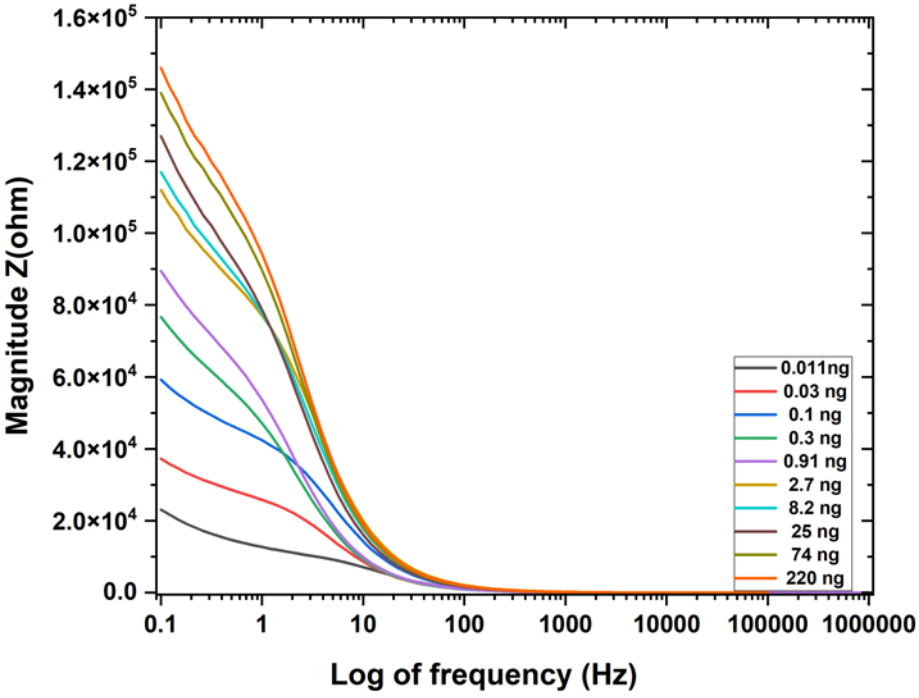


Figure 4.4 (A) Differential pulse voltammetry (DPV) responses the designed immunosensor to Aroclor 1254 concentrations(a) 0.011 ng/ml, (b) 0.033 ng/ml, (c) 0.101 ng/ml, (d) 0.304 ng/ml, (e) 0.91 ng/ml, (f) 2.7 ng/ml, (g) 8.2 ng/ml, (h) 25 ng/ml, (i) 74 ng/ml, and (j) 220 ng/ml.). **(B)** Plot of DPV current with respect to logarithms of different Aroclor 1254 concentrations. **(C)** EIS spectra for $[Fe(CN)6]^{3-/4-}$ after the binding of Aroclor 1254 at the immunosensor probe with different concentrations (a-j). **(D)** Plot of EIS the corresponding calibration obtained from EIS responses with respect to logarithms of different Aroclor 1254 concentrations. **(E)** The Bode impedance plots log of frequency vs. Magnitude Z(ohm).

Table 4.1 Performances of diverse electrochemical detection.

Method	Detection mode	Linear range	LOD	Amplification	Real sample	Ref.
DPV	----------	1–100	0.22 ng/L	None	Water	[185]
EIS	Noncompetitive	0.01–10	0.001 µg/L	None	Oil	[183]
DPV	Competitive	50–0.01	5.2 ppm	AP (ALP)	Food	[241]
LSV	Competitive	0.1–220	0.09 ng/ml	AP (ALP)	Water	[3]
DPV	Competitive	0.011–220	0.11 ng/ml	None	Soil	This work
EIS	Competitive	0.011-220	0.91 ng/ml	None	soil	This work

4.8.3 Reproducibility and stability of the designed immunosensor

Electrochemical immunosensors were tested with PCB concentrations as high as 25 ng/ml across seven electrodes to verify the reproducibility. The relative RSD was 2.43 %. According to the results, the fabricated immunosensor has high reproducibility and stability, which are important parameters in quantitative detection by immunosensors. In Figure 4.5, DPV was used for a complete assay every 5 days for a month (n=3). After storing the immunosensor for 10 days, it maintained 98 % of its original response, while maintaining 92 % after 20 days. This electrode displayed excellent stability (RSD 5.9 %) over a long period after being kept under dry conditions at 4 °C for 30 days. This might

be due to the antibody being firmly attached to the gold surface, which is a reason for the good stability.

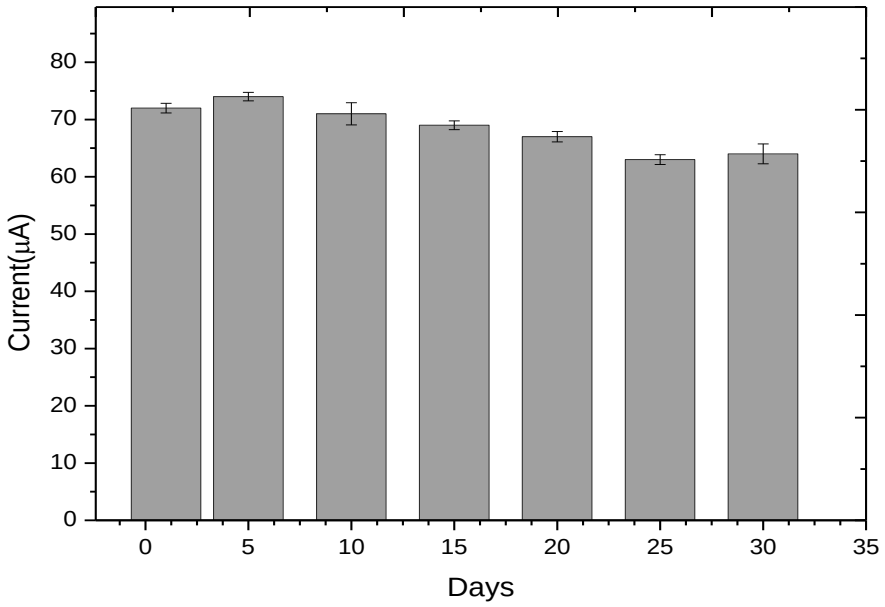


Figure 4.5 The stability of Aroclor 1254 detection by the immunosensor in 30 days.

4.8.4 Real sample analysis

Aroclor 1254, which was added to the soil samples using the standard addition technique, was determined using the developed immunosensor. As shown in Table 4.2, the developed sensing device showed recovery values in the range of 90–96 % for a spiked soil sample. All samples were run in triplicate. This indicated highly reliable results, with an RSD value of 2.5 % (n = 3). In comparison with the traditional ELISA method, the new immunosensor was effective and reliable in determining Aroclor 1254

prevalence in the soil samples. In this case, the developed electrode met higher performance standards than the standard instrument, so the results we obtained were more appealing. The fundamental analysis also revealed that the developed sensor had other advantages in terms of determining PCBs in soil samples, including the following: high accuracy, high selectivity, and high sensitivity.

Table 4.2 SPGE electrochemical and ELISA (immunoassay) approaches for the determination of Aroclor 1254 in soil samples (n=3).

Techniques	Sample	Added (ng/ml)	Found (ng/ml)	Recovery %	RSD % (n = 3).
ELISA	Soil	8.2	10.54	128.53	4.4 %
ELISA	Soil	25	26.41	105.64	3.6 %
Electrochemical	Soil	8.2	7.89	96.21	1.7 %
Electrochemical	Soil	25	22.74	90	2.5 %

4.9 Conclusions

In this work, a highly sensitive, cost-effective, and label-free electrochemical immunosensor was used for the determination of PCBs (Aroclor 1254). A self-assembled, monolayer-modified electrode was used in an indirectly competitive format and the results were compared with those of other methods. This immunosensor had a linear range of 0.011–220 ng/ml and a limit of detection (LOD) of 0.11 ng/ml and 0.91 ng/ml for DPV and EIS respectively, under optimum conditions. According to our analyses, the chip demonstrated good performance and stability and could be used to detect PCB compounds using the electrochemical immunosensor. This immunosensor could be incorporated into a portable device to carry out real-time measurements in the field. Moreover, the described technique can be improved using nanoparticles, such as gold nanoparticles (GNPs), to enhance the sensitivity and performance of the individual sensor measurements. This would improve the commercialization of the technique we present here. This would also reduce the steps required for immunoassay testing in the field. Hence, incorporating an organic-pollutant-monitoring platform into portable lab-on-a-chip technology would be a useful way to avoid the costly and inefficient analysis of samples in specialized laboratories.

4.10 References

1. Biziuk, M. Environmental fate and global distribution of polychlorinated biphenyls Related papers Environmental Fate and Global Distribution of Polychlorinated Biphenyls ARTICLE in REVIEWS OF ENVIRONMENTAL CONTAMINATION AND TOXICOLOGY · FEBRUARY 2009., doi:10.1007/978-1-4419-0032-6_5.

2. Lauby-Secretan, B.; Loomis, D.; Grosse, Y.; El Ghissassi, F.; Bouvard, V.; Benbrahim-Tallaa, L.; Guha, N.; Baan, R.; Mattock, H.; Straif, K.; et al. Carcinogenicity of polychlorinated biphenyls and polybrominated biphenyls. *Lancet Oncol.* **2013**, *14*, 287–288, doi:10.1016/S1470-2045(13)70104-9ï.

3. Alsefri, S.; Balbaied, T.; Moore, E. Electrochemical Development of an Immunosensor for Detection Polychlorinated biphenyls (PCBs) for Environmental Analysis. **2021**, doi:10.3390/chemosensors9110307.

4. Han, D.; Currell, M.J. Persistent organic pollutants in China's surface water systems. *Sci. Total Environ.* **2017**, *580*, 602–625, doi:10.1016/J.SCITOTENV.2016.12.007.

5. Fu, J.; Mai, B.; Sheng, G.; Zhang, G.; Wang, X.; Peng, P.; Xiao, X.; Ran, R.; Cheng, F.; Peng, X.; et al. Persistent organic pollutants in environment of the Pearl River Delta, China: an overview. *Chemosphere* **2003**, *52*, 1411–1422, doi:10.1016/S0045-6535(03)00477-6.

6. Laschi, S.; Fránek, M.; Mascini, M. Screen-Printed Electrochemical Immunosensors for PCB Detection. *Electroanalysis* **2000**, *12*, 1293–1298, doi:10.1002/1521-4109(200011)12:16<1293::AID-ELAN1293>3.0.CO;2-5.

7. Hong, S.; Kang, T.; Oh, S.; Moon, J.; Choi, I.; Choi, K.; Yi, J. Label-free sensitive optical detection of polychlorinated biphenyl (PCB) in an aqueous solution based on surface plasmon resonance measurements. *Sensors Actuators B Chem.* **2008**, *134*, 300–306, doi:10.1016/J.SNB.2008.05.006.

8. *Direct Electrochemical Immunosensor for Polychlorinated Biphenyls*; 1998;

9. Helen, C.; Lemasle, M.; Laplanche, A.; Genin, E. Determination of polychlorodibenzo-p-dioxins and polychlorodibenzofurans by gas chromatography/tandem mass spectrometry and gas chromatography/triple mass spectrometry in a quadrupole ion trap. *J. Mass Spectrom.* **2001**, *36*, 546–554,

doi:10.1002/JMS.156.

10. Ottonello, G.; Ferrari, A.; Magi, E. Determination of polychlorinated biphenyls in fish: Optimisation and validation of a method based on accelerated solvent extraction and gas chromatography–mass spectrometry. *Food Chem.* **2014**, *142*, 327–333, doi:10.1016/J.FOODCHEM.2013.07.048.

11. Popp, P.; Keil, P.; Möder, M.; Paschke, A.; Thuss, U. Application of accelerated solvent extraction followed by gas chromatography, high-performance liquid chromatography and gas chromatography–mass spectrometry for the determination of polycyclic aromatic hydrocarbons, chlorinated pesticides and polychlorinated dibenzo-p-dioxins and dibenzofurans in solid wastes. *J. Chromatogr. A* **1997**, *774*, 203–211, doi:10.1016/S0021-9673(97)00337-3.

12. Zajicek, J.L.; Tillitt, D.E.; Schwartz, T.R.; Schmitt, C.J.; Harrison, R.O. Comparison of an enzyme-linked immunosorbent assay (ELISA) to gas chromatography (GC) – measurement of polychlorinated biphenyls (PCBs) in selected US fish extracts. *Chemosphere* **2000**, *40*, 539–548, doi:10.1016/S0045-6535(99)00310-0.

13. Lasrado, J.A.; Santerre, C.R.; Zajicek, J.L.; Stahl, J.R.; Tillitt, D.E.; Deardorff, D. Determination of PCBs in Fish Using Enzyme-linked Immunosorbent Assay (ELISA). *J. Food Sci.* **2003**, *68*, 133–136, doi:10.1111/J.1365-2621.2003.TB14128.X.

14. Fillmann, G.; Galloway, T.S.; Sanger, R.C.; Depledge, M.H.; Readman, J.W. Relative performance of immunochemical (enzyme-linked immunosorbent assay) and gas chromatography–electron-capture detection techniques to quantify polychlorinated biphenyls in mussel tissues. *Anal. Chim. Acta* **2002**, *461*, 75–84, doi:10.1016/S0003-2670(02)00233-7.

15. Endo, T.; Okuyama, A.; Matsubara, Y.; Nishi, K.; Kobayashi, M.; Yamamura, S.; Morita, Y.; Takamura, Y.; Mizukami, H.; Tamiya, E. Fluorescence-based assay with enzyme amplification on a micro-flow immunosensor chip for monitoring coplanar polychlorinated biphenyls. *Anal. Chim. Acta* **2005**, *531*, 7–13, doi:10.1016/J.ACA.2004.08.077.

16. Inui, H.; Takeuchi, T.; Uesugi, A.; Doi, F.; Takai, M.; Nishi, K.; Miyake, S.; Ohkawa, H. Enzyme-Linked Immunosorbent Assay with Monoclonal and Single-Chain Variable Fragment Antibodies Selective to Coplanar Polychlorinated Biphenyls. **2012**, doi:10.1021/jf203585b.

17. Syahir, A.; Usui, K.; Tomizaki, K.; Kajikawa, K.; Mihara, H. Label and Label-Free Detection Techniques for Protein Microarrays. *Microarrays 2015, Vol. 4, Pages*

228-244 **2015**, *4*, 228–244, doi:10.3390/MICROARRAYS4020228.

18. Wang, S.; Zhao, S.; Wei, X.; Zhang, S.; Liu, J.; Dong, Y.; Florescu, M.; Jaffrezic-Renault, N. An Improved Label-Free Indirect Competitive SPR Immunosensor and Its Comparison with Conventional ELISA for Ractopamine Detection in Swine Urine. **2017**, doi:10.3390/s17030604.

19. Ge, L.; Li, S.P.; Lisak, G. Advanced sensing technologies of phenolic compounds for pharmaceutical and biomedical analysis. *J. Pharm. Biomed. Anal.* **2020**, *179*, 112913, doi:10.1016/J.JPBA.2019.112913.

20. Švorc, Ľ. *Determination of Caffeine: A Comprehensive Review on Electrochemical Methods*; 2013; Vol. 8;.

21. Zheng, X.; Li, H.; Xia, F.; Tian, D.; Hua, X.; Qiao, X.; Zhou, C. An Electrochemical Sensor for Ultrasensitive Determination the Polychlorinated Biphenyls. *Electrochim. Acta* **2016**, *194*, 413–421, doi:10.1016/J.ELECTACTA.2016.02.115.

22. Date, Y.; Aota, A.; Sasaki, K.; Namiki, Y.; Matsumoto, N.; Watanabe, Y.; Ohmura, N.; Matsue, T. Label-Free Impedimetric Immunoassay for Trace Levels of Polychlorinated Biphenyls in Insulating Oil. **2014**, doi:10.1021/ac4035289.

23. Haji-Hashemi, H.; Norouzi, P.; Safarnejad, M.R.; Ganjali, M.R. Label-free electrochemical immunosensor for direct detection of Citrus tristeza virus using modified gold electrode. *Sensors Actuators B Chem.* **2017**, *244*, 211–216, doi:10.1016/J.SNB.2016.12.135.

24. Liu, X.; Duckworth, P.A.; Wong, D.K.Y. Square wave voltammetry versus electrochemical impedance spectroscopy as a rapid detection technique at electrochemical immunosensors. *Biosens. Bioelectron.* **2010**, *25*, 1467–1473, doi:10.1016/J.BIOS.2009.10.047.

25. Frederix, F.; Bonroy, K.; Laureyn, W.; Reekmans, G.; Campitelli, A.; Dehaen, W.; Maes, G. Enhanced performance of an affinity biosensor interface based on mixed self-assembled monolayers of thiols on gold. *Langmuir* **2003**, *19*, 4351–4357, doi:10.1021/LA026908F.

26. Briand, E.; Salmain, M.; Herry, J.M.; Perrot, H.; Compère, C.; Pradier, C.M. Building of an immunosensor: How can the composition and structure of the thiol attachment layer affect the immunosensor efficiency? *Biosens. Bioelectron.* **2006**, *22*, 440–448, doi:10.1016/J.BIOS.2006.05.018.

27. Bhattarai, J.K.; Tan, Y.H.; Pandey, B.; Fujikawa, K.; Demchenko, A. V; Stine, K.J. Electrochemical impedance spectroscopy study of Concanavalin A binding to self-assembled monolayers of mannosides on gold wire electrodes. *J. Electroanal. Chem.* **2016**, *780*, 311–320, doi:https://doi.org/10.1016/j.jelechem.2016.09.045.

28. Fischer, L.M.; Tenje, M.; Heiskanen, A.R.; Masuda, N.; Castillo, J.; Bentien, A.; Émneus, J.; Jakobsen, M.H.; Boisen, A. Gold cleaning methods for electrochemical detection applications. *Microelectron. Eng.* **2009**, *86*, 1282–1285, doi:https://doi.org/10.1016/j.mee.2008.11.045.

29. Sci-Hub | Electrochemical Behavior of Au Colloidal Electrode through Layer-by-Layer Self-Assembly. Journal of Colloid and Interface Science, 248(2), 376–382 | 10.1006/jcis.2002.8238 Available online: https://sci-hub.se/10.1006/jcis.2002.8238 (accessed on Apr 23, 2022).

30. Fan, L.; Wang, G.; Liang, W.; Yan, W.; Guo, Y.; Shuang, S.; Dong, C.; Bi, Y. Label-free and highly selective electrochemical aptasensor for detection of PCBs based on nickel hexacyanoferrate nanoparticles/reduced graphene oxides hybrids. *Biosens. Bioelectron.* **2019**, *145*, 111728, doi:10.1016/J.BIOS.2019.111728.

31. Dutta, G.; Lillehoj, P.B. Wash-free, label-free immunoassay for rapid electrochemical detection of PfHRP2 in whole blood samples. Sci. Rep. **2018**, 8, 1–8, doi:10.1038/s41598-018-35471-8.

32. Bakshi, S.; Mehta, S.; Kumeria, T.; Shiddiky, M.J.A.; Popat, A.; Choudhury, S.; Bose, S.; Nayak, R. Rapid fabrication of homogeneously distributed hyper-branched gold nanostructured electrode based electrochemical immunosensor for detection of protein biomarkers. *Sensors Actuators B Chem.* **2021**, *326*, 128803, doi:10.1016/J.SNB.2020.128803.

33. Xiao, X.; Li, H.; Wang, en; Zhang, K.; Si, P. Examining the effects of self-assembled monolayers on nanoporous gold based amperometric glucose biosensors. **2014**, doi:10.1039/c3an01670f.

34. Centi, S.; Laschi, S.; Fránek, M.; Mascini, M. A disposable immunomagnetic electrochemical sensor based on functionalised magnetic beads and carbon-based screen-printed electrodes (SPCEs) for the detection of polychlorinated biphenyls (PCBs). *Anal. Chim. Acta* **2005**, *538*, 205–212, doi:10.1016/j.aca.2005.01.073.

35. Deng, A.; Franek, M.; Kolar, V. Food and Agricultural Immunology Determination of Atrazine in Soil Samples by ELISA Using Polyclonal and Monoclonal Antibodies. *Agric. Immunol.* **2010**, *11*, 135–144, doi:10.1080/09540109999816.

36. Chen, D.; Li, J. Interfacial design and functionization on metal electrodes through self-assembled monolayers. *Surf. Sci. Rep.* **2006**, *61*, 445–463, doi:https://doi.org/10.1016/j.surfrep.2006.08.001.

37. Laschi, S.; Mascini, M.; Scortichini, G.; Fra, M.; Nek, Ä.; Mascini, M. Polychlorinated Biphenyls (PCBs) Detection in Food Samples Using an Electrochemical Immunosensor. **2003**, doi:10.1021/jf0208637.

CHAPTER 5

Development of the QuEChERS Extraction Method and Comparison with (GC-MS)

5. Development of the QuEChERS Extraction Method for the Determination of Polychlorinated Biphenyls (Aroclor 1254) in Soil Samples by Using GC-MS

Note: This work has been published in the journal of ***Separations*** **2023**, *10*(4), 250

5.1 Abstract

Polychlorinated biphenyls (PCBs) have been found in soil, which has typically been the result of industrial pollution in the past two decades. Although they are banned, PCBs can still be found in soils and other environmental media. For this reason, it is critical to develop an analytical method that can reliably identify and monitor their sources. This study describes a gas chromatography with mass spectrometry (GC-MS) technique, which was used to detect PCBs in soil samples by using a fast extraction method. Using the QuEChERS (quick, easy, cheap, effective, rugged, and safe) method, PCBs were more effectively extracted from soil. Different related parameters, such as time of shaking and centrifuging, type of solvent, and clean-up adsorbents, were compared and optimized. As the extraction solvent, acetonitrile/water produced the best results, and as the dispersive solid-phase extraction sorbent, diatomaceous earth produced the best results. Procedures allowed recovery values between 95.3 % and 103.2 %. A limit of

detection of 1.9 μg/kg was determined with relative standard deviations (n = 3) of 2.1–4.0 % for intra-day assays and 3.6–5.8 % for inter-day assays. It was demonstrated that the method was simple, sensitive, efficient, and environmentally friendly when applied to soil samples. To our knowledge, an integrated approach based on QuEChERS for the determination of Aroclor 1254 in soil has not been published before. It is believed that this approach will eliminate the significant challenge of sample extraction in GC-MS processing, which was considered to be a procedural challenge in previous analyses. Furthermore, as part of a comparative study, analytical chromatographic techniques were used to compare the developed immunoassay system discussed in the previous chapters for detection of Aroclor 1254 in soil samples. This was to ensure that the developed immunoassay sensor method met the requirements of laboratory analytical methods. According to the comparison, the PCB test procedure was suitable. Moreover, the developed immunoassays were compared for reliability and sensitivity.

Key words: polychlorinated biphenyls (PCBs); quick; easy; cheap; effective; rugged; safe (QuEChERS); (GC-MS); sample preparation; extraction methods; soil environmental.

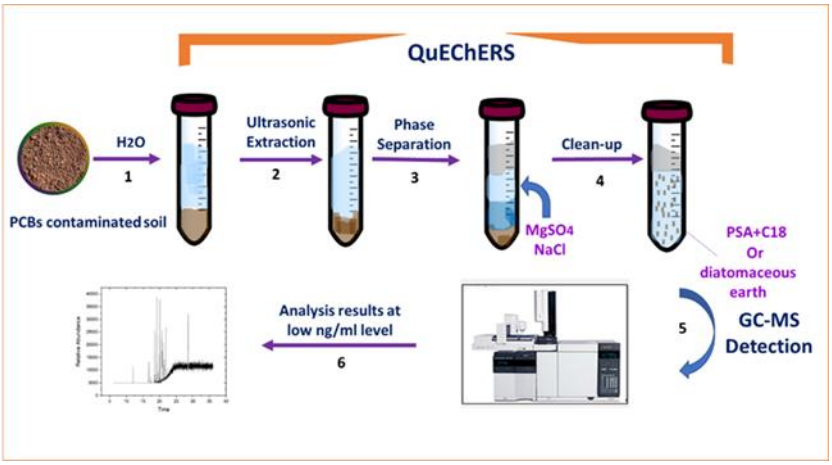


Figure 5.1 Graphical Abstract.

5.2 Introduction

Polychlorinated biphenyls (PCBs) are chemical compounds formed artificially by replacing hydrogen atoms within biphenyl molecules with chlorine atoms, classifying them as a persistent organic pollutant. A total of 209 possible PCB congeners exists due to different commercial names for PCBs, accumulating and posing an environmental hazard [1–3]. Despite the banning of using and/or producing PCBs, they are still widely spread in environmental media, including in agricultural soil [4]. Aroclor 1254 is one type of PCB that has attracted researchers in recent years. A product with dozens of highly chlorinated congeners, it has been widely used for numerous open and closed industrial applications due to its chemical and thermal stabilities [5–7]. Therefore, the possibility of exposing people to Aroclor 1254 has increased greatly in different ways, such as through dietary intake, dermal contact, or inhalation, which negatively affect the human body and cause serious conditions including neurotoxicity, dermatological disorders, and

lung problems. Thus, the detection of Aroclor 1254 in the environment has become very important and requires a sensitive analytical method [8,9].

Gas chromatography is most commonly used to detect polychlorinated biphenyls usually in conjunction with an electron capture detector or mass spectrometry [10,11]. Some of the features of these techniques are accuracy, reliability, and sensitivity [12]. Isolating PCBs from the soil matrix is a crucial step in GC-MS. The PCB analysis has been carried out using a wide range of extraction techniques, such as chemical methods involving soxhlet extraction [13–15], liquid–liquid extraction [16,17], and solid-phase extraction [18,19] or physical ones, involving ultrasonic extraction [20], microwave-assisted extraction [21], supercritical fluid extraction [22], and pressurized fluid extraction [23]. Despite their own advantages, these methods suffer from hazardous solvents, and sample preparation is expensive and time-consuming; therefore, Anastassiades et al. introduced a quick, easy, cheap, effective, rugged, and safe method, known as QuEChERS, as an alternative means of extraction [24].

The method involves acetonitrile extraction, followed by salt addition and dispersive solid-phase extraction (d-SPE) clean up. According to this alternative method, organic solvents are minimized, which was rarely discussed in the literature review [25]. PCBs have been removed from a variety of matrixes, including fish tissue [26–28], mussels [29], meat [30], and honey [31], and isolated by QuEChERS. Although different optimizations were discussed in the soil sample [32], further modification is required,

including combinations of solvents, sorbents, or salts, considering volume, type, and ratio, which mostly depends on the analyte and the matrix.

Through the use of the QuEChERS method combined with GC-MS, this study aimed to develop and validate an inexpensive and reliable method of analysing PCBs in soil. The QuEChERS method was examined for PCB extraction from six soil samples by examining the effect of water, solvent types, solvent volume, time of shaking, centrifuge time, speed, and types of sorbents used. To demonstrate the efficiency and accuracy of the methodology, blank samples spiked with standards were used to evaluate the precision and accuracy of the method.

5.3 Experiment

5.3.1 Instrumentation and Conditions for GC-MS

The GC-MS instrument used for the analysis of PCBs was an Agilent 6890/5973, which consisted of an Agilent 6890N GC equipped with an inert mass selective detector 5973. A capillary column HP-5MS [5%-phenyl-methylpolysiloxane] Agilent J&W GC column, with a dimension of 0.25 mm ID × 30 m and a 0.25 µm film coating thickness, was used for the separation of PCB congeners. Helium was used as the carrier gas, with a flow rate of 1.0 ml/min and a pressure of 18 psi. The injector was kept at a constant pressure and temperature of 250 ˚C. The oven temperature was programmed as follows: it was initially set at 70 ˚C and held for two minutes, then increased to 180 ˚C at a rate of 25 ˚C/min, then increased to 200 ˚C at a rate of 3 min, then increased to 280 ˚C at a rate of 8 min,

and held for 13 min. The injector and detector temperatures were both set at 280 ◦C. The injection volume was 5 µL in the splitless mode. The ionization voltage was 70 eV, and the solvent delay was set to 6 min. Detection of the compounds was performed in full scan mode with a scan range of 50 to 500 mass to charge ratios (m/z). The total run time was 36.07 min. The MS transfer line temperature was 280 ◦C, and the ion source temperature was 250 ◦C.



Figure 5.2 Agilent 6890/5973 gas chromatography-mass Spectrometry (GC-MS) instrument.

5.3.2 Chemicals and Instruments

The following were all obtained from Sigma (Dublin, Ireland): an Aroclor 1254 stock solution at a concentration of 200 µg/ml in methanol; a surrogate solution of a mixture in acetone containing 200 µg/ml of decachlorobiphenyl (deca-CB) and of tetrachloro-mxylene (TCMX); anhydrous $MgSO_4$ powder; sodium chloride NaCl powder;

diatomaceous earth; clean soil; acetonitrile; hexane; acetone; ethyl acetate; methanol. The reagents and solvents used in the experiments were generally of an analytical grade or higher. Ultrapure deionized water, with a resistivity of 18.2 MΩ·cm, was obtained from a Milli-Q system (Millipore, Molsheim, France). We used a QuEChERS Original Method extraction kit (5 g samples), 50/pk. The kit contents were as follows: 4 g $MgSO_4$, 1 g NaCl with 50 mL tubes, and a QuEChERS dispersive clean-up kit (PSA, C18, $MgSO_4$); these were purchased from Agilent Technologies Ireland Limited (Cork, Ireland). We also used a centrifuge (Heraeus Megafuge 16, Thermo Fisher, Bremen, Germany), analog vortex mixer (VWR Mixer Mini Vortex, Missouri CT, USA), ultrasonic Branson 5510 cleaner (Branson Ultrasonics Corporation, Brookfield, CT, USA), suitable hoods, glassware, volumetric flasks, pipettes, cylinders, beakers, vials, tubes for soil sample extraction, and filter paper for soil sample filtration.

5.3.3 Standard and Sample Solution Preparation

A six-point calibration curve was employed for the quantitative analysis. Standard solutions of Aroclor 1254 were prepared at levels of 0.32, 0.65, 1.25, 2.5, 5, and 10 ng/ml by diluting 200 μg/ml Aroclor 1254 stock solutions with methanol. Surrogate standard solutions for Deca-CB and TCMX were prepared at a concentration of 5 ng/ml via dilution with acetone from a 200 μg/ml stock solution. To assess extraction recovery, a surrogate standard was added, and the standards and working solutions were stored at 4 °C. For the recovery experiment, the soil used in this work (about 100 g) was purchased from Sigma. The soil samples were stored at room temperature 25 °C in dark-colored glass bottles. The physicochemical properties of the soil were as follows: The soil texture was

sandy; pH = 6.2; organic matter at levels of 0.1%. Afterwards, soil samples were spiked with PCBs standards at 10 μg/kg and 5 μg/kg. To obtain a homogeneous sample, a mechanical stirring apparatus was used. After that, to allow the solvent to evaporate, the samples were left in a ventilated area for eight hours. The standards are thought to bind the soil samples similarly to natural processes. For accurate recovery results, it is critical to use suitable extraction methods and solvents to avoid soil interference. The soil was pre-treated to remove the interfering compounds. Additionally, the potential contamination sources were controlled and evaluated throughout the process to obtain better recovery.

To calculate the recovery, a chromatogram with characteristic peak areas and retention times, or a "fingerprint" pattern, was produced by a single PCB mixture of Aroclor 1254. In this study, an Aroclor 1254 mixture containing tetra-CB, m/z 292; hexa-CB, m/z 360; hepta CB, m/z 394; penta-CB, m/z 326 with peak areas of penta-chlorinated biphenyls (penta-CBs) were selected and used to construct the calibration models for the quantification of Aroclor 1254, because penta-CBs are one of the major PCBs in Aroclor 1254 (48% weight). The areas of selected peaks in the sample were compared to the same areas in a standard PCB mixture, which was the method utilized.

Phase separation is a process in which a mixture is divided into two or more distinct phases, usually due to the presence of a separating agent. Salt is a commonly used separating agent, and its addition can induce phase separation. However, it is important to note that the effectiveness of the extraction system can also be influenced by the amount of salt used. In a recent study, the same amount of magnesium sulfate ($MgSO_4$)

has been used as in a previous study to induce phase separation [24]. Magnesium sulfate ($MgSO_4$) is often used as a drying agent to remove water from the organic phase and improve the efficiency of the extraction process. In addition to $MgSO_4$, NaCl can also be employed to minimize the effects of polar interference. This can be particularly useful when analysing samples that contain high levels of polar compounds, as these compounds can interfere with the extraction process and lead to inaccurate results. Therefore, careful consideration of the type and amount of separating agents used is crucial for the success of any extraction process.

5.3.4 Extraction and Clean-Up Procedure

Extraction was performed according to the QuEChERS method described by Anastassiades, Michelangelo Lehotay, Steven J. (2003) [24]. Approximately 5 g of soil samples were weighed into a 50 ml centrifuge tube and mixed with 15 ml of acetonitrile/water (75%: 25%, v/v) or hexane/water (75%: 25%, v/v) in a QuEChERS tube, followed by vortex homogenization for 4 min. Then, the tube containing samples was ultrasonically treated for 20 min. After that, 4 g of MgSO4 and 1 g of NaCl were added. After vortexing the mixture for 4 min, the extract was centrifuged at 4500 rpm for 10 min to remove the upper layer. Approximately 6 mL of the organic layer extract was transferred into a clean-up tube containing 900 mg $MgSO_4$ and 150 mg of sorbent mix (PSA/C18) or diatomaceous earth. After 4 min of vortex homogenization, the tubes were centrifuged for 10 min at 4500 rpm. Approximately 1.5 ml of the upper layer were

filtered before being transferred to GC vials for a GC-MS analysis, and 50 µL of deca-CB and TCMX internal standards were added the modified QuEChERS extraction method is shown in Figure 5.3. The blank samples (soils without PCBs) were treated the same way, but without the PCB standard solution. The experiments were replicated three times.

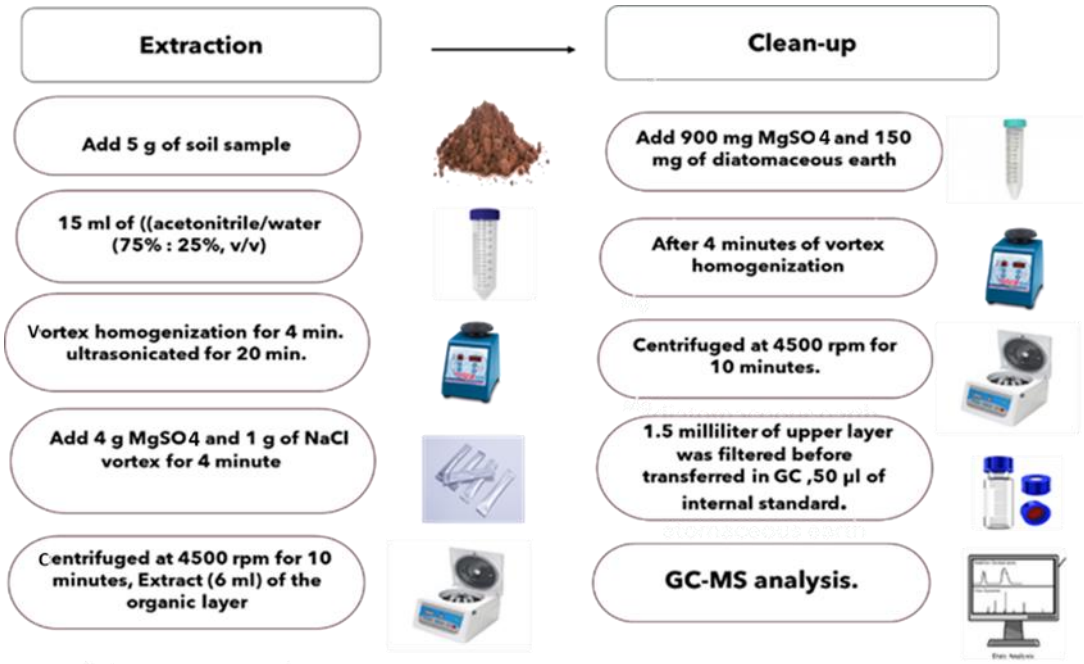


Figure 5.3 Schematic illustration of the modified QuEChERS extraction method.

5.3.5. Method validation

The analytical parameters used to validate the method for analysing PCBs include linearity, limit of detection (LOD), limit of quantification (LOQ), relative standard deviation (RSD), and recovery. The linearity of the relationship between concentration and the peak area was determined by analysing standard PCB solutions. Calibration curves used 6 standard solutions in the concentration range of 0.32–10 ng/ml for Aroclor 1254 in triplicate. LOD and LOQ were calculated using the formulas LOD = 3.3 SD of

intercept/slope and LOQ = 10 SD of intercept/slope. Precision was evaluated by measuring the inter-day and intra-day variability at two concentration levels within the linearity range, with three replicates on the same day or on three different days. Recovery was assessed by performing a study at two concentration levels within the linearity range to evaluate the accuracy of the GC-MS method. The results of these analytical parameters are presented in the results section of the study.

5.4. Results and Discussion

5.4.1. Optimization of Extraction Solvent Conditions

For the purpose of this study, Aroclor 1254 was selected to be analysed in soil samples. QuEChERS has been utilized in several studies to measure a variety of pollutants, including pesticides in soil samples [32][33], aromatic organochlorines [34], veterinary products, and pharmaceuticals [35][36]. In spite of this, the method has not been extensively used in the extraction of Aroclor 1254 from soil. The QuEChERS method should be optimized in order to obtain the best recovery. Several related parameters, including water effect, solvent effect, and solvent volume effect, were optimized.

A traditional QuEChERS extraction was performed with samples containing a high moisture content. Additionally, the QuEChERS method has been modified [37][38][39]. Humidity is an important factor when preparing soil samples [40]. It was necessary to add ultrapure water to soil samples in order to ensure moisture content and to improve the recovery of PCBs from soil samples. To achieve high extraction efficiency, different amounts of water (3, 5, 7, and 10 ml) were tested. According to the results, maximum

peak intensity and maximum recovery were achieved with 5 and 7 ml of water; as the amount of water increases, peak intensity decreases (see Fig.5.4 (a)). For the additional experiment we utilized 5 ml.

Extraction efficiency is highly dependent on the solvent used for extraction. In addition, the solvent must be less costly, compatible with analytical instruments, and eco-friendly [42]. To determine the most suitable solvent for the extraction of PCBs from soil samples, two different solvents were used: acetonitrile and hexane in combination with water. The original QuEChERS method used acetonitrile as the extract solvent, and many other studies involved QuEChERS procedures [24]. Therefore, this solvent was chosen for use in the present study as one of the solvents, while hexane was chosen as the other solvent since it is commonly used to extract PCBs from soil [43], although it is less eco-friendly. As shown in Fig. 5.4 (b), recovery rates of PCBs in the acetonitrile extraction were 85.53 %–102.72 %, showing better efficiency, the production of cleaner extracts, and overall higher recoveries for PCBs than the hexane extraction. In this study, acetonitrile was found to be the most suitable extraction solvent, as it extracts a lower amount of the matrix, which is consistent with the findings of the previous study [44][31].

Furthermore, the volume of solvent used is critical for effective recovery, and there should be enough solvent to allow the sample to be fully immersed and interact with the analyte. Various amounts of acetonitrile, including 3, 5, 7, 10, and 15 ml were tested, and it was found that 10 ml of acetonitrile yielded the highest peak intensity and recovery, as depicted in Fig.5.4 (c). Acetonitrile is considered to be a more selective solvent and produces a cleaner chromatogram compared to most other solvents used in the

QuEChERS technique [45]. When compared to other solvents utilized in QuEChERS, ACN separates from water more effectively in the presence of salts, producing good phase separation, which inhibits polar matrix interaction [46].

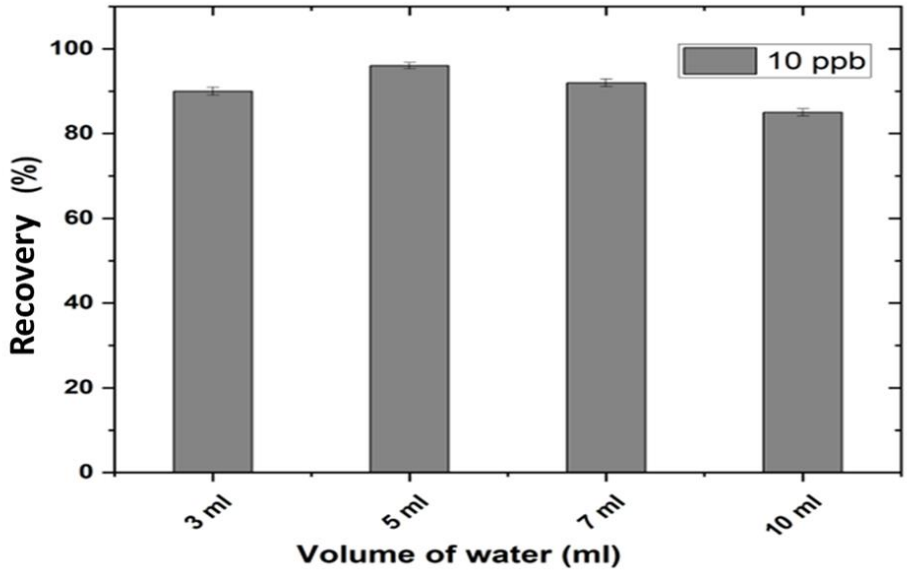


Figure 5.4 (a) The effect of water addition on extraction efficiency for the target Aroclor 1254 at 10 ng/ml.

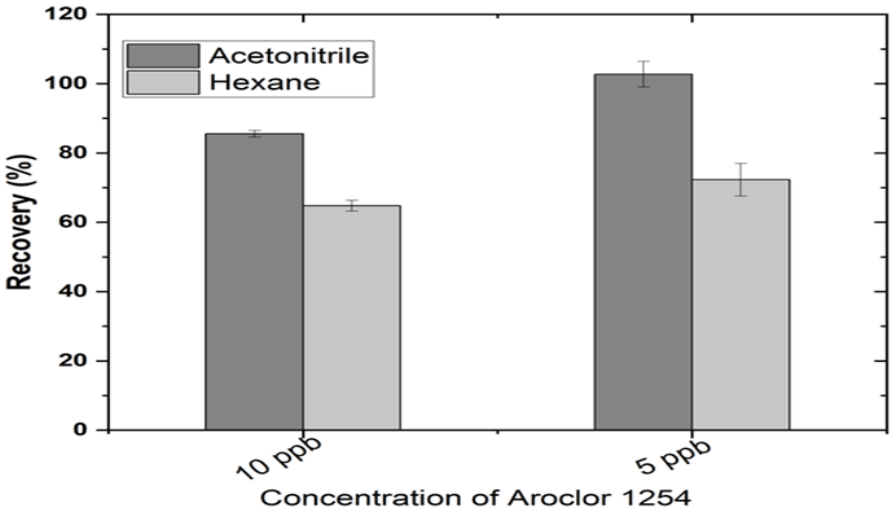


Figure 5.4 (b) The effect of acetonitrile and hexane as extraction solvents for the target Aroclor 1254 at 5 ng/ml and 10 ng/ml (n = 3).

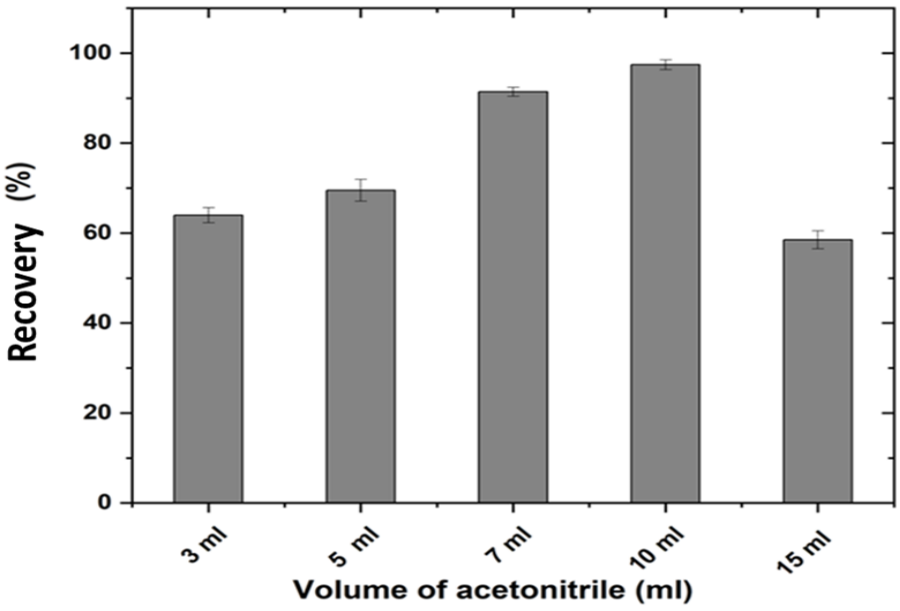


Figure 5.4 (c) The effects of different solvent volumes for the target Aroclor 1254 at 10 ng/ml (n = 3).

5.4.2 Optimization of Physical Extraction Condition

In this study, the effects of shaking time, centrifuge time, and speed were optimized and discussed. Several methods, including laboratory shakers, manual shakers, and vortexes, have been commonly used to extract targets from the soil. However, due to the strong binding characteristics of the soil, manual shaking for one minute, which was sufficient for the analysis of pesticides in fruits and vegetables according to the original QuEChERS method, resulted in lower recovery rates in this study. [24][47][48]. To compare the efficacy of manual shaking and vortex extraction, various extraction times ranging from 1 to 6 minutes were evaluated. The results showed that the recovery obtained with vortex extraction was higher than that obtained with manual shaking. Additionally, it was found that increasing the intensity of shaking was beneficial in breaking the strong interactions between analytes and matrix, resulting in improved extraction. Based on these findings, vortex extraction was selected as the preferred method of extraction for the targets from soil in this study. As shown in Fig. 5.5 (a), The optimal extraction time for the removal of target PCBs from soil was found to be 4 minutes, and extending the extraction time beyond this did not improve recovery rate.

There was a significant effect on centrifugation time and rate. In addition, different extraction times (1, 5, and 10 min) and rates (1500, 4500, and 5000 rpm) were investigated for 5 and 10 ng/ml concentration levels for PCB extraction. The results shown in Fig.5.5 (b) indicate that excellent recovery of PCBs was achieved at 10 minutes, which was chosen as the optimal centrifugation time. A centrifuge of 4500 rpm was

found to be sufficient to obtain good recovery of PCBs (Fig.5.5 (c)). Using a centrifuge facilitates increased contact between the solvent and the soil sample, which improves dissolution of the analyte [49][50] and reduces the extraction time.

As part of the preparation of complex matrixes such as soil, a clean-up step was necessary in order to reduce interference, improve quantification, and avoid disturbing the signal on the chromatographic system [51]. In addition to traditional sorbents used in the clean-up step of QuEChERS extraction from soil samples, C18 and PSA, diatomaceous earth was also used as alternative sorbents [52] [53].; they were less expensive and more eco-friendly than the traditional ones but have not been extensively investigated in d-SPE [52]. As shown in Fig. 5.5 (d), the sorbent has different effects on recovery and selectivity, and to achieve a satisfactory level of purification and recovery of PCBs, the effects of sorbent types were evaluated. The PSA retains a wide range of polar substances, including sugars, organic acids, and fatty acids. In addition, the nonpolar adsorbent, C18, retains trace amounts of nonpolar co-extractives and is capable of removing long chain fatty compounds and sterols from the extract. When PSA is used in conjunction with C18, additional lipids and sterols can be removed [53]. Diatomaceous earth consists of natural silica ($SiO_2 \bullet nH_2O$), with traces of metal oxides of specific structures, and its proposed use is as a simple alternative material and an environmentally friendly natural sorbent [54]. The use of diatomaceous earth improved phase separation during QuEChERS extraction. Calculations of the differences between spiked and blank soil samples were used to determine recovery rates.

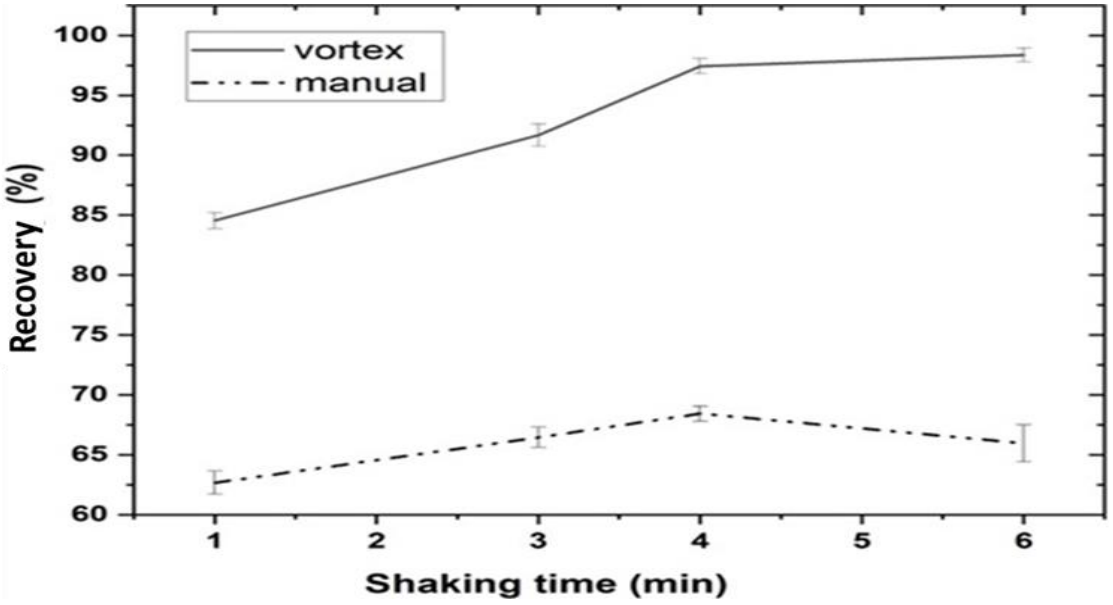


Figure 5.5 (A) Effect of shaking: 4 min, 15 mL of acetonitrile/water (75%: 25%, v/v), 5 g of soil, 4 g $MgSO_4$, 1 NaCl.

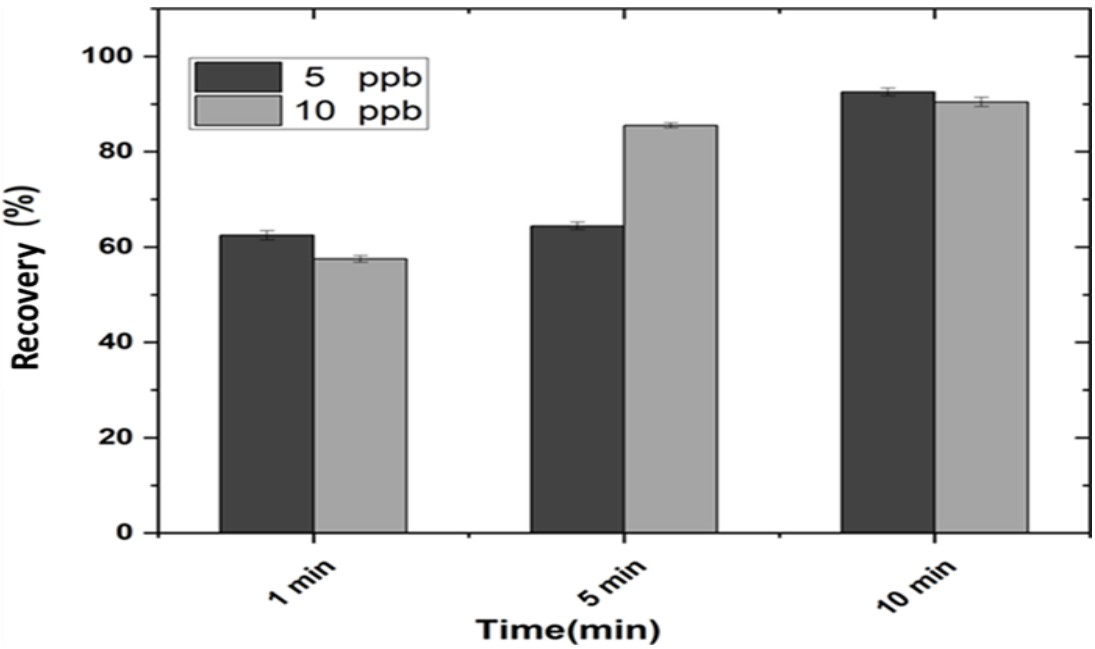


Figure 5.5(B) Effect of speed: 10 min, 15 mL of acetonitrile/water (75%: 25%, v/v), 5 grams of soil, 4 grams $MgSO_4$, 1 NaCl.

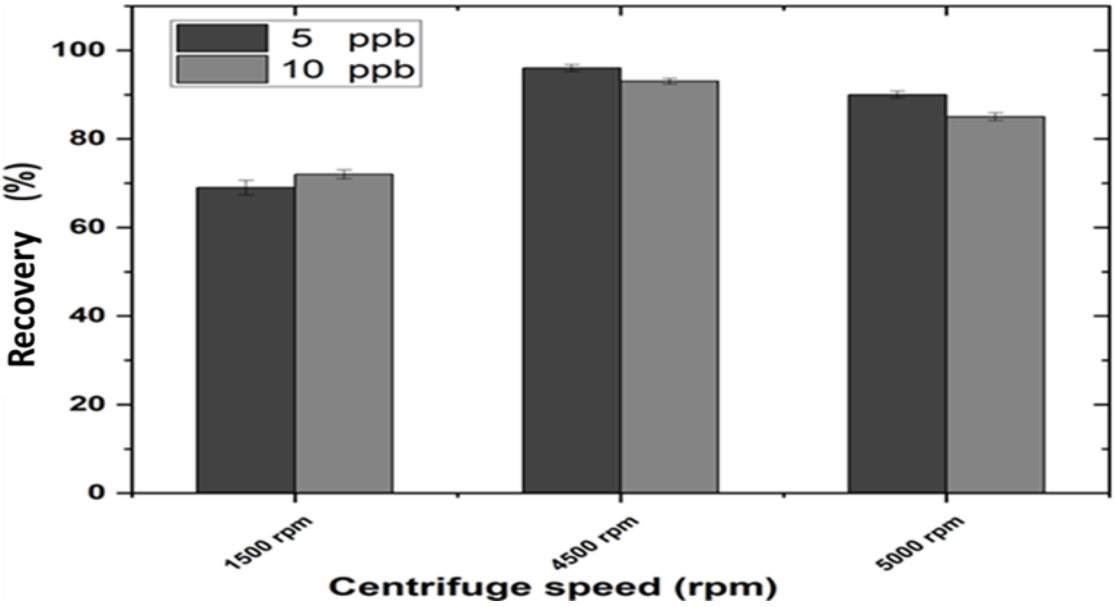


Figure 5.5 (C) Effect of centrifuge time: 4500 rpm, 15 mL of acetonitrile/water (75%: 25%, v/v), 5 g of soil, 4 g $MgSO_4$, 1 NaCl.

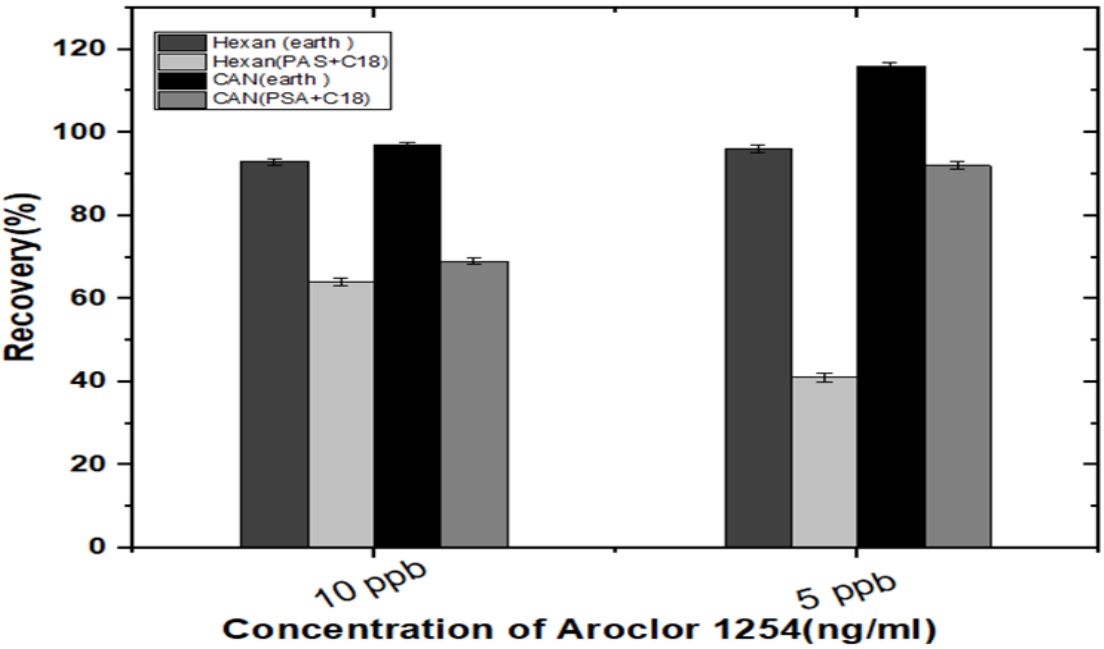


Figure 5.5 (D) Comparison of recovery rates for different sorbents in the QuEChERS extraction method (n = 3) The conditions for the experiment were: 5 grams of soil, 15 ml of acetonitrile/water (75%: 25%, v/v), 4 grams of $MgSO_4$, 1 gram of NaCl, 4500 rpm.

5.4.3 Method validation

Under optimized extraction and clean-up conditions, we studied analytical parameters such as selectivity, linearity, LOD, LOQ, precision, and recovery. In order to evaluate the selectivity of the method, a blank sample was extracted by the optimized QuEChERS method, and positive samples were confirmed by GC-MS (Fig.5.6 (a)). This confirms that the method has good selectivity, as no peaks interfered with analyte retention time. A standard calibration curve (Fig.5.6 (b)) has been prepared using concentrations ranging from 0.31 to 10 ng/ml (0.31, 0.65, 1.25, 2.5, 5, 10 ng/ml) of Aroclor 1254 with a coefficient of determination R^2 of 0.9933; the linear regression equation fit is shown as (Y = 38098(x) - 26023). The limit of detection (LOD) and limit of quantification (LOQ) were calculated based on three and ten times the standard deviation, respectively. The LOD value was 1.9 ng/ml and the LOQ value was 5.7 ng/ml, which indicated good sensitivity of this method.

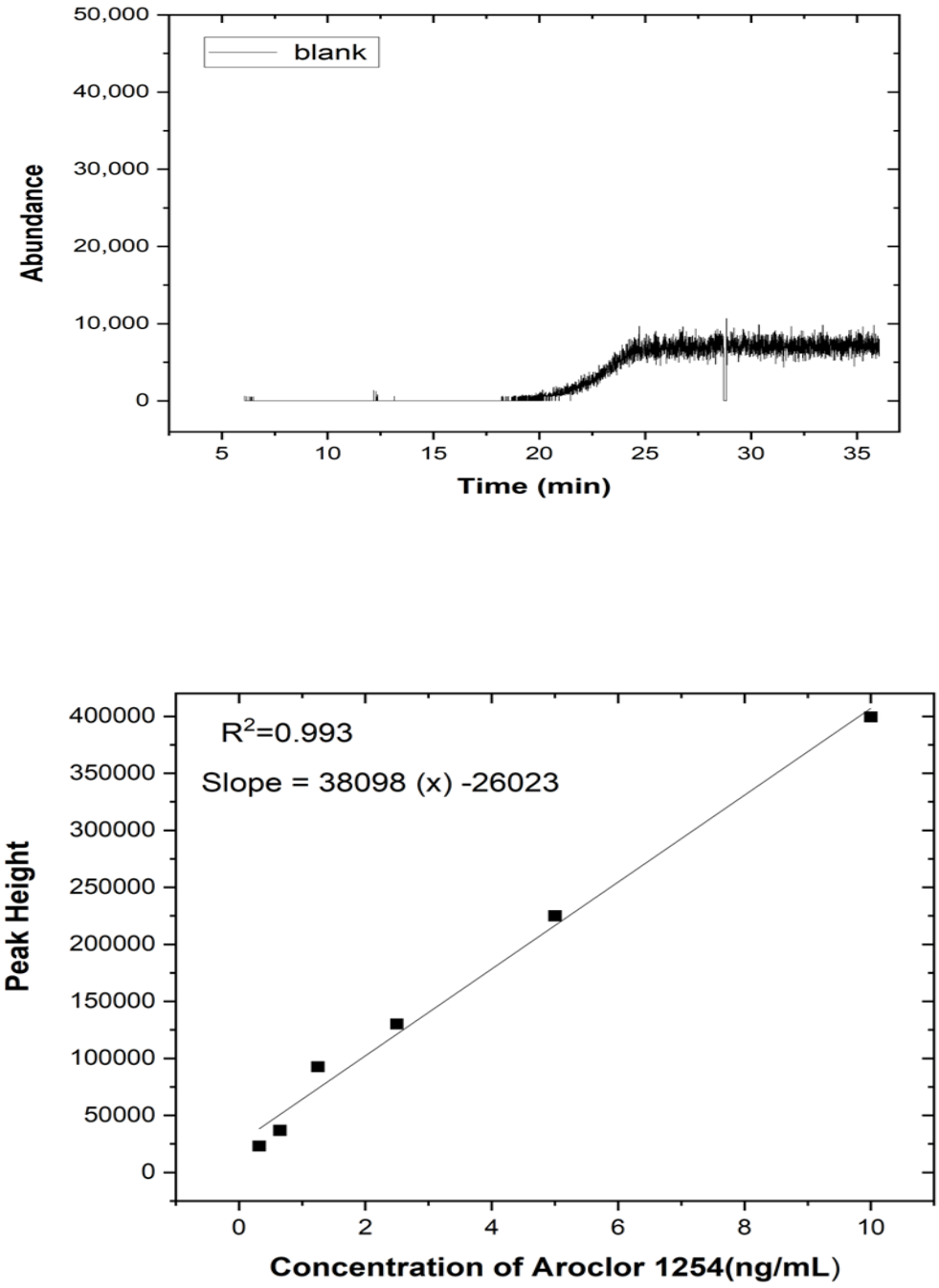


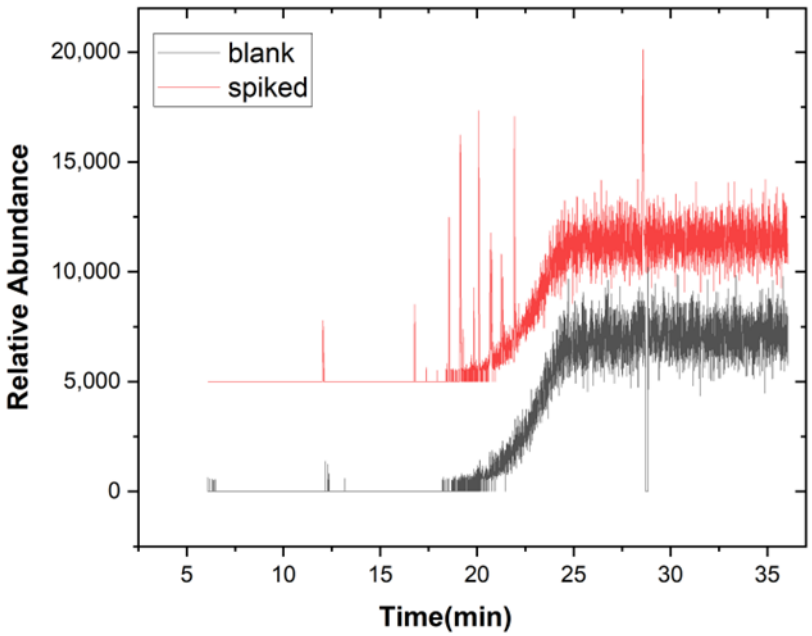
Figure 5.6 (a) GC analysis for the blank sample. (b) GC-MS calibration curve for standard Aroclor 1254.

5.4.4. Analysis of Aroclor 1254 in spiked soil samples (recovery and precision)

The validation of a method is crucial to ensure that the results obtained are accurate and reliable. In the case of analysing Aroclor 1254 in soil samples, sample spikes were used to improve the validation of the method. Two different levels of Aroclor 1254 standard solution were spiked into the soil samples at 5 and 10 µg/kg levels. The spiked samples were run in triplicate to evaluate the precision and repeatability of the assay. The RSD% was used to determine the precision, which was evaluated using two parameters: intra-day (repeatability) and inter-day precision. Repeatability was assessed by analysing three replicates of soil samples spiked at two levels (5 and 10 µg/kg) on the same day, while inter-day precision was determined by analysing samples on three different days over a period of two weeks.

The results of the analysis showed that the recovery of Aroclor 1254 from soil samples ranged from 95.3% to 103.2%, indicating the accuracy of the method. The RSD for inter-day precision ranged from 3.6 % to 5.8 %, while that for intra-day precision ranged from 2.1 % to 4 %, indicating the repeatability of the method. The developed modified QuECHERS method was compared with other recent studies in the literature, as demonstrated in Table 5.1. The present work shows great recovery value due to the use of different extraction solvents, which has a significant impact on the level of PCBs extraction from soil. Additionally, the comparison for blank (in black) and soil sample (in red) for 10 µg/kg and 5 µg/kg concentration are presented in Figure 5.7, which further supports the accuracy and reliability of the modified QuEChERS and GC-MS methods for

analysing Aroclor 1254 in soil samples. These findings are important for environmental studies and risk assessments, as accurate analysis of pollutants in soil is necessary for identifying potential risks and implementing effective mitigation strategies.



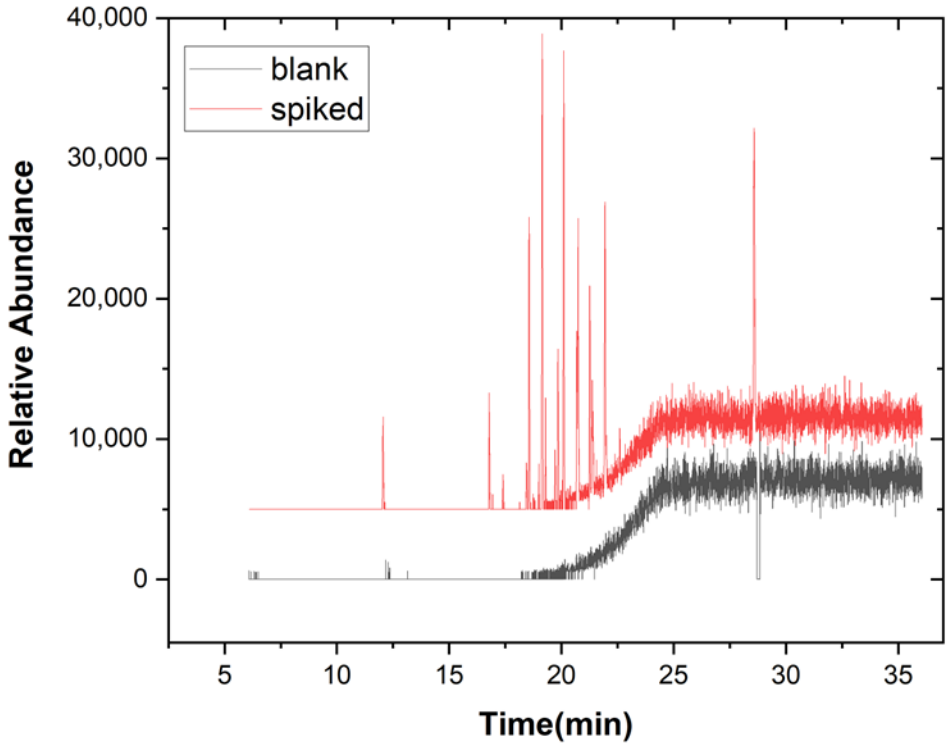


Figure 5.7 (a) GC/MS Total ion chromatogram of Aroclor 1254 (red line) and the blank (black line) for 10 µg /kg soil sample after QuEChERS extraction. (b) GC/MS Total ion chromatogram of Aroclor 1254 (red line) and the blank (black line) for 5 µg /kg soil sample after QuEChERS extraction.

Table 5.1 Comparison of the present study with other studies. For the present work recovery and RSD was included at different Aroclor 1254 concentrations in soil samples (n=3).

Sample	Extraction	Added (μg/kg)	Intra-day (RSD%)	Inter-day (RSD%)	Recovery (%)	Reference
water	acetonitrile	8 (μg/L)	≥15 %	---	90 – 95%	[242]
shrimp	water/ MeCN*	1, 5, 10	>20%	---	70–115%	[243]
sediment	water/ Ace/Hex* or water/Ace/DCM*	50	≥15 %	---	76–131%	[244]
Soil	Water/ acetonitrile	5	4	5.8	103.2%	Present work
Soil	water /acetonitrile	10	2.1	3.6	95.3%	Present work

***** MeCN (Acetonitrile), Ace (Acetone), Hex (Hexane), DCM (Dichloromethane).

5.5 Comparative summary of the different assay procedures used on SPGEs with optical and GC-MS

PCBs are found in various forms and concentrations in environmental regions, including water, air, and soil. As a result, there is a requirement to employ varied analytical methods depending on each particular case. Currently, Widely utilized traditional analytical methods for detecting PCBs involve the use of Gas Chromatography-Mass Spectrometry (GC-MS) and high-performance liquid chromatography (HPLC) with fluorescence detection[10,11].Many advantages are associated with the use of these Conventional analytical methods, such as accuracy, sensitivity and reliability .

Nevertheless, these methods have some limitations. One such disadvantage is including the fact that potential for high-risk loss of analytes during sample separation. Furthermore, these Techniques require the use of an extensive amount of harmful organic solvents [57]. This presents a concern due to its dual impact of increases costs and causing environmental contamination. The loss of analytes constitutes a significant source of low-quality analytical data for PCBs due to separation, pre-treatment, and sampling of analytes, These processes introduce errors that are unrelated to the final quantification step. Moreover, The use of these methods makes the approach of sample analysis, preparation, and quantification Extremely time-consuming and tedious[58].

In recent times, immunosensor techniques have become more popular to use instead of traditional techniques due to their numerous advantages and to overcome the limitations of GC-MS instruments. Therefore, immunosensor methods provide fast response times, on field measurement, requires only small volumes of sample and miniaturization.

The electrochemical immunosensor showed a good performance with a 3-fold decrease in sensitivity achieved after the surface modification. For the label free electrochemical showed good sensitivity and it was reducing the time of analysis to less than two hours by avoiding using labelled step. Many different tests and experiments could not be performed due to time limitations. We can improve and increase the sensitivity by modified the electrode using nanoparticles, such as gold nanoparticles (GNPs), to enhance the sensitivity and performance of the individual sensor measurements. Table 5.2 shows the comparison of optical and electrochemical immunosensors with GC-MS. As previously mentioned, the chromatographic techniques could detect at very low concentrations of PCBs.

Overall, the promising performance of the developed electrochemical immunosensors could satisfy the need for excellent biosensors. However, these developed immunosensors will not replace existing laboratory techniques, but will rather complement them.

Table 5.2 Comparison of optical and electrochemical immunosensors performance with GC-MS.

Detection	Support	Material for immunoreaction	LOD	Linear Rang (ng/ml)	R^2
Optical	96 well plate	Hydrophobic polystyrene	0.44 ng/ml	0.58 to 56 ng/ml	0.962
Electrochemical	SPE	Direct on gold bare electrode	0.20 ng/ml	0.304 to 220 ng/ml	0.96
Electrochemical	SPE	11-MUA Modified Sensor	0.09 ng/ml	0.1 to 220 ng/ml	0.99
Label Free Electrochemical	SPE	11-MUA Modified Sensor (DVP)	0.11 ng/ml	0.011 to 220 ng/ml	0.99
Label Free Electrochemical	SPE	11-MUA Modified Sensor (EIS)	0.91 ng/ml	0.011 to 220 ng/ml	0.98
GC-MS	---------- ---------	----------	1.9 ng/ml	1-10 ng/ml	-------

5.6 Conclusion

In this study, we have utilized a modified QuEChERS method, combined with GC-MS analysis, to analyze Aroclor 1254 in soil samples. This novel method has several advantages over traditional techniques, including its simplicity, cost-effectiveness, eco-friendliness, and minimal solvent extraction. We have modified the sample pre-treatment procedure by incorporating vortex shaking, a mixed solvent (either acetonitrile/water or hexane/water), and three adsorbents (PSA, C18, and diatomaceous earth) for the cleaning process. We have found that the best results were obtained when water/acetonitrile and diatomaceous earth were used. The method demonstrated excellent accuracy, linearity, LOD, LOQ, intra-day precision, and inter-day precision. Specifically, the recovery was in the range of 95.3-103.2 %, correlation coefficients were higher than 0.98, the limit of detection (LOD) was 1.9 µg/kg, and the limit of quantification (LOQ) was 5.7 µg/kg, intra-day precision varied between 2.1 % and 4 %, and inter-day precision was between 3.6 % and 5.8 %.

This optimized method offers several advantages over traditional techniques, including a reduction in overall analysis time, avoidance of the use of large levels of non-eco-friendly solvents, increased sensitivity, rapid results, and a reduction in the consumption of organic reagents. Compared to other common extraction methods, this streamlined procedure offers an efficient and effective technique for monitoring PCBs in the environment. Moreover, this technique has the potential to be applied to a wider range of sample types and applications, making it an even more valuable tool for environmental monitoring. Overall, the study provides a significant contribution to the

field of analytical chemistry and environmental science, demonstrating a novel and effective method for analysing Aroclor 1254 in soil samples.

The development electrochemical immunosensor showed a good sensitivity compared to optical immunosensors. The modified gold surface showed a 3-fold increase in sensitivity compared to the bare gold electrode. However, chromatographic techniques such as GC-MS seemed to be more promising in terms of high sensitivity, as they can detect to sub part per trillion level. As already mentioned earlier, this sensor was developed to screen and monitor the presence of PCBs, on the basis of “YES” or “NO”.

5.7 References

1. Robles Martínez, H.A.; Rodríguez, G.C.; Castillo, D.H. Determination of PCBs in Transformers Oil Using Gas Chromatography with Mass Spectroscopy and Aroclors (A1254:A1260). Chem. Soc 2005, 49, 263–270.

2. Shin, S.K.; Kim, T.S. Levels of polychlorinated biphenyls (PCBs) in transformer oils from Korea. J. Hazard. Mater. 2006, 137, 1514–1522, doi:10.1016/j.jhazmat.2006.04.031.

3. Shen, F.; Xu, Y.J.; Wang, Y.; Zhu, P.Y.; Dai, X.L.; Chen, J.; Zou, Q. Determination of Aroclor 1254 in Water Samples Using Polystyrene–Divinylbenzene Solid-Phase Extraction and Gas Chromatography. J. Anal. Test. 2018, 2, 306–311, doi:10.1007/s41664-018-0063-7.

4. Kim, L.; Jeon, J.W.; Lee, Y.S.; Jeon, H.J.; Park, B.J.; Lee, H.S.; Choi, S.D.; Lee, S.E. Monitoring and risk assessment of polychlorinated biphenyls (PCBs) in agricultural soil collected in the vicinity of an industrialized area. Appl. Biol. Chem. 2016, 59, 655–659, doi:10.1007/s13765-016-0207-2.

5. Kaya, D.; Imamoglu, I.; Sanin, F.D.; Payne, R.B.; Sowers, K.R. Potential risk reduction of Aroclor 1254 by microbial dechlorination in anaerobic Grasse River sediment microcosms. J. Hazard. Mater. 2017, 321, 879–887, doi:10.1016/j.jhazmat.2016.10.009.

6. Swanson, G.M.; Ratcliffe, H.E.; Fischer, L.J. Human Exposure to Polychlorinated Biphenyls (PCBs): A Critical Assessment of the Evidence for Adverse Health Effects. Regul. Toxicol. Pharmacol. 1995, 21, 136–150, doi:https://doi.org/10.1006/rtph.1995.1018.

7. Zhong, Y.; Guo, P.; Wang, X.; An, J. Aroclor 1254 inhibits cell viability and induces apoptosis of human A549 lung cancer cells by modulating the intracellular Ca2+ level and ROS production through the mitochondrial pathway. J. Environ. Sci. Heal. Part A 2015, 50, 806–813, doi:10.1080/10934529.2015.1019797.

8. Ozcan, S. Analyses of polychlorinated biphenyls in waters and wastewaters using vortex-assisted liquid-liquid microextraction and gas chromatography-mass spectrometry. J. Sep. Sci. 2011, 34, 574–584, doi:10.1002/jssc.201000623.

9. Ozcan, S.; Tor, A.; Aydin, M.E. Determination of selected polychlorinated biphenyls in water samples by ultrasound-assisted emulsification-microextraction and gas chromatography-mass-selective detection. Anal. Chim. Acta 2009, 647, 182–188, doi:10.1016/j.aca.2009.06.037.

10. Derouiche, A.; Driss, M.R.; Morizur, J.P.; Taphanel, M.H. Simultaneous analysis of polychlorinated biphenyls and organochlorine pesticides in water by headspace solid-phase microextraction with gas chromatography-tandem mass spectrometry. J. Chromatogr. A 2007, 1138, 231–243, doi:10.1016/j.chroma.2006.10.064.

11. Güzel, B.; Canlı, O. An environmental friendly and stable analytical method for the determination of indicator polychlorinated biphenyls (PCBs) in solid and waste oil samples by gas chromatography-electron capture detector (GC-ECD). Microchem. J. 2022, 178, doi:10.1016/j.microc.2022.107325.

12. Santos, F.J.; Galceran, M.T. The application of gas chromatography to environmental analysis. TrAC - Trends Anal. Chem. 2002, 21, 672–685, doi:10.1016/S0165-9936(02)00813-0.

13. Bandh, C.; Björklund, E.; Mathiasson, L.; Näf, C.; Zebühr, Y. Comparison of accelerated solvent extraction and Soxhlet extraction for the determination of PCBs in Baltic Sea sediments. Environ. Sci. Technol. 2000, 34, 4995–5000, doi:10.1021/es991064g.

14. Wang, P.; Zhang, Q.; Wang, Y.; Wang, T.; Li, X.; Ding, L.; Jiang, G. Evaluation of Soxhlet extraction, accelerated solvent extraction and microwave-assisted extraction for the determination of polychlorinated biphenyls and polybrominated diphenyl ethers in soil and fish samples. Anal. Chim. Acta 2010, 663, 43–48, doi:10.1016/j.aca.2010.01.035.

15. Luque-García, J.L.; Luque De Castro, M.D. Extraction of polychlorinated biphenyls from soils by automated focused microwave-assisted Soxhlet extraction. J. Chromatogr. A 2003, 998, 21–29, doi:10.1016/S0021-9673(03)00652-6.

16. Barri, T.; Bergström, S.; Norberg, J.; Jönsson, J.Å. Miniaturized and Automated Sample Pretreatment for Determination of PCBs in Environmental Aqueous Samples Using an On-Line Microporous Membrane Liquid-Liquid Extraction-Gas Chromatography System. Anal. Chem. 2004, 76, 1928–1934, doi:10.1021/ac035089g.

17. Rezaei, F.; Bidari, A.; Birjandi, A.P.; Milani Hosseini, M.R.; Assadi, Y. Development of a dispersive liquid-liquid microextraction method for the determination of polychlorinated biphenyls in water. J. Hazard. Mater. 2008, 158, 621–627, doi:10.1016/j.jhazmat.2008.02.005.

18. Westbom, R.; Thörneby, L.; Zorita, S.; Mathiasson, L.; Björklund, E. Development of a solid-phase extraction method for the determination of polychlorinated biphenyls in water. J. Chromatogr. A 2004, 1033, 1–8, doi:10.1016/j.chroma.2004.01.022.

19. Zhang, Z.; Rhind, S.M. Optimized determination of polybrominated diphenyl ethers and polychlorinated biphenyls in sheep serum by solid-phase extraction-gas chromatography-mass spectrometry. Talanta 2011, 84, 487–493, doi:10.1016/j.talanta.2011.01.042.

20. Huo, L.G.; Li, H.D.; Zhao, C. Le; Wang, W.B.; Chen, Z.L.; Ding, R.Y.; Dong, Z.; Wang, F.E.; Yang, G.S.; Lu, X.; et al. The Determination of PCBs in Meat and Sea Food by GC-QqQ-MS/MS. Food Anal. Methods 2012, 5, 1481–1491, doi:10.1007/s12161-012-9391-9.

21. Ecd, G.C.; Benedicto, J.; Beckert, F. Determination of PCBs in Soils / Sediments by Microwave-Assisted Extraction. 1995, 29, 2709–2712.

22. Reddy, A.V.B.; Moniruzzaman, M.; Aminabhavi, T.M. Polychlorinated biphenyls (PCBs) in the environment: Recent updates on sampling, pretreatment, cleanup technologies and their analysis. Chem. Eng. J. 2019, 358, 1186–1207.

23. Camel, V. Recent extraction techniques for solid matrices - Supercritical fluid extraction, pressurized fluid extraction and microwave-assisted extraction: Their potential and pitfalls. Analyst 2001, 126, 1182–1193, doi:10.1039/b008243k.

24. Anastassiades, M.; Lehotay, S.J.; Štajnbaher, D.; Schenck, F.J. Fast and Easy Multiresidue Method Employing Acetonitrile Extraction/Partitioning and "Dispersive Solid-Phase Extraction" for. J. AOAC Int. 2003, 86, 412–31.

25. Chamkasem, N.; Lee, S.; Harmon, T. Analysis of 19 PCB congeners in catfish tissue using a modified QuEChERS method with GC-MS/MS. Food Chem. 2016, 192, 900–906, doi:10.1016/j.foodchem.2015.07.088.

26. Norli, H.R.; Christiansen, A.; Deribe, E. Application of QuEChERS method for extraction of selected persistent organic pollutants in fish tissue and analysis by gas chromatography mass spectrometry. J. Chromatogr. A 2011, 1218, 7234–7241, doi:10.1016/j.chroma.2011.08.050.

27. Cui, Y.; Wang, Z.; Cong, J.; Wang, L.; Liu, Y.; Wang, X.; Xie, J. Determination of polychlorinated biphenyls in fish tissues from Shanghai seafood markets using a modified QuEChERS method. Anal. Sci. 2017, 33, 973–977, doi:10.2116/analsci.33.973.

28. Madureira, T.V.; Santos, C.; Velhote, S.; Cruzeiro, C.; Rocha, E.; Rocha, M.J. Contamination levels of polychlorinated biphenyls in wild versus cultivated samples of female and male mussels (Mytilus sp.) from the Northwest Coast of Iberian Peninsula-new application for QuEChERS (Quick, Easy, Cheap, Effective, Rugged, and Safe) metho. Environ. Sci. Pollut. Res. 2014, 21, 1528–1540, doi:10.1007/s11356-013-2017-y.

29. Kuzukiran, O.; Filazi, A. Determination of Selected Polychlorinated Biphenyl Residues in Meat Products by QuEChERS Method Coupled with Gas Chromatography–Mass Spectrometry. Food Anal. Methods 2016, 9, 1867–1875, doi:10.1007/s12161-015-0367-4.

30. Al-Alam, J.; Fajloun, Z.; Chbani, A.; Millet, M. A multiresidue method for the analysis of 90 pesticides, 16 PAHs, and 22 PCBs in honey using QuEChERS–SPME. Anal. Bioanal. Chem. 2017, 409, 5157–5169, doi:10.1007/s00216-017-0463-y.

31. Fernandes, V.C.; Domingues, V.F.; Mateus, N.; Delerue-Matos, C. Multiresidue pesticides analysis in soils using modified QuEChERS with disposable pipette extraction and dispersive solid-phase extraction. J. Sep. Sci. 2013, 36, 376–382, doi:10.1002/jssc.201200673.

32. Yu, Y.; Liu, X.; He, Z.; Wang, L.; Luo, M.; Peng, Y.; Zhou, Q. Development of a multi-residue method for 58 pesticides in soil using QuEChERS and gas chromatography-tandem mass spectrometry. Anal. Methods 2016, 8, 2463–2470, doi:10.1039/c6ay00337k.

33. Rouvire, F.; Buleté, A.; Cren-Olivé, C.; Arnaudguilhem, C. Multiresidue analysis of aromatic organochlorines in soil by gas chromatography-mass spectrometry and QuEChERS extraction based on water/dichloromethane partitioning. Comparison with accelerated solvent extraction. Talanta 2012, 93, 336–344, doi:10.1016/j.talanta.2012.02.048.

34. Robert Baudot, L.W. Comparison of Two Analytical Methods for the Determination of Traces of Veterinary Antibiotics and Steroid Hormones in Soil Based on Pressurised Liquid Extraction (PLE) and Quick, Easy, Cheap, Effective, Rugged, Safe (Modified-Quechers) Extraction. Pharm. Anal. Acta 2014, 05, doi:10.4172/2153-2435.1000315.

35. De Mastro, F.; Cocozza, C.; Traversa, A.; Cacace, C.; Mottola, F.; Mezzina, A.; Brunetti, G. Validation of a modified QuEChERS method for the extraction of multiple classes of pharmaceuticals from soils. Chem. Biol. Technol. Agric. 2022, 9, 1–14, doi:10.1186/s40538-022-00305-3.

36. Lacina, O.; Zachariasova, M.; Urbanova, J.; Vaclavikova, M.; Cajka, T.; Hajslova, J. Critical assessment of extraction methods for the simultaneous determination of pesticide residues and mycotoxins in fruits, cereals, spices and oil seeds employing ultra-high performance liquid chromatography-tandem mass spectrometry. J. Chromatogr. A 2012, 1262, 8–18, doi:10.1016/j.chroma.2012.08.097.

37. Walorczyk, S. Development of a multi-residue screening method for the determination of pesticides in cereals and dry animal feed using gas chromatography-triple quadrupole tandem mass spectrometry. J. Chromatogr. A 2007, 1165, 200–212, doi:10.1016/j.chroma.2007.07.071.

38. Cajka, T.; Sandy, C.; Bachanova, V.; Drabova, L.; Kalachova, K.; Pulkrabova, J.; Hajslova, J. Streamlining sample preparation and gas chromatography-tandem mass spectrometry analysis of multiple pesticide residues in tea. Anal. Chim. Acta 2012, 743, 51–60, doi:10.1016/j.aca.2012.06.051.

39. Salama, G.; Gindy, A. El; Hameed, E.A.A. The use of experimental design for optimisation of QuEChERS extraction of commonly used pesticides in Egyptian soil and drainage water and their determination by GC/MS. Int. J. Environ. Anal. Chem. 2022, 102, 4238–4249, doi:10.1080/03067319.2020.1781837.

40. SALIMIASL, S.M.; KHODAYAR, M.J.; MOUSAVI, Z.; AKHGARI, M. Comparison of the Modified QuEChERS Method and the Conventional Method of Extraction in Forensic Medicine to Detect Methadone in Post-Mortem Urine by GCMS. Asia Pacific J. Med. Toxicol. 2017, 6, 81–87.

41. Zhang, C.; Deng, Y.; Zheng, J.; Zhang, Y.; Yang, L.; Liao, C.; Su, L.; Zhou, Y.; Gong, D.; Chen, L.; et al. The application of the QuEChERS methodology in the determination of antibiotics in food: A review. TrAC - Trends Anal. Chem. 2019, 118, 517–537, doi:10.1016/j.trac.2019.06.012.

42. Szostek, B.; Tinklenberg, J.A.; Aldstadt, J.H. A simple method for the quantitative microextraction of polychlorinated biphenyls from soils and sediments. Chemosphere 1999, 38, 3131–3139, doi:10.1016/S0045-6535(98)00519-0.

43. Pajewska-Szmyt, M.; Sinkiewicz-Darol, E.; Bernatowicz-Łojko, U.; Kowalkowski, T.; Gadzała-Kopciuch, R.; Buszewski, B. QuEChERS extraction coupled to GC-MS for a fast determination of polychlorinated biphenyls in breast milk from Polish women. Environ. Sci. Pollut. Res. 2019, 26, 30988–30999, doi:10.1007/s11356-019-06201-y.

44. He, Z.; Wang, L.; Peng, Y.; Luo, M.; Wang, W.; Liu, X. Determination of selected polychlorinated biphenyls in soil and earthworm (Eisenia fetida) using a QuEChERS-based method and gas chromatography with tandem MS. J. Sep. Sci. 2015, 38, 3766–3773, doi:https://doi.org/10.1002/jssc.201500624.

45. Núñez, M.; Borrull, F.; Pocurull, E.; Fontanals, N. Sample treatment for the determination of emerging organic contaminants in aquatic organisms. TrAC - Trends Anal. Chem. 2017, 97, 136–145, doi:10.1016/j.trac.2017.09.007.

46. Al-Thaiban, H.; Al-Tamimi, N.; Helaleh, M. Development of QuEChERS method for the determination of polycyclic aromatic hydrocarbons in smoked meat products using GC-MS from Qatar. J. Anal. Methods Chem. 2018, 2018, doi:10.1155/2018/9206237.

47. Vera, J.; Correia-Sá, L.; Paíga, P.; Bragança, I.; Fernandes, V.C.; Domingues, V.F.; Delerue-Matos, C. QuEChERS and soil analysis. An Overview. Sample Prep. 2014, 1, doi:10.2478/sampre-2013-0006.

48. Hvězdová, M.; Kosubová, P.; Košíková, M.; Scherr, K.E.; Šimek, Z.; Brodský, L.; Šudoma, M.; Škulcová, L.; Sáňka, M.; Svobodová, M.; et al. Currently and recently used pesticides in Central European arable soils. Sci. Total Environ. 2018, 613–614, 361–370, doi:10.1016/j.scitotenv.2017.09.049.

49. Kouzayha, A.; Al Iskandarani, M.; Mokh, S.; Rabaa, A.R.; Budzinski, H.; Jaber, F. Optimization of a solid-phase extraction method using centrifugation for the determination of 16 polycyclic aromatic hydrocarbons in water. J. Agric. Food Chem. 2011, 59, 7592–7600, doi:10.1021/jf200123v.

50. Farajzadeh, M.A.; Sohrabi, H.; Mohebbi, A. Combination of Modified QuEChERS Extraction Method and Dispersive Liquid–Liquid Microextraction as an Efficient Sample Preparation Approach for Extraction and Preconcentration of Pesticides from Fruit and Vegetable Samples. Food Anal. Methods 2019, 12, 534–543, doi:10.1007/s12161-018-1384-x.

51. Łozowicka, B.; Rutkowska, E.; Jankowska, M. Influence of QuEChERS modifications on recovery and matrix effect during the multi-residue pesticide analysis in soil by GC/MS/MS and GC/ECD/NPD. Environ. Sci. Pollut. Res. 2017, 24, 7124–7138, doi:10.1007/s11356-016-8334-1.

52. Arias, J.L. de O.; Rombaldi, C.; Caldas, S.S.; Primel, E.G. Alternative sorbents for the dispersive solid-phase extraction step in quick, easy, cheap, effective, rugged and safe method for extraction of pesticides from rice paddy soils with determination by liquid chromatography tandem mass spectrometry. J. Chromatogr. A 2014, 1360, 66–75, doi:10.1016/j.chroma.2014.07.082.

53. Cabrera, L.D.C.; Caldas, S.S.; Prestes, O.D.; Primel, E.G.; Zanella, R. Evaluation of alternative sorbents for dispersive solid-phase extraction clean-up in the QuEChERS method for the determination of pesticide residues in rice by liquid chromatography with tandem mass spectrometry. J. Sep. Sci. 2016, 39, 1945–1954, doi:10.1002/jssc.201501204.

54. Shi, J.-W.; Zhao, Y.-G.; Fu, Z.-J.; Li, J.-G.; Wang, Y.-F.; Yang, T.-C. Development of a Screening Method for the Determination of PCBs in Water Using QuEChERS Extraction and Gas Chromatography–Triple Quadrupole Mass Spectrometry. Anal. Sci. 2012, 28, 167.

55. Han, L.; Sapozhnikova, Y.; Lehotay, S.J. Streamlined sample cleanup using combined dispersive solid-phase extraction and in-vial filtration for analysis of pesticides and environmental pollutants in shrimp. Anal. Chim. Acta 2014, 827, 40–46.

56. Ben Salem, F.; Ben Said, O.; Duran, R.; Monperrus, M. Validation of an adapted QuEChERS method for the simultaneous analysis of polycyclic aromatic hydrocarbons, polychlorinated biphenyls and organochlorine pesticides in sediment by gas chromatography–mass spectrometry. Bull. Environ. Contam. Toxicol. 2016, 96, 678–684.

57. Potter, D.W.; Pawliszyn, J. Rapid Determination of Polyaromatic Hydrocarbons and Polychlorinated Biphenyls in Water Using Solid-Phase Microextraction and GC/MS. Environ. Sci. Technol. **1994**, 28, 298–305, doi:10.1021/es00051a017.

58. Gilgenast, E.; Boczkaj, G.; Przyjazny, A.; Kamiński, M. Sample preparation procedure for the determination of polycyclic aromatic hydrocarbons in petroleum vacuum residue and bitumen. Anal. Bioanal. Chem. **2011**, 401, 1059–1069, doi:10.1007/s00216-011-5134-9.

Appendix

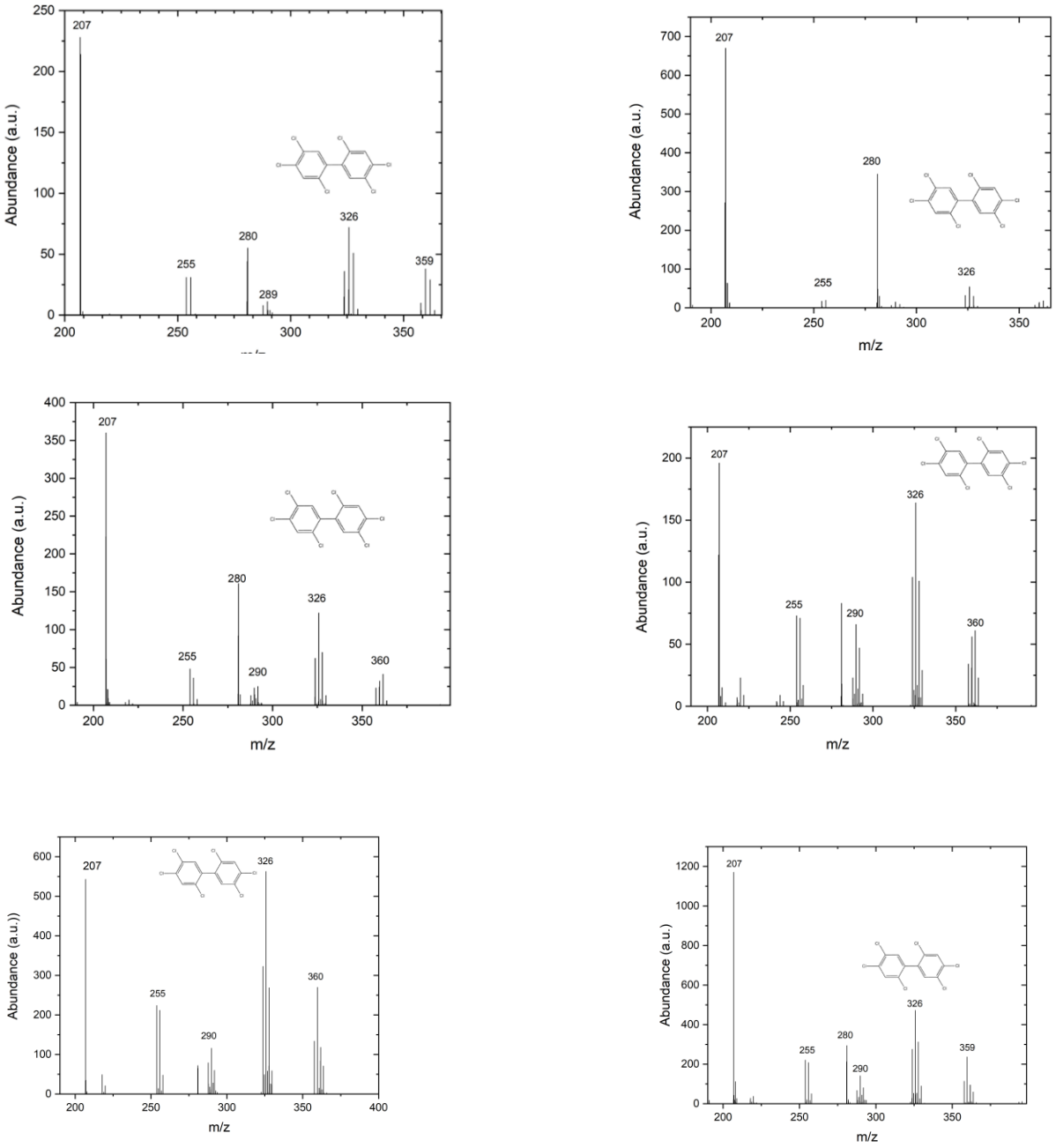


Figure 1.A: The example of mass spectrum of the polychlorinated biphenyls (PCBs) the isotope distributions are identifiable in spectra, around m/z 326.

CHAPTER 6

General conclusions and suggestions for future work

6.1. Conclusion

Concern for environmental pollution of PCBs has led to the development of new technologies to find better solutions to monitor this problem more effectively. The mixture of PCBs usually forms in similar molecules, which make it difficult to detect. Extensive research has been performed in the areas of PCBs extraction, separation, and specific detection.

For the last few decades, researchers have made progress with various techniques of detection, depending on the properties of the substances to be measured, such as the level of concentration, physicochemical properties, etc. They are mainly focused on analytical based chromatographic methods, either gas or liquid chromatography, in combination with different detectors, namely flame ionisation, electron capture, mass spectrometry, fluorescence and UV spectrophotometry, however, these techniques rely on expensive laboratory-based instrument with often additional extra cost needed to perform the analysis. Also, they are not suited to in-field measurements and online Soil monitoring.

Another proposed alternative for PCBs determination in soil monitoring is by using an immunoassay technique, which is designed to detect specific chemicals by measuring chemicals response to specific antibodies. This technique has been widely used in the field of clinical science. Recent development however has seen it is application extended to areas such as food science, health screening, determination of pollutants in the environment and for illicit drug detection. in comparison with other immunoassay

detection methods, electrochemical enzyme immunoassay offers the advantages of sensitivity and low detection limit. Moreover, this technique introduced the miniaturised device that allows for simple and low-cost instrumentation with only small sample volume required.

In this thesis, we have developed a novel electrochemical immunosensor based on screen-printed gold electrodes as an analytical tool for the analysis and monitoring of PCBs in environmental applications. An integrated electrode of a three-electrode system consisting of gold as the working electrode, gold as the counter electrode and an Ag/AgCl reference electrode was utilized. This system provides fast response times, on field measurement and requires only small volumes of sample. Modification of the gold electrode surface could enhance the binding of the antigen to an antibody, thus improving the sensitivity of the sensor towards PCBs. Analysis on real sample was conducted using this immunosensor format. optimisation studies on different assay components were conducted in order to achieve the optimal concentration and conditions for a maximum antibody-antigen binding.

The purpose of this thesis is to present, for the first time to our knowledge, the development of a novel electrochemical immunosensor based on self-assembled monolayer SAMs for enhanced sensitivity in the detection of PCBs in environmental samples. An important aspect in a biosensor development is to attach the biological elements to the surface of the sensor. in order to enhance the sensitivity of the developed biosensors, the gold working electrode was modified with the 11-MUA SAM. Activation of water soluble carbodiimide was performed using EDC and NHS before the protein immobilisation. The performance of 11-MUA SAM in ethanolic solution has been demonstrated as a result to improve the binding of the protein towards the gold surface for the detection of Aroclor 1254 in the soil samples. Characterisation of the SAM formation on the gold electrode was performed using cyclic Voltammetry (CV), electrochemical impedance spectroscopy (EIS) and contact angle measurement. Impedance measurements were carried out at a potential of +0.21 V versus Ag/AgCl with 0.1 V amplitude, in the frequency range of 0.1 Hz to 1 MHz. The results confirmed that with the presence of SAM on the gold electrode, the binding of antibodies to the surface was improved and thus sensitivity of the sensor increased. the detection limit of the modified gold electrode using voltammetric measurement was found at 0.09 ng/ml and was more sensitive compared to unmodified bare gold electrode with 0.20 ng/ml, which increased in 3-folds sensitivity. As a result of this chapter, we have been able to answer the key research question, can we provide a robust method that is easily adopted for on-site analysis? Yes, we have done this by developing our method. Also, can we improve the limit of detection and the sensitivity for the detection of PCBs in soil? Yes, we have

done this by modifying the electrode. The sensitivity increased and the limit of detection decreased as described above.

To simplify the assay procedure and reduce overall costs and time, in this research we developed a label-free immunosensor solution for PCB determination. Additionally, it increases sensitivity and allows for real-time monitoring. The similar modification and method we used previously but without label. indirect competitive electrochemical immunosensor was first developed with a PCB-BSA conjugate. It has been successfully immobilized on an 11-mercaptoundecanoic acid (11-MUA)-modified gold electrode via a carbodiimide-coupling reaction using cross-linking 1-ethyl-3-(3-dimethylaminopropyl) carbodiimide (EDC) and N-hydroxy succinimide (NHS) on the electrode surface. The immunosensor was investigated by cyclic voltammetry (CV), impedance spectroscopy (EIS) and differential pulse voltammetry (DPV) in a standard solution of $[Fe(CN)6]^{3-/4-}$. A linear range was 0.011–220 ng/mL for both (DPV) and (EIS) and a limit of detection (LOD) of 0.11 ng/ml and 0.91 ng/ml for PCBs detection were achieved by the developed immunosensor respectively. The proposed immunosensor has good sensitivity, stability and it can prove to be an adequate real-time monitoring solution for PCBs in soil samples or other samples. Using label-free method would also reduce the steps required for immunoassay testing in the field. As a result of this chapter, we were able to answer our key research question about is it possible to develop a portable electrochemical immunosensor for the detection of PCBs in the environment on-site? A potential future application of this method is the ability to integrate it into portable devices.

In the future, this immunosensor could be incorporated into a portable device to perform measurements in the field in real time. Hence, incorporating an organic-pollutant-monitoring platform into portable lab-on-a-chip technology would be a useful way to avoid costly and inefficient sample analysis in specialized laboratories.

To validate the developed immunosensor, chromatographic techniques-based, gas chromatography-mass spectrometry was performed for detection of PCBs in real Soil samples. Chromatographic technique is one of the promising traditional techniques for determination of PCBs in various sample matrices. Using GC-MS, a low detection limit was achieved for (Aroclor 1254) (1.9) ng/ml. Beside the validation we developed here the extraction method by using the QuEChERS (quick, easy, cheap, effective, rugged, and safe) method, and we found it more effectively for PCBs extracted from soil. Different related parameters were compared and optimized. As the extraction solvent, acetonitrile/water produced the best results, and as the dispersive solid-phase extraction sorbent, diatomaceous earth produced the best results. Procedures allowed recovery values between 95.3% and 103.2%. It was demonstrated that the method was simple, sensitive, efficient, and environmentally friendly when applied to soil samples.

6.2. Future work

This thesis developed a novel electrochemical immunosensor based on self-assembled monolayers. In future work, it may be possible to study how the assays developed in this thesis can be integrated into a lab-on-chip system. The following sections discuss different approaches.

One of the first potential areas for future study is sensor fabrication can be improved, using a novel material, such as nanomaterials, graphene, or quantum dots. These materials offer improved sensitivity, selectivity, and stability. These advanced materials can be incorporated into sensor structures to enhance their performance and enable detection of analytes at lower concentrations as shown in figure 6.1 [2][3].

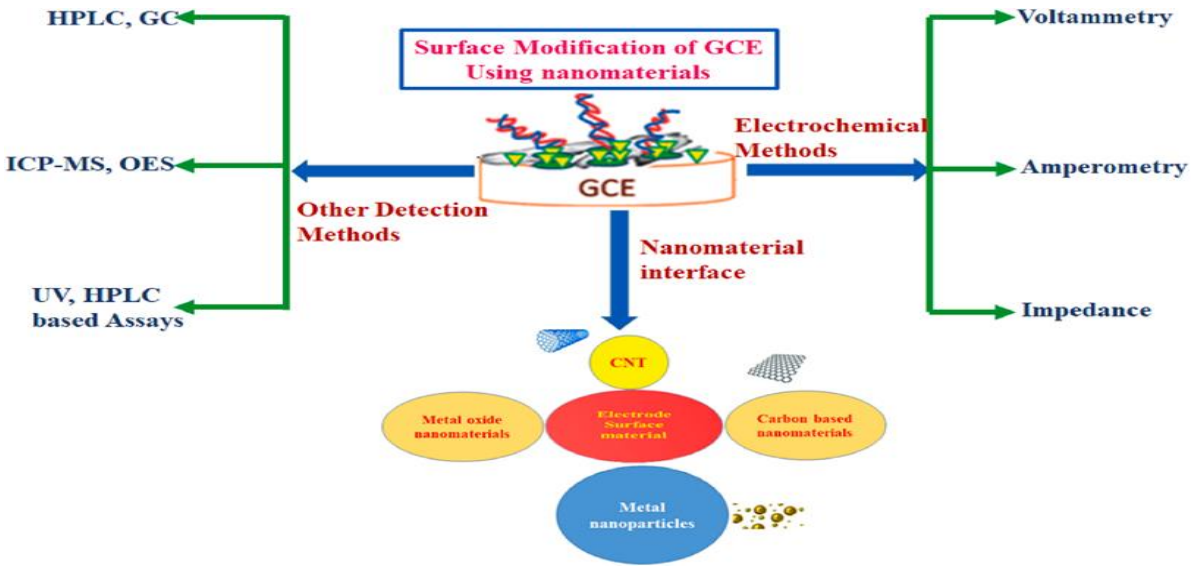


Figure 6.1 Schematic view of analytical methods over various electrochemical methods for SMX detection towards nanomaterial interfacial aspects [4].

Another potential area could be improved instead of use antibodies as biorecognition elements in electrochemical immunosensors, exploration of new biorecognition elements such as aptamers, peptides, and proteins could provide better specificity and sensitivity[5][6]. By doing so, both time and expenditure can be reduced.

Another area of improvement lies in manufacturing techniques advancement. Techniques like additive manufacturing (3D printing) and micro/nanofabrication technologies allow for the production of complex sensor structures with high precision and miniaturization. These techniques enable the integration of multiple sensing elements, increase sensor functionality, and reduce fabrication costs [7][8].

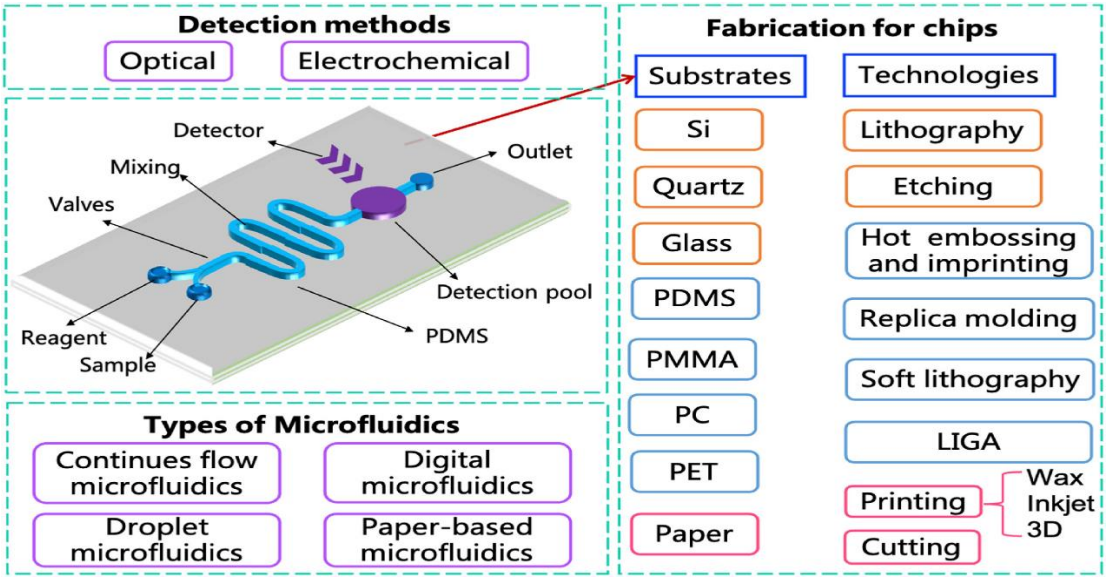


Figure 6.2 Summary of microfluidics, such as substrates materials, fabrication technologies, detection method and types of microfluidics [7].

Furthermore, the integration of electrochemical immunosensors with smartphone technology can make the method more accessible and user-friendly[9][10].Since smartphones already contain the technology required to analyze and communicate results, they are an excellent option for portable electrochemical analyses. A customized attachment is then added to the phone so that electrochemical detection can be performed [11]. Future research could focus on developing electrochemical immunosensors that can be connected to smartphones and provide real-time measurements and analysis.

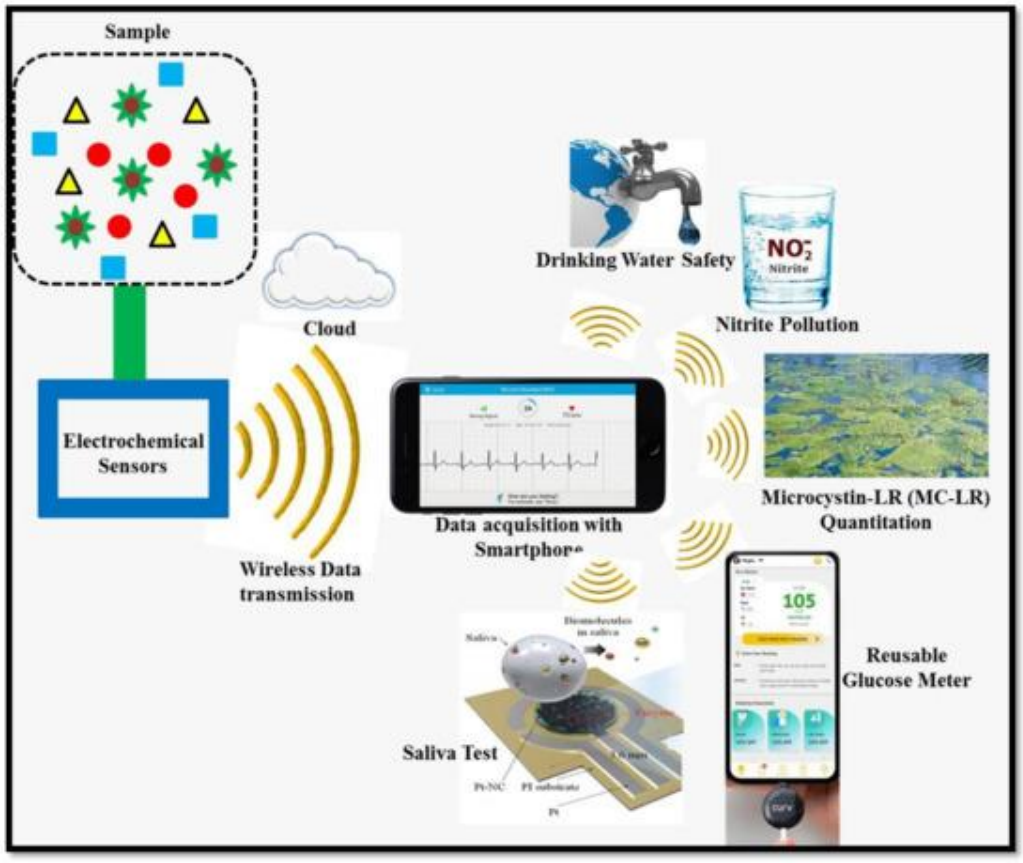


Figure 6.3 Applications of smartphone-based wireless electrochemical sensors.

The development of electrochemical biosensors based on such small chips could provide a number of advantages over conventional devices in terms of analytical performance; however, their greatest advantage would be their ability to work with small volumes of biomolecules and small volumes of sample, both of which could prove to be critical. Moreover, the miniaturization of the three-electrode system on a chip provides a platform with a dedicated connector that is easy to use.

In addition, the integration of the immunosensors to a micro fluidic platform using online voltammetric measurements or similar electrochemical approaches capable of controlling sample and substrate movement will progress the work further towards becoming a commercial product and promise to be an important area of research in years to come.

6.3 References

1. Přibyl, J.; Hepel, M.; Skládal, P. Piezoelectric immunosensors for polychlorinated biphenyls operating in aqueous and organic phases. *Sensors Actuators B* **2006**, *113*, 900–910, doi:10.1016/j.snb.2005.03.077.

2. Iftikhar, T.; Asif, M.; Aziz, A.; Ashraf, G.; Jun, S.; Li, G.; Liu, H. Topical advances in nanomaterials based electrochemical sensors for resorcinol detection. *Trends Environ. Anal. Chem.* **2021**, *31*, e00138, doi:https://doi.org/10.1016/j.teac.2021.e00138.

3. Tajik, S.; Orooji, Y.; Ghazanfari, Z.; Karimi, F.; Beitollahi, H.; Varma, R.S.; Jang, H.W.; Shokouhimehr, M. Nanomaterials modified electrodes for electrochemical detection of Sudan I in food. *J. Food Meas. Charact.* **2021**, *15*, 3837–3852, doi:10.1007/s11694-021-00955-1.

4. Padmalaya, G.; Krishna Kumar, K.; Senthil Kumar, P.; Sreeja, B.S.; Bose, S. A recent advancement on nanomaterials for electrochemical sensing of sulfamethaoxole and its futuristic approach. *Chemosphere* **2022**, *290*, 133115, doi:https://doi.org/10.1016/j.chemosphere.2021.133115.

5. Oberhaus, F. V.; Frense, D.; Beckmann, D. Immobilization techniques for aptamers on gold electrodes for the electrochemical detection of proteins: A review. *Biosensors* **2020**, *10*, doi:10.3390/BIOS10050045.

6. Nan, M.-N.; Bi, Y.; Xue, H.-L.; Long, H.-T.; Xue, S.-L.; Pu, L.-M.; Prusky, D.

Modification performance and electrochemical characteristics of different groups of modified aptamers applied for label-free electrochemical impedimetric sensors. *Food Chem.* **2021**, *337*, 127761, doi:https://doi.org/10.1016/j.foodchem.2020.127761.

7. Li, Z.; Liu, H.; Wang, D.; Zhang, M.; Yang, Y.; Ren, T. Recent advances in microfluidic sensors for nutrients detection in water. *TrAC Trends Anal. Chem.* **2023**, *158*, 116790, doi:https://doi.org/10.1016/j.trac.2022.116790.

8. Didier, C.M.; Kundu, A.; Deroo, D.; Rajaraman, S. Development of in vitro 2D and 3D microelectrode arrays and their role in advancing biomedical research. *J. Micromechanics Microengineering* **2020**, *30*, doi:10.1088/1361-6439/ab8e91.

9. Kholafazad-Kordasht, H.; Hasanzadeh, M.; Seidi, F. Smartphone based immunosensors as next generation of healthcare tools: Technical and analytical overview towards improvement of personalized medicine. *TrAC Trends Anal. Chem.* **2021**, *145*, 116455.

10. Umapathi, R.; Ghoreishian, S.M.; Sonwal, S.; Rani, G.M.; Huh, Y.S. Portable electrochemical sensing methodologies for on-site detection of pesticide residues in fruits and vegetables. *Coord. Chem. Rev.* **2022**, *453*, 214305.

11. Kishore, S.C.; Samikannu, K.; Atchudan, R.; Perumal, S.; Immanuel Edison, T.N.J.; Alagan, M.; Sundramoorthy, A.K.; Lee, Y.R. Smartphone-Operated Wireless Chemical Sensors: A Review. *Chemosensors* **2022**, *10*, 1–22, doi:10.3390/chemosensors10020055.

Appendix A

A.1 Awards

1. Bronze awardee of the 2022 School of Chemistry Postgraduate Research Publication Prize.

A.2 Publications

1. **Alsefri, S.;** Balbaied, T.; Moore, E. Electrochemical Development of an Immunosensor for Detection Polychlorinated biphenyls (PCBs) for Environmental Analysis. **2021**, doi:10.3390/chemosensors9110307.

2. **Alsefri, S.;** Balbaied, T.; Albalawi, I.; Alatawi, H.; Moore, E. A Novel Label-Free Electrochemical Immunosensor Based on a Self-Assembled Monolayer-Modified Electrode for Polychlorinated Biphenyl (PCB) in Environmental Analysis. *Electrochem* **2022**, *3*, 451–462, doi:10.3390/electrochem3030031.

3. **Alsefri, S.;** Balbaied, T.; Alatawi, H.; Albalawi, I.; Hogan, A.; Moore, E. Development of the QuEChERS Extraction Method for the Determination of Polychlorinated Biphenyls (Aroclor 1254) in Soil Samples by Using GC-MS. *Separations* **2023**, *10*, 250.

4. **Alsefri, S.;** Balbaied, T.; Moore, E. The development of optical immunosensors based on indirect competitive enzyme-linked immunosorbent assay methods for

detection of Aroclor1254 in environmental samples. **Under review 2023**, for publication in journal of the Royal Society of Chemistry.

5. Albalawi, I.; Alatawi, H.; **Alsefri, S.**; Moore, E. Electrochemical Synthesis of Reduced Graphene Oxide/Gold Nanoparticles in a Single Step for Carbaryl Detection in Water. *Sensors* **2022**, *22*, 5251.

6. Alatawi, H.; Hogan, A.; Albalawi, I.; O'Sullivan-Carroll, E.; **Alsefri, S.;** Wang, Y.; Moore, E. Rapid determination of NSAIDs by capillary and microchip electrophoresis with capacitively coupled contactless conductivity detection in wastewater. *Electrophoresis* **2022**, *43*, 1944–1952.

7. Albalawi, I.; Hogan, A.; Alatawi, H.; **Alsefri, S**.; Moore, E. A novel comparative study for simultaneous determination of Cd (II) and Pb (II) based on ruthenium complex-nanoparticles-nafion modified screen-printed gold electrode. *Sensors Actuators B Chem.* **2023**, *380*, 133273, doi:10.1016/j.snb.2022.133273.

8. Alatawi, H.; Hogan, A.; Albalawi, I.; **Alsefri, S.;** Moore, E. Efficient determination of non-steroidal anti-inflammatory drugs by micellar electrokinetic chromatography in wastewater. *Anal. Methods* **2023**, *15*, 1402–1409.

A.3 Oral Presentation

- All Hazards Forensics Conference – 27th – 28th November ,2018 (University College Cork) (Attendee).

- LSI day, Tyndall, cork 2020 (Tyndall National Institute – Cork).

- Environ 2021 - 31st Annual Irish Environmental Researchers Colloquium (University College Cork).
- School of chemistry postgraduate research day ,2021 (University College Cork).
- Analytical research forum ARF 2022 (Royal Society of Chemistry – London -UK).
- Environ 2022, Jointly hosted by Environmental Sciences Association of Ireland & Ulster University (Belfast).
- 74th Irish Universities Chemistry Research Colloquium (University of Galway) (2023).

A.4 Poster Presentation

- School of Chemistry Postgraduate Research Day 2019 (University College Cork)
- ISE Satellite Student Regional Symposium on Electrochemistry (Trinity College Dublin) (2019)
- Environ 2020, 30th Irish Environmental Researchers Colloquium (Dublin City University)
- SCI Electrochemistry Conference 2021 (University of Manchester)
- Analytical research forum ARF21.2021 ((Royal Society of Chemistry – London - UK)

A.5 Dissemination Activities

- Schools Analyst Competition May 2019
- Cork Carnival of Science, Cork, Ireland, 2019
- Demonstration for undergraduate & master's degree (S1/S2) 2019
- 4 outreaches at Tyndall 2019
- Demonstration for Final Year Chemistry Student Projects,2020
- Demonstration for undergraduate & master's degree (S1/S2) 2021
- Cork Carnival of Science, Cork, Ireland, 2022
- Demonstration for Final Year Forensic Student Projects,2022
- Primary Science Quiz 2022
- Demonstration for undergraduate & master's degree (S1/S2) 2022

A.6 Modules

- PG6001 - STEPS Scientific Training for Enhanced PG Studies (2019)
- PG6009 - Graduate Information Literacy Skills (2019)
- CM6007- Teaching & demonstrating skills (2019)
- ST6013 - Statistics and Data Analysis for Postgraduate (2019)

A.7 Workshops

- How to Plan Your PhD, 21 Feb 2019, Brookfield Health Science building, UCC, Cork, Ireland. This workshop helped me a lot in planning my PhD project. It gave me an idea how to set daily, monthly, and mid-term objectives to meet the annual aims.

- The Seven Secrets of Highly Successful Research Students,21 Feb 2019, Brookfield Health Science building, UCC, Cork, Ireland. This workshop clarified the steps of presenting the lab report to a publishingpaper.

- Presenting your Research with Confidence ,,22 Feb 2019, Brookfield Health Science building, UCC, Cork, Ireland. This workshop clarified the steps of presenting the lab report to a publishingpaper.

- PhD Workshop: Turbocharge your writing and scientific writing ,22nd Feb 2019, Brookfield Health Science building, UCC, Cork, Ireland. This workshop let me recognise the small details in writing my PhD thesis.

- webinar about electrochemical, enzymatic biosensors, palmsens (Amsterdam, Netherlands) (2019).

chemosensors

MDPI

Article

Electrochemical Development of an Immunosensor for Detection Polychlorinated biphenyls (PCBs) for Environmental Analysis

Samia Alsefri, Thanih Balbaied and Eric Moore *

Sensing & Separation Group, School of Chemistry and Life Science Interface, Tyndall National Institute, University College Cork, T12R5CP Cork, Ireland; 112220405@umail.ucc.ie (S.A.); thanih.balbaied@tyndall.ie (T.B.)
* Correspondence: e.moore@ucc.ie

Abstract: Polychlorinated biphenyls (PCBs) are a highly toxic family of synthetic chemical compounds. PCBs are widely spread in the environment and their toxicity can cause serious ailments to living organisms such as cancer; therefore, developing a device for the detection of PCBs in the environment is significant. In this paper, polyclonal primary anti-PCB antibodies were immobilized onto a gold screen-printed electrode with the purpose of creating an electrochemical immunosensor for the detection of Aroclor 1254. It was modified with 11-mercaptoundecanoic acid (11-MUA) and the activation of the carboxylic acid terminal was performed by cross-linking 1-ethyl-3-(3-dimethylaminopropyl) carbodiimide (EDC) and N-hyrodsuccinmide (NHS) on the electrode surface. Cyclic voltammetry, electrochemical impedance spectroscopy (EIS), linear sweep voltammetry, atomic force microscopy (AFM), scanning electron microscopy (SEM), and contact angle measurement were employed to characterize SAM development on the gold electrode. Using a competitive assay, a 0.09 ng/mL^{-1} limit of detection and a linear range of 0.101–220 ng/mL^{-1} were determined. The self-assembled monolayers (SAM) were successful in encapsulating the PCBs on the immunosensor. The electrochemical detection showed better resolution when compared to traditional methods such as the ELISA optical technique. The novel electrochemical immunosensor approach that is discussed in this paper has the potential to offer rapid sample screening in a portable, disposable format and could contribute to the effective control and prevention of PCBs in the environment.

Keywords: polychlorinated biphenyls; disposable screen-printed gold electrode; linear sweep voltammetry; immunosensors; immunoassays; self-assembled monolayers

check for updates

Citation: Alsefri, S.; Balbaied, T.; Moore, E. Electrochemical Development of an Immunosensor for Detection Polychlorinated biphenyls (PCBs) for Environmental Analysis. *Chemosensors* **2021**, *9*, 307. https://doi.org/10.3390/chemosensors9110307

Academic Editor: Mehmet Senel

Received: 13 September 2021
Accepted: 25 October 2021
Published: 28 October 2021

Publisher's Note: MDPI stays neutral with regard to jurisdictional claims in published maps and institutional affiliations.

Copyright: © 2021 by the authors. Licensee MDPI, Basel, Switzerland. This article is an open access article distributed under the terms and conditions of the Creative Commons Attribution (CC BY) license (https://creativecommons.org/licenses/by/4.0/).

1. Introduction

Polychlorinated biphenyls (PCBs) are a family of artificial organic compounds with two to ten chlorine atoms attached to the biphenyl [1,2]. Since 1929, PCBs have been commercially manufactured under the trade name Aroclor. Aroclor consists of a combination of chlorinated biphenyls, including over 100 different unique PCBs. Congeners are defined and numbered according to the total amount of chlorine in the mixture [3]. Aroclor 1254 ($C1_2H_5Cl_5$) is one of the commercial products, and it is a viscous, light-yellow liquid with an average molecular weight of 328, containing approximately 21% $C1_2H_6Cl_4$, 48% $C1_2H_5Cl_5$, 23% $C1_2H_4Cl_6$, and 6% $C1_2H_3Cl_7$ with an average chlorine content of 54% [4]. Figure 1 shows the structure of Arcolor 1254.

These compounds have been used as plasticizers, surface coatings, inks, additives for insulating liquids, pesticides, and lubricants [5,6], all of which have contaminated the environment. Further contamination may result from the disposal of obsolete electrical equipment containing PCBs, as well as leaks from industrial sites. Furthermore, PCBs have significant teratogenic, carcinogenic, and mutagenic impacts on the human body. PCBs are persistent in the environment and until today a large proportion of PCBs are still present in old transformers and power capacitors, which have the potential to be released into the environment. PCB congeners also enhance the degree of structural uniformity and

chlorination increases. Lastly, the PCBs high stability and lipophilicity nature resulted in them being widely distributed in the world ecosystem. PCBs occur in all environments matrixes and can be found in a variety of environmental media (water, atmosphere, soil, sediment, and creatures) [7–10]. These chemicals have become a significant danger to the environment and the health and safety of humans. All of these facts make the development of an effective and economical testing method for PCBs very important [11,12].

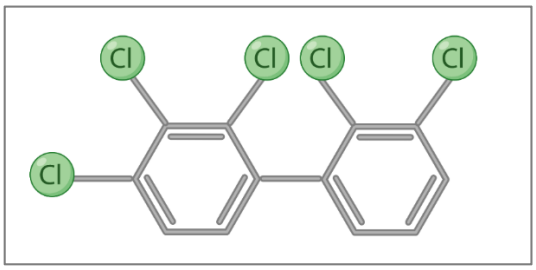


Figure 1. Structure of Arcolor 1254.

The methods used to determine PCBs so far are: tandem mass spectrometry [13,14], bioanalytical techniques [15], and spectral analysis [16]. These methods, although sensitive, are generally time-consuming and expensive and typically require sample preparation before the chromatographic separation [17,18]. On the other hand, electrochemical techniques have been utilized in a variety of prospective applications and environmental research due to their relative advantages, such as low costs, easy operation, and fast response.

Only a few papers have been published to date that are based on electrochemical immunosensors for PCBs [19,20]. All of these have used modified materials to enhance the immobilization of antibodies, such as nanoparticles [19,21–23], self-assembled monolayers (SAM), including [24,25] cysteamine [26] and 11-mercaptoundecanoic acid (11-MUA) [24].

SAM is typically formed by activating the carboxylic acid groups with [1-ethyl-3-(3-dimethylaminopropyl) carbodiimide] (EDC) in conjunction with N-hydroxy succinimide (NHS) before protein immobilization through the use of an alkylthiol reaction [27]. This reaction decreases the random orientation of the antibodies that bind the surface proteins to the carboxylic acid end-groups enhancing the immunosensor sensitivity and selectivity [24,28]. Research has shown that SAM forms better on a gold surface [29–31] as the gold strongly absorbs the protein molecules and creates a hydrophobic interaction through the strong S–Au bonds [32,33]. This facilitates the immobilization of the desired protein on the specific target area and limits non-specific binding [34]. Electrode surfaces provide no sites for covalent bonding, making it necessary to coat a thin film of functional groups to covalently bond with the amino groups of the used antibodies [35]. In this research paper, the anti-PCB were compounded onto the chip (made of the gold sensor) by covalent coupling technique and with the aid of [1-ethyl-3-(3-dimethylamino propyl) carbodiimide] (EDC) in collaboration with NHS N-hydroxy succinimide [36,37]. Figure 2 illustrates the fabrication of an immunosensor in a gold electrode with 11-MUA SAM, as well as its activation by EDC/NHS. The desired protein and antigen are then presented.

The indirect competitive assay using (alkaline phosphate) AP as an enzymatic label was used. A bovine albumin (BSA) conjugate, BSA-PCB was the basis for the PCB immobilization procedure. After the experiment, the amount of anti-PCB that reacted with immobilized PCB was determined using a secondary antibody with alkaline phosphate, labeled *p*-aminophenyl phosphate (*p*APP), which detected the presence of alkaline phosphate. Liner sweep volumetry was used as the electrochemical detection technique. A number of characterization methods were reported including contact angle measurement, cyclic voltammetry, impedance measurement, SEM, and AFM. To the best of our knowledge, this is the first study to investigate the SAM modified on gold electrodes with PCBs compounds. The measurement of the electrochemical detection for the biochip was achieved via detection of the quantity of antibodies that react with the target Aroclor 1254 compound. The assay was then compared with the traditional optical method (ELISA).

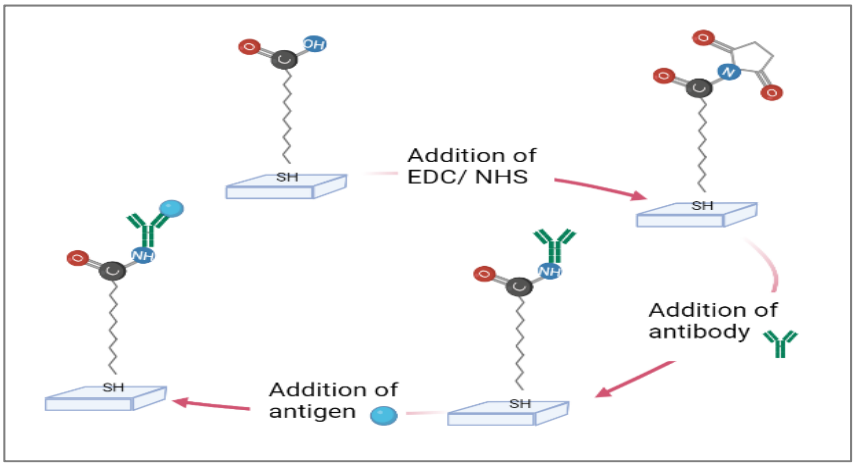


Figure 2. The graphic depicts the synthesis of SAM from 11-MUA on a gold electrode in combination with antibody immobilization. (Note abbreviations were included in Appendix A).

2. Materials and Methods

2.1. Reagents and Chemicals

Polyclonal chicken antibody (IgY) specific to PCB, alkaline phosphatase (AP) labeled goat anti-chicken (IgY) antibodies were bought from GmbH (Heidelberg, Germany). Aroclor 1254 and PCB were bought from (Cole-Parmer Instrument Company Ltd., Eaton Socon, Saint Neots, UK). A total of 2 mg of PCB-BSA conjugate (Aroclor 1254) was bought from (BioTeZ Berlin-Buch GmbH (Heidelberg, Germany)). *p*-nitrophenyl phosphate (*p*NPP) substrate, diethanolamine reagent (DEA) phosphate-buffered saline (PBS), sodium hydrogen carbonate, sodium chloride, Tween-20, tris (hydroxymethyl) aminomethane, potassium chloride (KCl) and bovine serum albumin (BSA) were bought from Sigma (Dublin, Ireland). To adjust pH, hydrochloric acid (HCl) 37%, sodium hydroxide, ammonium hydroxide solution and sodium cyanoborohydride (NaCNBH4) were bought from Sigma (Dublin, Ireland). 11-mercaptoundecanoic acid (11-MUA), 1-ethyl-3-(3-dimethylaminopropyl) carbodiimide (EDC), NHS, potassium ferricyanide ($K_3[Fe(CN)_6]$), potassium ferrocyanide ($K_3[Fe(CN)_6]$), acetone, 1-isopropyl alcohol, ethanol, and alkaline phosphatase (AP) were also bought from Sigma (Dublin, Ireland). For the electrochemical tests, the substrate was *p*-aminophenyl phosphate (*p*APP) salt, which was bought from Sigma (Dublin, Ireland). Disposable electrochemical screen-printed gold electrodes (AuE), model C220 BT, were purchased from (Drop Sens, Asturias, Spain). To ensure optimal detection, a standard 96 well ELISA microplate was bought from Greiner bio-one (Frickenhausen, Germany). All other reagents were analytical grade or higher, with daily buffer solutions made using nanopore water (18.2 mΩ-cm).

2.2. Equipment and Instrumentation

Optical detection was carried out using the EL Read 2000 microplate reader was provided by biochrom.co.UK. Incubation was made possible using a Biometra OV3 Incubator (Gottingen, Germany), which was set at 37 °C. Cyclic voltammetry was recorded using a PalmSens handheld potentiostat (Palm Instrument BV Houten, Houten, The Netherlands). Impedance measurements were performed in a faraday cage with minimal noise using a CHI potentiostat 1100/620B (CH Instruments Inc., Austin, TX, USA). The removal of the surface organic molecules was achieved using a plasma cleaner (Harrick Plasma Ithaca, New York, NY, USA). A nitrogen spray gun facilitated the drying of SPEs between measurements using the Contact Angle Instrument (OCA) by Data Physics Instruments GmbH (Filderstadt, Germany). SEM measurements were carried out on an FEI Quanta 650 Scanning electron microscope (FEI Company, Hillsboro, OR, USA). AFM measurements were carried out using "SCANASYST-AIR" by Bruker AFM Probes (Bruker AFM Probes, Camarillo, CA, USA). Specificity (Cross-Reactivity) obtained using a PalmSens handheld

potentiostat (Palm Instrument BV Houten, Houten, The Netherlands) and Data obtained from Origin Pro 8.5.1 software. Measurements were taken at room temperature between −0.2 and 0.6 V in $[Fe(CN)_6]^{3-/4-}$ and 0.1 M of KCl solution with a scan rate of 50 mV·s^{-1}.

2.3. Modification of Gold SPE with SAM (LSV)

In order to prepare self-assembled monolayers (SAM) on the gold working electrodes, solutions of 5 mM 11-mercaptoundecanoic acid (11-MUA) were separately prepared in absolute ethanol (N2 bubbled for 30 min to eliminate the presence of oxygen) [38–40]. The gold electrodes were immersed in the SAM solution for 20 h at room temperature. Upon removing the biochips from the solution, the electrodes were rinsed thoroughly with absolute ethanol to remove any unbound molecules. They were then dried with N_2. To activate the carboxylic terminal end after SAM formation, the electrodes were immersed in a solution of 50 mM EDC and NHS for 1 h and were rinsed with deionized water and dried with N_2. CVs were carried out in 5 mM $[Fe(CN)_6]^{3-/4-}$ and 0.1 M of KCl solution, and the potential that was applied was in the range (−0.2 to 0.6 V) [34,35]. The scan rate applied was 50 mV·s^{-1}. Figure 3 shows the steps involved in the formation of self-assembled monolayers on the gold electrodes. Immobilization of protein on the gold surface after the activation of EDC/NHS was performed by incubating 5 µg mL^{-1} of BSA-Aroclor 1254 coating conjugate at 37 °C for 1 h.

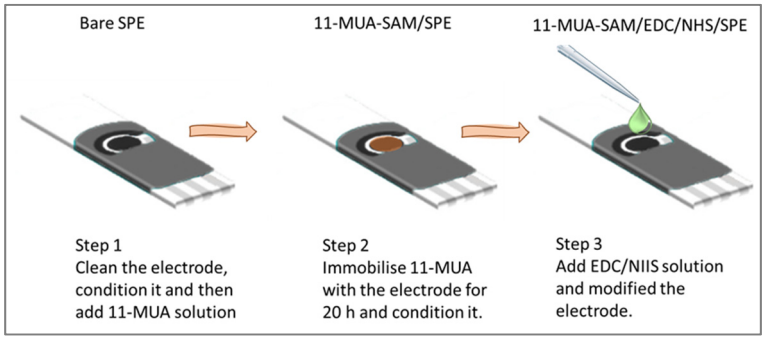


Figure 3. The steps involved in the formation of self-assembled monolayers on the gold electrode.

2.4. Topography Characterization

2.4.1. Contact Angle Measurement

The sessile drop contact angle method was utilized to evaluate the surface hydrophobicity of the SAM substrates. A 1 µL drop of deionized water was supplied to the surface of the gold electrodes at a medium rate of 1 µL per second. Measurements were repeated on each electrode for three drops.

2.4.2. Scanning Electron Microscopy (SEM)

SEM measurements at the surface of the bare gold electrode were observed using a FEI Quanta 650 Scanning electron microscope (SEM). The SEM was coated and imaged at ×100 magnification for clean bare AuE and SAM-modified AuE. These were observed and compared before and after the modification.

2.4.3. Atomic Force Microscopy (AFM)

The experiments were performed using an atomic force microscope (Bruker AFM Probes, Camarillo, CA, USA), which used "scanasyst-Air" as its measurement mode. The force constant of the scanasyst-Air was 2 N/m. The frequency used for the tapping mode was 95 ± 45 kHz with a scan size of 0.5 µm. For the purposes of comparison, three scans were taken per sample. Data acquisition was performed using NanoScope Analysis 1.9 software.

2.5. Electrochemichal Characterization

2.5.1. Stability Study of the Coated Electrodes

A stability study was performed on the coated BSA-Aroclor 1254 coating conjugate on the gold electrodes by immobilizing the electrodes with a few layers of the assay components, which is similar to the steps mentioned in Section 2.6. Using an Indirect Competitive Assay, the gold electrode was coated with 5 μg mL^{-1} of BSA-Aroclor 1254 coating conjugate overnight and kept at a temperature of 4 °C. The next morning the electrodes were washed, dried, and placed in a blocking solution (BSA-tris buffer) for one hour. The electrodes were then rinsed with a washing buffer and nonpure water. The biochips were stored dry at 4 °C for further use. A complete capture assay test was performed on three electrodes daily for 10 days using LSV.

2.5.2. Cyclic Voltammetry (CV)

CV was performed in 0.1 M KCl with a 5 mM ferri/ferrocyanide redox pair with an applied voltage ranging from −0.2 to +0.6 V. The scan rate was set at 0.05 V s^{-1}. In this experiment, screen-printed electrodes (SPEs) were utilized. The gold electrode had a working area of 4 mm. The Ag/AgCl reference electrode was used to refer to all potentials reported in this study.

2.5.3. Impedance Measurement

A frequency response analysis (FRA) was utilized to apply a modest amplitude AC signal to the biochip for impedance measurements. The impedance behavior of the electrode was evaluated by analyzing the AC voltage and current response at frequencies ranging from 0.1 Hz to 1 MHz. The measurements were performed in the presence of a 5 mM redox probe $[Fe(CN)_6]^{3-/4-}$ in 0.1 M KCl at an applied potential of +0.2 V and an amplitude of 0.1 V.

2.5.4. Amperometric Detection

PalmSens (Palm Instrument BV Houten, Houten, The Netherlands). was used to carry out the amperometric detection using a portable potentiostat. Before each measurement, a coating was applied to the chips with layers of a biocomponent assay, which was stored in 14,000 μL DEA buffer with pH 9.5 and at a temperature of 4 °C. The aim of this was to prevent loss of activity of the antibodies. The detection was carried out on the coated electrode using the AP as the labeled enzyme and the *p*APP as the substrate. The measurement was set to 60 s, and the potential was applied at 450 mV versus Ag/AgCl. The measurement of the current was taken to acquire stability in the baseline. At 45 s, 100 μL of *p*APP was injected into the working electrode. The final concentration of the *p*APP in the buffer was 5 μg mL^{-1}. The increase in the current was taken as the data signal for evaluation. As *p*APP is sensitive to light and moisture, the solution was made daily.

2.5.5. Specificity (Cross-Reactivity)

The specificity was determined by testing the cross-reactivity (CR) of the antibody with a variety of Aroclors. The reaction was carried out using liner sweep voltammetry (LSV) by adding these compounds (instead of Aroclor 1254 in the respective assays) at 11 serial dilutions, using the same concentration range (0.01 to 660 ng mL^{-1}) that was used to detect the target (Aroclor 1254). The CR values can be calculated using the following formula:

$$\text{cross} - \text{reactivity}\ (\%) = \frac{\text{IC50 of Aroclor 1254}}{\text{IC50 of other compounds}} \times 100$$

2.6. Indirect Competitive Assay

Indirect competitive assay was applied by ELISA or by linear sweep voltammetry. Immobilization of antibodies was carried out directly on microwell plates or on the clean electrode surface to enhance the maximum signal. The immobilization of biocomponents

was performed on the working electrode and wells. A total of 100 µL or 10 µL of the coating antigen BSA-Aroclor1254 (5 µg mL^{-1}) (pH 7.4) was added to microwell plates or electrode surfaces and incubated overnight at 4 °C. The microwell plates or electrodes surfaces were then washed three times with 0.05 M Tris, pH 7.4 (0.05% Tween 20) and blocked with 1% BSA-Tris Solution (0.05 M Tris-HCI) for 30 min at 37 °C. After incubation, the microwell plates or electrode surface was washed three times to remove any unbound coating conjugate. For the competition step, the serial dilution of Aroclor 1254 PCB was mixed with polyclonal chicken antibody (IgY) specific to PCB with concentrations of 0.465 µg/mL^{-1} or 0.123 µg/mL^{-1} used for ELISA or linear sweep voltammetry. The mixture was left to incubate for 15 min. A volume of 100 or 10 µL was introduced to the microwell plates or electrode surface. The microwell plates and electrode surfaces were allowed to bind for 1 h at 37 °C. To standardize the assay, a 1/5000 dilution of commercially available (AP) labeled goat anti-chicken (IgY) antibodies was prepared, and 100 or 10 µL of the solution was added to the microwell plates or electrode surfaces and allowed to react for 1 h or 30 min at 37 °C. After washing, 100 or 10 µL of the substrate solution *p*NPP or *p*APP diluted in DEA buffer (pH 9.5, 1 mg mL^{-1}) was added to surfaces. The electrochemical substrates were incubated, and measurements were taken using the PalmSens potentiostat.

2.7. Real Sample

The analysis was carried out in a river water sample were collected from River Lee (Cork, Ireland) in April 2020, and the tap water was taken from Kane Building (chemistry department)—UCC (University College Cork). To protect the water samples from contaminants, glass vessels with Teflon caps were used for storage. Immediately after collecting the samples, they were diluted with equal amounts of methanol to prevent losses to the polystyrene tubes or the glass containments. To remove all the suspended materials in the sample, 0.45 µm filter aid materials were used before testing. The water samples used in this experiment contained 50% methanol. the final assay result was multiplied by a factor of 2 [41]. For the highly contaminated samples, those outside the assay's calibration range were further diluted and analyzed.

3. Results

3.1. Topography Characterization

In order to study SAM behavior, a characterization of the monolayer on the gold electrode was carried out using contact angle, SEM and AFM. The contact angle data showed significant variations in hydrophobicity/hydrophilicity when the substrate was modified. The gold immobilized SAM electrode was tested using contact angles for structural information about the modified surface, as shown in Figure 4A,B. SEM and AFM are complementary techniques in assessing SAM formation. SAMs are usually smooth, structurally ordered and chemically defined at the microscopic scale [42]. Therefore, they are ideal for SEM and AFM measurements. Comparisons were made before and after SAM and protein immobilization was performed on the same gold surface. Furthermore, the interaction between SAM and proteins immobilized on the gold electrode was examined. The bare gold and the modified electrode images were taken at ×100 magnification using SEM corresponding to the various stacks, as shown in Figure 4C,D. AFM high-resolution images were taken to measure the roughness of the gold surface electrode during the electrode modification process. This process began with the bare electrode (Figure 4E), then the electrode when 11-MUA was adsorbed (Figure 4F), then the electrode after the activation of EDC/NHS (Figure 4G), and, finally, the electrode after the protein layer of BSA-Aroclor 1254 was formed (Figure 4H).

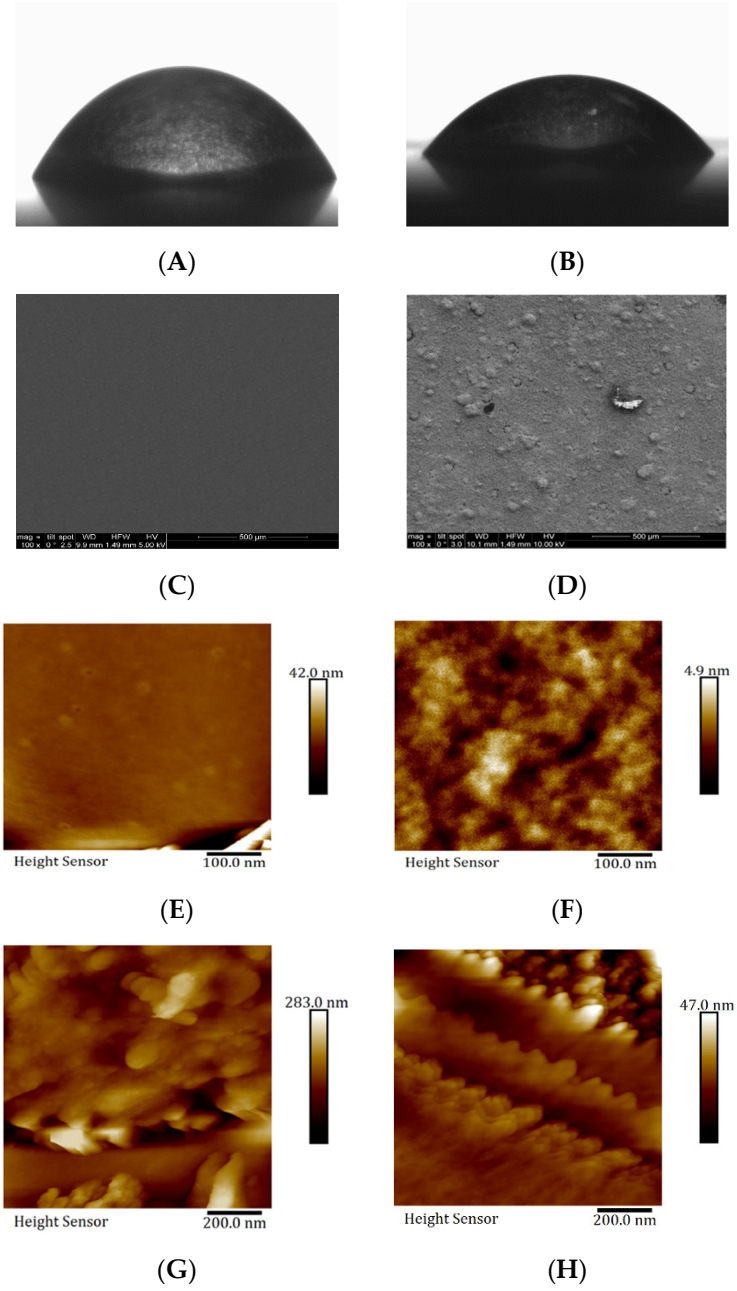


Figure 4. Typical topography of the bare electrode surfaces of gold SPE and modified with SAM. Contact angle graphs of bare electrode (**A**) and SAM-modified electrode (**B**); SEM micrographs of bare electrode (**C**) and 11MUA-SAM-modified electrode (**D**); top cross-section (×100 magnification); AFM micrographs (**E**) bare Au, (**F**) 11-MUA SAM (20 h), (**G**) EDC/NHS (1 h), (**H**) BSA-Aroclor 1254 coating conjugate.

3.1.1. Contact Angle Measurement

The thiol end groups utilized in the fabrication of the modified SAM gold electrodes impacted on the water contact angle. The contact angle for bare gold electrodes is 59.4 degrees [24,43]. However, as shown in Figure 4A,B, after 20 h of SAM synthesis, the contact angle value decreased in comparison with the gold bare electrode value, showing the presence of a hydrophilic surface. Hydroxyl-terminated (OH) and methyl-terminated (CH3) SAMs will usually possess a smaller hydrophobic surface over amine-terminated (NH2) or carboxylic acid-terminated (COOH) SAMs [42,44]. Previous research has indicated that the low contact angle value of carboxylic acid-terminated monolayers suggests that the

monolayer surface is covered with dense arrays of thiol tail groups. Findings by Wang et al. indicated that SAM carboxyl acid terminus had a minimum contact angle of 10°, depending on the kind of SAM synthesis utilized [42,45]. On the other hand, the contact angle for SAM produced in ethanolic solution has been measured as 35°. This corresponds with the contact angle values obtained twenty hours after SAM modification, as indicated in Table 1. SAM adjustment had 2.2% percent relative standard deviation and decreased the water contact angle for five tests that were recorded per electrode.

Table 1. The water contact angle of gold electrodes treated with thiol SAM.

	Before SAM	After SAM
Contact angle θ (°)	56.9	35.4
Relative standard deviation (%)	3.7%	2.2%

Measurement was taken five times for each electrode.

3.1.2. Scanning Electron Microscopy (SEM)

The surfaces of the electrodes were photographed using SEM so as to identify at a high resolution the spatial variations in the electrodes before and after modification. The bare gold electrode surface appeared smoother (Figure 4C) than the modified electrode and had a more uneven structure (Figure 4D). As was previously reported [21], the images in Figure 4D show the transition in the surface morphology of the electrodes as the various stacks attached to the gold surface.

3.1.3. Atomic Force Microscopy (AFM)

AFM was applied at 0.5 uM^2 to evaluate the interactions between SAM and the proteins that were immobilized on the bare gold electrodes. Figure 4E shows that there was a smooth surface structure for the bare gold electrodes to a resolution of 42 nm. The topography image after the adsorption of 11-MUA revealed a flat surface, with the calculated average of the surface roughness being 2.80 nM (Figure 4F). It was found that the protein layer of the BSA coating conjugate, which formed on the surface, resulted in greater roughness (Figure 4H) than the surface following the activation of EDC/NHS (Figure 4G). Surface roughness and particle diameter are important because they can aid in the study of the effects of tribological behavior on surfaces. Table 2 shows the surface roughness and particle diameter size of the gold electrode before and after the introduction of SAM, EDC/NHS, and the protein layer. It has been reported that surface roughness increases with the addition of protein [46]; however, this research found that the surface roughness decreased after the addition of the protein. The maximum particle diameter was 141.20 nm. As has been argued by Kim [47], it may be possible that the roughness could be due to the different shapes of the protein layer. In addition, it shows inhomogeneous particles size after the addition of the BSA-Arcolor 1254 coating conjugate. This is due to the aggregation of antibodies.

Table 2. Surface roughness and particle diameters of bare and modified gold electrodes.

	Bare Gold Electrode	SAM (20 h)	EDC/NHS (1 h)	Bsa-Alcoler1254 Coating Conjugate
Surface Roughness	4.74	2.8	2.88	2.94
Min particles diameter (nm)	11.86	-	-	11.86
Max particles diameter (nm)	107.74	-	-	141.2

Data obtained from NanoScope Analysis 1.9 software.

3.2. Electrochemical Characterization

LSV and CV, as shown in Figure 5A,B, were utilized to investigate the SAM redox process in relation to the gold electrode [46,48]; however, their limitations made this difficult. For example, it was difficult to avoid double layer charging and to measure current on low overpotential [47,49]. For these reasons, EIS was applied, as shown in Figure 5C [50]. EIS

is a sensitive method for investigating electron transport over a thin monolayer [48,50]. Amperometry was utilized in the presence of *p*AP, which is transformed to *p*-aminophenol, to prove the enzymatic process before adding the target analyte (*p*AP). At +300 mV (vs. Ag/AgCl), detection of *p*AP was possible. Electrodes may be amperometrically measured because of the low substrate specificity of AP (Figure 5D).

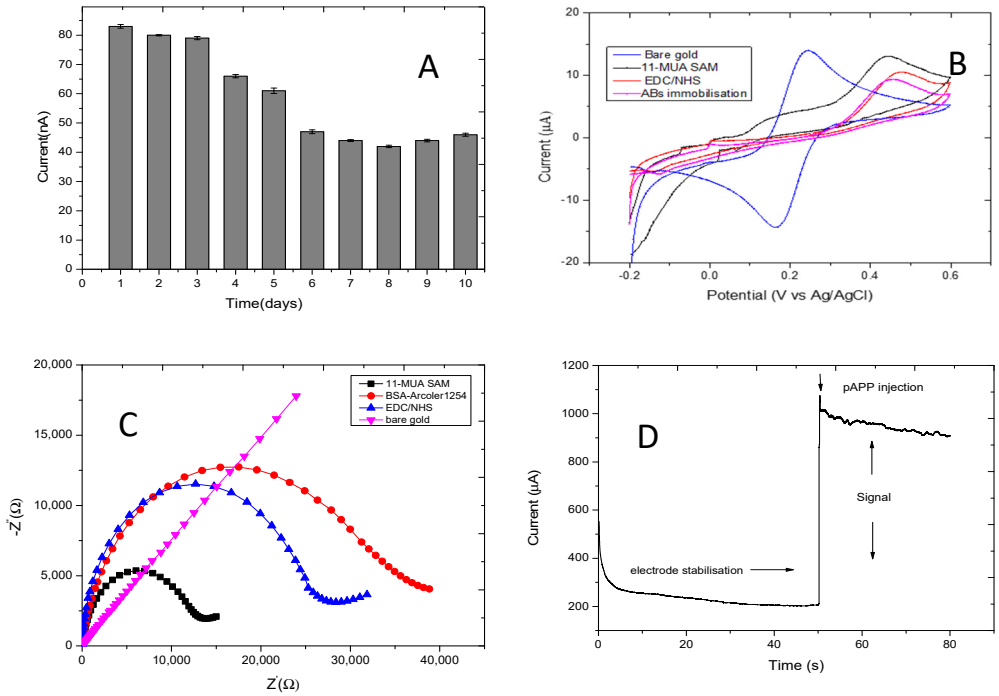


Figure 5. Electrochemical characterization of modified electrode. (**A**) A stability study of the coated BSA-Aroclor 1254 on a gold electrode surface was performed using linear sweep voltammetry. Prior to the measurements, the coated electrode was stored at 4 °C. Three electrodes were measured every day for 10 days. (**B**) The voltammogram of CV for the bare gold electrode and the gold electrode after SAM modification with 11-MUA. (**C**) Impedance spectra of the bare gold electrode, after 20 h SAM, activation with EDC/NHS and immobilization with 5 μg/mL^{-1} BSA-Aroclor 1254. The redox couple was 5 Mm [Fe (CN)$_6$]$^{3-/4-}$ in 0.1 KCl. Frequency measured from 0.1 Hz to 1 MHz, with amplitude of 0.1 V, potential applied at 0.21 V. The inserted circuit is Randle's equivalent, where Rs represents the dynamic solution resistance, Rct represents the charge transfer resistance of the immobilize recognition layer, CdI indicates the capacitance measured between the gold electrode and the electrolyte solution on a double layer basis, and Zw is the Warburg element describing the time frequency. (**D**) Amperometric detection of a chip modified AP containing bilayer (competitive assay) was measured in DEA buffer pH 9.5 at potential of 0.45 V vs. Ag/AgCl. The substrate *p*APP was injected at 40 s.

3.2.1. Stability Study of the Coated Electrodes

Before the linear sweep voltammetry deduction was used, the electrodes underwent a complete capture assay. A total of 0.123 ug/mL^{-1} of the primary antibody was immobilized on the electrode surface, followed by the addition of the labeled secondary antibody in 1/5000 dilution. In total, 10 uL of the substrate solution *p*APP was diluted in DEA buffer (pH 9.5, 1 mg mL^{-1}) and added to the electrode surfaces. The electrochemical substrates were incubated, and measurements were taken using the PalmSens potentiostat. The electrodes were washed and dried before using LSV. Measurements were performed daily for 10 days using the three electrodes (n = 3). Figure 5A shows the 10-day performance of the coated BSA-Aroclor 1254 coating conjugate on the gold electrode using LSV detection. From the graphs, it was observed that the coated electrode remained stable for the first 5 days with a decrease in signal being observed from day 6.

3.2.2. Cyclic Voltammetry

To identify the electrochemical properties of the electrode modification, an 11-MUA self-assembly on the gold electrode CV was used. The peaks of the ferricyanide/ferrocyanide couple were utilized to investigate the SAM electron-transfer efficiency on the gold surfaces. It was found that when the SAM molecules bonded to the gold electrode surface, this gradually inhibited electron transport. Figure 5B displays the electrode CVs before and after SAM modification with 11-MUA. Findings indicated a decrease in $[Fe(CN)_6]^{3-/4-}$ cathodic and anodic peak current following the gold surface's immobilization of 11-MUA SAM. This is consistent with the findings of Lu et al. [51]. Water-soluble NHS and EDC to carboxylic acid immobilization ended as SAMs increased protein coverage [52]. The coating conjugate and primary monoclonal antibody were immobilized using the competitive ELISA method.

3.2.3. Impedance Measurement

To gather further kinetic data, impedance was next applied in this study over a broader time constant limit. The impedance measurements applied ranged from 0.1 Hz to 1 MHz. An amplitude of 0.1 V and a potential of 0.21 V were used. It was observed that at higher frequencies, a semi-circle followed by a straight line appeared at the lower frequencies for the bare gold electrode, demonstrating the presence of Warburg resistance, as shown in Figure 5C. The diffusion processes occurred at the surface of the electrode when it was connected to the equivalent circuit that corresponded to the charge-transfer resistance (Re) [53]. With regard to the bare gold (Au) electrodes, there was an increase in impedance value, and the l1-MUA gold electrode was immobilized for electron transfer [54]. A highly insulated surface on the gold electrode was formed after SAM formation. Upon the addition of the protein layer (BSA-Aroclor 1254) coating conjugate, the impedance value significantly increased at both high and low frequencies. This increase relates to the higher molecular weight of protein-BSA (M = 66.5 kDa), compared to 11-MUA (M = 218.36 g/mol). This result is supported by the fact that almost all the faradaic current was blocked, which increased the surface resistance [27]. The Randle's equivalent shown in Figure 5C depended on mass transport and is comparable to data obtained for electron transfer in an earlier study [54]. The parameter assessment for the Randle's equivalent circuit on the gold electrode for 11-MUA SAM is shown in Table 3. Findings indicated that the value C_{dI} for the monolayer electrode was lower than the one recorded for the bare gold electrode (1.18×10^{-6} F/cm^{-2}). This low C_{dI} value is a sign that the electrodes are coated by well-formed SAM of carboxylic-acid-ended long chain thiols [55]. Upon the activation of EDC/NHS and the addition of the protein layer, the C_{dI} values fell to 8.10×10^{-7} and 5.74×10^{-7} F/cm^{-2}, in that order. This was due to the presence of the immobilized protein (BSA-Aroclor 1254 coating conjugate) on the gold surface, which resulted in the reduced access of the solution ions to the gold surface.

Table 3. Parameter evaluation for the Randle's model on a gold electrode.

Surface	RS (Ω)	Rct (KΩ)	CdI (F/cm^2) $\times 10^{-6}$
Bare gold	7.52	0.385	8.20
SAM (20 h)	7.79	12.56	1.18
EDC/NHS (1 h)	7.74	27.13	0.81
BSA-Arcoler 1254	7.79	34.92	0.57

Data obtained from CHI 1100/620B software.

3.2.4. Amperometric Detection

Amperometry can detect the current flow resulting from the enzymatic redox reaction in real-time. Before the amperometric measurements were taken, the electrodes were washed and stored in DEA buffer. *p*APP was the substrate that was used for the amperometric sensor. Figure 5D shows the amperometric response of the immunoassay system. Findings revealed that when the *p*APP was introduced at 50 s, the amperometric

signal increased and reached a steady-state value in less than 80 s. A steady background amperometric signal was also obtained when there was no addition of *p*-aminophenyl phosphate (*p*APP), which demonstrated electrode stabilization. The enzyme that was utilized for electrochemical detection was AP, which was also used for the ELISA work. Enzyme AP converts *p*NPP into the molecule *p*-nitrophenol, which is spectrophotometrically detectable in conventional ELISAs. Considerable differences in redox potentials between phosphorylated and free forms were observed due to a lack of electrode fouling by electro polymerization and a low redox potential when converted to (*p*AP) at (+300 mV (vs. Ag/AgCl) *p*AP is detectable [56,57]. Measurement of the electrodes both amperometrically and spectrophotometrically was possible due to the low substrate specificity of AP.

3.2.5. Specificity (Cross-Reactivity)

The specificity of the assay was evaluated by the CR (cross-reactivity) of the polyclonal antibody with five different types of compounds of Aroclors such as (Aroclor 1248, Aroclor 1016, Aroclor 1242, Aroclor 1260, Aroclor 1262). The CR values were calculated according to the following formula: CR (%) = (IC50 of Aroclor 1254)/(IC50 of other compounds) × 100. The cross-reactivity of five Aroclors compounds against Aroclor 1254 was measured, and the results are displayed in Table 4. A low IC50 value was recorded for Aroclor 1254, which proved the sensitivity of the assay toward the PCBs detection. Based on the CR values, the assay evidently provided higher responses to formulations with highly chlorinated biphenyls (Aroclors 1254, 1260, and 1262), which had a similar structure arrangement to Aroclor 1254. On the other hand, it recorded the lowest cross-reactivity with a lower chlorination level (Aroclor 1248, 1242, 1016) because of the significant difference in their molecular structures with Aroclor 1254. Therefore, this method showed good specificity for the detection of Aroclor 1254.

Table 4. The cross-reactivities of the antibody against Aroclor 1254 and other Aroclor using competitive assay.

Compound	IC50 (ng/mL^{-1})	CR (%)
Aroclor 1254	3.94	100
Aroclor 1248	14.4	27.36
Aroclor 1260	5.20	75.765
Aroclor 1242	11.57	34
Aroclor 1262	6.30	62.53
Aroclor 1016	13.27	29.6

3.3. Indirect Competitive Assay

Linear sweep voltammetry was performed to generate the curves of indirect competitive assay using bare gold electrodes and SAM modified electrodes, as shown in Figure 6. Prior to surface modification, the biochips were cleaned using plasma cleaner. After SAM formation, and to eliminate any unbound molecules from the surface of the gold, the electrodes were cleaned using absolute ethanol. Following SAM formation, a mixture of EDC and NHS was immobilized onto the surface of the gold electrode. The resulting intermediate NHS esters were stable at neutral conditions and did not hydrolyze easily. The unmodified bare gold electrode had a limit of detection (LOD) of 0.202 ng/mL^{-1} and R^2 value of 0.96. These findings are lower than other investigators' reported values, but they are still within reasonable parameters. A linear range from 0.304 to 220 ng/mL^{-1} was attained. When the electrode was changed, it was found that the modification electrode displayed a LOD of 0.09 ng/mL$^{-1,}$ a sensitivity level that was much lower than that of the unmodified electrode. The sensor recorded a linear detection range of between 220 and 0.101 ng/mL^{-1} with an R^2 value of 0.99. This novel modification had good value among other literature reviews, as illustrated in Table 5.

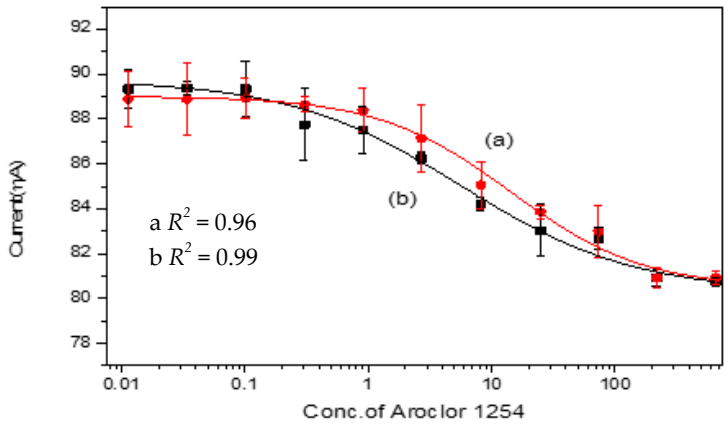


Figure 6. A competitive assay was conducted in which the performance of the gold electrode modified with 11-MUA was compared with the assay performance using (a) a bare gold electrode and (b) SAM modification gold electrode.

Table 5. Comparison with previously reported electrochemical PCB immunosensors with present work.

Immunosensor	Analyte	LOD	Linear Range	Ref.
MoS2-rGO/Thi/AuNP/GCE	PCB77	80 ag mL^{-1}	0.3 fg mL^{-1}–0.1 ng mL^{-1}	[58,59]
SnS2/β-CD modified screen-printed electrode	Aroclor1016	5 µM	0.625 to 80 µM	[19]
β-CDP/rGO/PPy/PGE	PCB	0.50 pM	1.0 pM–10.0 µM	[5]
Gold bare electrode	Aroclor of 1254	0.20 ng/mL^{-1}	0.304–220 ng/mL^{-1}	This work
Au SPE/11MUA-SAM/EDC/NHS	Aroclor of 1254	0.09 ng/mL^{-1}	0.1 to 220 ng/mL^{-1}	This work

3.4. Real Sample Analysis

11-MUA-SAM/EDC/NHS/SPGE was applied to determine Aroclor 1254 in the tap and river samples collected using the standard addition technique. The river and tap samples were further diluted with tris-BSA buffer solution pH 7.4 and analyzed by LSV and ELISA. As highlighted in Table 6, the developed sensor's results showed that the recovery values of the spiked samples were in the range of 91–97% for both the river and the tap water, which indicated highly reliable results, with an RSD value that was below 3% (n = 3). On the other hand, the Aroclor 1254 results obtained by ELISA showed that the recovery values of the spiked samples were in the range of 107.26–120% with an RSD of approximately 7% (n = 3) Therefore, the 11-MUA-SAM/EDC/NHS/SPGE was an effective technique in determining Aroclor 1254 in water samples. Similarly, the analytical results that were obtained from the 11-MUA-SAM/EDC/NHS/SPGE showed that the procedures of the sample analysis were significantly easy as it benefits from a lower determination time and fewer potential errors produced from the elaborate sample preparation. These results were more effective and reliable when compared to the results obtained from ELISA measurements, which is a traditional technique. In terms of detecting Aroclor 1254, it was clear from the results that ELISA could not accurately quantify the variables that were being tested. Therefore, this meant that the developed electrode was more sensitive and precise when compared to the standard instrument, which made the results obtained more satisfactory. The results of the fundamental analysis also showed that the developed sensor had other benefits such as high accuracy, selectivity, and sensitivity in the determination of the PCBs in the water samples.

Table 6. MUA-SAM/EDC/NHS/SPGE and ELISA (immunoassay) for the determination of Aroclor 1254 in tap and river water.

Techniques	Sample	Added (ng/mL^{-1})	Found (ng/mL^{-1})	Recovery %	RSD % (n = 3)
11-MUA-SAM/EDC/NHS/SPGE	River water	75	72.75	97	1.34
11-MUA-SAM/EDC/NHS/SPGE	Tap water	75	68.25	91	2.35
ELISA	River water	75	90	120	6.88
ELISA	Tap water	75	80.44	107.26	4.96

4. Conclusions

The modification of Au SPE/11MUA-SAM/EDC/NHS in this paper was successfully employed to determine PCBs (Aroclor 1254). In this paper, contact angle, SEM and AFM, the typical topography characterization techniques were used to examine the surface of bare and modified electrodes. In addition, investigation of biochips' electrochemical behavior was carried out by way of impedance and cyclic voltammetry, through the use of 5 mM potassium ferricyanide/ferrocyanide in the presence of 0.1 M KCI as the redox probe. This redox pair was selected as they are one of the most studied redox complexes in electrochemistry. LSV and amperometry were used to test the stability of the coated electrode as well as the enzymatic redox reaction. The competitive assay was applied to test the developed SPE. The findings demonstrated a significant increase in sensitivity and analytical performance when compared to the SPE. Utilizing the 11-MUA SAM solution, modification of the electrode with the gold surface for detecting Aroclor 1254 determined an LOD of 0.09 ng/mL^{-1} and a linear range (220–0.101 ng/mL^{-1}).

In an immunoassay, immobilizing protein to targeted sites without non-specific binding is critical. SAM was employed to reduce the random orientation of antibodies attaching to the surface. Findings indicated that the presence of SAM on the gold electrode increased the binding of the antibody to the surface, and therefore, sensor sensitivity was increased.

It was observed that the electrode became more insulated after the immersion of EDC/NHS and BSA-Aroclor 1254 coating conjugate. Overall, the developed chip showed good performance and stability and could be utilized for detection of PCB compounds using the proposed electrochemical immunosensor. This immunosensor could be used in conjunction with a portable device, allowing for in-field measurements. Moreover, much more work could be carried out to improve the commercialization of the described technique, such as minimizing the number of stages for the assay and the incubation time. In addition, further study could seek to increase the sensitivity and performance of the individual sensor measurements. This would also reduce the steps required for immunoassay testing in the field. Therefore, the integration into a real-time portable lab-on-a-chip solution could represent a future platform for monitoring organic pollution such as PCBs in the environment and avoid costly and non-efficient analysis of the samples in dedicated laboratories.

Author Contributions: Supervision, E.M.; writing—original draft, S.A.; reviewing—original draft, T.B. All authors have read and agreed to the published version of the manuscript.

Funding: This research was funded by the Ministry of Higher Education of Saudi Arabia.

Institutional Review Board Statement: Not applicable.

Informed Consent Statement: Not applicable.

Data Availability Statement: Not applicable.

Acknowledgments: The authors would like to acknowledge the financial support of the Ministry of Higher Education of Saudi Arabia. The author would like to thank Emma O'Sullivan-Carroll for constructive criticism of the manuscript.

Conflicts of Interest: The authors declare that there is no conflict of interest from any parts.

Appendix A

The following abbreviations were used in this manuscript:

ΔEp	peak-to-peak separation
11-MUA	11-mercaptoundecanoic acid
Ag/AgCl	silver/silver chloride
AP	alkaline phosphatase
AFM	atomic force microscopy
Au	gold
BSA	bovine serum albumin
CV	cyclic voltammetry
EDC	1-Ethyl-3-(3-(dimethylamino)-propyl) carbodiimide
EIS	electrochemical impedance spectroscopy
ELISA	enzyme-linked immunosorbent assay
HPLC	high performance liquid chromatography
$K_3Fe\ (CN)_6$	potassium ferricyanide
$K_4Fe\ (CN)_6$	potassium ferrocyanide
KCI	potassium chloride
LOD	limit of detection
LSV	linear sweep voltammetry
MeOH	methanol
NaCl	sodium chloride
NaCNBH4	sodium cyanoborohydride
NaOH	sodium hydroxide
NHS	N-hydroxy succinimide
PAb	polyclonal antibodies
*p*APP	*p*-aminophenyl phosphate
PBS	Phosphate-buffered saline
PCB	polychlorinated biphenyls
*p*NPP	*p*-nitrophenyl phosphate
Rct	charge transfer resistance
SAM	self-assembled monolayer
SEM	scanning electron microscopy
SPGE	screen-printed gold electrodes
TRIS	tris(hydroxylmethyl)aminomethane

References

1. Varanasi, P.; Fullana, A.; Sidhu, S. Remediation of PCB contaminated soils using iron nano-particles. *Chemosphere* **2007**, *66*, 1031–1038. [CrossRef]
2. Chana, A.; Concejero, M.A.; De Frutos, M.; Gonzá Lez, M.J.; Herradón, B. Computational Studies on Biphenyl Derivatives. Analysis of the Conformational Mobility, Molecular Electrostatic Potential, and Dipole Moment of Chlorinated Biphenyl: Searching for the Rationalization of the Selective Toxicity of Polychlorinated Biphenyls (PCBs)†. *Chem. Res. Toxicol.* **2002**, *15*, 1514–1526. [PubMed]
3. Cao, S.; Capozzi, S.L.; Kjellerup, B.V.; Davis, A.P. Polychlorinated biphenyls in stormwater sediments: Relationships with land use and particle characteristics. *Water Res.* **2019**, *163*, 114865. [CrossRef] [PubMed]
4. The Risk Assessment Information System. Available online: https://rais.ornl.gov/tox/profiles/aroclor_1254_f_V1.html (accessed on 9 October 2021).
5. Zheng, X.; Li, H.; Xia, F.; Tian, D.; Hua, X.; Qiao, X.; Zhou, C. An Electrochemical Sensor for Ultrasensitive Determination the Polychlorinated Biphenyls. *Electrochim. Acta* **2016**, *194*, 413–421. [CrossRef]
6. Yang, G.; Zhuang, H.; Chen, H.; Ping, X.; Bu, D. A gold nanoparticle based immunosorbent bio-barcode assay combined with real-time immuno-PCR for the detection of polychlorinated biphenyls. *Sens. Actuators B Chem.* **2015**, *214*, 152–158. [CrossRef]
7. Gabryszewska, M.; Gworek, B. Impact of municipal and industrial waste incinerators on PCBs content in the environment. *PLoS ONE* **2020**, *15*, e0242698. [CrossRef]
8. Deng, A.P.; Kolář, V.; Ulrich, R.; Fránek, M. Direct competitive ELISA for the determination of polychlorinated biphenyls in soil samples. *Anal. Bioanal. Chem.* **2002**, *373*, 685–690. [CrossRef] [PubMed]
9. Yang, G.; Zhuang, H.; Chen, H.; Ping, X. An indirect competitive enzyme-linked immunosorbent assay for the determination of 3,4-dichlorobiphenyl in sediment using a specific polyclonal antibody†. *Anal. Methods* **2014**, *6*, 893–899. [CrossRef]

10. Petrovic, M.; Sremacki, M.; Radonic, J.; Mihajlovic, I.; Obrovski, B.; Vojinovic Miloradov, M. Health risk assessment of PAHs, PCBs and OCPs in atmospheric air of municipal solid waste landfill in Novi Sad, Serbia. *Sci. Total Environ.* **2018**, *644*, 1201–1206. [CrossRef]
11. Reddy, A.V.B.; Moniruzzaman, M.; Aminabhavi, T.M. Polychlorinated biphenyls (PCBs) in the environment: Recent updates on sampling, pretreatment, cleanup technologies and their analysis. *Chem. Eng. J.* **2019**, *358*, 1186–1207. [CrossRef]
12. Wei, Y.; Kong, L.-T.; Yang, R.; Wang, L.; Liu, J.-H.; Huang, X.-J. Electrochemical impedance determination of polychlorinated biphenyl using a pyrenecyclodextrin-decorated single-walled carbon nanotube hybridw. *Chem. Commun* **2011**, *47*, 5340–5342. [CrossRef] [PubMed]
13. Zhang, J.; Pan, M.; Gan, N.; Cao, Y.; Wu, D. Employment of a novel magnetically multifunctional purifying material for determination of toxic highly chlorinated polychlorinated biphenyls at trace levels in soil samples. *J. Chromatogr. A* **2014**, *1364*, 36–44. [CrossRef] [PubMed]
14. Ayris, S.; Currado, G.M.; Smith, D.; Harrad, S. GC/MS procedures for the determination of PCBs in environmental matrices. *Chemosphere* **1997**, *35*, 905–917. [CrossRef]
15. Van Emon, J.M.; Chuang, J.C. Development and application of immunoaffinity chromatography for coplanar PCBs in soil and sediment. *Chemosphere* **2013**, *90*, 1–6. [CrossRef] [PubMed]
16. Cheng, J.; Wang, P.; Su, X.-O. Surface-enhanced Raman spectroscopy for polychlorinated biphenyl detection: Recent developments and future prospects. *TrAC Trends Anal. Chem.* **2020**, *125*, 115836. [CrossRef]
17. West, C.; Lesellier, E. A unified classification of stationary phases for packed column supercritical fluid chromatography. *J. Chromatogr. A* **2008**, *1191*, 21–39. [CrossRef]
18. Ramón-Azcón, J.; Valera, E.; Rodríguez, Á.; Barranco, A.; Alfaro, B.; Sanchez-Baeza, F.; Marco, M.P. An impedimetric immunosensor based on interdigitated microelectrodes (IDμE) for the determination of atrazine residues in food samples. *Biosens. Bioelectron.* **2008**, *23*, 1367–1373. [CrossRef]
19. Liu, X.; Sakthivel, R.; Cheng, C.-Y.; Luo, J.; Song, L.; Wu, J.; He, W.; Younis, U.; Chung, R.-J. 3A-Amino-3A-Deoxy-(2AS, 3AS)-β-Cyclodextrin Hydrate/Tin Disulfide Modified Screen-Printed Carbon Electrode for the Electrochemical Detection of Polychlorinated Biphenyls. *Nanoscale Res. Lett.* **2020**, *15*, 4. [CrossRef]
20. Yu, Y.; Chen, X.; Wei, Y.; Liu, J.-H.; Huang, X.-J. Strategy for Polychlorinated Biphenyl Detection Based on Specific Inhibition of Charge Transport Using a Nanogapped Gold Particle Film. *Anal. Chem.* **2012**, *84*, 9818–9824. [CrossRef]
21. Moldovan, C.; Mihailescu, C.; Stan, D.; Ruta, L.; Iosub, R.; Gavrila, R.; Purica, M.; Vasilica, S. Characterization of self-assembled monolayers (SAMs) on silicon substrate comparative with polymer substrate for *Escherichia coli* O157:H7 detection§. *Appl. Surf. Sci.* **2009**, *255*, 8953–8959. [CrossRef]
22. Centi, S.; Laschi, S.; Fránek, M.; Mascini, M. A disposable immunomagnetic electrochemical sensor based on functionalised magnetic beads and carbon-based screen-printed electrodes (SPCEs) for the detection of polychlorinated biphenyls (PCBs). *Anal. Chim. Acta* **2005**, *538*, 205–212. [CrossRef]
23. Khesuoe, M.P.; Okumu, F.O.; Matoetoe, M.C. Development of a silver functionalised polyaniline electrochemical immunosensor for polychlorinated biphenyls†. *Anal. Methods* **2016**, *8*, 7087–7095. [CrossRef]
24. Ahmad, A.; Moore, E. Electrochemical immunosensor modified with self-assembled monolayer of 11-mercaptoundecanoic acid on gold electrodes for detection of benzo[a]pyrene in water. *Analyst* **2012**, *137*, 5839–5844. [CrossRef]
25. Briand, E.; Salmain, M.; Herry, J.M.; Perrot, H.; Compère, C.; Pradier, C.M. Building of an immunosensor: How can the composition and structure of the thiol attachment layer affect the immunosensor efficiency? *Biosens. Bioelectron.* **2006**, *22*, 440–448. [CrossRef] [PubMed]
26. Mendes, R.K.; Ferreira, D.C.M.; Carvalhal, R.F.; Peroni, L.A.; Kubota, L.T. Development of an Electrochemical Immunosensor for. *J. Braz. Chem. Soc.* **2009**, *20*, 795–801. [CrossRef]
27. Tlili, A.; Abdelghani, A.; Ameur, S.; Jaffrezic-Renault, N. Impedance spectroscopy and affinity measurement of specific antibody–antigen interaction. *Mater. Sci. Eng. C* **2006**, *26*, 546–550. [CrossRef]
28. Gutiérrez-Zúñiga, G.G.; Hernández-López, J.L. Sensitivity improvement of a sandwich-type ELISA immunosensor for the detection of different prostate-specific antigen isoforms in human serum using electrochemical impedance spectroscopy and an ordered and hierarchically organized interfacial supramolecular architecture. *Anal. Chim. Acta* **2016**, *902*, 97–106. [PubMed]
29. Chaki, N.K.; Vijayamohanan, K. Self-assembled monolayers as a tunable platform for biosensor applications. *Biosens. Bioelectron.* **2002**, *17*, 1–12. [CrossRef]
30. Arya, S.K.; Solanki, P.R.; Datta, M.; Malhotra, B.D. Recent advances in self-assembled monolayers based biomolecular electronic devices. *Biosens. Bioelectron.* **2009**, *24*, 2810–2817. [CrossRef]
31. Ulman, A. Self-Assembled Monolayers of 4-Mercaptobiphenyls and the Garcia MRSEC for Polymers at Engineered Interfaces. *Acc. Chem. Res.* **2001**, *34*, 855–863. [CrossRef]
32. Gooding, J.J.; Ciampi, S. The molecular level modification of surfaces: From self-assembled monolayers to complex molecular assemblies. *Chem. Soc. Rev* **2011**, *40*, 2704–2718. [CrossRef]
33. Sayikli Şimşek, Ç.; Nur Sonuç Karaboğa, M.; Sezgintürk, M.K. A new immobilization procedure for development of an electrochemical immunosensor for parathyroid hormone detection based on gold electrodes modified with 6-mercaptohexanol and silane. *Talanta* **2015**, *144*, 210–218. [CrossRef]

34. Bonroy, K.; Frederix, F.; Reekmans, G.; Dewolf, E.; De Palma, R.; Borghs, G.; Declerck, P.; Goddeeris, B. Comparison of random and oriented immobilisation of antibody fragments on mixed self-assembled monolayers. *J. Immunol. Methods* **2006**, *312*, 167–181. [CrossRef]
35. Tsugimura, K.; Ohnuki, H.; Wu, H.; Endo, H.; Tsuya, D.; Izumi, M. Oriented antibody immobilization on self-assembled monolayers applied as impedance biosensors. *J. Phys. Conf. Ser.* **2017**, *924*, 012015. [CrossRef]
36. Andreescu, S.; Sadik, O.A. Trends and challenges in biochemical sensors for clinical and environmental monitoring. *Pure Appl. Chem.* **2004**, *76*, 861–878. [CrossRef]
37. Mollarasouli, F.; Kurbanoglu, S.; Ozkan, S.A. The role of electrochemical immunosensors in clinical analysis. *Biosensors* **2019**, *9*, 86. [CrossRef]
38. Bakshi, S.; Mehta, S.; Kumeria, T.; Shiddiky, M.J.A.; Popat, A.; Choudhury, S.; Bose, S.; Nayak, R. Rapid fabrication of homogeneously distributed hyper-branched gold nanostructured electrode based electrochemical immunosensor for detection of protein biomarkers. *Sens. Actuators B Chem.* **2021**, *326*, 128803. [CrossRef]
39. Xiao, X.; Li, H.; Wang, M.; Zhang, K.; Si, P. Examining the effects of self-assembled monolayers on nanoporous gold based amperometric glucose biosensors. *Analyst* **2014**, *139*, 488–494. [CrossRef]
40. Haji-Hashemi, H.; Norouzi, P.; Safarnejad, M.R.; Ganjali, M.R. Label-free electrochemical immunosensor for direct detection of Citrus tristeza virus using modified gold electrode. *Sens. Actuators B Chem.* **2017**, *244*, 211–216. [CrossRef]
41. Lawruk, T.S.; Lachman, C.E.; Jourdan, S.W.; Fleeker, J.R.; Hayes, M.C.; Herzog, D.P.; Rubio, F.M. Quantitative determination of PCBs in soil and water by a magnetic particle-based immunoassay. *Environ. Sci. Technol.* **1996**, *30*, 695–700. [CrossRef]
42. Wang, M.S.; Palmer, L.B.; Schwartz, J.D.; Razatos, A. Evaluating Protein Attraction and Adhesion to Biomaterials with the Atomic Force Microscope. *Langmuir* **2004**, *20*, 7753–7759. [CrossRef] [PubMed]
43. Narayan, T.; Kumar, S.; Kumar, S.; Augustine, S.; Yadav, B.K.; Malhotra, B.D. Protein functionalised self assembled monolayer based biosensor for colon cancer detection. *Talanta* **2019**, *201*, 465–473. [CrossRef] [PubMed]
44. Chuang, W.-H.; Lin, J.-C. Surface characterization and platelet adhesion studies for the mixed self-assembled monolayers with amine and carboxylic acid terminated functionalities. *J. Biomed. Mater. Res. Part A* **2007**, *82*, 820–830. [CrossRef]
45. Baio, J.E.; Weidner, T.; Brison, J.; Graham, D.J.; Gamble, L.J.; Castner, D.G. Amine terminated SAMs: Investigating why oxygen is present in these films. *J. Electron Spectrosc. Relat. Phenom.* **2009**, *172*, 2–8. [CrossRef]
46. Rechendorff, K.; Hovgaard, M.B.; Foss, M.; Zhdanov, V.P.; Besenbacher, F. Enhancement of Protein Adsorption Induced by Surface Roughness. *Appl. Phys. Lett* **2003**, *5*, 10885–10888. [CrossRef]
47. Kim, S.Y.; Yu, J.; Son, S.J.; Min, J. Signal enhancement in a protein chip array using a 3-D nanosurface. *Ultramicroscopy* **2010**, *110*, 659–665. [CrossRef]
48. Finklea, H.O.; Hanshew, D.D. American Chemical Society Electron-Transfer Kinetics in Organized Thiol Monolayers with Attached Pentaammine(pyridine)ruthenium Redox Centers. *J. Am. Chem. Soc.* **1992**, *114*, 3173–3181. [CrossRef]
49. Miller, C.; Cuendet, P.; Grätzel, M. Adsorbed ω-hydroxy thiol monolayers on gold electrodes: Evidence for electron tunneling to redox species in solution. *J. Phys. Chem.* **1991**, *95*, 877–886. [CrossRef]
50. Xing, Y.F.; O'Shea, S.J.; Li, S.F.Y. Electron transfer kinetics across a dodecanethiol monolayer self assembled on gold. *J. Electroanal. Chem.* **2003**, *542*, 7–11. [CrossRef]
51. Patel, N.; Davies, M.C.; Heaton, R.J.; Roberts, C.J.; Tendler, S.J.B.; Williams, P.M. A scanning probemicroscopy study of the physisorption and chemisorption of protein molecules onto carboxylate terminated self-assembledmonolayers. *Appl. Phys. A Mater. Sci. Process.* **1998**, *66*, 569–574. [CrossRef]
52. Lu, X.; Li, M.; Yang, C.; Zhang, L.; Li, Y.; Jiang, L.; Li, H.; Jiang, L.; Liu, C.; Hu, W. Electron Transport through a Self-Assembled Monolayer of Thiol-End-Functionalized Tetraphenylporphines and Metal Tetraphenylporphines. *Langmuir* **2006**, *22*, 3035–3039. [CrossRef]
53. Radi, A.E.; Muñoz-Berbel, X.; Cortina-Puig, M.; Marty, J.L. An electrochemical immunosensor for ochratoxin A based on immobilization of antibodies on diazonium-functionalized gold electrode. *Electrochim. Acta* **2009**, *54*, 2180–2184. [CrossRef]
54. Molinero, V.; Calvo, E.J. Electrostatic interactions at self assembled molecular films of charged thiols on gold. *J. Electroanal. Chem.* **1998**, *445*, 17–25. [CrossRef]
55. Cecchet, F.; Marcaccio, M.; Margotti, M.; Paolucci, F.; Rapino, S.; Rudolf, P. Redox mediation at 11-mercaptoundecanoic acid self-assembled monolayers on gold. *J. Phys. Chem. B* **2006**, *110*, 2241–2248. [CrossRef]
56. Fähnrich, K.A.; Pravda, M.; Guilbault, G.G. Disposable amperometric immunosensor for the detection of polycyclic aromatic hydrocarbons (PAHs) using screen-printed electrodes. *Biosens. Bioelectron.* **2003**, *18*, 73–82. [CrossRef]
57. Moore, E.J.; Pravda, M.; Kreuzer, M.P.; Guilbault, G.G. Comparative study of 4-aminophenyl phosphate and ascorbic acid 2-phosphate, as substrates for alkaline phosphatase based amperometric immunosensor. *Anal. Lett.* **2003**, *36*, 303–315. [CrossRef]
58. Kaya, S.I.; Cetinkaya, A.; Bakirhan, N.K.; Ozkan, S.A. Trends in sensitive electrochemical sensors for endocrine disruptive compounds. *Anal. Chem.* **2020**, *28*, e00106.
59. Mohammadi, A.; Heydari-Bafrooei, E.; Foroughi, M.M.; Mohammadi, M. Electrochemical aptasensor for ultrasensitive detection of PCB77 using thionine-functionalized MoS 2-rGO nanohybrid. *Microchem. J.* **2020**, *155*, 104747. [CrossRef]

electrochem

MDPI

Article

A Novel Label-Free Electrochemical Immunosensor Based on a Self-Assembled Monolayer-Modified Electrode for Polychlorinated Biphenyl (PCB) in Environmental Analysis

Samia Alsefri, Thanih Balbaied, Ibtihaj Albalawi, Hanan Alatawi and Eric Moore *

Sensing & Separation Group, School of Chemistry and Life Science Interface, Tyndall National Institute, University College Cork, T12 R5CP Cork, Ireland

* Correspondence: e.moore@ucc.ie

Abstract: PCBs (polychlorinated biphenyls) are a very large group of organic compounds that have between two and ten chlorine atoms attached to the biphenyl. These compounds have an acute impact as environmental pollutants, causing cancer and other adverse health effects in humans. It is therefore imperative to develop techniques for the cost-effective detection of PCBs at very low concentrations in ecosystems. In this paper, a novel label-free, indirect, competitive electrochemical immunosensor was first developed with a PCB-BSA conjugate. It is shown herein to compete with free PCBs for binding to the anti-PCB polyclonal primary antibody (IgY). Then, we used a secondary antibody to enhance the sensitivity of the sensor for the detection of PCB in a sample. It has been successfully immobilized on an 11-mercaptoundecanoic acid (11-MUA)-modified gold electrode via a carbodiimide-coupling reaction using cross-linking 1-ethyl-3-(3-dimethylaminopropyl) carbodiimide (EDC) and N-hydroxysuccinimide (NHS) on the electrode surface. The immunosensor was investigated by cyclic voltammetry and differential pulse voltammetry in a standard solution of $[Fe(CN)_6]^{3-/4-}$. A linear range of 0.011–220 ng/mL^{-1} and a limit of detection (LOD) of 0.11 ng/mL^{-1} for PCBs detection were achieved by the developed immunosensor, showing advantages over conventional assays. The novel label-free electrochemical immunosensor discussed in this paper is a solution for simple, rapid, cost-effective sample screening in a portable, disposable format. The proposed immunosensor has good sensitivity, and it can prove to be an adequate real-time monitoring solution for PCBs in soil samples or other samples.

Keywords: polychlorinated biphenyls; label-free disposable screen-printed gold electrode; differential pulse voltammetry; immunosensors; self-assembled monolayers (SAM)

check for updates

Citation: Alsefri, S.; Balbaied, T.; Albalawi, I.; Alatawi, H.; Moore, E. A Novel Label-Free Electrochemical Immunosensor Based on a Self-Assembled Monolayer-Modified Electrode for Polychlorinated Biphenyl (PCB) in Environmental Analysis. *Electrochem* **2022**, *3*, 451–462. https://doi.org/10.3390/electrochem3030031

Academic Editors: Michael EG Lyons and Masato Sone

Received: 5 July 2022
Accepted: 18 August 2022
Published: 22 August 2022

Publisher's Note: MDPI stays neutral with regard to jurisdictional claims in published maps and institutional affiliations.

Copyright: © 2022 by the authors. Licensee MDPI, Basel, Switzerland. This article is an open access article distributed under the terms and conditions of the Creative Commons Attribution (CC BY) license (https://creativecommons.org/licenses/by/4.0/).

1. Introduction

Polychlorinated biphenyls (PCBs) are organic compounds containing two to ten chlorine atoms attached to the biphenyl [1,2]. Aroclor 1254 ($C_{12}H_5Cl_5$) is a mixture of polychlorinated biphenyls, and is a viscous, light-yellow liquid with a molecular weight of 328, containing 21% $C_{12}H_6Cl_4$, 48% $C_{12}H_5Cl_5$, 23% $C_{12}H_4Cl_6$, and 6% $C_{12}H_3Cl_7$, with an average chlorine content of 54% [3]. Owing to its severe harm to the environment, the chemical was banned despite its wide use in industry. Nevertheless, it is still present in electrical power generation, plastic manufacturing, chemical production, printing, and other industries; therefore, PCB contamination is still a global issue. It can be found in air, soil, and aquatic environments, and in human bodies [4–6] PCBs disrupt endogenous hormones and immune functions, and can lead to tumor formation [7,8]. It is therefore important and urgent to develop reliable, on-site screening systems that use simple analytical methods with high specificity and sensitivity for PCB detection. These methods can be applied to trace levels of PCBs that pose a major threat to the environment and to public health.

For PCB detection, standard methods such as gas chromatography–mass spectrometry (GC-MS) and high-performance liquid chromatography–mass spectrometry (HPLC-MS)

have been commonly used [9–11]. Although they are sensitive and accurate, these instrumental analyses have some limitations and are mainly used in laboratory settings. Therefore, immunoassay techniques seem to be a viable solution for portable devices. For example, enzyme-linked immunosorbent assays (ELISA) [12–14] have detection limits of less than 1.0 μg/mL with high specificity [15,16]. Traditional ELISA involves many steps and long incubations, which must be reduced in order to enable rapid, on-site detection of PCBs. Therefore, electrochemical methods will replace optical ones because they enable faster response times and miniaturization. Electrochemical biosensors can be labeled or label-free [17]; label-free-based immunoassays have attracted considerable attention recently due to their fast, simple, and low-cost on-site analysis, and the fact that do not require the modification of biological samples [18–21]. A competitive immunoassay is the common scheme used with label-free immunosensors [3,6,17,22], whereby the formation of antibody–antigen complexes changes the thickness and mass of an electrode surface, which in turn blocks the transfer of electrons to the electrode surface [23,24]. Therefore, the key factor here is the immobilization of the antibody or antigen on the electrode surface with no nonspecific binding [25,26].

In view of the rarity of studies using label-free electrochemical immunosensors for PCB detection [7,8,13,27–30], in this study, a novel, sensitive, and label-free electrochemical immunosensor was developed based on an indirect competitive assay on modified electrodes for the quantification of total polychlorinated biphenyls (PCBs). Detailed instructions for electrode modification were provided in our previous study [3]. This study applied the Aroclor 1254–bovine serum albumin (BSA) conjugate, which became the solution for the competition assay and enabled our development of the immunosensor modified with 11-mercaptodecylic acid (MUA). PCB-BSA competed with antigens in solution for polyclonal antibodies (anti-PCB), resulting in two types of anti-PCB: one which binds freely to PCB in solution, while the other binds to PCB-BSA. Secondary antibodies were then applied, which in turn competed with these two types of anti-PCB, changing the electrochemical signals and increasing the sensitivity of the immunosensor. Differential pulse voltammetry (DPV) was applied to record the interaction of antibodies with PCB antigens on the modified electrode, using $[Fe(CN)_6]^{3-/4-}$ solution as a redox probe. PCBs were therefore competitively bound to this particular antibody, resulting in Aroclor 1254–BSA complex formation, which then dissociated from the electrode, causing significant decreases in DPV. Capture assays were used in optimization, and the analyte concentrations remained constant, allowing the use of direct ELISA. Competitive assays were used in the sensitivity measurements, and the analyte concentration gradually changed, allowing the use of indirect ELISA.

PCBs were determined using the proposed immunosensor in both standard and real samples. The details of the preparation, characterization, and possible application of the immunosensors were investigated as follows. The presented immunosensor's linear dynamic range and limit of detection were compared with a labeled immunosensor, ELISA, and other previously described immunoassays for PCB detection. We believe that the findings of this study, a label-free detection technique, will have a significant impact on the development of an ultrasensitive platform for detecting and quantifying PCBs in the environment. Figure 1 illustrates the functionalization process of SPGE and the detection process of the PCB contaminant.

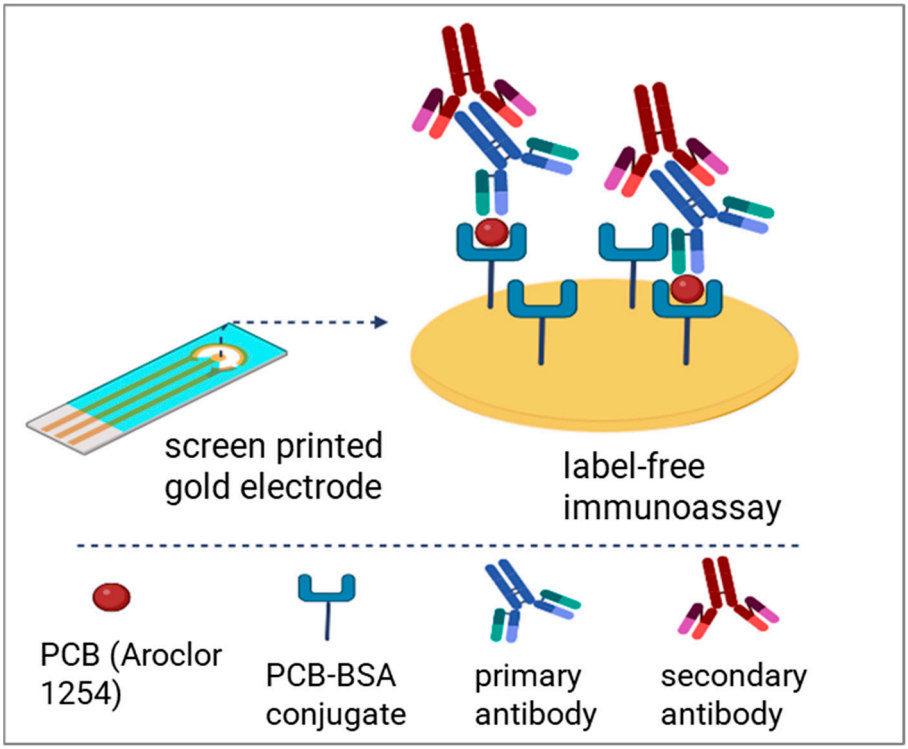


Figure 1. Functionalization steps of PCB immunoassay on SPGE, reprinted from reference [31], Springer Nature, 2018.

2. Materials and Methods

2.1. Chemicals and Materials

Aroclor 1254 PCB was purchased from Cole-Parmer Instrument Company Ltd., Eaton Socon, Saint Neots, UK. Reagents, such as buffers (Tris base: PBS—phosphate-buffered saline, DEA—diethanolamine); solutions (NaHCO3—sodium bicarbonate, NaCl—sodium chloride, KCl—potassium chloride, HCl 37%—hydrochloric acid, NaBH3CN—sodium cyanoborohydride, NH4OH—ammonium hydroxide, NaOH—sodium hydroxide); chemicals (NHS—N-hydroxysuccinimide 98%, EDC—1-ethyl-3-(3-dimethylaminopropyl) carbodiimide, 11-MUA—11-mercaptoundecanoic acid 95%, $K_4[Fe(CN)_6^-]$—potassium ferrocyanide, $K_3[Fe(CN)_6^-]$—potassium ferricyanide, BSA—bovine serum albumin); Tween-20 detergent; acetone; alcohol (1-isopropyl; ethanol); and clean soil, were bought from Sigma (Dublin, Ireland). Other biochemicals, including polyclonal chicken antibody (IgY), specific to PCB; goat anti-chicken IgY (heavy and light chain) unconjugated antibody; and PCB-BSA conjugate (Aroclor 1254), were purchased from GmbH (Heidelberg, Germany). All the reagents were of analytical grade or higher, and all the buffers and solutions were made from water filtered with nanopores (18.2 mΩ-cm).

2.2. Equipment and Instruments

For the optical assays, a microplate reader (EL Read 2000 from biochrom.co, Cambridge, UK) and 96-well ELISA microplates (Greiner bio-one from Frickenhausen, Germany) were used. For electrochemical assays, a Palm Sens potentiostat (Palm Instrument BV Houten, The Netherlands) and disposable electrochemical screen-printed gold electrodes (AuE) with a size L 3.4 × W 1.0 × H 0.05 cm and a diameter of 4 mm (Drop Sens, Asturias, Spain) were used. For incubation and pretreatments, a 37 °C Biometra OV3 Incubator (Gottingen, Germany) and a plasma cleaner (Harrick Plasma Ithaca, Ithaca, NY, USA) were used. Between measurements, nitrogen spray guns were used to dry the SPEs.

2.3. Cyclic Voltammetry for Pretreatment of Electrodes

For electrochemical measurements, it is necessary to ensure that the electrode surfaces are clean. As a result, the optimization of various SPGE cleaning protocols was carried out. At a scan rate of 50 mV s^{-1}, the chips were cycled in 5 mM $[Fe(CN)_6]^{3-/4-}$ in 0.1 M KCl. The potential was chosen between −0.2 and 0.6 versus Ag/AgCl. The following are the different chip-cleaning protocols: (a) SPGE was given a plasma cleaner treatment for 20–30 min; (b) SPGE was ultrasonically cleaned for 5 min in acetone, then for another 5 min in 1-isopropyl alcohol before being rinsed with deionized water for 5 min; (c) on a hot plate, a 1:1:5 mixture of 29% ammonia solution, 30% H_2O_2, and ultrapure water was heated to 80 °C, and the SPGEs were immersed in the solution for 5 min; (d) the SPGE was cycled from 0 to +1.6 V in 0.5 M for 3 scans in 0.5 M sulfuric acid, H2SO4. The SPGE, on the other hand, was scanned between −0.2 and 0.6 V in 5 mM $[Fe(CN)_6]^{3-/4-}$ in 0.1 M KCl to investigate the effect of the scan rate. Different scan rates of 5–200 mV s versus Ag/AgCl were used in the experiments.

2.4. Modification of SPG Electrodes

Our method for modifying the electrode was discussed in our previous paper [3]. We briefly describe the method here: 5 mM of 11-MUA used as SAM was applied on the gold working electrodes. 11-MUA was diluted in absolute ethanol and bubbled with N2 for the purpose of reducing the oxygen [23,32,33]; then, the electrodes were immersed in this mixture for 20 h at 25 °C. Next, the electrodes were rinsed thoroughly with ethanol and dried with N2. After that, 50 mM EDC and NHS solution was used to immerse electrodes for 1 h, and then the electrodes were rinsed with deionized water and dried again with N2. The electrodes were then exposed to protein as a final step. A measure of 5 μg mL^{-1} of Aroclor 1254–BSA coating conjugate was immobilized for 1 h at 37 °C.

2.5. Optimization of Label-Free Immunoassay

These different experimental parameters were optimized using an Aroclor 1254 solution at 25 ng mL^{-1} concentration without a competition test (we used fixed-concentration PCBs at 25 ng mL^{-1} Aroclor 1254 concentration). Therefore, instead of performing the competitive assay, we applied a capture assay with DPV techniques to optimize several conditions, including the concentrations of BSA–Aroclor 1254, the concentrations of anti-PCB Ab, and the competition time. Under optimized experimental conditions, the label-free immunoassay was performed using an indirect competitive immunoassay scheme using DPV, which was applied in order to find the calibration plot and compare the other methods. The electrode surfaces were incubated at 37 °C for one hour with 15 μL of BSA–Aroclor 1254 coating antigen (5 μg mL^{-1}) (pH 7.4). For washing the electrode surfaces, 0.05 M Tris, pH 7.4 (0.05% Tween 20) was sprayed on them three times, and then the electrodes were blocked for 30 min at 37 °C with 1% BSA–Tris (0.05 M Tris–HCI). To eliminate unbound coating conjugates, the electrode surface was washed three times following the incubation process. Aroclor 1254 PCB, serially diluted with PCB-specific polyclonal chicken antibody (IgY), was mixed and left to incubate for 15 min with 0.246 μg/mL^{-1} of the polyclonal chicken antibody (IgY). The electrode surface was exposed to 15 μL of each dilution, and binding occurred for 30 min at 37 °C. The SPGE surface was coated with a 1/5000 dilution of unlabeled anti-rabbit IgG antibody and allowed to react for 30 min at 37 °C in order to standardize the assay. A 100 μL-volume wash buffer was used to wash the electrodes before the electrochemical reading. The DPV analysis utilized a voltage range from −0.2 to +0.6 V at a scan rate of 0.05 V s^{-1} and a response amplitude of 0.05 V. In addition to the step potential, the modulation time and interval time were all fixed during the assay: 0.01 V and 0.1 s, respectively, were used in 0.1 M KCl in 4 mL PBS, containing a 5 mM redox probe $[Fe(CN)_6]^{3-/4-}$.

2.6. Real Sample Analysis

For the real sample analysis, ten grams of soil were placed in a glass flask and spiked with a known amount of Aroclor 1254 before being extracted for recovery studies. A measure of 5 g of the spiked sample was added to 10 mL of methanol. The flask was sealed, shaken frequently for 2 min, and then left at room temperature for 30 min. The sample was centrifuged at 2500 rpm for 10 min [34,35]. After waiting 5 min for the solid particles to settle, the soil was filtered through a 0.45 m nitrocellulose filter. The extract was then evaporated to a volume of 1 mL before processing, as described in Section 2.5.

3. Results and Discussion

3.1. Electrochemical Characterization of the Electrode

Cleaning and substrate preparation are important steps in studying the surface phenomenon, because they can improve the surface state for better electrochemical activity to take place. There are different common pretreatment methods for producing a clean gold surface, and most are performed just before the modification of the surface. Different pretreatment procedures, either individual or combined, are employed. Common pretreatment methods include thermal treatment, mechanical polishing with a slurry of alumina, oxygen plasma cleaning, chemical oxidation with piranha solution or ethanol, and electrochemical polishing using potential cycling [27,36]. In this study, we used four different protocols to clean the electrode, as follows: plasma cleaning, ultrasonicating, NH_3 + H_2O_2, and H_2SO_4. Electrode cleanliness can be measured by examining the potential difference of the peak-to-peak separation (ΔEp) of anodic and cathodic peaks. According to Fischer et al., a smaller ΔEp indicates a cleaner surface, where any increase in the ΔEp value indicates that some sort of contamination has occurred on the electrode surface [28]. Considering that the theoretical value of ΔEp is 59 mV for the single-electron transfer of $[Fe(CN)_6]^{3-/4-}$, the closest experimental value of ΔEP (58 mV) was achieved when the CV was performed using the plasma-cleaner-treated electrode. Compared with the other cleaning protocols, the plasma cleaning method shows well-defined peaks(see Figure 2). For this reason, we used this method as our cleaning procedure for further electrochemical investigations. The data generated from the curves are summarized in Table 1.

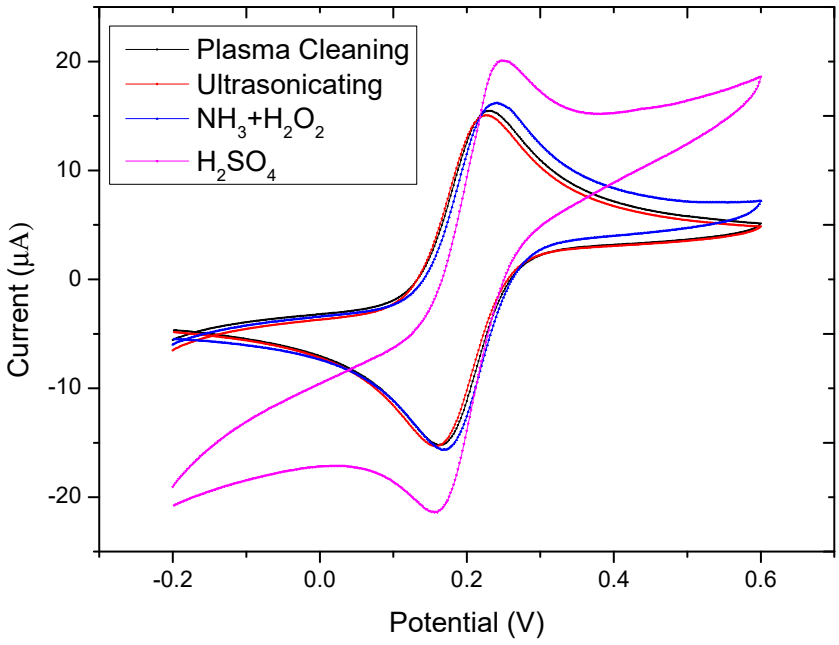


Figure 2. Studies on different chip-cleaning procedures. CV was scanned in mM $[Fe(CN)_6]^{3-/4-}$ redox coupled with a 50 mV/s scan rate.

Table 1. The values of peak-to-peak separation using different cleaning protocols.

Cleaning Protocols	E_{pa} (V)	E_{pc} (V)	ΔE_P (mV) *
Plasma cleaning	0.226	0.168	58
Ultrasonicating	0.226	0.160	66
$NH_3 + H_2O_2$	0.242	0.172	70
H_2SO_4	0.246	0.160	86

* $\Delta E_P = E_{Pa} - E_{pc}$.

Secondly, the influence of the scan rates was investigated by performing the CVs over the range 5–200 mV/s^{-1}. As shown in Figure 3, a large peak separation was observed when the scan rates were increased. The redox couple used was 5 mM ferricyanide/ferrocyanide in 0.1 MKCL. The peak-to-peak separation achieved for the scan rate of 50 mV/s was 64 mV, which is a better performance compared to those reported by M. Lu with 75 mV [29]. A good linear correlation was obtained between the anodic peak height and the square root of the applied scan rates, as shown in Figure 3. The values of the correlation coefficients (R2) of the anodic peak (0.999) and the cathodic peak (0.998) confirm that the electrochemical system was under the diffusion control process. Table 2 shows the calculated CV data for the oxidation of 5 mM $[Fe(CN)_6]^{3-/4-}$ in 1 M kCL with different scan rates. The measurements were performed at room temperature, 25 °C. Table 2 shows that the data of Ipa increased as the scan rate increased. It also shows the ΔEpa for each scan rate within the practical range (70–40 mV). In addition, the theoretical value of 58 mV was recorded twice at that range, at scan rates of 100 and 200 mV/s. Furthermore, it shows all the redox reactions across the different scan rates applied at ≈200 mV.

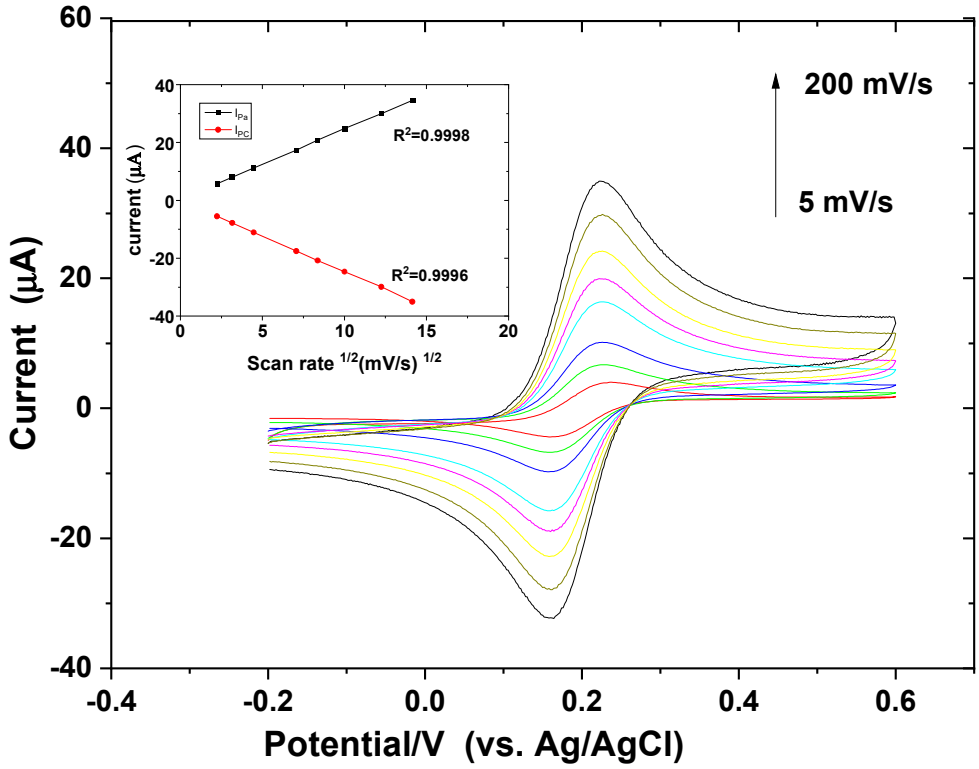


Figure 3. Influence of the scan rates on the CV signals measured in 5 mM $[Fe(CN)_6]^{3/4}$ in 1 M KCL. The potential applied was from −0.2 to 0.6 V.

Table 2. Influence of the scan rate on the half-peak potential and the peak current for the oxidation component of the process. The scan rates studied were 5, 10, 20, 50, 70, 100, 150, and 200 mV s^{-1}.

Scan Rate (mV/s)	Ipa (μA) [c]	ΔEp (mV) [b]	Emid vs. Ag/Ag CL (Mv) [a]
200	34.59	58	193
150	30.01	64	194
100	24.80	58	193
70	20.83	62	191
50	17.38	64	192
20	11.18	68	192
10	7.98	68	194
5	5.71	70	198

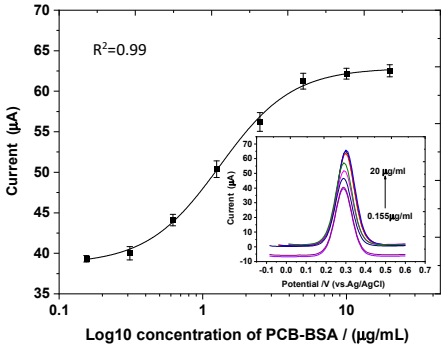
[a] Measured from the value 1/2 (Epc + Epa) versus Ag/AgCl reference electrode; [b] ΔEp = (Epc − Epa); [c] Ep anodic data as a function of scan rate.

3.2. Optimization of the Assay Conditions

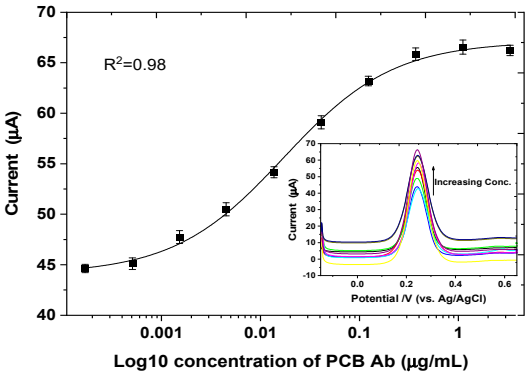
Different concentrations of BSA–Aroclor 1254 conjugate and anti-PCB Ab, and different competition times were selected to test the immunosensor. This test was performed using a capture assay and the concentration of BSA–Aroclor 1254 conjugate varied from 20 to 0.155 μg mL^{-1} in this study. The BSA–Aroclor 1254 conjugate was immobilized on the sensor surface in three independent experiments. As the concentration of BSA–Aroclor 1254 increased, there was an increase in the peak sensor currents. The concentration of the BSA–Aroclor 1254 conjugate (5–20 μg mL^{-1}) did not affect the DPV current further; therefore, 5 μg mL^{-1} was chosen as the optimal concentration to use during the experiments, as shown in Figure 4a. Furthermore, 5 μg mL^{-1} BSA–Aroclor 1254 coating conjugate was immobilized on the electrodes and used to cover the electrodes completely, followed by blocking the chips with 1% BSA in Tris buffer (pH 7.4). The primary PCB antibody was serially diluted in concentrations ranging between 10 μg mL^{-1} and 0.0005 ng ml^{-1}. As shown in Figure 4b, the optimal concentration of anti-PCB Ab was 0.246 μg/mL^{-1}. The competitive times for PCB–BSA and PCBs standards were also optimized because of the competition with the finite anti-PCBs, which is a factor that affects the DPV response of the biosensor. Figure 4c shows the peak current progressed at a dramatic rate until it reached minimal intensity at 25 min (containing 25 ng mL^{-1} Aroclor 1254 concentration). Most of the PCB was bound specifically to anti-PCB, as shown in the data from 10 to 35 min. It is therefore optimal to have a 25 min competition time.

3.3. Sensitivity of the Immunosensor for PCB Aroclor 1254 Determination

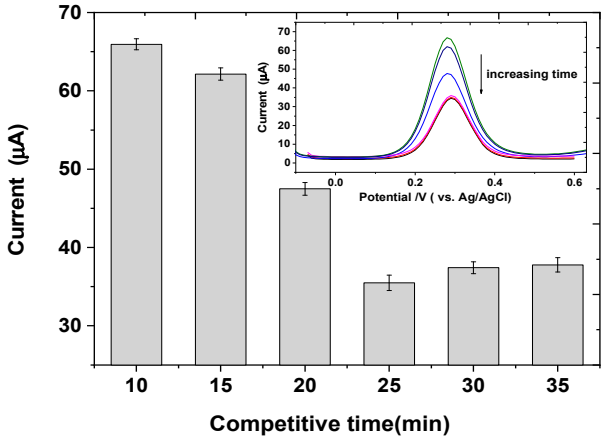
Aroclor 1254 was examined under optimized conditions using DPV in PBS (pH 7.4) to assess its effects on analytical capability. The DPV redox peak currents shown in Figure 5 are clearly shown to decrease with increasing concentrations of Aroclor 1254. Results indicate that Aroclor 1254 and PCB-BSA were successfully incorporated. Figure 5B shows the current had a linear relationship with Aroclor-1254 concentration on a semilogarithmic scale. The concentration was between 0.011 and 220 ng mL^{-1}. Additionally, the linear regression equation fit is shown ($Y = -4.623\ln(x) + 39.8$) ($R^2 = 0.99$), and the limit of detection was estimated to be 0.11 ng mL^{-1}. This was estimated to be three times that of the SD of the blank sample/slope. Table 3 shows a comparison with other existing PCB detection methods; the immunosensor demonstrated a wider linear dynamic range and an acceptable detection limit with a sensitivity of 4.62 μA ng^{-1}.



(**a**)

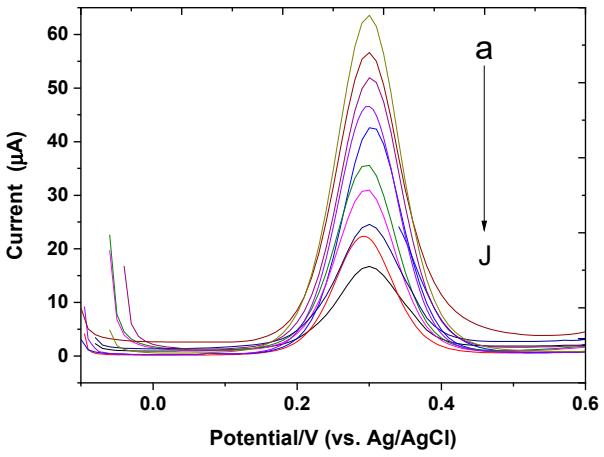


(**b**)

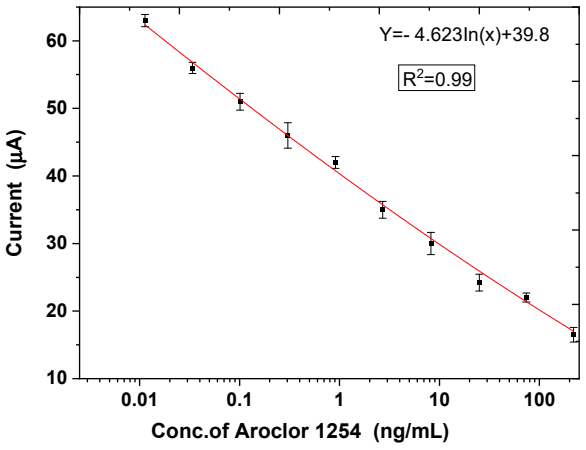


(**c**)

Figure 4. (**a**) Optimized concentration of PCB-BSA conjugate using capture assay. Detection was DPV (n = 3). The optimized concentration of the PCB-BSA conjugate was 5 µg/mL. (**b**) Optimized concentration of PCB using capture assay. Detection was DPV (n = 3). The optimized concentration of PCB was 0.246 µg/mL, which is less than the optical, which was 0.465 µg/mL. (**c**) Competition time for immunosensor response. Detection was DPV (n = 3).



(**A**)



(**B**)

Figure 5. (**A**) Typical DPV response of the designed immunosensor to Aroclor 1254 concentrations: (a) 0.011, (b) 0.033, (c) 0.101, (d) 0.304, (e) 0.91, (f) 2.7, (g) 8.2, (h) 25, (i) 74, and (j) 220 ng/mL^{-1}. (**B**) Plot of DPV current with respect to logarithms of different Aroclor 1254 concentrations.

Table 3. Performance of diverse electrochemical detection methods.

Method	Detection Mode	Linear Range	LOD	Amplification	Real Sample	Ref.
DPV	-	1–100	0.22 ng/L	None	Water	[30]
EIS	Noncompetitive	0.01–10 µg/L	0.001 µg/L	None	Oil	[22]
DPV	Competitive	0.01–50 ppm	5.2 ppm	AP (ALP)	Food	[37]
LSV	Competitive	0.1–220	0.09 ng/mL^{-1}	AP (ALP)	Water	[3]
DPV	Competitive	0.011–220	0.11 ng/mL^{-1}	None	Soil	This work

3.4. Reproducibility and Stability of the Designed Immunosensor

Electrochemical immunosensors were tested with PCB concentrations as high as 25 ng mL^{-1} across seven electrodes to verify the reproducibility. The relative RSD was 2.43%. According to the results, the fabricated immunosensor has high reproducibility and stability, which are important parameters in quantitative detection by immunosensors. In Figure 6, DPV was used for a complete assay every 5 days for a month (n = 3). After storing the immunosensor for 10 days, it maintained 98% of its original response, while maintaining 92% after 20 days. This electrode displayed excellent stability (RSD 5.9%) during a long period after being kept under dry conditions at 4 °C for 30 days. This might be due to the antibody being firmly attached to the gold surface, which is a reason for the good stability.

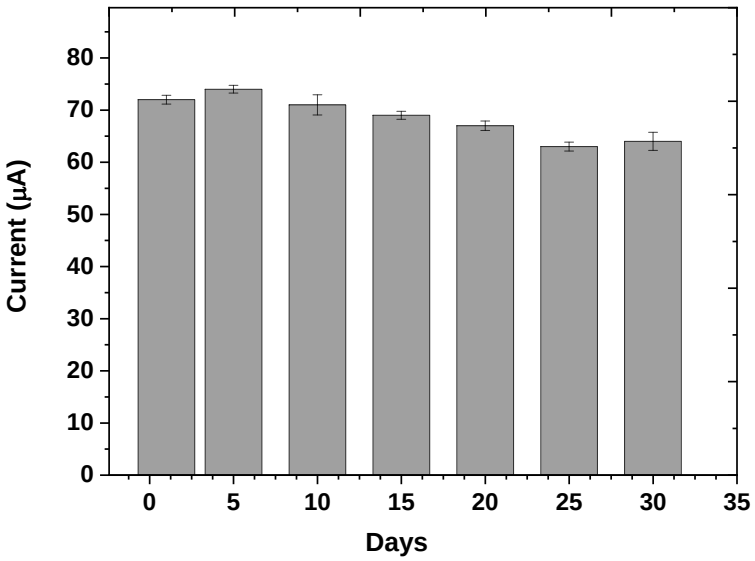


Figure 6. The stability of Aroclor 1254 detection by the immunosensor during 30 days.

3.5. Real Sample Analysis

Aroclor 1254, which was added to the soil samples using the standard addition technique, was determined using the developed immunosensor. As shown in Table 4, the developed sensing device showed recovery values in the range 90–96% for a spiked soil sample. All samples were run in triplicate. This indicated highly reliable results, with an RSD value of 2.5% (n = 3). In comparison with the traditional ELISA method, the new immunosensor was effective and reliable in determining Aroclor 1254 prevalence in the soil samples. In this case, the developed electrode met higher performance standards than the standard instrument, so the results we obtained were more appealing. The fundamental analysis also revealed that the developed sensor had other advantages in terms of determining PCBs in soil samples, including high accuracy, high selectivity, and high sensitivity.

Table 4. SPGE electrochemical and ELISA (immunoassay) approaches for the determination of Aroclor 1254 in soil samples (n = 3).

Techniques	Sample	Added (ng/mL^{-1})	Found (ng/mL^{-1})	Recovery %	RSD % (n = 3).
ELISA	Soil	8.2	10.54	128.53	4.4%
ELISA	Soil	25	26.41	105.64	3.6%
Electrochemical	Soil	8.2	7.89	96.21	1.7%
Electrochemical	Soil	25	22.74	90	2.5 %

4. Conclusions

In this work, a highly sensitive, cost-effective, and label-free electrochemical immunosensor was used for the determination of PCBs (Aroclor 1254). A self-assembled, monolayer-modified electrode was used in an indirectly competitive format and the results were compared with those of other methods. This immunosensor had a linear range of 0.011–220 ng/mL^{-1} and a limit of detection (LOD) of 0.11 ng/mL^{-1} under optimum conditions. According to our analyses, the chip demonstrated good performance and stability and could be used to detect PCB compounds using the electrochemical immunosensor. This immunosensor could be incorporated into a portable device to carry out real-time measurements in the field. Moreover, the technique described can be improved using nanoparticles, such as gold nanoparticles (GNPs), to enhance the sensitivity and performance of the individual sensor measurements. This would improve the commercialization of the technique we present here. This would also reduce the steps required for immunoassay testing in the field. Hence, incorporating an organic-pollutant-monitoring platform into portable lab-on-a-chip technology would be a useful way to avoid the costly and inefficient analysis of samples in specialized laboratories.

Author Contributions: Supervision, E.M.; writing—original draft, S.A.; reviewing—original draft, T.B.; Data curation, Investigation, Methodology, I.A.; Investigation and Review and editing. H.A. All authors have read and agreed to the published version of the manuscript.

Funding: The Saudi Ministry of Higher Education and Cultural Bureau, Dublin supported this work.

Institutional Review Board Statement: Not applicable.

Informed Consent Statement: Not applicable.

Data Availability Statement: Data are contained within the article.

Conflicts of Interest: The authors declare that there is no conflict of interest from any parts.

Abbreviations

The following abbreviations were used in this manuscript:

ΔEp	peak-to-peak separation
11-MUA	11-mercaptoundecanoic acid
Ag/AgCl	silver/silver chloride
Au	gold
BSA	bovine serum albumin
CV	cyclic voltammetry
EDC	1-Ethyl-3-(3-(dimethylamino)-propyl) carbodiimide
ELISA	enzyme-linked immunosorbent assay
HPLC	high performance liquid chromatography
$K_3Fe(CN)_6$	potassium ferricyanide
$K_4Fe(CN)_6$	potassium ferrocyanide
KCI	potassium chloride
LOD	limit of detection
MeOH	methanol
NaCl	sodium chloride
$NaCNBH_4$	sodium cyanoborohydride

NaOH	sodium hydroxide
NHS	N-hydroxy succinimide
PAb	polyclonal antibodies
PBS	phosphate-buffered saline
PCB	polychlorinated biphenyls
Rct	charge transfer resistance
SAM	self-assembled monolayer
SPGE	screen-printed gold electrodes
TRIS	tris(hydroxylmethyl)aminomethane

References

1. Biziuk, M. Environmental fate and global distribution of polychlorinated biphenyls Related papers Environmental Fate and Global Distribution of Polychlorinated Biphenyls. *Artic. Rev. Environ. Contam. Toxicol.* **2009**, *201*, 137–158. [CrossRef]
2. Lauby-Secretan, B.; Loomis, D.; Grosse, Y.; El Ghissassi, F.; Bouvard, V.; Benbrahim-Tallaa, L.; Guha, N.; Baan, R.; Mattock, H.; Straif, K.; et al. Carcinogenicity of polychlorinated biphenyls and polybrominated biphenyls. *Lancet Oncol.* **2013**, *14*, 287–288. [CrossRef]
3. Alsefri, S.; Balbaied, T.; Moore, E. Electrochemical Development of an Immunosensor for Detection Polychlorinated biphenyls (PCBs) for Environmental Analysis. *Chemosensors* **2021**, *9*, 307. [CrossRef]
4. Han, D.; Currell, M.J. Persistent organic pollutants in China's surface water systems. *Sci. Total Environ.* **2017**, *580*, 602–625. [CrossRef]
5. Fu, J.; Mai, B.; Sheng, G.; Zhang, G.; Wang, X.; Peng, P.; Xiao, X.; Ran, R.; Cheng, F.; Peng, X.; et al. Persistent organic pollutants in environment of the Pearl River Delta, China: An overview. *Chemosphere* **2003**, *52*, 1411–1422. [CrossRef]
6. Laschi, S.; Fránek, M.; Mascini, M. Screen-Printed Electrochemical Immunosensors for PCB Detection. *Electroanal. Int. J. Devoted Fundam. Pract. Asp. Electroanal.* **2000**, *12*, 1293–1298. [CrossRef]
7. Hong, S.; Kang, T.; Oh, S.; Moon, J.; Choi, I.; Choi, K.; Yi, J. Label-free sensitive optical detection of polychlorinated biphenyl (PCB) in an aqueous solution based on surface plasmon resonance measurements. *Sens. Actuators B Chem.* **2008**, *134*, 300–306. [CrossRef]
8. Bender, S.; Sadik, O.A. Direct Electrochemical Immunosensor for Polychlorinated Biphenyls. *Environ. Sci. Technol.* **1998**, *32*, 788–797. [CrossRef]
9. Helen, C.; Lemasle, M.; Laplanche, A.; Genin, E. Determination of polychlorodibenzo-p-dioxins and polychlorodibenzofurans by gas chromatography/tandem mass spectrometry and gas chromatography/triple mass spectrometry in a quadrupole ion trap. *J. Mass Spectrom.* **2001**, *36*, 546–554. [CrossRef]
10. Ottonello, G.; Ferrari, A.; Magi, E. Determination of polychlorinated biphenyls in fish: Optimisation and validation of a method based on accelerated solvent extraction and gas chromatography–mass spectrometry. *Food Chem.* **2014**, *142*, 327–333. [CrossRef]
11. Popp, P.; Keil, P.; Möder, M.; Paschke, A.; Thuss, U. Application of accelerated solvent extraction followed by gas chromatography, high-performance liquid chromatography and gas chromatography–mass spectrometry for the determination of polycyclic aromatic hydrocarbons, chlorinated pesticides and polychlorinated dibenzo-p-dioxins and dibenzofurans in solid wastes. *J. Chromatogr. A* **1997**, *774*, 203–211. [CrossRef]
12. Zajicek, J.L.; Tillitt, D.E.; Schwartz, T.R.; Schmitt, C.J.; Harrison, R.O. Comparison of an enzyme-linked immunosorbent assay (ELISA) to gas chromatography (GC)—Measurement of polychlorinated biphenyls (PCBs) in selected US fish extracts. *Chemosphere* **2000**, *40*, 539–548. [CrossRef]
13. Lasrado, J.A.; Santerre, C.R.; Zajicek, J.L.; Stahl, J.R.; Tillitt, D.E.; Deardorff, D. Determination of PCBs in Fish Using Enzyme-linked Immunosorbent Assay (ELISA). *J. Food Sci.* **2003**, *68*, 133–136. [CrossRef]
14. Fillmann, G.; Galloway, T.S.; Sanger, R.C.; Depledge, M.H.; Readman, J.W. Relative performance of immunochemical (enzyme-linked immunosorbent assay) and gas chromatography–electron-capture detection techniques to quantify polychlorinated biphenyls in mussel tissues. *Anal. Chim. Acta* **2002**, *461*, 75–84. [CrossRef]
15. Endo, T.; Okuyama, A.; Matsubara, Y.; Nishi, K.; Kobayashi, M.; Yamamura, S.; Morita, Y.; Takamura, Y.; Mizukami, H.; Tamiya, E. Fluorescence-based assay with enzyme amplification on a micro-flow immunosensor chip for monitoring coplanar polychlorinated biphenyls. *Anal. Chim. Acta* **2005**, *531*, 7–13. [CrossRef]
16. Inui, H.; Takeuchi, T.; Uesugi, A.; Doi, F.; Takai, M.; Nishi, K.; Miyake, S.; Ohkawa, H. Enzyme-Linked Immunosorbent Assay with Monoclonal and Single-Chain Variable Fragment Antibodies Selective to Coplanar Polychlorinated Biphenyls. *J. Agric. Food Chem.* **2012**, *60*, 1605–1612. [CrossRef]
17. Syahir, A.; Usui, K.; Tomizaki, K.; Kajikawa, K.; Mihara, H. Label and Label-Free Detection Techniques for Protein Microarrays. *Microarrays* **2015**, *4*, 228–244. [CrossRef]
18. Wang, S.; Zhao, S.; Wei, X.; Zhang, S.; Liu, J.; Dong, Y.; Florescu, M.; Jaffrezic-Renault, N. An Improved Label-Free Indirect Competitive SPR Immunosensor and Its Comparison with Conventional ELISA for Ractopamine Detection in Swine Urine. *Sensors* **2017**, *17*, 604. [CrossRef]
19. Ge, L.; Li, S.P.; Lisak, G. Advanced sensing technologies of phenolic compounds for pharmaceutical and biomedical analysis. *J. Pharm. Biomed. Anal.* **2020**, *179*, 112913. [CrossRef]

20. Švorc, Ľ. Determination of Caffeine: A Comprehensive Review on Electrochemical Methods. *Int. J. Electrochem. Sci.* **2013**, *8*, 5755–5773.
21. Zheng, X.; Li, H.; Xia, F.; Tian, D.; Hua, X.; Qiao, X.; Zhou, C. An Electrochemical Sensor for Ultrasensitive Determination the Polychlorinated Biphenyls. *Electrochim. Acta* **2016**, *194*, 413–421. [CrossRef]
22. Date, Y.; Aota, A.; Sasaki, K.; Namiki, Y.; Matsumoto, N.; Watanabe, Y.; Ohmura, N.; Matsue, T. Label-Free Impedimetric Immunoassay for Trace Levels of Polychlorinated Biphenyls in Insulating Oil. *Anal. Chem.* **2014**, *86*, 2989–2996. [CrossRef] [PubMed]
23. Haji-Hashemi, H.; Norouzi, P.; Safarnejad, M.R.; Ganjali, M.R. Label-free electrochemical immunosensor for direct detection of Citrus tristeza virus using modified gold electrode. *Sens. Actuators B Chem.* **2017**, *244*, 211–216. [CrossRef]
24. Liu, X.; Duckworth, P.A.; Wong, D.K.Y. Square wave voltammetry versus electrochemical impedance spectroscopy as a rapid detection technique at electrochemical immunosensors. *Biosens. Bioelectron.* **2010**, *25*, 1467–1473. [CrossRef]
25. Frederix, F.; Bonroy, K.; Laureyn, W.; Reekmans, G.; Campitelli, A.; Dehaen, W.; Maes, G. Enhanced performance of an affinity biosensor interface based on mixed self-assembled monolayers of thiols on gold. *Langmuir* **2003**, *19*, 4351–4357. [CrossRef]
26. Briand, E.; Salmain, M.; Herry, J.M.; Perrot, H.; Compère, C.; Pradier, C.M. Building of an immunosensor: How can the composition and structure of the thiol attachment layer affect the immunosensor efficiency? *Biosens. Bioelectron.* **2006**, *22*, 440–448. [CrossRef]
27. Bhattarai, J.K.; Tan, Y.H.; Pandey, B.; Fujikawa, K.; Demchenko, A.V.; Stine, K.J. Electrochemical impedance spectroscopy study of Concanavalin A binding to self-assembled monolayers of mannosides on gold wire electrodes. *J. Electroanal. Chem.* **2016**, *780*, 311–320. [CrossRef]
28. Fischer, L.M.; Tenje, M.; Heiskanen, A.R.; Masuda, N.; Castillo, J.; Bentien, A.; Émneus, J.; Jakobsen, M.H.; Boisen, A. Gold cleaning methods for electrochemical detection applications. *Microelectron. Eng.* **2009**, *86*, 1282–1285. [CrossRef]
29. Lu, M.; Li, X.; Yu, B.; Li, H. Electrochemical Behavior of Au Colloidal Electrode through Layer-by-Layer Self-Assembly. *J. Colloid Interface Sci.* **2002**, *248*, 376–382. [CrossRef]
30. Fan, L.; Wang, G.; Liang, W.; Yan, W.; Guo, Y.; Shuang, S.; Dong, C.; Bi, Y. Label-free and highly selective electrochemical aptasensor for detection of PCBs based on nickel hexacyanoferrate nanoparticles/reduced graphene oxides hybrids. *Biosens. Bioelectron.* **2019**, *145*, 111728. [CrossRef]
31. Dutta, G.; Lillehoj, P.B. Wash-free, label-free immunoassay for rapid electrochemical detection of PfHRP2 in whole blood samples. *Sci. Rep.* **2018**, *8*, 1–8. [CrossRef] [PubMed]
32. Bakshi, S.; Mehta, S.; Kumeria, T.; Shiddiky, M.J.A.; Popat, A.; Choudhury, S.; Bose, S.; Nayak, R. Rapid fabrication of homogeneously distributed hyper-branched gold nanostructured electrode based electrochemical immunosensor for detection of protein biomarkers. *Sens. Actuators B Chem.* **2021**, *326*, 128803. [CrossRef]
33. Xiao, X.; Li, H.; Wang, M.; Zhang, K.; Si, P. Examining the effects of self-assembled monolayers on nanoporous gold based amperometric glucose biosensors. *Analyst* **2014**, *139*, 488–494. [CrossRef]
34. Centi, S.; Laschi, S.; Fránek, M.; Mascini, M. A disposable immunomagnetic electrochemical sensor based on functionalised magnetic beads and carbon-based screen-printed electrodes (SPCEs) for the detection of polychlorinated biphenyls (PCBs). *Anal. Chim. Acta* **2005**, *538*, 205–212. [CrossRef]
35. Deng, A.; Franek, M.; Kolar, V. Food and Agricultural Immunology Determination of Atrazine in Soil Samples by ELISA Using Polyclonal and Monoclonal Antibodies. *Agric. Immunol.* **2010**, *11*, 135–144. [CrossRef]
36. Chen, D.; Li, J. Interfacial design and functionization on metal electrodes through self-assembled monolayers. *Surf. Sci. Rep.* **2006**, *61*, 445–463. [CrossRef]
37. Laschi, S.; Mascini, M.; Scortichini, G.; Fra, M.; Nek, Ä.; Mascini, M. Polychlorinated Biphenyls (PCBs) Detection in Food Samples Using an Electrochemical Immunosensor. *J. Agric. Food Chem.* **2003**, *51*, 1816–1822. [CrossRef]

separations

MDPI

Article

Development of the QuEChERS Extraction Method for the Determination of Polychlorinated Biphenyls (Aroclor 1254) in Soil Samples by Using GC-MS

Samia Alsefri [1], Thanih Balbaied [1], Hanan Alatawi [1], Ibtihaj Albalawi [1], Anna Hogan [2] and Eric Moore [2,3,*]

[1] Sensing and Separation Group, School of Chemistry and Life Science Interface, Tyndall National Institute, University College Cork, T12R5CP Cork, Ireland; 112220405@umail.ucc.ie (S.A.); thanih.balbaied@gmail.com (T.B.); 110122737@umail.ucc.ie (H.A.); 110125574@umail.ucc.ie (I.A.)
[2] School of Chemistry, University College Cork, T12R5CP Cork, Ireland; annamaria.hogan@ucc.ie
[3] Tyndall National Institute, T12R5CP Cork, Ireland
* Correspondence: e.moore@ucc.ie

Abstract: Polychlorinated biphenyls (PCBs) have been found in soil, which has typically been the result of industrial pollution in the past two decades. Although they are banned, PCBs can still be found in soils and other environmental media. For this reason, it is critical to develop an analytical method that can reliably identify and monitor their sources. This study describes a gas chromatography with mass spectrometry (GC-MS) technique, which was used to detect PCBs in soil samples by using a fast extraction method. Using the QuEChERS (quick, easy, cheap, effective, rugged, and safe) method, PCBs were more effectively extracted from soil. Different related parameters, such as time of shaking and centrifuging, type of solvent, and clean-up adsorbents, were compared and optimized. As the extraction solvent, acetonitrile/water produced the best results, and as the dispersive solid-phase extraction sorbent, diatomaceous earth produced the best results. Procedures allowed recovery values between 95.3% and 103.2%. A limit of detection of 1.9 µg/kg was determined with relative standard deviations (n = 3) of 2.1–4.0% for intra-day assays and 3.6–5.8% for inter-day assays. It was demonstrated that the method was simple, sensitive, efficient, and environmentally friendly when applied to soil samples. To our knowledge, an integrated approach based on QuEChERS for the determination of Aroclor 1254 in soil has not been published before. It is believed that this approach will eliminate the significant challenge of sample extraction in GC-MS processing, which was considered to be a procedural challenge in previous analyses.

Keywords: polychlorinated biphenyls (PCBs); quick; easy; cheap; effective; rugged; safe (QuEChERS); (GC-MS); sample preparation; extraction methods; soil environmental

check for updates

Citation: Alsefri, S.; Balbaied, T.; Alatawi, H.; Albalawi, I.; Hogan, A.; Moore, E. Development of the QuEChERS Extraction Method for the Determination of Polychlorinated Biphenyls (Aroclor 1254) in Soil Samples by Using GC-MS. *Separations* **2023**, *10*, 250. https://doi.org/10.3390/separations10040250

Academic Editor: Massimo Del Bubba

Received: 7 March 2023
Revised: 7 April 2023
Accepted: 11 April 2023
Published: 12 April 2023

Copyright: © 2023 by the authors. Licensee MDPI, Basel, Switzerland. This article is an open access article distributed under the terms and conditions of the Creative Commons Attribution (CC BY) license (https://creativecommons.org/licenses/by/4.0/).

1. Introduction

Polychlorinated biphenyls (PCBs) are chemical compounds formed artificially by replacing hydrogen atoms within biphenyl molecules with chlorine atoms, classifying them as a persistent organic pollutant. A total of 209 possible PCB congeners exist due to different commercial names for PCBs, accumulating and posing an environmental hazard [1–3]. Despite the banning of using and/or producing PCBs, they are still widely spread in environmental media, including in agricultural soil [4].

Aroclor 1254 is one type of PCB that has attracted researchers in recent years. A product with dozens of highly chlorinated congeners, it has been widely used for numerous open and closed industrial applications due to its chemical and thermal stabilities [5–7]. Therefore, the possibility of exposing people to Aroclor 1254 has increased greatly in different ways, such as through dietary intake, dermal contact, or inhalation, which negatively affect the human body and cause serious conditions including neurotoxicity, dermatological disorders, and

lung problems. Thus, the detection of Aroclor 1254 in the environment has become very important and requires a sensitive analytical method [8,9].

Gas chromatography is most commonly used to detect polychlorinated biphenyls usually in conjunction with an electron capture detector or mass spectrometry [10,11]. Some of the features of these techniques are accuracy, reliability, and sensitivity [12]. Isolating PCBs from the soil matrix is a crucial step in GC-MS. The PCB analysis has been carried out using a wide range of extraction techniques, such as chemical methods—involving soxhlet extraction [13–15], liquid–liquid extraction [16,17], and solid-phase extraction [18,19]—or physical ones, involving ultrasonic extraction [20], microwave-assisted extraction [21], supercritical fluid extraction [22], and pressurized fluid extraction [23].

Despite their own advantages, these methods suffer from hazardous solvents, and sample preparation is expensive and time-consuming; therefore, Anastassiades et al. introduced a quick, easy, cheap, effective, rugged, and safe method, known as QuEChERS, as an alternative means of extraction [24].

The method involves acetonitrile extraction, followed by salt addition and dispersive solid-phase extraction (d-SPE) cleanup. According to this alternative method, organic solvents are minimized, which was rarely discussed in the literature review [25]. PCBs have been removed from a variety of matrixes, including fish tissue [26–28], mussels [29], meat [30], and honey [31], and isolated by QuEChERS. Although different optimizations were discussed in the soil sample [32], further modification is required, including combinations of solvents, sorbents, or salts, considering volume, type, and ratio, which mostly depends on the analyte and the matrix.

Through the use of the QuEChERS method combined with GC-MS, this study aimed to develop and validate an inexpensive and reliable method of analyzing PCBs in soil. The QuEChERS method was examined for PCB extraction from six soil samples by examining the effect of water, solvent types, solvent volume, time of shaking, centrifuge time, speed, and types of sorbents used. To demonstrate the efficiency and accuracy of the methodology, blank samples spiked with standards were used to evaluate the precision and accuracy of the method.

2. Experiment

2.1. Instrumentation and Conditions for GC-MS

The GC-MS instrument used for the analysis of PCBs was an Agilent 6890/5973, which consisted of an Agilent 6890N GC equipped with an inert mass selective detector 5973. A capillary column HP-5MS [5%-phenyl)-methylpolysiloxane] Agilent J&W GC column, with a dimension of 0.25 mm ID × 30 m and a 0.25 µm film coating thickness, was used for the separation of PCB congeners. Helium was used as the carrier gas, with a flow rate of 1.0 mL/min and a pressure of 18 psi. The injector was kept at a constant pressure and temperature of 250 °C. The oven temperature was programmed as follows: it was initially set at 70 °C and held for two minutes, then increased to 180 °C at a rate of 25 °C/min, then increased to 200 °C at a rate of 3 °C/min, then increased to 280 °C at a rate of 8 °C/min, and held for 13 min. The injector and detector temperatures were both set at 280 °C. The injection volume was 5 µL in the splitless mode. The ionization voltage was 70 eV, and the solvent delay was set to 6 min. Detection of the compounds was performed in full scan mode with a scan range of 50 to 500 mass to charge ratios (*m/z*). The total run time was 36.07 min. The MS transfer line temperature was 280 °C, and the ion source temperature was 250 °C.

2.2. Chemicals and Instruments

The following were all obtained from Sigma (Dublin, Ireland): an Aroclor 1254 stock solution at a concentration of 200 µg/mL in methanol; a surrogate solution of a mixture in acetone containing 200 µg/mL of decachlorobiphenyl (deca-CB) and of tetrachloro-m-xylene (TCMX); anhydrous $MgSO_4$ powder; sodium chloride NaCl powder; diatomaceous earth; clean soil; acetonitrile; hexane; acetone; ethyl acetate; methanol. The reagents

and solvents used in the experiments were generally of an analytical grade or higher. Ultrapure deionized water, with a resistivity of 18.2 MΩ·cm, was obtained from a Milli-Q system (Millipore, Molsheim, France). We used a QuEChERS Original Method extraction kit (5 g samples), 50/pk. The kit contents were as follows: 4 g $MgSO_4$, 1 g NaCl with 50 mL tubes, and a QuEChERS dispersive clean-up kit (PSA, C18, $MgSO_4$); these were purchased from Agilent Technologies Ireland Limited (Cork, Ireland). We also used a centrifuge (Heraeus Megafuge 16, Thermo Fisher, Bremen, Germany), analog vortex mixer (VWR Mixer Mini Vortex, Missouri CT, USA), ultrasonic Branson 5510 cleaner (Branson Ultrasonics Corporation, Brookfield, CT, USA), suitable hoods, glassware, volumetric flasks, pipettes, cylinders, beakers, vials, tubes for soil sample extraction, and filter paper for soil sample filtration.

2.3. Standard and Sample Solution Preparation

A six-point calibration curve was employed for the quantitative analysis. Standard solutions of Aroclor 1254 were prepared at levels of 0.32, 0.65, 1.25, 2.5, 5, and 10 ng/mL by diluting 200 µg/mL Aroclor 1254 stock solutions with methanol. Surrogate standard solutions for Deca-CB and TCMX were prepared at a concentration of 5 ng/mL via dilution with acetone from a 200 µg/mL stock solution. To assess extraction recovery, a surrogate standard was added, and the standards and working solutions were stored at 4 °C. For the recovery experiment, the soil used in this work (about 100 g) was purchased from Sigma. The soil samples were stored at room temperature 25 °C in dark-colored glass bottles. The physicochemical properties of the soil were as follows: The soil texture was sandy; pH = 6.2; organic matter at levels of 0.1%. Afterwards, soil samples were spiked with PCBs standards at 10 µg/kg and 5 µg/kg. To obtain a homogeneous sample, a mechanical stirring apparatus was used. After that, to allow the solvent to evaporate, the samples were left in a ventilated area for eight hours. The standards are thought to bind the soil samples similarly to natural processes. For accurate recovery results, it is critical to use suitable extraction methods and solvents to avoid soil interference. The soil was pretreated to remove the interfering compounds. Additionally, the potential contamination sources were controlled and evaluated throughout the process to obtain better recovery.

To calculate the recovery, a chromatogram with characteristic peak areas and retention times, or a "fingerprint" pattern, was produced by a single PCB mixture of Aroclor 1254. In this study, an Aroclor 1254 mixture containing tetra-CB, *m/z* 292; hexa-CB, *m/z* 360; hepta-CB, *m/z* 394; penta-CB, *m/z* 326 with peak areas of penta-chlorinated biphenyls (penta-CBs) were selected and used to construct the calibration models for the quantification of Aroclor 1254, because penta-CBs are one of the major PCBs in Aroclor 1254 (48% weight). The areas of selected peaks in the sample were compared to the same areas in a standard PCB mixture, which was the method utilized.

Phase separation is a process in which a mixture is divided into two or more distinct phases, usually due to the presence of a separating agent. Salt is a commonly used separating agent, and its addition can induce phase separation. However, it is important to note that the effectiveness of the extraction system can also be influenced by the amount of salt used. In a recent study, the same amount of magnesium sulfate ($MgSO_4$) has been used as in a previous study to induce phase separation [24]. Magnesium sulfate ($MgSO_4$) is often used as a drying agent to remove water from the organic phase and improve the efficiency of the extraction process. In addition to $MgSO_4$, NaCl can also be employed to minimize the effects of polar interference. This can be particularly useful when analyzing samples that contain high levels of polar compounds, as these compounds can interfere with the extraction process and lead to inaccurate results. Therefore, careful consideration of the type and amount of separating agents used is crucial for the success of any extraction process.

2.4. Extraction and Clean-Up Procedure

Extraction was performed according to the QuEChERS method described by Anastassiades, Michelangelo Lehotay, Steven J. (2003) [24]. Approximately 5 g of soil samples were weighed into a 50 mL centrifuge tube and mixed with 15 mL of acetonitrile/water (75%: 25%, *v/v*) or hexane/water (75%: 25%, *v/v*) in a QuEChERS tube, followed by vortex homogenization for 4 min. Then, the tube containing samples was ultrasonically treated for 20 min. After that, 4 g of $MgSO_4$ and 1 g of NaCl were added. After vortexing the mixture for 4 min, the extract was centrifuged at 4500 rpm for 10 min to remove the upper layer. Approximately 6 mL of the organic layer extract was transferred into a clean-up tube containing 900 mg $MgSO_4$ and 150 mg of sorbent mix (PSA/C18) or diatomaceous earth. After 4 min of vortex homogenization, the tubes were centrifuged for 10 min at 4500 rpm. Approximately 1.5 milliliters of the upper layer were filtered before being transferred to GC vials for a GC-MS analysis, and 50 µL of deca-CB and TCMX internal standards were added the modified QuEChERS extraction method is shown in Figure 1. The blank samples (soils without PCBs) were treated the same way, but without the PCB standard solution. The experiments were replicated three times.

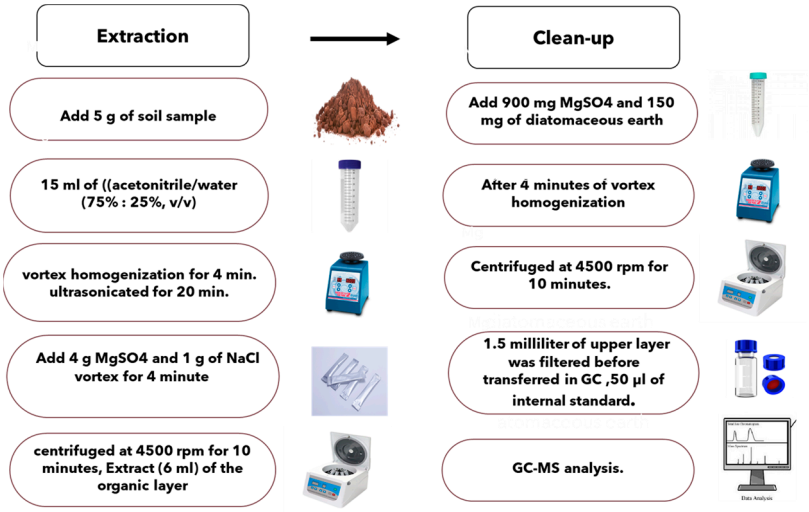


Figure 1. Schematic illustration of the modified QuEChERS extraction method.

2.5. Method Validation

The analytical parameters used to validate the method for analyzing PCBs include linearity, limit of detection (LOD), limit of quantification (LOQ), relative standard deviation (RSD), and recovery. The linearity of the relationship between concentration and peak area was determined by analyzing standard PCB solutions. Calibration curves used 6 standard solutions in the concentration range of 0.32–10 ng/mL for Aroclor 1254 in triplicate. LOD and LOQ were calculated using the formulas LOD = 3.3 SD of intercept/slope and LOQ = 10 SD of intercept/slope. Precision was evaluated by measuring the inter-day and intra-day variability at two concentration levels within the linearity range, with three replicates on the same day or on three different days. Recovery was assessed by performing a study at two concentration levels within the linearity range to evaluate the accuracy of the GC-MS method. The results of these analytical parameters are presented in the results section of the study.

3. Results and Discussion

3.1. Optimization of Extraction Solvent Conditions

For the purpose of this study, Aroclor 1254 was selected to be analyzed in soil samples. QuEChERS has been utilized in several studies to measure a variety of pollutants, including pesticides in soil samples [32,33], aromatic organochlorines [34], veterinary products, and pharmaceuticals [35,36]. In spite of this, the method has not been extensively used in the

extraction of Aroclor 1254 from soil. The QuEChERS method should be optimized in order to obtain the best recovery. Several related parameters, including water effect, solvent effect, and solvent volume effect, were optimized.

A traditional QuEChERS extraction was performed with samples containing a high moisture content. Additionally, the QuEChERS method has been modified [37–39]. Humidity is an important factor when preparing soil samples [40,41]. It was necessary to add ultrapure water to soil samples in order to ensure moisture content and to improve the recovery of PCBs from soil samples. To achieve high extraction efficiency, different amounts of water (3, 5, 7, and 10 mL) were tested. According to the results, maximum peak intensity and maximum recovery were achieved with 5 and 7 mL of water; as the amount of water increases, peak intensity decreases (see Figure 2a). For the additional experiment we utilized 5 mL.

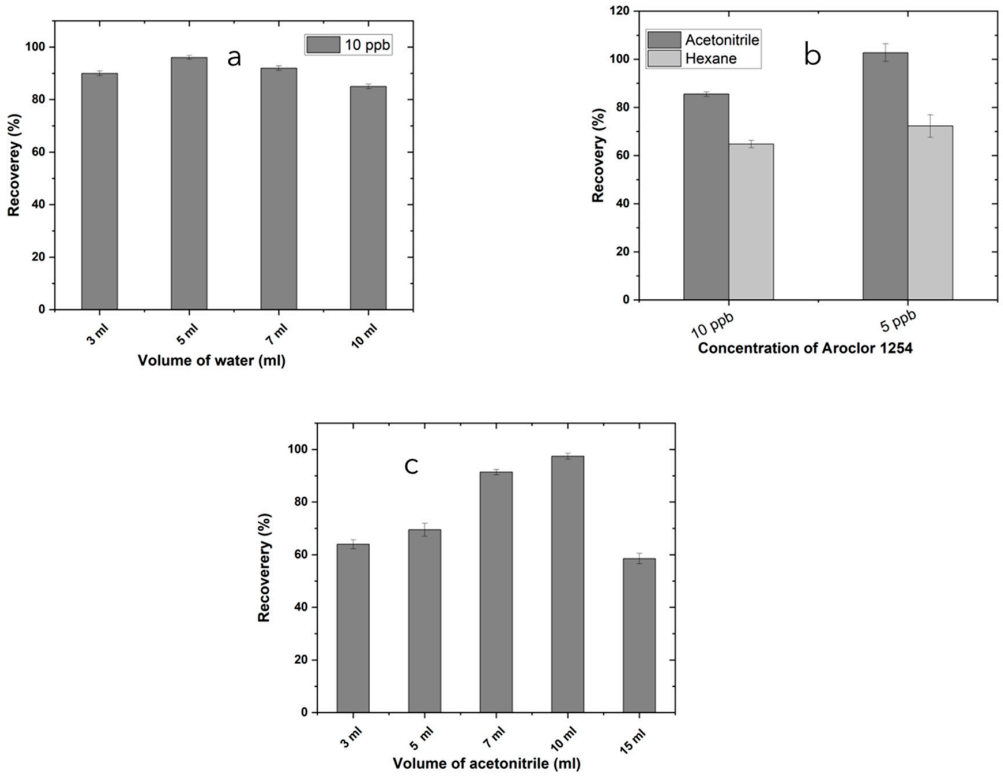


Figure 2. (**a**) The effect of water addition on extraction efficiency for the target Aroclor 1254 at 10 ng/mL; (**b**) the effect of acetonitrile and hexane as extraction solvents for the target Aroclor 1254 at 5 ng/mL and 10 ng/mL (n = 3); (**c**) the effects of different solvent volumes for the target Aroclor 1254 at 10 ng/mL (n = 3).

Extraction efficiency is highly dependent on the solvent used for extraction. In addition, the solvent must be less costly, compatible with analytical instruments, and eco-friendly [42]. To determine the most suitable solvent for the extraction of PCBs from soil samples, two different solvents were used: acetonitrile and hexane in combination with water. The original QuEChERS method used acetonitrile as the extract solvent, as did many other studies involving QuEChERS procedures [24]. Therefore, this solvent was chosen for use in the present study as one of the solvents, while hexane was chosen as the other solvent since it is commonly used to extract PCBs from soil [43], although it is less eco-friendly. As shown in Figure 2b, recovery rates of PCBs in the acetonitrile extraction were 85.53–102.72%, showing better efficiency, the production of cleaner extracts, and overall higher recoveries for PCBs than the hexane extraction. In this study, acetonitrile was found to be the most suitable extraction solvent, as it extracts a lower amount of the matrix, which is consistent with the findings of the previous study [31,44].

Furthermore, the volume of solvent used is critical for effective recovery, and there should be enough solvent to allow the sample to be fully immersed and interact with the analyte. Various amounts of acetonitrile, including 3, 5, 7, 10, and 15 mL were tested, and it was found that 10 mL of acetonitrile yielded the highest peak intensity and recovery, as depicted in Figure 2c. Acetonitrile is considered to be a more selective solvent and produces a cleaner chromatogram compared to most other solvents used in the QuEChERS technique [45]. When compared to other solvents utilized in QuEChERS, ACN separates from water more effectively in the presence of salts, producing good phase separation, which inhibits polar matrix interaction [46].

3.2. Optimization of Physical Extraction Condition

In this study, the effects of shaking time, centrifuge time, and speed were optimized and discussed. Several methods, including laboratory shakers, manual shakers, and vortexes, have been commonly used to extract targets from the soil. However, due to the strong binding characteristics of the soil, manual shaking for one minute, which was sufficient for the analysis of pesticides in fruits and vegetables according to the original QuEChERS method, resulted in lower recovery rates in this study. [24,47,48]. To compare the efficacy of manual shaking and vortex extraction, various extraction times ranging from 1 to 6 min were evaluated. The results showed that the recovery obtained with vortex extraction was higher than that obtained with manual shaking. Additionally, it was found that increasing the intensity of shaking was beneficial in breaking the strong interactions between analytes and matrix, resulting in improved extraction. Based on these findings, vortex extraction was selected as the preferred method of extraction for the targets from soil in this study. As shown in Figure 3a, the optimal extraction time for the removal of target PCBs from soil was found to be 4 min, and extending the extraction time beyond this did not improve recovery rate.

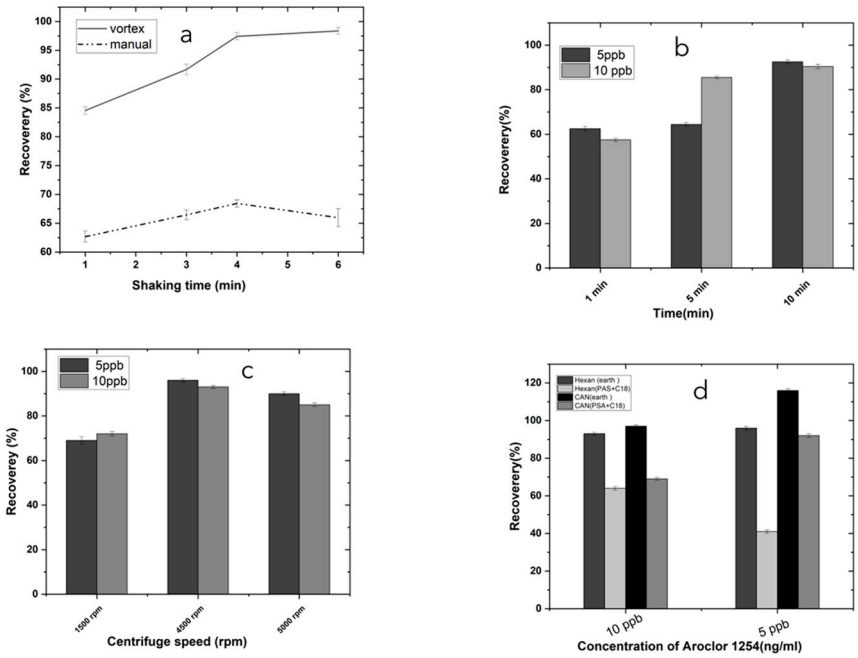


Figure 3. (**a**) Effect of shaking: 4 min, 15 mL of acetonitrile/water (75%:25%, *v/v*), 5 g of soil, 4 g $MgSO_4$, 1 NaCl. (**b**) Effect of centrifuge time: 4500 rpm, 15 mL of acetonitrile/water (75%:25%, *v/v*), 5 g of soil, 4 g $MgSO_4$, 1 NaCl. (**c**) Effect of speed: 10 min, 15 mL of acetonitrile/water (75%:25%, *v/v*), 5 g of soil, 4 g $MgSO_4$, 1 NaCl. (**d**) Comparison of recovery rates for different sorbents in the QuEChERS extraction method (n = 3). The conditions for the experiment were: 5 g of soil, 15 mL of acetonitrile/water (75%:25%, *v/v*), 4 g of $MgSO_4$, 1 g of NaCl, 4500 rpm.

There was a significant effect on centrifugation time and rate. In addition, different extraction times (1, 5, and 10 min) and rates (1500, 4500, and 5000 rpm) were investigated for 5 and 10 ng/mL concentration levels for PCB extraction. The results shown in Figure 3b indicate that excellent recovery of PCBs was achieved at 10 min, which was chosen as the optimal centrifugation time. A centrifuge of 4500 rpm was found to be sufficient to obtain good recovery of PCBs (Figure 3c). Using a centrifuge facilitates increased contact between the solvent and the soil sample, which improves dissolution of the analyte [49,50] and reduces the extraction time.

As part of the preparation of complex matrixes such as soil, a clean-up step was necessary in order to reduce interference, improve quantification, and avoid disturbing the signal on the chromatographic system [51]. In addition to traditional sorbents used in the clean-up step of QuEChERS extraction from soil samples, C18 and PSA, diatomaceous earth was also used as alternative sorbents [52,53]; they were less expensive and more eco-friendly than the traditional ones, but have not been extensively investigated in d-SPE [52]. As shown in Figure 3d, the sorbent has different effects on recovery and selectivity, and to achieve a satisfactory level of purification and recovery of PCBs, the effects of sorbent types were evaluated. The PSA retains a wide range of polar substances, including sugars, organic acids, and fatty acids. In addition, the nonpolar adsorbent, C18, retains trace amounts of nonpolar co-extractives and is capable of removing long chain fatty compounds and sterols from the extract. When PSA is used in conjunction with C18, additional lipids and sterols can be removed [53]. Diatomaceous earth consists of natural silica (SiO_2 nH_2O), with traces of metal oxides of specific structures, and its proposed use is as a simple alternative material and an environmentally-friendly natural sorbent [54]. The use of diatomaceous earth improved phase separation during QuEChERS extraction. Calculations of the differences between spiked and blank soil samples were used to determine recovery rates.

3.3. Method Validation

Under optimized extraction and clean-up conditions, we studied analytical parameters such as selectivity, linearity, LOD, LOQ, precision, and recovery. In order to evaluate the selectivity of the method, a blank sample was extracted by the optimized QuEChERS method, and positive samples were confirmed by GC-MS (Figure 4A). This confirms that the method has good selectivity, as no peaks interfered with analyte retention time. A standard calibration curve (Figure 4B) has been prepared using concentrations ranging from 0.31 to 10 ng/mL (0.31, 0.65, 1.25, 2.5, 5, 10 ng/mL) of Aroclor 1254 with a coefficient of determination R^2 of 0.9933; the linear regression equation fit is shown as (Y = 38,098 (x) − 26,023). The limit of detection (LOD) and limit of quantification (LOQ) were calculated based on three and ten times the standard deviation, respectively. The LOD value was 1.9 ng/mL and the LOQ value was 5.7 ng/mL, which indicated good sensitivity of this method.

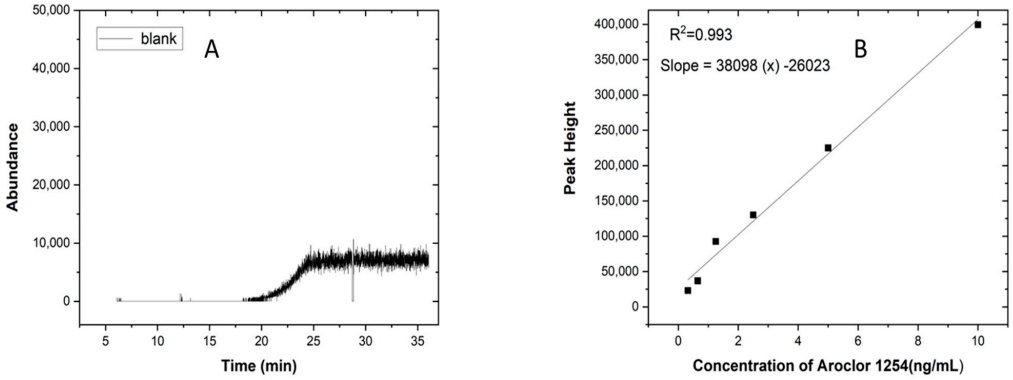


Figure 4. (**A**) GC analysis for the blank sample. (**B**) GC-MS calibration curve for standard Aroclor 1254.

3.4. Analysis of Aroclor 1254 in Spiked Soil Samples (Recovery and Precision)

The validation of a method is crucial to ensure that the results obtained are accurate and reliable. In the case of analyzing Aroclor 1254 in soil samples, sample spikes were used to improve the validation of the method. Two different levels of Aroclor 1254 standard solution were spiked into the soil samples at 5 and 10 µg/kg levels. The spiked samples were run in triplicate to evaluate the precision and repeatability of the assay. The RSD% was used to determine the precision, which was evaluated using two parameters: intra-day (repeatability) and inter-day precision. Repeatability was assessed by analyzing three replicates of soil samples spiked at two levels (5 and 10 µg/kg) on the same day, while inter-day precision was determined by analyzing samples on three different days over a period of two weeks.

The results of the analysis showed that the recovery of Aroclor 1254 from soil samples ranged from 95.3% to 103.2%, indicating the accuracy of the method. The RSD for inter-day precision ranged from 3.6% to 5.8%, while that for intra-day precision ranged from 2.1% to 4%, indicating the repeatability of the method. The developed modified QuEChERS method was compared with other recent studies in the literature, as demonstrated in Table 1. The present work shows great recovery value due to the use of different extraction solvents, which has a significant impact on the level of PCBs extraction from soil. Additionally, the comparison for blank (in black) and soil sample (in red) for 10 µg/kg and 5 µg/kg concentrations are presented in Figure 5, which further supports the accuracy and reliability of the modified QuEChERS and GC-MS methods for analyzing Aroclor 1254 in soil samples. These findings are important for environmental studies and risk assessments, as accurate analysis of pollutants in soil is necessary for identifying potential risks and implementing effective mitigation strategies.

Table 1. Comparison of the present study with other studies. For the present work recovery and RSD was included at different Aroclor 1254 concentrations in soil samples (n = 3).

Sample	Extraction	Added (µg/kg)	Intra-Day (RSD%)	Inter-Day (RSD%)	Recovery (%)	Reference
Water	acetonitrile	8 (µg /L)	≥15%	-	90–95%	[54]
Shrimp	water/MeCN *	1, 5, 10	>20%	-	70–115%	[55]
Sedimen	water/Ace/Hex * or wter/Ace/DCM *	50	≥15%	-	76–131%	[56]
Soil	Water/acetonitrile	5	4	5.8	103.2%	Present work
Soil	water/acetonitrile	10	2.1	3.6	95.3%	Present work

* MeCN (Acetonitrile), Ace (Acetone), Hex (Hexane), DCM (Dichloromethane).

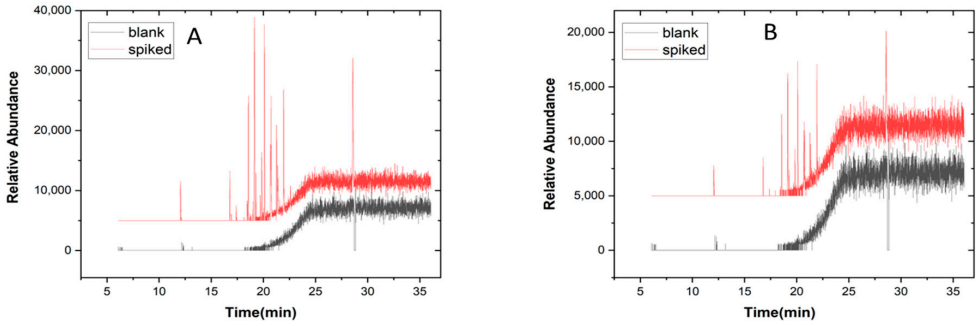


Figure 5. (**A**) GC/MS Total ion chromatogram of Aroclor 1254 (red line) and the blank (black line) for 10 µg /kg soil sample after QuEChERS extraction. (**B**) GC/MS Total ion chromatogram of Aroclor 1254 (red line) and the blank (black line) for 5 µg /kg soil sample after QuEChERS extraction.

4. Conclusions

In this study, we have utilized a modified QuEChERS method, combined with GC-MS analysis, to analyze Aroclor 1254 in soil samples. This novel method has several advantages

over traditional techniques, including its simplicity, cost-effectiveness, eco-friendliness, and minimal solvent extraction. We have modified the sample pretreatment procedure by incorporating vortex shaking, a mixed solvent (either acetonitrile/water or hexane/water), and three adsorbents (PSA, C18, and diatomaceous earth) for the cleaning process. We have found that the best results were obtained when water/acetonitrile and diatomaceous earth were used. The method demonstrated excellent accuracy, linearity, LOD, LOQ, intra-day precision, and inter-day precision. Specifically, the recovery was in the range of 95.3–103.2%, correlation coefficients were higher than 0.98, the limit of detection (LOD) was 1.9 µg/kg, and the limit of quantification (LOQ) was 5.7 µg/kg, intra-day precision varied between 2.1% and 4%, and inter-day precision was between 3.6% and 5.8%.

This optimized method offers several advantages over traditional techniques, including a reduction in overall analysis time, an avoidance of the use of large levels of non-eco-friendly solvents, increased sensitivity, rapid results, and a reduction in the consumption of organic reagents. Compared to other common extraction methods, this streamlined procedure offers an efficient and effective technique for monitoring PCBs in the environment. Moreover, this technique has the potential to be applied to a wider range of sample types and applications, making it an even more valuable tool for environmental monitoring. Overall, the study provides a significant contribution to the field of analytical chemistry and environmental science, demonstrating a novel and effective method for analyzing Aroclor 1254 in soil samples.

Author Contributions: S.A.: writing—original draft; T.B.: writing—review and editing; H.A.: validation and investigation; I.A.: validation and investigation; A.H.: supervision; E.M.: supervision. All authors have read and agreed to the published version of the manuscript.

Funding: This research was funded by the Ministry of Higher Education of Saudi Arabia.

Data Availability Statement: Not applicable.

Acknowledgments: The authors would like to thank the Ministry of Higher Education of Saudi Arabia for their financial support. The authors would also like to thank the School of Chemistry and University College Cork for providing laboratory facilities.

Conflicts of Interest: The authors declare no conflict of interest.

References

1. Robles Martínez, H.A.; Rodríguez, G.C.; Castillo, D.H. Determination of PCBs in Transformers Oil Using Gas Chromatography with Mass Spectroscopy and Aroclors (A1254:A1260). *Chem. Soc.* **2005**, *49*, 263–270.
2. Shin, S.K.; Kim, T.S. Levels of polychlorinated biphenyls (PCBs) in transformer oils from Korea. *J. Hazard. Mater.* **2006**, *137*, 1514–1522. [CrossRef] [PubMed]
3. Shen, F.; Xu, Y.J.; Wang, Y.; Zhu, P.Y.; Dai, X.L.; Chen, J.; Zou, Q. Determination of Aroclor 1254 in Water Samples Using Polystyrene–Divinylbenzene Solid-Phase Extraction and Gas Chromatography. *J. Anal. Test.* **2018**, *2*, 306–311. [CrossRef]
4. Kim, L.; Jeon, J.W.; Lee, Y.S.; Jeon, H.J.; Park, B.J.; Lee, H.S.; Choi, S.D.; Lee, S.E. Monitoring and risk assessment of polychlorinated biphenyls (PCBs) in agricultural soil collected in the vicinity of an industrialized area. *Appl. Biol. Chem.* **2016**, *59*, 655–659. [CrossRef]
5. Kaya, D.; Imamoglu, I.; Sanin, F.D.; Payne, R.B.; Sowers, K.R. Potential risk reduction of Aroclor 1254 by microbial dechlorination in anaerobic Grasse River sediment microcosms. *J. Hazard. Mater.* **2017**, *321*, 879–887. [CrossRef] [PubMed]
6. Swanson, G.M.; Ratcliffe, H.E.; Fischer, L.J. Human Exposure to Polychlorinated Biphenyls (PCBs): A Critical Assessment of the Evidence for Adverse Health Effects. *Regul. Toxicol. Pharmacol.* **1995**, *21*, 136–150. [CrossRef]
7. Zhong, Y.; Guo, P.; Wang, X.; An, J. Aroclor 1254 inhibits cell viability and induces apoptosis of human A549 lung cancer cells by modulating the intracellular Ca^{2+} level and ROS production through the mitochondrial pathway. *J. Environ. Sci. Health Part A* **2015**, *50*, 806–813. [CrossRef]
8. Ozcan, S. Analyses of polychlorinated biphenyls in waters and wastewaters using vortex-assisted liquid-liquid microextraction and gas chromatography-mass spectrometry. *J. Sep. Sci.* **2011**, *34*, 574–584. [CrossRef]
9. Ozcan, S.; Tor, A.; Aydin, M.E. Determination of selected polychlorinated biphenyls in water samples by ultrasound-assisted emulsification-microextraction and gas chromatography-mass-selective detection. *Anal. Chim. Acta* **2009**, *647*, 182–188. [CrossRef]
10. Derouiche, A.; Driss, M.R.; Morizur, J.P.; Taphanel, M.H. Simultaneous analysis of polychlorinated biphenyls and organochlorine pesticides in water by headspace solid-phase microextraction with gas chromatography-tandem mass spectrometry. *J. Chromatogr. A* **2007**, *1138*, 231–243. [CrossRef]

11. Güzel, B.; Canlı, O. An environmental friendly and stable analytical method for the determination of indicator polychlorinated biphenyls (PCBs) in solid and waste oil samples by gas chromatography-electron capture detector (GC-ECD). *Microchem. J.* **2022**, *178*, 107325. [CrossRef]
12. Santos, F.J.; Galceran, M.T. The application of gas chromatography to environmental analysis. *TrAC—Trends Anal. Chem.* **2002**, *21*, 672–685. [CrossRef]
13. Bandh, C.; Björklund, E.; Mathiasson, L.; Näf, C.; Zebühr, Y. Comparison of accelerated solvent extraction and Soxhlet extraction for the determination of PCBs in Baltic Sea sediments. *Environ. Sci. Technol.* **2000**, *34*, 4995–5000. [CrossRef]
14. Wang, P.; Zhang, Q.; Wang, Y.; Wang, T.; Li, X.; Ding, L.; Jiang, G. Evaluation of Soxhlet extraction, accelerated solvent extraction and microwave-assisted extraction for the determination of polychlorinated biphenyls and polybrominated diphenyl ethers in soil and fish samples. *Anal. Chim. Acta* **2010**, *663*, 43–48. [CrossRef] [PubMed]
15. Luque-García, J.L.; Luque De Castro, M.D. Extraction of polychlorinated biphenyls from soils by automated focused microwave-assisted Soxhlet extraction. *J. Chromatogr. A* **2003**, *998*, 21–29. [CrossRef]
16. Barri, T.; Bergström, S.; Norberg, J.; Jönsson, J.Å. Miniaturized and Automated Sample Pretreatment for Determination of PCBs in Environmental Aqueous Samples Using an On-Line Microporous Membrane Liquid-Liquid Extraction-Gas Chromatography System. *Anal. Chem.* **2004**, *76*, 1928–1934. [CrossRef]
17. Rezaei, F.; Bidari, A.; Birjandi, A.P.; Milani Hosseini, M.R.; Assadi, Y. Development of a dispersive liquid-liquid microextraction method for the determination of polychlorinated biphenyls in water. *J. Hazard. Mater.* **2008**, *158*, 621–627. [CrossRef]
18. Westbom, R.; Thörneby, L.; Zorita, S.; Mathiasson, L.; Björklund, E. Development of a solid-phase extraction method for the determination of polychlorinated biphenyls in water. *J. Chromatogr. A* **2004**, *1033*, 1–8. [CrossRef]
19. Zhang, Z.; Rhind, S.M. Optimized determination of polybrominated diphenyl ethers and polychlorinated biphenyls in sheep serum by solid-phase extraction-gas chromatography-mass spectrometry. *Talanta* **2011**, *84*, 487–493. [CrossRef]
20. Huo, L.G.; Li, H.D.; Zhao, C.L.; Wang, W.B.; Chen, Z.L.; Ding, R.Y.; Dong, Z.; Wang, F.E.; Yang, G.S.; Lu, X.; et al. The Determination of PCBs in Meat and Sea Food by GC-QqQ-MS/MS. *Food Anal. Methods* **2012**, *5*, 1481–1491. [CrossRef]
21. Ecd, G.C.; Benedicto, J.; Beckert, F. Determination of PCBs in Soils / Sediments by Microwave-Assisted Extraction. *Environ. Sci. Technol.* **1995**, *29*, 2709–2712.
22. Reddy, A.V.B.; Moniruzzaman, M.; Aminabhavi, T.M. Polychlorinated biphenyls (PCBs) in the environment: Recent updates on sampling, pretreatment, cleanup technologies and their analysis. *Chem. Eng. J.* **2019**, *358*, 1186–1207. [CrossRef]
23. Camel, V. Recent extraction techniques for solid matrices—Supercritical fluid extraction, pressurized fluid extraction and microwave-assisted extraction: Their potential and pitfalls. *Analyst* **2001**, *126*, 1182–1193. [CrossRef] [PubMed]
24. Anastassiades, M.; Lehotay, S.J.; Štajnbaher, D.; Schenck, F.J. Fast and Easy Multiresidue Method Employing Acetonitrile Extraction/Partitioning and "Dispersive Solid-Phase Extraction" for the Determination of Pesticide Residues in Produce. *J. AOAC Int.* **2003**, *86*, 412–431. [CrossRef]
25. Chamkasem, N.; Lee, S.; Harmon, T. Analysis of 19 PCB congeners in catfish tissue using a modified QuEChERS method with GC-MS/MS. *Food Chem.* **2016**, *192*, 900–906. [CrossRef]
26. Norli, H.R.; Christiansen, A.; Deribe, E. Application of QuEChERS method for extraction of selected persistent organic pollutants in fish tissue and analysis by gas chromatography mass spectrometry. *J. Chromatogr. A* **2011**, *1218*, 7234–7241. [CrossRef]
27. Cui, Y.; Wang, Z.; Cong, J.; Wang, L.; Liu, Y.; Wang, X.; Xie, J. Determination of polychlorinated biphenyls in fish tissues from Shanghai seafood markets using a modified QuEChERS method. *Anal. Sci.* **2017**, *33*, 973–977. [CrossRef]
28. Madureira, T.V.; Santos, C.; Velhote, S.; Cruzeiro, C.; Rocha, E.; Rocha, M.J. Contamination levels of polychlorinated biphenyls in wild versus cultivated samples of female and male mussels (Mytilus sp.) from the Northwest Coast of Iberian Peninsula-new application for QuEChERS (Quick, Easy, Cheap, Effective, Rugged, and Safe) metho. *Environ. Sci. Pollut. Res.* **2014**, *21*, 1528–1540. [CrossRef]
29. Kuzukiran, O.; Filazi, A. Determination of Selected Polychlorinated Biphenyl Residues in Meat Products by QuEChERS Method Coupled with Gas Chromatography–Mass Spectrometry. *Food Anal. Methods* **2016**, *9*, 1867–1875. [CrossRef]
30. Al-Alam, J.; Fajloun, Z.; Chbani, A.; Millet, M. A multiresidue method for the analysis of 90 pesticides, 16 PAHs, and 22 PCBs in honey using QuEChERS–SPME. *Anal. Bioanal. Chem.* **2017**, *409*, 5157–5169. [CrossRef]
31. Fernandes, V.C.; Domingues, V.F.; Mateus, N.; Delerue-Matos, C. Multiresidue pesticides analysis in soils using modified QuEChERS with disposable pipette extraction and dispersive solid-phase extraction. *J. Sep. Sci.* **2013**, *36*, 376–382. [CrossRef] [PubMed]
32. Yu, Y.; Liu, X.; He, Z.; Wang, L.; Luo, M.; Peng, Y.; Zhou, Q. Development of a multi-residue method for 58 pesticides in soil using QuEChERS and gas chromatography-tandem mass spectrometry. *Anal. Methods* **2016**, *8*, 2463–2470. [CrossRef]
33. Rouvire, F.; Buleté, A.; Cren-Olivé, C.; Arnaudguilhem, C. Multiresidue analysis of aromatic organochlorines in soil by gas chromatography-mass spectrometry and QuEChERS extraction based on water/dichloromethane partitioning. Comparison with accelerated solvent extraction. *Talanta* **2012**, *93*, 336–344. [CrossRef] [PubMed]
34. Robert Baudot, L.W. Comparison of Two Analytical Methods for the Determination of Traces of Veterinary Antibiotics and Steroid Hormones in Soil Based on Pressurised Liquid Extraction (PLE) and Quick, Easy, Cheap, Effective, Rugged, Safe (Modified-Quechers) Extraction. *Pharm. Anal. Acta* **2014**, *5*, 1000315. [CrossRef]
35. De Mastro, F.; Cocozza, C.; Traversa, A.; Cacace, C.; Mottola, F.; Mezzina, A.; Brunetti, G. Validation of a modified QuEChERS method for the extraction of multiple classes of pharmaceuticals from soils. *Chem. Biol. Technol. Agric.* **2022**, *9*, 49. [CrossRef]

36. Lacina, O.; Zachariasova, M.; Urbanova, J.; Vaclavikova, M.; Cajka, T.; Hajslova, J. Critical assessment of extraction methods for the simultaneous determination of pesticide residues and mycotoxins in fruits, cereals, spices and oil seeds employing ultra-high performance liquid chromatography-tandem mass spectrometry. *J. Chromatogr. A* **2012**, *1262*, 8–18. [CrossRef]
37. Walorczyk, S. Development of a multi-residue screening method for the determination of pesticides in cereals and dry animal feed using gas chromatography-triple quadrupole tandem mass spectrometry. *J. Chromatogr. A* **2007**, *1165*, 200–212. [CrossRef]
38. Cajka, T.; Sandy, C.; Bachanova, V.; Drabova, L.; Kalachova, K.; Pulkrabova, J.; Hajslova, J. Streamlining sample preparation and gas chromatography-tandem mass spectrometry analysis of multiple pesticide residues in tea. *Anal. Chim. Acta* **2012**, *743*, 51–60. [CrossRef]
39. Salama, G.; El Gindy, A.; Hameed, E.A.A. The use of experimental design for optimisation of QuEChERS extraction of commonly used pesticides in Egyptian soil and drainage water and their determination by GC/MS. *Int. J. Environ. Anal. Chem.* **2022**, *102*, 4238–4249. [CrossRef]
40. Salimiasl, S.M.; Khodayar, M.J.; Mousavi, Z.; Akhgari, M. Comparison of the Modified QuEChERS Method and the Conventional Method of Extraction in Forensic Medicine to Detect Methadone in Post-Mortem Urine by GCMS. *Asia Pac. J. Med. Toxicol.* **2017**, *6*, 81–87.
41. Zhang, C.; Deng, Y.; Zheng, J.; Zhang, Y.; Yang, L.; Liao, C.; Su, L.; Zhou, Y.; Gong, D.; Chen, L.; et al. The application of the QuEChERS methodology in the determination of antibiotics in food: A review. *TrAC—Trends Anal. Chem.* **2019**, *118*, 517–537. [CrossRef]
42. Szostek, B.; Tinklenberg, J.A.; Aldstadt, J.H. A simple method for the quantitative microextraction of polychlorinated biphenyls from soils and sediments. *Chemosphere* **1999**, *38*, 3131–3139. [CrossRef]
43. Pajewska-Szmyt, M.; Sinkiewicz-Darol, E.; Bernatowicz-Łojko, U.; Kowalkowski, T.; Gadzała-Kopciuch, R.; Buszewski, B. QuEChERS extraction coupled to GC-MS for a fast determination of polychlorinated biphenyls in breast milk from Polish women. *Environ. Sci. Pollut. Res.* **2019**, *26*, 30988–30999. [CrossRef] [PubMed]
44. He, Z.; Wang, L.; Peng, Y.; Luo, M.; Wang, W.; Liu, X. Determination of selected polychlorinated biphenyls in soil and earthworm (Eisenia fetida) using a QuEChERS-based method and gas chromatography with tandem MS. *J. Sep. Sci.* **2015**, *38*, 3766–3773. [CrossRef] [PubMed]
45. Núñez, M.; Borrull, F.; Pocurull, E.; Fontanals, N. Sample treatment for the determination of emerging organic contaminants in aquatic organisms. *TrAC—Trends Anal. Chem.* **2017**, *97*, 136–145. [CrossRef]
46. Al-Thaiban, H.; Al-Tamimi, N.; Helaleh, M. Development of QuEChERS method for the determination of polycyclic aromatic hydrocarbons in smoked meat products using GC-MS from Qatar. *J. Anal. Methods Chem.* **2018**, *2018*, 9206237. [CrossRef]
47. Vera, J.; Correia-Sá, L.; Paíga, P.; Bragança, I.; Fernandes, V.C.; Domingues, V.F.; Delerue-Matos, C. QuEChERS and soil analysis. An Overview. *Sample Prep.* **2014**, *1*, 54–77. [CrossRef]
48. Hvězdová, M.; Kosubová, P.; Košíková, M.; Scherr, K.E.; Šimek, Z.; Brodský, L.; Šudoma, M.; Škulcová, L.; Sáňka, M.; Svobodová, M.; et al. Currently and recently used pesticides in Central European arable soils. *Sci. Total Environ.* **2018**, *613–614*, 361–370. [CrossRef]
49. Kouzayha, A.; Al Iskandarani, M.; Mokh, S.; Rabaa, A.R.; Budzinski, H.; Jaber, F. Optimization of a solid-phase extraction method using centrifugation for the determination of 16 polycyclic aromatic hydrocarbons in water. *J. Agric. Food Chem.* **2011**, *59*, 7592–7600. [CrossRef]
50. Farajzadeh, M.A.; Sohrabi, H.; Mohebbi, A. Combination of Modified QuEChERS Extraction Method and Dispersive Liquid–Liquid Microextraction as an Efficient Sample Preparation Approach for Extraction and Preconcentration of Pesticides from Fruit and Vegetable Samples. *Food Anal. Methods* **2019**, *12*, 534–543. [CrossRef]
51. Łozowicka, B.; Rutkowska, E.; Jankowska, M. Influence of QuEChERS modifications on recovery and matrix effect during the multi-residue pesticide analysis in soil by GC/MS/MS and GC/ECD/NPD. *Environ. Sci. Pollut. Res.* **2017**, *24*, 7124–7138. [CrossRef] [PubMed]
52. de Arias, J.L.O.; Rombaldi, C.; Caldas, S.S.; Primel, E.G. Alternative sorbents for the dispersive solid-phase extraction step in quick, easy, cheap, effective, rugged and safe method for extraction of pesticides from rice paddy soils with determination by liquid chromatography tandem mass spectrometry. *J. Chromatogr. A* **2014**, *1360*, 66–75. [CrossRef] [PubMed]
53. Cabrera, L.D.C.; Caldas, S.S.; Prestes, O.D.; Primel, E.G.; Zanella, R. Evaluation of alternative sorbents for dispersive solid-phase extraction clean-up in the QuEChERS method for the determination of pesticide residues in rice by liquid chromatography with tandem mass spectrometry. *J. Sep. Sci.* **2016**, *39*, 1945–1954. [CrossRef] [PubMed]
54. Shi, J.-W.; Zhao, Y.-G.; Fu, Z.-J.; Li, J.-G.; Wang, Y.-F.; Yang, T.-C. Development of a Screening Method for the Determination of PCBs in Water Using QuEChERS Extraction and Gas Chromatography–Triple Quadrupole Mass Spectrometry. *Anal. Sci.* **2012**, *28*, 167. [CrossRef] [PubMed]
55. Han, L.; Sapozhnikova, Y.; Lehotay, S.J. Streamlined sample cleanup using combined dispersive solid-phase extraction and in-vial filtration for analysis of pesticides and environmental pollutants in shrimp. *Anal. Chim. Acta* **2014**, *827*, 40–46. [CrossRef]
56. Ben Salem, F.; Ben Said, O.; Duran, R.; Monperrus, M. Validation of an adapted QuEChERS method for the simultaneous analysis of polycyclic aromatic hydrocarbons, polychlorinated biphenyls and organochlorine pesticides in sediment by gas chromatography–mass spectrometry. *Bull. Environ. Contam. Toxicol.* **2016**, *96*, 678–684. [CrossRef]

Disclaimer/Publisher's Note: The statements, opinions and data contained in all publications are solely those of the individual author(s) and contributor(s) and not of MDPI and/or the editor(s). MDPI and/or the editor(s) disclaim responsibility for any injury to people or property resulting from any ideas, methods, instructions or products referred to in the content.